

**University of Alberta**

Caspase activity and regulation in *Drosophila melanogaster*  
innate immunity

by

Silvia Guntermann

A thesis submitted to the Faculty of Graduate Studies and Research  
in partial fulfillment of the requirements for the degree of

Doctor of Philosophy

in

Immunology

Medical Microbiology and Immunology

©Silvia Guntermann  
Spring 2014  
Edmonton, Alberta

Permission is hereby granted to the University of Alberta Libraries to reproduce single copies of this thesis and to lend or sell such copies for private, scholarly or scientific research purposes only.

Where the thesis is converted to, or otherwise made available in digital form, the University of Alberta will advise potential users of the thesis of these terms.

The author reserves all other publication and other rights in association with the copyright in the thesis and, except as herein before provided, neither the thesis nor any substantial portion thereof may be printed or otherwise reproduced in any material form whatsoever without the author's prior written permission.

*To Peter, our families, and friends*

## ABSTRACT

The fine balance struck between life and death is key for the health of all multicellular organisms and therefore the pathways that govern life and death decisions are evolutionarily highly conserved. For example, the human TNF and the *Drosophila* IMD pathways coordinate signaling elements such as conserved JNK, NF- $\kappa$ B, and caspase modules to drive appropriate responses. Caspases are an evolutionarily conserved family of cysteinyl aspartate proteases with fundamental roles in the opposing processes of cell-survival and cell-death. The caspase Dredd is an essential pro-survival regulator of the IMD mediated immune response. However, the detailed involvement of Dredd in the sequential activation of the IMD cascade, the position of Dredd, and Dredd's interactions with the IMD pathway were unknown. In addition, the molecular mechanism of Dredd activation and regulation was unclear. In this study I conducted a thorough structural and functional analysis of the mechanism of Dredd activity in IMD signaling. I revealed numerous interactions of Dredd with early activators of the IMD pathway. I showed that the caspase activity inhibitor p35 blocked Dredd activation in a mechanism that is distinct from the general mechanism of p35-dependent caspase inhibition. In addition, Dredd activation appears independent of auto-processing which might be explained by the lack of Dredd linker residues that support auto-processing and may explain Dredd's sole function in pro-survival responses. In a combination of cell culture and *in vivo* assays, I demonstrated that Dredd is required for the activation of dJNK signaling upstream of dTAK1 and determined that Dredd additionally functions downstream of Imd activation. Furthermore, my data uncovered a dual regulation of dIAP2 by RING domain mediated destruction and Dronc mediated N-terminal

proteolytic cleavage. In summary, the data indicate a distinct activation mechanism for Dredd and establish dual functions for Dredd in the IMD signaling cascade, where Dredd is required in a proximal signaling complex for the early transduction of a phospho-relay to Rel and dJNK as well as for the subsequent activation of Rel. The data also uncover a novel role for Dronc in immune signaling. Combined the findings underline the importance and complexity of non-apoptotic roles of caspases.

## ACKNOWLEDGEMENT

Looking back, I feel very lucky about the many people I have met, and about my friends and family who have been with me during the time of my Ph.D thesis. It would have been impossible to stay on track all these years and to finish this doctoral thesis without the support, help, and encouragement of all the kind people around me, to only some of whom it is possible to give particular mention here.

Foremost, I would like to thank my supervisor Dr. Edan Foley. Thank you so much for welcoming me in your lab and for providing me with the opportunity to complete my Ph.D. thesis. I know this project has always been important to you and I am grateful for your trust in me and the opportunity to turn it into my project. I am very thankful for all your patience, motivation, enthusiasm, and your guidance to help me to improve my theoretical and practical skills. Thank you for being always so supportive when I felt frustrated, and for always letting me know that “everything will be fine”.

My gratitude goes out as well to my committee members Dr. Kirst King-Jones and Dr. Stefan Pukatzki, and to my examination committee Dr. Joel Dacks and Dr. Savraj Grewal. Thank you for sharing your expertise and knowledge, and for your critical comments and suggestions towards my work and my thesis.

I want to thank present and past members of the Foley lab. In particular, Anja, Brendon, Brittany, David B., David P., Kristina, and Tanja. Thank you all so much for being great colleagues but most importantly for being wonderful friends throughout my time in the lab. I have enjoyed all our conversations, shared lunches and coffee breaks. I am sad that those moments will be less frequently but I am sure that in the future our friendships will extend well beyond our shared time in the lab.

I wish to thank all my friends I made during my time in Canada and to all my “good-old” friends back in Germany who were always a great source of laughter, joy, and support. Thanks to my dearest friend Stephanie who I am friend with for as long as I can remember. You have always been there for me.

Thanks to the Asmuth family for supporting Peter and me in all our decisions and to always make me feel like part of the family.

Thanks to my siblings Anja, Lea, Lina, and Michael. I am so grateful to be part of this crazy wonderful bunch I can call family and I am looking forward to all the time together to come. Best Family ever!

Thanks to Marie-Luise for being the best stepmom anybody could wish for.

Immeasurable thanks goes to my Mom and Dad who I owe everything. Thanks to my Mom, who unfortunately cannot be here but I am sure she has been there all along. Thanks to my Dad who has done an unbelievable job in

raising and taking care of us kids and for always supporting us in every step of our lives.

Finally to Peter, who has been by my side throughout this Ph.D. thesis supporting me every single minute. Without your loving support, I would not have had the courage to embark on this journey and I would not have had the endurance to finish it. You are the best!

# TABLE OF CONTENTS

## Table of Contents

### Abbreviations, Symbols and Nomenclature

<b>Chapter 1. Introduction</b>	<b>1</b>
1.1. Innate Immunity .....	2
1.2. <i>Drosophila</i> innate immunity .....	5
1.3. TNF signaling pathway .....	6
1.4. IMD signaling pathway .....	9
1.5. Caspases .....	13
1.5.1. Caspase structure and classification .....	15
1.5.2. Caspase activation .....	19
1.5.3. Caspase regulation .....	22
1.5.4. Caspases in apoptotic signaling .....	26
1.5.5. Non-apoptotic caspases .....	27
1.5.6. Caspase-8 .....	29
1.5.7. Dredd .....	32
1.6. Objectives .....	36
<b>Chapter 2. Materials and Methods</b>	<b>38</b>
2.1. Buffers and solutions .....	39
2.2. DNA cloning .....	46
2.2.1. Expression constructs .....	46
2.2.2. Polymerase chain reaction (PCR) with Pfx polymerase .....	52
2.2.3. Polymerase chain reaction (PCR) with <i>Taq</i> polymerase .....	52
2.2.4. Reverse transcription polymerase chain reaction (RT-PCR) .....	53
2.2.5. Polymerase chain reaction (PCR) purification .....	53

2.2.6.	Agarose gel electrophoresis .....	53
2.2.7.	DNA isolation from excised gel fragments .....	54
2.2.8.	TOPO TA cloning and recombination (Gateway recombination cloning technology) .....	54
2.2.9.	Generation of chemically competent bacteria .....	57
2.2.10.	Transformation of bacteria .....	57
2.2.11.	Analytical polymerase chain reaction (PCR) from bacterial colonies .....	58
2.2.12.	DNA preparation of bacterial mini cultures from bacterial colonies .....	58
2.2.13.	DNA preparation of bacterial midi cultures from mini cultures .....	59
2.2.14.	Measurement of DNA concentration and purity .....	59
2.2.15.	Analytical restriction digest .....	59
2.2.16.	Preparation of DNA samples for sequencing .....	60
2.2.17.	Preparation of glycerol stocks and set up of bacterial cultures from a glycerol stock .....	61
2.3.	Generation of dsRNA .....	61
2.3.1.	<i>De novo</i> synthesis of dsRNA .....	61
2.3.2.	Amplification of T7 tagged DNA .....	62
2.3.3.	Generation of dsRNA .....	63
2.4.	Cell lines and cell culture .....	65
2.4.1.	<i>Drosophila</i> cell line culture .....	65
2.4.2.	Human cell line culture .....	65
2.4.3.	Determination of the concentration of viable cells in a suspension .....	66
2.5.	Cell treatments .....	67
2.5.1.	S2 cell treatments .....	67
2.5.2.	Determination of the apoptotic index .....	67
2.5.3.	HeLa cell treatments .....	67
2.6.	DNA transfection in cell culture .....	68
2.6.1.	DNA transfection in S2 cell culture .....	68

2.6.2. DNA transfection in HeLa cell culture .....	68
2.7. RNAi treatment .....	69
2.7.1. dsRNA in S2 cells culture .....	69
2.7.2. siRNA in HeLa cell culture .....	70
2.8. Immunoprecipitation .....	72
2.9. Quantitative real-time PCR (qRT-PCR) .....	72
2.9.1. RNA purification .....	72
2.9.2. Measurement of RNA concentration and purity .....	73
2.9.3. Synthesis of cDNA .....	73
2.9.4. qRT-PCR with SYBR green method .....	74
2.9.5. Boxplots .....	77
2.10. SDS-PAGE and Western blotting .....	77
2.10.1. Sample preparation .....	77
2.10.2. SDS-PAGE .....	77
2.10.3. Transfer .....	78
2.10.4. Western blotting .....	78
2.10.5. In cell western .....	82
2.11. TMRE assay for the detection of the IMM potential .....	82
2.12. Fly lines and fly husbandry .....	83
2.12.1. Septic injury .....	85
<b>Chapter 3. The role of Dredd in <i>Drosophila</i> IMD signaling in cell culture</b> .....	<b>86</b>
3.1. Background .....	87
3.2. Dredd is an essential component of the IMD/dJNK pathway in cell culture .....	87
3.2.1. Dredd is required for IMD/dJNK activation in cell culture .....	87
3.2.2. Baculovirus p35 inhibits Dredd-dependent activation of dJNK in cell culture .....	94
3.3. Dredd interaction with the IMD pathway .....	103

3.3.1. Dredd acts upstream of dTAK1 in dJNK phosphorylation in cell culture .....	103
3.3.2. Dredd interacts with early IMD pathway components .....	107
3.4. Summary .....	119
<b>Chapter 4. The role of Dredd in <i>Drosophila</i> IMD signaling <i>in vivo</i></b>	<b>121</b>
4.1. Background .....	122
4.2. Dredd is an essential component of the IMD/dJNK pathway <i>in vivo</i> .....	123
4.2.1. Baculovirus p35 inhibits dJNK activation <i>in vivo</i> .....	123
4.2.2. Dredd is required for dJNK activation in IMD signaling <i>in vivo</i> ....	129
4.3. Dredd is an essential component in IMD/Rel signaling downstream of Imd activation <i>in vivo</i> .....	131
4.3.1. Dredd is required downstream of Imd activation .....	131
4.3.2. Dredd does not rescue the <i>dredd</i> <sup>B118</sup> mutation .....	143
4.4. Summary .....	150
<b>Chapter 5. Caspase function in <i>Drosophila</i> IMD signaling</b>	<b>152</b>
5.1. Background .....	153
5.2. Dredd structure and activation is distinct from Caspase-8 in cell culture .....	155
5.2.1. Dredd forms homodimers in S2 cells .....	155
5.2.2. Dredd and Caspase-8 have distinct proteolytic activities .....	157
5.2.3. Dredd and Caspase-8 have distinct interaction profiles .....	170
5.3. Dronc regulates dIAP2 protein levels in cell culture .....	172
5.3.1. N-terminal processing of dIAP2 is distinct from RING-dependent turnover of the full-length protein .....	172
5.3.2. Dronc is required for dIAP2 cleavage .....	181
5.3.3. Identification of dIAP2 cleavage site .....	191
5.3.4. Loss of <i>dronc</i> activity alters the IMD pathway response in S2 cells .....	193

5.4. Summary .....	195
<b>Chapter 6. Discussion</b>	<b>197</b>
6.1. Background - The role of Dredd in <i>Drosophila</i> IMD signaling in cell culture .....	198
6.1.1. Dredd is an essential component of the IMD/dJNK pathway in cell culture .....	198
6.1.2. Dredd interacts with early IMD pathway components .....	200
6.2. Background - The role of Dredd in <i>Drosophila</i> IMD signaling <i>in vivo</i> .....	202
6.2.1. Dredd is an essential component of the IMD/dJNK pathway <i>in vivo</i> .....	203
6.2.2. Dredd is an essential component in IMD/Rel signaling downstream of Imd activation <i>in vivo</i> .....	204
6.3. Background - Caspase function in <i>Drosophila</i> IMD signaling .....	207
6.3.1. Dredd structure and activation is distinct from Caspase-8 in cell culture .....	208
6.3.2. Dronc regulates dIAP2 protein levels in cell culture .....	216
6.4. Model .....	220
6.5. Significance .....	222
<b>Chapter 7. Bibliography</b>	<b>224</b>
<b>Appendix - Supplementary data</b>	<b>249</b>

# FIGURES

## Chapter 1. Introduction

Figure 1.1.	TNF and IMD signaling .....	4
Figure 1.2.	TNF signaling pathway .....	8
Figure 1.3.	IMD signaling pathway .....	12
Figure 1.4.	Non-apoptotic functions of caspases .....	14
Figure 1.5.	Caspase structure .....	16
Figure 1.6.	Human and <i>Drosophila</i> Caspases .....	18
Figure 1.7.	Caspase activation .....	21
Figure 1.8.	Caspase inhibition .....	25
Figure 1.9.	Caspase-8 in apoptosis .....	31
Figure 1.10.	Dredd history .....	33
Figure 1.11.	Historical model of IMD signaling .....	35
Figure 1.12.	Objectives .....	37

## Chapter 2. Materials and Methods

Figure 2.1.	Three step PCR to generate chimeric constructs .....	48
-------------	--	----

## Chapter 3. The role of Dredd in *Drosophila* IMD signaling in cell culture

Figure 3.1.	PGN induces a transient Phospho-dJNK response in cell culture .....	89
Figure 3.2.	RNAi-mediated depletion of <i>dredd</i> substantially eliminates Dredd protein .....	91
Figure 3.3.	Dredd is required for IMD/dJNK activation in cell culture .....	93
Figure 3.4.	Baculovirus p35 prevents Phospho-dJNK in cell culture .....	95
Figure 3.5.	Baculovirus p35 blocks transcriptional induction of dJNK-dependent transcripts in cell culture .....	98
Figure 3.6.	Dredd interacts with Baculovirus p35 in cell culture .....	100
Figure 3.7.	Dredd is essential in IMD signaling .....	102

Figure 3.8.	Constitutively active dTAK1 cell line activates dJNK in the IMD pathway .....	104
Figure 3.9.	Dredd acts upstream of dTAK1 in dJNK phosphorylation in the IMD pathway .....	106
Figure 3.10.	Confirmation of HA- or Myc-tagged expression constructs in cell culture .....	108
Figure 3.11.	dFADD interact with Imd and dIAP2 in cell culture .....	110
Figure 3.12.	Dredd interacts with dFADD and dIAP2 in cell culture .....	112
Figure 3.13.	Dredd does not compete with dFADD for binding with dIAP2 in cell culture .....	114
Figure 3.14.	Dredd and dIAP2 expression constructs for S2 cells .....	116
Figure 3.15.	Dredd:dIAP2 interaction in cell culture .....	118
Figure 3.16.	Summary of section 3 .....	120

#### **Chapter 4. The role of Dredd in *Drosophila* IMD signaling *in vivo***

Figure 4.1.	Confirmation of baculovirus p35 expression <i>in vivo</i> .....	125
Figure 4.2.	Baculovirus p35 inhibits dJNK activation <i>in vivo</i> .....	127
Figure 4.3.	Dredd is required for dJNK activation in IMD signaling <i>in vivo</i> ..	130
Figure 4.4.	Dredd in IMD signaling .....	134
Figure 4.5.	UAS/GAL4 GAL80[ts] TARGET system .....	136
Figure 4.6.	Expression of Imdcl induces an antimicrobial response <i>in vivo</i> .....	138
Figure 4.7.	Dredd functions downstream of or parallel to cleaved Imd (Imdcl) <i>in vivo</i> .....	140
Figure 4.8.	P[dredd+] rescues the <i>dredd</i> <sup>B118</sup> mutation in Imdcl flies .....	142
Figure 4.9.	<i>Dredd</i> does not rescue the <i>dredd</i> <sup>B118</sup> mutation in Imdcl flies .....	145
Figure 4.10.	Dredd does not rescue the <i>dredd</i> <sup>B118</sup> mutation .....	148
Figure 4.11.	Summary of section 4 .....	151

#### **Chapter 5. Caspase function in *Drosophila* IMD signaling**

Figure 5.1.	Dredd forms homodimers in S2 cells .....	156
-------------	--	-----

Figure 5.2.	Examination of caspase expression constructs in S2 cells and flies .....	159
Figure 5.3.	Caspase-8 is processed in a zVAD-FMK dependent manner in cell culture .....	161
Figure 5.4.	Processing of Caspase-8 is independent of Dredd .....	163
Figure 5.5.	Caspase-8 induces Dredd processing in cell culture .....	165
Figure 5.6.	Processing of Caspase-8 does not influence IMD signaling .....	167
Figure 5.7.	Dredd does not substitute for Caspase-8 during apoptosis in HeLa cells .....	169
Figure 5.8.	Dredd and Caspase-8 have distinct interaction profiles .....	171
Figure 5.9.	N-terminal processing of dIAP2 is distinct from a RING-dependent turnover of a full-length protein .....	174
Figure 5.10.	N-terminal processing of dIAP2 is impaired by zVAD-FMK treatment .....	177
Figure 5.11.	zVAD-FMK stabilizes MycdIAP2 protein .....	179
Figure 5.12.	Dronc influences N-terminal processing of dIAP2 .....	182
Figure 5.13.	Dronc is required for dIAP2 protein cleavage .....	184
Figure 5.14.	Dronc catalytic activity is required for dIAP2 cleavage .....	186
Figure 5.15.	dIAP2 protein stability .....	188
Figure 5.16.	Dronc and not Drice cleaves dIAP2 .....	190
Figure 5.17.	Dronc cleaves dIAP2 at two specific Aps residues .....	192
Figure 5.18.	Loss of <i>dronc</i> alters the IMD pathway response in cell culture .....	194
Figure 5.19.	Summary of section 5 .....	196

## Chapter 6. Discussion

Figure 6.1.	Proposed model .....	221
-------------	----------------------	-----

## Appendix - Supplementary data

Figure 1.	The IMD signaling pathway does not induce apoptosis .....	250
Figure 2.	Caspase sequence alignment .....	251

# TABLES

## Chapter 1. Introduction

Table 1.1.	Non-apoptotic functions of caspases .....	28
------------	---	----

## Chapter 2. Materials and Methods

Table 2.1.	Components of the resolving and stacking SDS-polyacrylamide gel .....	45
Table 2.2.	List of primer sequences for PCR assays .....	49
Table 2.3.	List of Gateway destination clones used in Gateway LR clonase assays .....	56
Table 2.4.	List of primer sequences for generating dsRNA in a PCR reactions .....	64
Table 2.5.	List of siRNAs .....	71
Table 2.6.	List of qRT-PCR primer sequences used in qRT-PCR assays ...	76
Table 2.7.	List of primary antibodies used in Western blot assays .....	79
Table 2.8.	List of secondary antibodies used in Western blot assays .....	81
Table 2.9.	List of fly lines .....	84

## Chapter 4. The role of Dredd in *Drosophila* IMD signaling *in vivo*

Table 4.1.	Fly strains for section 4.2. ....	124
Table 4.2.	Fly strains for section 4.3.1. ....	133
Table 4.3.	Fly strains for section 4.3.2. ....	144

## Chapter 5. Caspase function in *Drosophila* IMD signaling

Table 5.1.	Fly strains for section 5.2.1. ....	154
------------	-------------------------------------	-----

## ABBREVIATIONS, SYMBOLS AND NOMENCLATURE

### ABBREVIATIONS AND SYMBOLS:

#	–	Number
%	–	Percent
°C	–	Degree Celsius
A	–	Ampere
A260	–	Absorption at 260 nm
A280	–	Absorption at 280 nm
aa	–	Amino acids
Ab	–	Antibody
Act	–	Actin
AMP	–	Antimicrobial peptide
AP-1	–	Activator protein 1
APAF-1	–	Apoptotic Peptidase Activating Factor 1
APS	–	Ammonium persulfate
ARK	–	Apaf-1-related-killer
Asp	–	Aspartic acid (D)
Att	–	Attacin
Bcl-2	–	B-cell lymphoma 2
Bid	–	BH3-interacting domain death agonist
bp	–	Base pair
BSA	–	Bovine serum albumin
CaCl <sub>2</sub>	–	Calcium chloride
CARD	–	Caspase recruitment domain
caspase	–	Cysteine-dependent aspartate-directed protease
cDNA	–	Complementary deoxyribonucleic acid
c-FLIP <sub>L</sub>	–	Cellular FLICE-like Inhibitory Protein, long
CG	–	Computed Gene (formerly Celera Genome)
CHX	–	Cycloheximide
clAP	–	Cellular inhibitor of Apoptosis Protein

c-IAP1	–	Cellular Inhibitor of Apoptosis Protein 1
c-IAP2	–	Cellular Inhibitor of Apoptosis Protein 2
cl	–	Cleaved
CO <sub>2</sub>	–	Carbon dioxide
CrmA	–	cytokine response modifier A
D	–	Dalton
Damm	–	Death associated molecule related to Mch2
DAP-PGN	–	Diaminopimelic acid peptidoglycan
dATP	–	Deoxyadenosine triphosphate
Dcp-1	–	Death caspase-1
DD	–	Death Domain
Decay	–	Death executioner caspase related to Apopain/Yama
DED	–	Death-Effector Domain
dFADD	–	<i>Drosophila</i> Fas-Associated protein with Death Domain
dH <sub>2</sub> O	–	Distilled water
DH5α	–	<i>Escherichia coli</i> strain
dIAP1	–	<i>Drosophila</i> Inhibitor of Apoptosis protein 1
dIAP2	–	<i>Drosophila</i> Inhibitor of Apoptosis protein 2
DID	–	Death Inducing Domain
dIKK	–	<i>Drosophila</i> Inhibitor of nuclear factor Kappa-B Kinase
Dipt	–	Diptericin
dJNK	–	<i>Drosophila</i> c-Jun N-terminal Kinase
dMKK4	–	<i>Drosophila</i> Mitogen-activated Kinase Kinase 4
dMKK7	–	<i>Drosophila</i> Mitogen-activated Kinase Kinase 7
DMSO	–	Dimethyl sulfoxide
DNA	–	Deoxyribonucleic acid
DNase	–	Deoxyribonuclease
Dnr1	–	Defense repressor 1
dNTP	–	Deoxyribonucleotide triphosphate
Dredd	–	Death related ced-3/Nedd2-like protein
Drice	–	<i>Drosophila</i> interleukin-converting enzyme
Dronc	–	Dronc

dsRNA	–	Double-stranded ribonucleic acid
dTAB2	–	<i>Drosophila</i> TAK1-Associated Binding protein 2
dTAK1	–	<i>Drosophila</i> TGF- $\beta$ -Activated Kinase 1
DTT	–	Dithiothreitol
<i>E. coli</i>	–	<i>Escherichia coli</i>
E1	–	Ubiquitin activating enzyme
E2	–	Ubiquitin conjugating enzyme
E3	–	Ubiquitin ligase
FADD	–	Fas-Associated Death Domain protein
FBS	–	Fetal Bovine Serum
g	–	Gram
h	–	Hour
H <sub>2</sub> O	–	Water
Hep	–	Hemipterous
HEPES	–	Hydroxyethyl piperazineethanesulfonic acid
Hid	–	Head involution defective
IB	–	Immunoblot
IBM	–	IAP-binding motif
ICW	–	In-Cell Western
IgG	–	Immunoglobulin G
IKK	–	Inhibitor of nuclear factor Kappa-B Kinase
IKK- $\alpha$	–	Inhibitor of nuclear factor Kappa-B Kinase alpha
IKK- $\beta$	–	Inhibitor of nuclear factor Kappa-B Kinase beta
IL	–	Interleukin
IL-1	–	Interleukin-1
Imd	–	Immune deficiency
IMM	–	Inner Mitochondrial Membrane
I.P.	–	Immunoprecipitation
Ird5	–	Immune response deficient 5
I- $\kappa$ B	–	Inhibitor of kappa-B
I- $\kappa$ B- $\alpha$	–	Inhibitor of nuclear factor kappa-B alpha
JNK	–	c-Jun N-terminal Kinase

k	–	Kilo
$K_2HPO_4$	–	Potassium dihydrogen phosphate
K48	–	Lysine 48 linkage between ubiquitin molecules
K63	–	Lysine 63 linkage between ubiquitin molecules
KCl	–	Potassium chloride
Key	–	Kenny
l	–	Liter
LB	–	Luria Bertani bacterial growth medium
LPS	–	Lipopolysaccharide
m	–	Meter
$\mu$	–	Micro
m	–	Milli
m	–	Mol
M	–	Molar
MAP	–	Mitogen Associated Protein
MAPK	–	Mitogen Associated Protein Kinase
MAPKK	–	Mitogen Associated Protein Kinase Kinase
MAPKKK	–	Mitogen Associated Protein Kinase Kinase Kinase
MG132	–	(Z-Leu-Leu-Leu-CHO) peptide aldehyde
$MgCl_2$	–	Magnesium chloride
min	–	Minute
ML-IAP	–	Melanoma-Inhibitor of Apoptosis
MMP-1	–	Matrix Metalloproteinase-1
MOMP	–	Mitochondrial Outer Membrane Permeabilization
mRNA	–	Messenger RNA
MW	–	Molecular weight
n	–	Nano
NaCl	–	Sodium chloride
NaOH	–	Sodium hydroxide
NEMO	–	NF- $\kappa$ B essential modifier
NF- $\kappa$ B	–	Nuclear Factor of kappa light polypeptide gene enhancer in B-cells

OMM	–	Outer Mitochondrial Membrane
ORF	–	Open Reading Frame
OTE	–	Off-target effect
p10	–	Small caspase subunit of around 10 kD
p20	–	Large caspase subunit of around 20 kD
p35	–	Baculovirus antiapoptotic protein
PAMP	–	Pathogen Associated Molecular Pattern
PARP	–	Poly [ADP-ribose] polymerase
PBS	–	Phosphate Buffered Saline
PBT	–	Phosphate Buffered Saline with Triton X-100
PCR	–	Polymerase Chain Reaction
P-dJNK	–	Phosphorylated c-Jun N-terminal Kinase
PGN	–	Peptidoglycan
PGRP	–	Peptidoglycan Recognition Protein
PGRP-LC	–	Peptidoglycan Recognition Protein - Long Chain
pH	–	Measure of the activity of the solvated hydrogen ion
Pi	–	Inorganic phosphate
PMSF	–	Phenylmethylsulfonyl fluoride
PRR	–	Pattern Recognition Receptor
Puc	–	Puckered
p-value	–	Probability value
qRT-PCR	–	Quantitative Real-time Polymerase Chain Reaction
Rel	–	Relish
RHD	–	Rel Homology Domain
RHG	–	Reaper, Hid, Grim
RIPK1	–	Receptor-Interacting serine/threonine-Protein Kinase 1
RNA	–	Ribonucleic acid
RNAi	–	RNA Interference
RNase	–	Ribonuclease
rNTP	–	Ribonucleotide triphosphate
rpm	–	Revolutions per minute
Rpr	–	Reaper

RT	–	Reverse transcriptase
RT-PCR	–	Reverse Transcription Polymerase Chain Reaction
RuCl <sub>2</sub>	–	Rubidium chloride
s	–	Second
S2	–	Schneiders 2 cells
SDS	–	Sodiumdodecyl sulphate
SDS-PAGE	–	Sodium dodecyl sulphate-polyacrylamide gel electrophoresis
siRNA	–	Short interfering RNA
Strica	–	Serine-threonine rich caspase
TAB1	–	TAK1-Associated Binding Protein1
TAB2	–	Transforming growth factor beta-activated kinase 1-binding protein 2
TAE	–	Tris base, acetic acid, EDTA
TAK1	–	Tumor necrosis factor-β Activated Kinase
<i>Taq</i>	–	<i>Taq</i> polymerase
tBid	–	Truncated Bid
TE	–	Tris base, EDTA
TEMED	–	Tetramethylethylenediamine
TLR	–	Toll-like Receptors
TMRE	–	Tetramethylrhodamine ethyl ester
TNF	–	Tumor Necrosis Factor
TNFR	–	Tumor Necrosis Factor Receptor
TNF-R1	–	Tumor Necrosis Factor Receptor 1
TRADD	–	Tumor Necrosis Factor Receptor 1-associated Death
TRAF	–	Tumor Necrosis Factor Receptor-associated Factor
ts	–	Temperature sensitive
U	–	Units
UAS	–	Upstream Activating Sequence
UV	–	Ultraviolet
V	–	Volts
v	–	Volume

v/v	–	Volume per volume
w	–	Weight
w/v	–	Weight per volume
WB	–	Western blot
x g	–	X standard acceleration due to gravity
XIAP	–	X-linked Inhibitor of Apoptosis Protein
z-VAD-FMK	–	Carbobenzoxy-valyl-alanyl-aspartyl-[O-methyl]- fluoromethylketone
$\Delta\Psi$	–	Mitochondrial membrane potential

NOMENCLATURE:

CLASS	CHARACTER	EXAMPLE
Gene	italics	<i>imd</i>
Allele	italics and superscript	<i>imd</i> <sup>shadok</sup>
Protein	first letter capitalized	Imd
Pathway	all letters capitalized	IMD
Chromosome	(,)	gene symbols within a chromosome are separated by a comma
	(/)	homologous chromosomes are separated by a forward slash
	(;)	heterologous chromosomes are separated by a semicolon (in flies: 1;Y;2;3;4)
	(+)	wild type chromosomes are indicated by a plus

## **Chapter 1. Introduction**

## 1.1. Innate Immunity

The main role of the immune system is to defend the body from invasion by pathogens<sup>1,2</sup>. The system can be divided into two main branches: the innate immune system and the adaptive immune system<sup>3</sup>. The adaptive immune system has evolved more recently in early vertebrates and allows for a stronger immune response as well as immunological memory<sup>3,4</sup>. The innate immune system is the first line of defense in all multicellular organisms and it is activated immediately after encounter of a pathogen<sup>5-7</sup>. Innate immunity is mediated by non-rearranging germline encoded gene products that activate potent antimicrobial defenses<sup>2,8</sup>. The innate immunity includes physical barriers such as the skin, humoral responses, and immune cells that attack foreign cells<sup>2</sup>. The relative simplicity of the innate immune system compared to the adaptive immune system has made it initially an understudied aspect of immunity. However, failures in innate immune responses have been implicated in a range of autoimmune, neurological, and cancerous diseases, underlining the importance of this aspect of immunity<sup>3</sup>.

The activation of the innate immune system is based on three distinct steps. The first step is the recognition of a pathogen (Pathogen-Associated Molecular Pattern; PAMP) by a receptor (Pattern Recognition Receptor; PRR)<sup>2</sup>. This is followed by the induction of a series of signaling events that finally elicit appropriate immune responses. The pathways that drive immunity show high degree of conservation among multicellular species<sup>9-11</sup>. This was first demonstrated with the discovery of the *Drosophila* receptor Toll<sup>12</sup>. Toll was first discovered for its role in axis formation in the early embryo, but further research demonstrated Toll's substantial role in fly immunity. Importantly, these discoveries prompted the search for, and subsequent discovery of, human Toll-like receptors (TLRs)<sup>12-18</sup>. This fundamental receptor family plays key roles in the mammalian innate immune response<sup>19</sup>.

The *Drosophila* Immune Deficiency (IMD) pathway is another example of the evolutionary conservation of immune responses across distantly related species<sup>10,20,21</sup>. Studies of the IMD pathway have revealed significant parallels to the human Tumor Necrosis Factor (TNF) pathway (Figure 1.1.). The high degree

---

of conservation and the sophisticated array of genetic and molecular tools make *Drosophila* an excellent model to study the function and regulation of signaling pathways<sup>10,13,17,22-24</sup>.

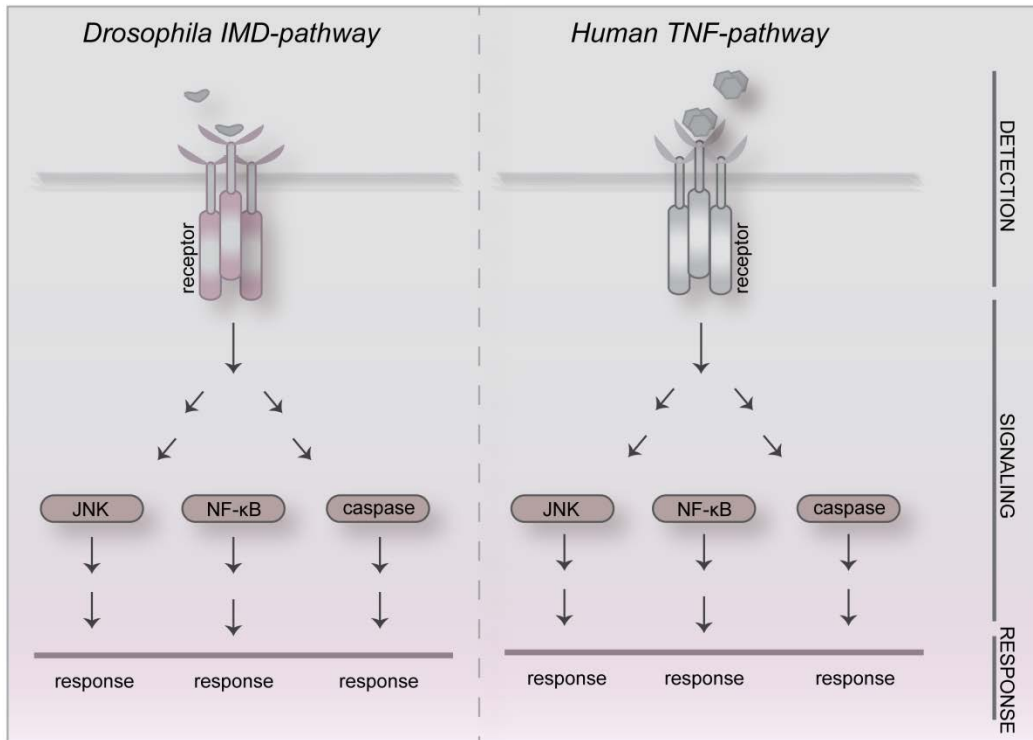


**Figure 1.1. TNF and IMD signaling:** Illustration of the human TNF and *Drosophila* IMD signaling pathways. The pathways driving immunity are often highly conserved among multicellular species. For example, the IMD signaling pathway has overt similarities to the TNF pathway, as both cascades signal through conserved c-Jun N-terminal Kinase (JNK), Nuclear Factor of kappa light polypeptide gene enhancer in B-cells (NF-κB), and caspase modules to elicit appropriate physiological responses.

## 1.2. *Drosophila* innate immunity

Similar to all multicellular organisms, *Drosophila* is surrounded by an immeasurable amount of micro-organisms, and therefore relies on a multilayered defense system to fight potential attacks by invading pathogens. If pathogens pass the first physical barrier and enter the body of the fly, a combination of humoral and cellular responses is activated<sup>10,25,26</sup>. The humoral and cellular responses involve three distinct mechanisms: the mobilization of blood cells to either phagocytose or encapsulate invading microbes, the activation of proteolytic signaling cascades resulting in melanization and coagulation reactions, and a humoral mechanism leading to synthesis of antimicrobial peptides (AMP)<sup>10,27-29</sup>.

In *Drosophila*, the vast majority of AMP are produced in the fat body, which is considered the functional analog of the mammalian liver<sup>10,24,30</sup>. The fat body is a multifunctional organ that plays a major role in the life of the fly by regulating metabolic functions like storage, utilization of energy, and infection-triggered synthesis of AMP. AMP are secreted from the fat body into the hemolymph (blood) within hours after an infection and they fight pathogens by disrupting their membranes, interfering with their metabolism, or targeting cytoplasmic components<sup>31,32</sup>.

There are seven known AMP in *Drosophila* and their production is regulated by two different signaling pathways. The Toll signaling pathway is activated by gram-positive bacteria or by fungi. Toll activation leads to the expression of the AMP *drosomycin (drs)*, *metchnikowin (mtk)*, and *defensin (def)*<sup>33-35</sup>. The IMD signaling pathway responds to the detection of diaminopimelic acid peptidoglycan (DAP-PGN) produced primarily by gram-negative bacteria and results in the expression of the AMP *dipterocin (dipt)*, *attacin (att)*, *cecropin (cec)*, and *drosocin (dro)*<sup>36-40</sup>.

### 1.3. TNF signaling pathway

The human TNF pathway is triggered by the recognition of Tumor Necrosis Factor (TNF)<sup>41,42</sup>. TNF is an essential cytokine that regulates numerous physiological events, including inflammation, differentiation, and apoptosis and it has been implicated in the pathogenesis of a wide spectrum of human diseases, including sepsis, diabetes, cancer, osteoporosis, multiple sclerosis, rheumatoid arthritis, and inflammatory bowel diseases<sup>43-46</sup>. TNF pathway signaling can initiate the activation of three signaling arms, the Nuclear Factor of kappa light polypeptide gene enhancer in B-cells (NF- $\kappa$ B), JNK, or Caspase-8 arm<sup>47-51</sup>. The nature of the response induced by NF- $\kappa$ B, c-Jun N-terminal Kinase (JNK), or Caspase-8 can be either pro- or anti-apoptotic, and the fine balance struck between the individual signaling modules is very important to avoid deregulation<sup>42,52,53</sup>.

Initially, the interaction of trimeric TNF with the TNF-receptor (TNFR1) triggers the formation of a multiprotein signaling complex (complex 1) at the cell membrane that consists of a series of signal transducers, like TNF Receptor-associated Factor 2 or 5 (TRAF2/5), TNFR-associated via Death Domain (TRADD), cellular Inhibitor of Apoptosis 1 and 2 (c-IAP1 and c-IAP2), and Receptor-Interacting serine/threonine-Protein Kinase 1 (RIPK1) (Figure 1.2.)<sup>47,48,54-59</sup>. Complex 1 serves as a platform for c-IAP mediated ubiquitination of several complex-1 components including RIPK1, c-IAP themselves, and possibly TRAF2 and TRADD<sup>56,57,60-63</sup>. It is suggested that the ubiquitin chains enable the recruitment of the Inhibitor of nuclear factor Kappa-B Kinase (IKK) complex (composed of NEMO/IKK $\alpha$ /IKK $\beta$ ) and the Transforming growth factor-beta-activated Kinase 1 (TAK1) complex<sup>64-66</sup>. The TAK1 complex consists of TAK1, and TAK1-binding proteins 2 and 3 (TAB2 and 3)<sup>64,67</sup>, and facilitates phosphorylation and activation of the IKK complex that promotes NF- $\kappa$ B activation<sup>68</sup>.

Activation of NF- $\kappa$ B mediates the induction of genes involved in a broad range of biological processes including innate and adaptive immunity, inflammation, and stress responses<sup>69</sup>. In the absence of TNF stimulation, the Inhibitor of

nuclear factor kappa-B (I- $\kappa$ B) inhibits NF- $\kappa$ B by masking its nuclear localization signals, and therefore retains NF- $\kappa$ B in the cytoplasm. Upon IKK-mediated phosphorylation, I $\kappa$ B is ubiquitinated and destroyed by the proteasome<sup>70-72</sup>. The liberated NF- $\kappa$ B dimers translocate to the nucleus and initiate gene transcription.

TAK1 also initiates a kinase cascade through the MAP Kinase Kinases (MAPKK) 4 and 7 that promotes phosphorylation and activation of the MAP-Kinase (MAPK) c-Jun NH(2)-terminal Kinase (JNK)<sup>73-78</sup>. JNK signaling leads to the induction of Activator Protein 1 (AP-1)-dependant target genes that are involved in inflammation, apoptosis, and stress responses<sup>74,79,80</sup>.

In addition to NF- $\kappa$ B and JNK signaling, TNF can also activate a caspase-mediated pro-apoptotic response by initiating the formation of a second complex termed complex II<sup>49,73</sup>. It is suggested that the cytoplasmic complex II derives from the internalized complex I<sup>81-83</sup>. Formation of complex II recruits the adapter molecule FADD, which in turn recruits Caspase-8<sup>47,73,82</sup>. At the complex, proximity-induced dimerization and autoproteolytic cleavage generates an active stable Caspase-8<sup>73,84,85</sup>, that is released from the complex to cleave and activate downstream substrates<sup>85-87</sup>.

Under non-apoptotic conditions, NF- $\kappa$ B signaling induces anti-apoptotic gene products to secure cell survival after TNF stimulation. For example, cellular FLICE-like Inhibitory Protein long (cFLIP<sub>L</sub>) is important to secure cell survival<sup>88-90</sup>. cFLIP<sub>L</sub> and Caspase-8 have a very similar domain structure, but cFLIP<sub>L</sub> lacks a catalytic site. cFLIP<sub>L</sub> forms heterodimers with Caspase-8 at complex II to prevent Caspase-8 autoproteolytic cleavage, stabilization, and subsequent induction of apoptosis<sup>73,91</sup>. Surprisingly, the cFLIP<sub>L</sub>/Caspase-8 heterodimer has catalytic activity<sup>91-94</sup>. However the activity is not sufficient to cleave apoptotic substrates like effector caspase-3 or BH3-interacting domain death agonist (Bid), and therefore fails to induce apoptosis. It is believed that a full-length Caspase-8 performs the non-apoptotic roles of Caspase-8<sup>95</sup>.

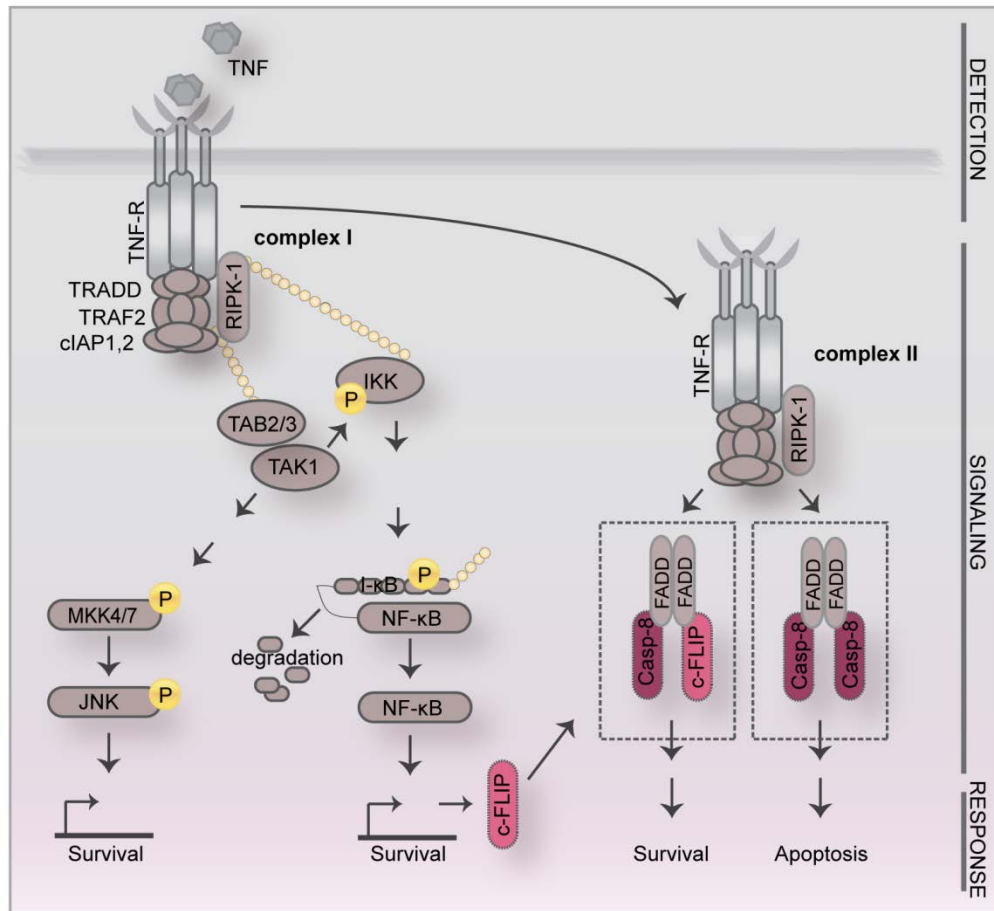


**Figure 1.2. TNF signaling pathway:** Illustration of the human TNF pathway. TNF activates the TNF signaling pathway that triggers the formation of a signaling complex (complex I). Complex I is important for the activation of the NF-κB and JNK arm of TNF signaling and consequently the induction of survival responses. For example, NF-κB signaling up-regulates the transcription of cFLIP<sub>L</sub> that blocks Caspase-8, and therefore inhibits the induction of apoptosis. TNF signaling can also induce apoptosis by generating a second internalized complex (complex II). Under non-apoptotic conditions, cFLIP<sub>L</sub> and Caspase-8 form heterodimers that fail to induce apoptosis. In the absence of pro-survival factors like cFLIP<sub>L</sub>, the cytoplasmic complex II incorporates Caspase-8 homodimers that initiates the full activation of Caspase-8 and induction of apoptosis.

#### 1.4. IMD signaling pathway

The IMD pathway is an immune response pathway in flies with significant parallels to the human TNF pathways<sup>20,96-98</sup>. Both pathways signal through conserved NF- $\kappa$ B, JNK, and caspase modules (Figure 1.1.-1.3.). Detection of bacterial DAP-PGN by the Peptidoglycan Recognition Proteins LC and LE (PGRP-LC and PGRP-LE) activates the IMD pathway (Figure 1.3.)<sup>99-104</sup>. Activation of the pathway leads to the initiation of a signal transduction cascade, mediated by the Imd, Fas associated Death Domain (dFADD), TAK1 Binding Protein 2 (dTAB2), Bendless, Effete, and Inhibitor of Apoptosis 2 (dIAP2) proteins<sup>105-115</sup>.

*Early receptor-proximal signaling events:* The detailed mechanisms of early IMD signal transduction are not fully understood. At the start of this study, it was proposed that Imd is the most proximal protein recruited to PGRP-LC and PGRP-LE<sup>100,116,117</sup>. Here, Imd interacts with dFadd by homotypic death domain-mediated (DD) binding<sup>106,115</sup>. More recent data indicated that immune challenge triggers the caspase-mediated cleavage of Imd and that N-terminal cleavage promotes Imd activation by exposing a binding site for the E3 ubiquitin ligase dIAP2<sup>114</sup>. dIAP2-mediated K63-polyubiquitination of the Imd protein is essential for IMD/Rel activation and appears to require the E2s Effete and Bendless<sup>113,114</sup>. It is suggested that ubiquitination of Imd generates a scaffold to recruit the *Drosophila* TAK1 homolog, dTAK1 via the ubiquitin binding domain of its partner dTAB2, and to recruit the *Drosophila* IKK (IKK $\beta$ /*ird5* and IKK $\gamma$ /*kenny*) complex via the ubiquitin binding domain of IKK $\gamma$ <sup>107,108,118-120</sup>. Activation of dTAK1 mediates the induction of two divergent cascades, which culminate in IMD/Relish (Rel, p105 NF- $\kappa$ B homolog) and IMD/dJNK (JNK homolog) activation.

*IMD/Rel signaling:* dTAK1 activates the IKK complex, which is required for the initiation of the IMD/Rel arm<sup>118,119,121,122</sup>. Rel is a composite protein with an N-terminal NF- $\kappa$ B transcription factor domain and an auto-inhibitory C-terminal ankyrin repeat domain<sup>123-127</sup>. Activation of Rel requires two distinct posttranslational modifications: phosphorylation of the NF- $\kappa$ B domain of Rel and endoproteolytic separation of the NF- $\kappa$ B domain from the C-terminal ankyrin

repeat domain<sup>121,125-128</sup>. The liberated Phospho-NF- $\kappa$ B transcription factor domain translocates to the nucleus and induces the prolonged expression of a broad cohort of pro-immune genes such as AMP (Att and Dipt)<sup>125</sup>.

The IKK complex has two distinct roles in IMD/Rel activation. The catalytically active IKK drives the IMD/Rel transcriptional response through the phosphorylation of Rel, while the IKK complex also supports Rel cleavage in a non-catalytic manner. Phosphorylation of Rel is not a requirement for Rel cleavage, but it is required for the recruitment of the RNA polymerase II and expression of Rel-responsive transcripts<sup>128</sup>. Proteolytic cleavage of Rel at the putative caspase cleave site (LQHD) requires the protein Death related ced-3/Nedd2-like protein (Dredd), which is the *Drosophila* ortholog of Caspase-8<sup>125,126,129-131</sup>. However, *in vitro* cleavage assays failed to convincingly demonstrate the direct cleavage of Rel by Dredd<sup>125,126,128</sup>.

*IMD/dJNK signaling:* dTAK1 also activates a cascade of MAP Kinases (MAPK). Signal transduction through the MAP kinase pathway is evolutionarily conserved in all eukaryotic organisms<sup>132,133</sup>. It involves the activation of a triple kinase module including MAPK Kinase Kinase (MKKK), which phosphorylates and activates MAPK Kinase (MKK), which in turn activates MAPK by dual phosphorylation on Thr and Tyr residues<sup>134</sup>. The phosphorylation event triggers the conformational change of the MAPK structure that results in the exposure of the active site in the kinase domain. MAPK phosphorylates target proteins that mediate cellular responses as diverse as cell growth, cell survival, neural functions, and the immune response<sup>135</sup>.

In *Drosophila*, active dTAK1 (dMAPKKK) triggers the activation of the MAP Kinase 4 (dMKK4) and MAP Kinase Kinase 7 (dMKK7), which results in the transient phosphorylation of the MAPK, dJNK<sup>98,136-138</sup>. Phospho-dJNK activates a subset of immune-responsive AP1-dependent target genes (Puckered (Puc) and Matrix Metalloproteinase-1 (MMP-1))<sup>28,132,139,140</sup>.

The phosphatase activity of Puc generates a self-limiting negative feedback loop by dephosphorylating Phospho-dJNK<sup>137,141,142</sup>. The function of dJNK signaling in the IMD pathway remains controversial as the contribution of dJNK to AMP induction has generated conflicting results. Initial studies suggested that

dJNK signaling is required for the early induction of AMP while later reports demonstrated *in vivo* that the reduction in dJNK pathway activity increased AMP genes<sup>143-145</sup>.

As describe above, the processes that activate and regulate the IMD/dJNK arm are still poorly understood. To enhance our understanding of IMD/dJNK signaling, our laboratory performed a quantitative high-throughput RNAi screen for dJNK modifiers<sup>146</sup>. In addition to the identification of numerous novel hits, the screen indicated a role of *Drosophila* caspase Dredd in the phosphorylation of dJNK<sup>146</sup>. However, the exact role and contribution of the Dredd to the IMD/dJNK response were still elusive.

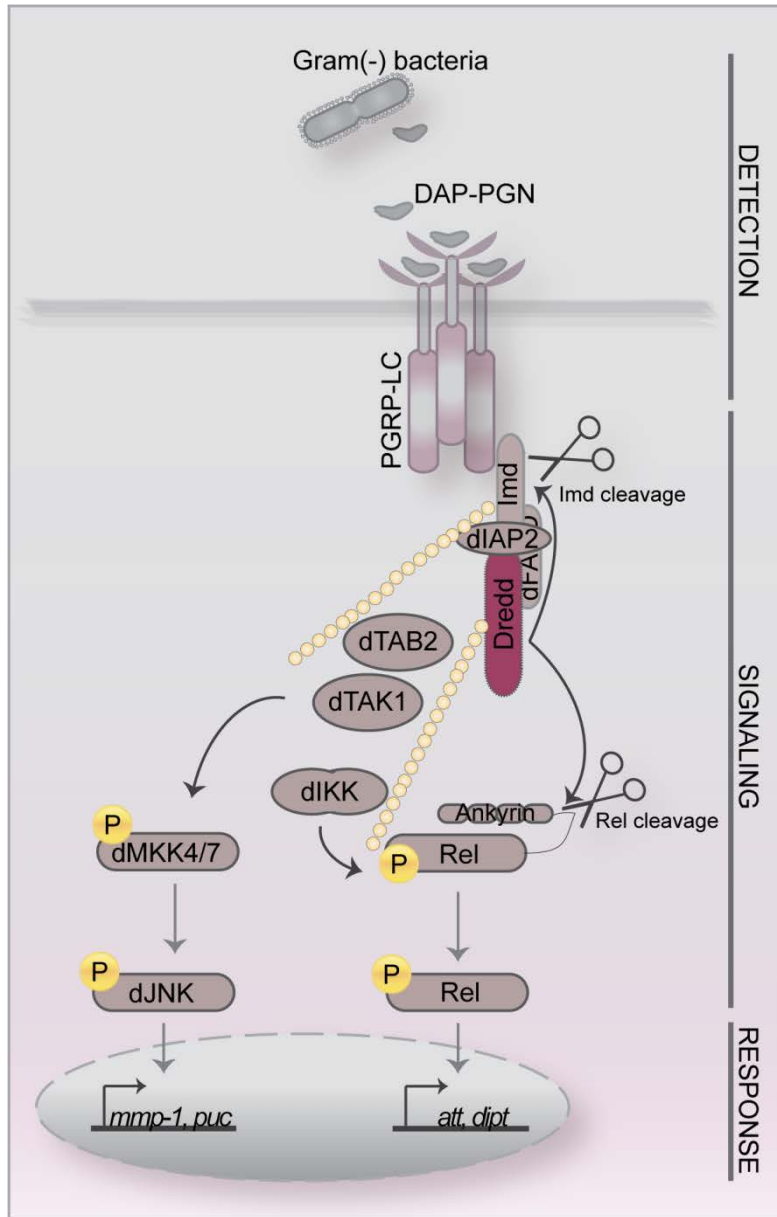


**Figure 1.3. IMD signaling pathway:** Illustration of the proposed model of the *Drosophila* IMD pathway. PGN activates the *Drosophila* IMD signaling pathway that triggers recruitment of Imd, dFADD, and Dredd. Dredd cleaves Imd, which enables binding of dIAP2 and subsequent ubiquitination of Imd. The ubiquitin chains function as a scaffold to recruit TAB2, dTAK1, and IKK. Activation of dTAK1 and IKK enables the downstream activation of the IMD/Rel and IMD/dJNK arm, which results in the induction of appropriate target gene expression.

## 1.5. Caspases

Caspases are intracellular cysteinyl aspartate proteases with an important role in programmed cell death, proliferation, and immunity<sup>147-149</sup>. The importance for caspases in the process of apoptosis was initially established by the discovery of the *ced-3* gene, which encodes for a caspase important for programmed cell death in *C. elegans*<sup>148,150</sup>. The discovery of the *ced-3* caspase led to the identification of numerous apoptotic caspases in other species. Based on the initial discovery in apoptosis, caspases became synonymous with cell death for a long time<sup>151</sup>. Interestingly, the mammalian homolog of *ced-3* encodes Caspase-1, which mediates inflammation rather than cell death<sup>152,153</sup>. More recently, it became clear that apoptotic caspases have additional and very important non-apoptotic functions in survival, proliferation, differentiation, and immunity (Figure 1.4.)<sup>154-157</sup>.

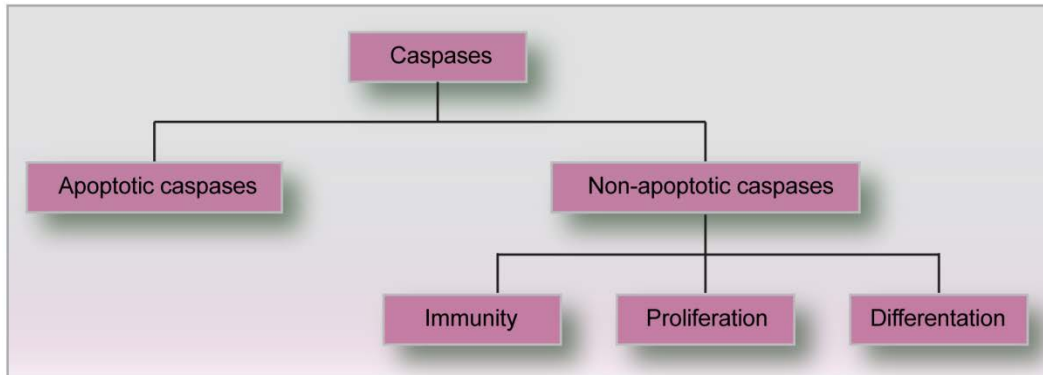


**Figure 1.4. Non-apoptotic functions of caspases:** Illustration of caspase functions. Caspases were initially described in apoptosis. However, recent research implicated caspases in other important non-apoptotic function ranging from immunity to proliferation to differentiation.

### 1.5.1. Caspase structure and classification

Caspases can be classified into two types: initiator and effector caspases. Initiator caspases are activated first and trigger the activation of effector caspases by proteolytic cleavage of the inactive pro-form of effector caspases. Activated effector caspases cleave a broad range of structural and regulatory substrates that finally triggers cell death<sup>158-163</sup>.

To prevent erroneous activation of the caspase pathway, caspases are synthesized as inactive zymogens. Caspases possess an N-terminal prodomain and a C-terminal caspase-domain that is composed of a small and a large subunit. Initiator caspases have longer prodomains compared to effector caspases, which contain protein interaction motifs that integrate the initiator caspases into macromolecular complexes (Figure 1.5.)<sup>148</sup>. More specifically, the prodomain of initiator caspases contains specific protein interaction regions (e.g. caspase activation and recruitment domain (CARD) or death effector domain (DED)) that are important for their interaction with other adaptor proteins<sup>164-168</sup>. The prodomain and the small and large subunits are connected by linker sequences that are often proteolytically cleaved at an aspartic acid (Asp) during the caspase activation process<sup>169</sup>. C-terminal cleavage at the aspartic acid peptide bonds within the caspases and substrate proteins is a feature that is common to all caspases<sup>169,170</sup>. The large subunit contains the catalytic site cysteine while the small subunit provides conserved residues to form the substrate binding pocket<sup>169</sup>.

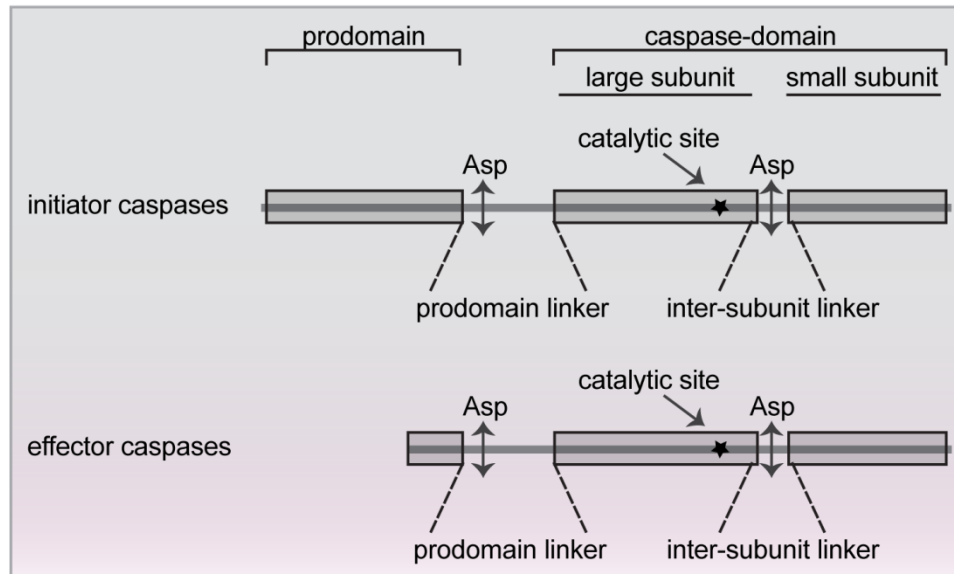


**Figure 1.5. Caspase structure:** Illustration of the general caspase structure of initiator and effector caspases. Caspases are synthesized as inactive pro-caspases. Caspases possess a prodomain and a caspase domain consisting of a small and a large subunit. Initiator caspases have longer prodomains compared to effector caspases. The prodomain contains specific protein interaction regions (e.g. a CARD domain or a death effector domain DED). The star represents the catalytic site cysteine. During activation, caspases are generally cleaved at an aspartate (Asp) within the inter-subunit linker and the prodomain linker.

By now twelve caspases are identified in humans and most of the caspases to date are described in the context of programmed cell death (Figure 1.6.)<sup>171</sup>. A lot of effort went towards the understanding of the regulatory functions of caspases during apoptosis.

Seven caspases have been described in *Drosophila* (Figure 1.6.), with Nedd2-like caspase (Dronc)<sup>172</sup> and Dredd<sup>129</sup> defined as initiator caspases, and *Drosophila* interleukin-1 converting enzyme (Drice)<sup>173</sup>, Death caspase-1 (Dcp-1)<sup>174</sup>, Death executioner caspase related to Apopain/Yama (Decay)<sup>175</sup>, and Death Associated Molecule related to Mch2 (Damm)<sup>176</sup> as effector caspases. The seventh caspase, Serine-threonine rich caspase (Strica)<sup>177,178</sup>, has a long prodomain typical for initiator caspases, but lacks any caspase recruitment domain or death effector domain. Since the cellular function of Strica is unclear, further research is required to clarify if Strica functions as a potential initiator caspase.

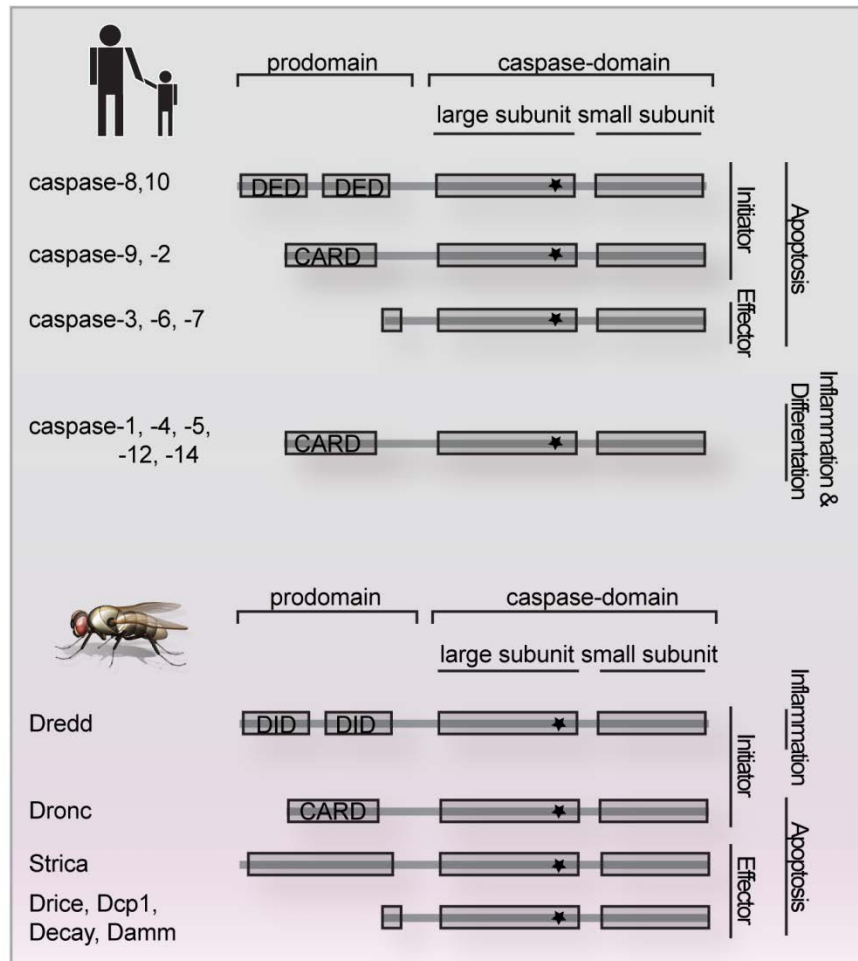


**Figure 1.6. Human and *Drosophila* Caspases:** Illustration of the twelve human (top) and seven *Drosophila* (bottom) caspases. The apoptotic caspases are subdivided into two groups: the initiation and effector caspases. Initiator caspases have longer prodomains compared to effector caspases. The prodomain, caspase-domain, the interaction motifs (CARD and DED), and the catalytic site are indicated.

### 1.5.2. Caspase activation

The full activation and stabilization of initiator caspases usually requires dimerization and auto-processing, while effector caspases require proteolytic cleavage by an initiator caspase (Figure 1.7.)<sup>179,180</sup>. In contrast to initiator caspases, effector caspases form inactive homodimeric complexes in the absence of apoptotic signals. The linker between the small and large subunit of effector caspases sterically blocks the active site, and therefore activation requires the proteolytic cleavage of the inter-subunit linker by an initiator caspase. Proteolytic cleavage triggers rearrangement of the subunits in order to form the catalytic site<sup>166,169,181-183</sup>.

The activation mechanism of initiator caspases is still not fully understood. Initiator caspases are inactive monomeric zymogens and they require signal mediated dimerization in order to become active<sup>184</sup>. In general, this is initiated by the recruitment of the caspase to a signaling complex<sup>185-190</sup>. Caspases bind the complex through prodomain-mediated homotypic interactions, and caspase recruitment to the complex triggers proximity-induced dimerization and activation of the caspase molecule<sup>85,181,191,192</sup>. Dimerization triggers autoproteolytic cleavage in the inter-subunit linker that results in the separation of the small and large subunit. The additional cleavage of the linker between the prodomain and the large subunit releases the active caspase from the complex which consist of a tetrameric structure of the two small subunits surrounded by the two large subunits<sup>84,85,91,181,192-196</sup>. The two heterodimers interact with each other predominantly through the interaction between the small subunits. The association of the subunits generates two active sites in the mature caspase molecule and it is proposed that each site function autonomously<sup>197</sup>.

The requirement of dimerization or/and proteolytic cleavage for the activation of caspases is still under debate. For example, dimerization, but not cleavage is required for Caspase-8 function in T-cell proliferation whereas cleavage of Caspase-8 is required for induction of apoptosis<sup>95,198</sup>. It is proposed that proteolytic cleavage stabilizes Caspase-8 to achieve adequate stability to function in the cytosol after its release from the complex<sup>85,194-196,198,199</sup>. So far, it is

not understood if the differences in the activation process trigger the diverse function of Caspase-8 in apoptotic and non-apoptotic processes. The specific requirements for Caspase-9 activation are still unclear since some studies suggested that cleavage and dimerization are not required for the full activation of Caspase-9<sup>200-202</sup>. Similarly, the Caspase-9 ortholog Dronc appears to only require dimerization, and while cleavage occurs during apoptosis, it is not essential for Dronc activation<sup>203,204</sup>. The molecular activation mechanism of the non-apoptotic initiator caspase Dredd, which is considered the Caspase-8 ortholog, is unknown.

While a lot of effort has been made to understand caspase activation in the process of apoptosis, further research is necessary to determine more details of caspase activation and how differences in their activation process might mediate the opposing physiological function in apoptosis, survival, and differentiation.

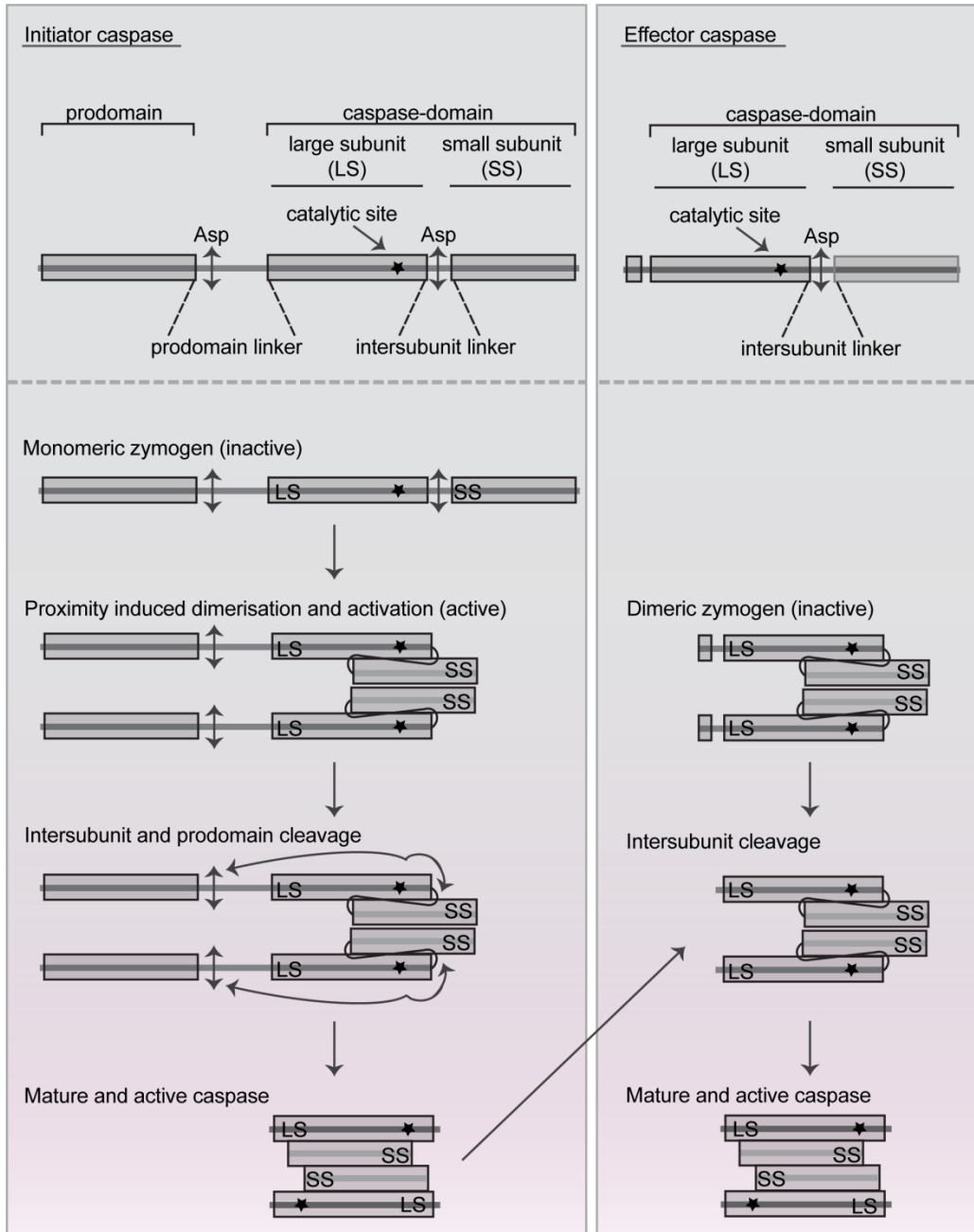


**Figure 1.7. Caspase activation:** Illustration of the general caspase activation process. Caspases are synthesized as inactive pro-caspases. Initiator caspases are recruited to an activation platform where they become active by proximity induced dimerization. The subsequent cleavage in the subunit linker stabilizes the molecule and triggers the release of the mature, active caspase. Effector caspases require the proteolytic cleavage of their inter-subunit linker by an initiator caspase to become active.

### 1.5.3. Caspase regulation

In apoptosis, activation of caspases triggers the proteolytic cleavage of vital cellular proteins and ultimately causes disassembly of the cell<sup>205-207</sup>. Several mechanisms of caspase inhibition have been described to avoid unwanted caspase activation that could be devastating for the organism (Figure 1.8.).

*Viral inhibition:* Viral inhibition extends host cell viability and blocks the activation of the host immune response, therefore increasing the time for viral replication in the host<sup>208</sup>. Two well-studied viral inhibitors are the cowpox virus inhibitor cytokine response modifier A (CrmA)<sup>209-213</sup> and the baculovirus p35<sup>211,214-220</sup>. Both inhibitors are so-called suicide inhibitors that irreversibly block the caspase. The viral inhibitor gets processed by caspases like a substrate, but generates a stable irreversible inhibitor-enzyme complex through a covalent thioester bond<sup>216,221-224</sup>.

*Chemical inhibition:* Chemical caspase inhibitors have been developed as a research and clinical tool to prevent apoptosis. For example, the cell-permeable pan caspase inhibitor zVAD-FMK competes with the substrate for binding and irreversibly interacts with the catalytic site to prevent induction of apoptosis<sup>225,226</sup>.

*Cellular inhibition (IAPs):* Inhibitor of apoptosis proteins (IAP) are a conserved family of proteins across species as diverse as viruses, yeast, flies, and humans<sup>227-229</sup>. IAP proteins were originally identified in baculovirus infected insect cells<sup>230-232</sup>. Two motifs are representative for the members of the IAP family and are highly conserved amongst IAP proteins. The ~70 amino acid long N-terminal baculovirus IAP repeat domain(s) (BIR) are Zink Finger like structures that mediate protein-protein interactions<sup>230,232-234</sup>. The C-terminal Really Interesting Gene domain (RING) provides E3 ubiquitin ligase activity<sup>233,235,236</sup>. Some IAPs also contain structures like the caspase activation recruitment domain or the conserved Ubiquitin-associated domain (UBA) that binds monomeric ubiquitin and ubiquitin chains<sup>237,238</sup>.

The mammalian cellular Inhibitor of Apoptosis Protein 1 (c-IAP1), cellular Inhibitor of Apoptosis Protein 2 (c-IAP2), X-linked Inhibitor of Apoptosis Protein (XIAP), and Melanoma-Inhibitor of Apoptosis (ML-IAP) and the *Drosophila* dIAP1

and dIAP2 possess RING domains with E3 ligase activities. In general, E3 ligase activity enables auto-ubiquitination and cross-ubiquitination of the substrate<sup>236,239-241</sup>. Ubiquitin is a small protein that has a central role in a wide array of degradative and non-degradative processes<sup>242,243</sup>. Ubiquitin chains are synthesized of ubiquitin monomers joined by covalent bonds between the C-terminus of one ubiquitin and the internal K48 (48rd lysine of ubiquitin) or K63 (63rd lysine of ubiquitin) lysine residues in the next ubiquitin. The attachment of ubiquitin involves the sequential action of a ubiquitin-activating enzyme (E1), a ubiquitin-conjugating enzyme (E2), and a ubiquitin ligase (E3)<sup>244,245</sup>. The type of lysine linkages of ubiquitin chains determines the cellular outcomes<sup>246-249</sup>. While K48-linked chains target the substrate for proteasomal destruction, non-degradative K63-ubiquitin chains are involved in regulatory processes such as DNA repair, signal transduction, and receptor endocytosis<sup>248,250-253</sup>.

IAPs are considered the guardians of the apoptotic machinery by binding caspases and inhibiting their active site<sup>254</sup>. This sterically blocks the caspase, sequesters the caspase away from its substrate, or promotes proteasomal degradation of the caspase<sup>255,256</sup>. Caspases are only bound by IAPs after the caspase is processed, and consequently IAPs are considered the very last line of defense to ensure the survival of a cell. The only known exception to date is the *Drosophila* caspase Dronc which is bound by dIAP1 in the monomeric zymogen state<sup>257</sup>.

Currently eight human IAPs and four *Drosophila* IAPs have been described<sup>258,259</sup>. In humans, XIAP inhibits Caspase-9 and -7<sup>260-262</sup>. Caspase-8 is not inhibited by IAPs, but XIAP blocks the Caspase-8 substrate Caspase-3<sup>231,261</sup>. In *Drosophila*, dIAP1 inhibits the caspases Dronc, Drice, and Dcp-1<sup>263-265</sup>.

By now, the name inhibitor of apoptosis is a bit of a misnomer since recent reports suggested that only some IAPs (like XIAP in mammals and dIAP1 in flies) block caspase function under physiological conditions. By now, IAPs have also been linked to processes like cell-cycle regulation, cell-signaling, protein degradation, and immunity<sup>266</sup>. For example, cIAP1 and 2 ubiquitinate many components in the TNFR-complex I that mediates the recruitment of further downstream molecules important for NF- $\kappa$ B and MAPK activation<sup>56,60-62</sup>. In

*Drosophila*, dIAP2 is important to mediate appropriate immune responses. Initially, dIAP2 was described in the context of apoptosis<sup>227,267,268</sup>. However, in contrast to *dIAP1*, *dIAP2* mutants are viable and healthy, and don't have developmental or stress-induced apoptosis defects<sup>111,112,269-271</sup>. Importantly, follow up studies demonstrated that *diap2* mutant flies are incapable to fight of gram-negative bacterial infection and die quickly after an infection<sup>109-112,269,272,273</sup>. Combined, the data established dIAP2 as an essential component in immunity.

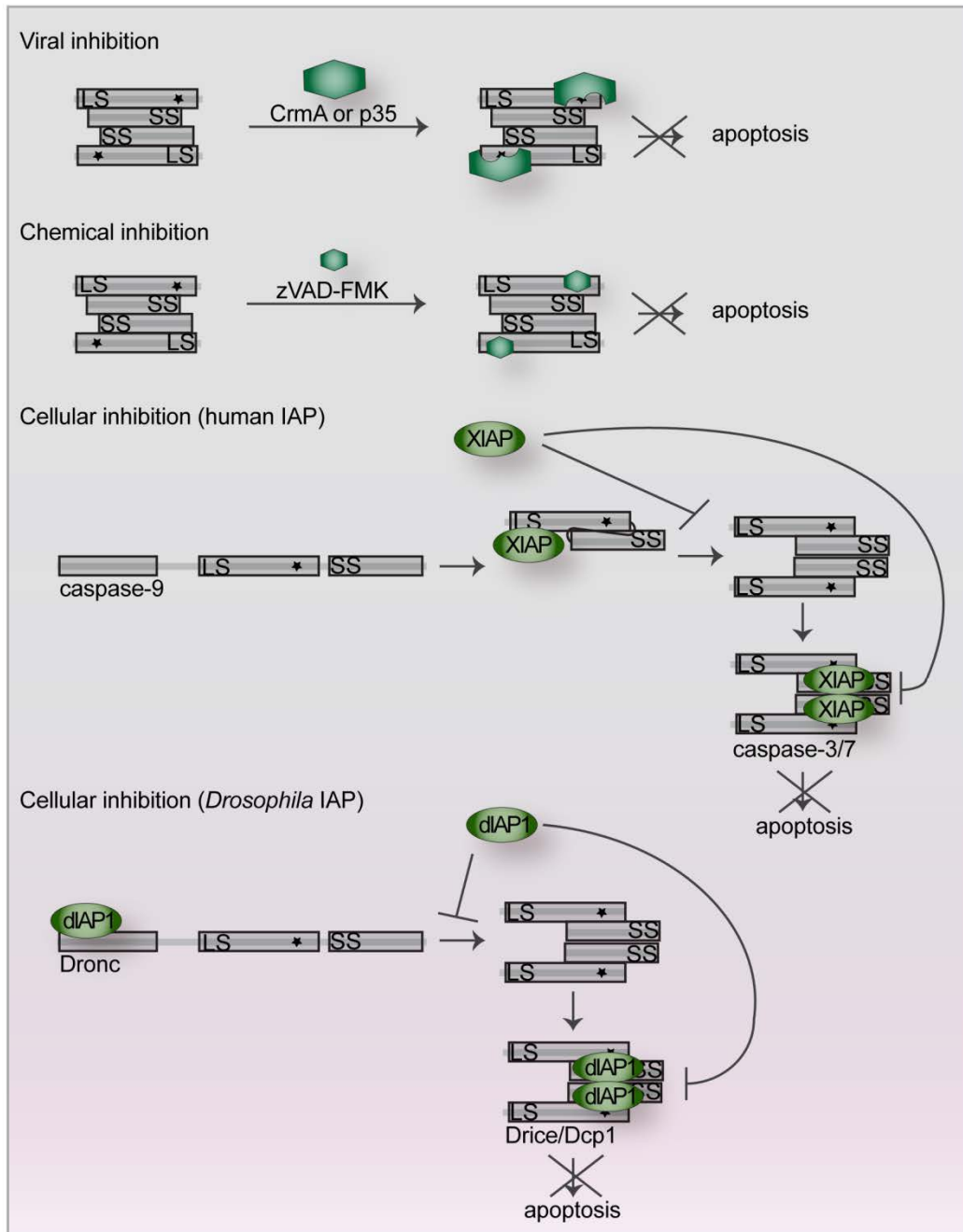


**Figure 1.8. Caspase inhibition:** Illustration of caspase inhibition. Viral inhibitors like CrmA and p35, as well as synthetic peptide inhibitors like z-VAD-FMK, bind as pseudosubstrates to the active catalytic sites (stars) of caspases, thereby inhibiting their catalytic activity. The human IAP (XIAP) binds the large subunit of Caspase-9, thereby preventing activation. XIAP also inhibits effector caspases by blocking their active catalytic sites (star). dIAP1 binds Dronc at the prodomain and targets Dronc for proteasomal degradation. dIAP1 also blocks effector

caspases by binding to the processed ends of the caspases (see text for more details).

#### 1.5.4. Caspases in apoptotic signaling

*Mammalian caspases:* Caspase-2,-8,-9, and -10 are initiator caspases while caspase-3, -6, and -7 are effector caspases during mammalian cell death. Apoptosis is initiated by one of the two signaling cascades, termed the intrinsic or the extrinsic pathways. Both pathways activate effector caspases<sup>169</sup>.

Caspase-8 is one of the crucial initiator caspases during the extrinsic death receptor-mediated apoptosis by the TNF family members<sup>274,275</sup>. Under conditions where pro-survival signals are blocked, receptor activation initiates the internalization of the receptor that recruits Caspase-8 to the receptor complex through the interaction with Fadd. Recruitment and binding initiates full activation of Caspase-8 by proximity induced dimerization and auto-processing, which ultimately initiates apoptosis through effector caspase activation (see 1.3. TNF signaling for more details)<sup>162,184,194,276</sup>.

The activation of the intrinsic pathway leads to the release of cytochrome c from the mitochondria and association with the Apoptotic Protease Activating Factor 1 (APAF1)<sup>277,278</sup>. This causes oligomerization of APAF1 and the recruitment of Caspase-9<sup>186,279</sup>. The formed multimeric complex, called apoptosome, initiates proximity induced dimerization and activation of Caspase-9, which ultimately initiates apoptosis through effector caspase activation<sup>186,280-282</sup>.

Caspase-10 and -2 functions are not completely understood, but it appears that Caspase-10 might overlap with Caspase-8 function, while Caspase-2 might be more similar in function to Caspase-9<sup>170</sup>.

*Drosophila caspases:* As in the mammalian system, *Drosophila* caspases drive apoptosis. In the fly, the initiator caspase Dronc and the effector caspases Drice and Dcp-1 facilitate the induction of cell death. Induction of cell death requires a reversal of dIAP1-mediated inhibition of *Drosophila* caspases. This is facilitated by IAP antagonists Reaper, Hid, and Grim (RHG proteins)<sup>227,283-286</sup>. The RHG proteins are transcriptionally activated in response to many different pro-

apoptotic signals, including developmental signals, radiation, and various forms of cellular stress or injury<sup>287-290</sup>.

RHG proteins bind via their IAP binding motif (IBM) directly to the BIR domains of dIAP1 and induces auto-ubiquitination and degradation of dIAP1<sup>291-294</sup>. The release of dIAP1-mediated Dronc inhibition promotes the assembly of the fly apoptosome consisting of Dronc and the adaptor molecule Apaf-1-related-killer (ARK)<sup>172,204</sup>. Dimerization within the apoptosome induces Dronc activation, and the active apoptosome in turn cleaves and activates Drice and Dcp-1 effector caspases that causes the induction of apoptosis<sup>204</sup>.

### 1.5.5. Non-apoptotic caspases

Human Caspase-1, 3, 5, 8, 10, and 12 have non-apoptotic caspase function, ranging from cell-cycle regulation, embryonic development, monocyte differentiation, T- and B-cell proliferation to NF- $\kappa$ B activation (Table 1.1.)<sup>295-317</sup>.

Similarly, the *Drosophila* caspases Dronc, Drice, and Dcp-1 have non-apoptotic roles like compensatory proliferation, spermatogenesis, and cell differentiation (Table 1.1.)<sup>318-325</sup>. Also, Dredd was originally identified as a Caspase-8 ortholog with minimal phenotypic information<sup>129</sup>. Subsequent genetic screens to dissect the components of the IMD innate immune signaling pathway implicated Dredd in the control of immune responses to gram-negative bacteria<sup>130,326</sup>. Dredd is the only caspase thus far with functions in innate immune signaling in the model system *Drosophila*.

Immunological requirements for caspases are often understated and therefore the exact molecular basis for caspase activity and activation in non-apoptotic pathways are still mostly elusive.

Orgnaism	Caspase	Phenotype
<i>Drosophila</i>	Dronc	compensatory proliferation, dendritic pruning, spermatogenesis, neuronal differentiation, border cell migration
	Dredd	immunity
	Drice	compensatory proliferation, spermatogenesis, neuronal differentiation
	Dcp-1	compensatory proliferation
Mammals	Caspase-1	innate immunity
	Caspase-2	innate immunity
	Caspase-3	adaptive immunity, lymphocyte proliferation, lens epithelia cells, sceletal muscel cells, stem-cell maturation
	Caspase-5	innate immunity
	Caspase-8	innate immunity, adaptive immunity, embryonic development, lymphocyte proliferation, macrophage differentiation
	Caspase-10	innate immunity
	Caspase-11	innate immunity, macrophage cell migration
	Caspase-12	innate immunity
Caspase-14	keratin differentiation	

**Table 1.1. Non-apoptotic functions of caspases:** Summary of non-apoptotic caspases functions in *Drosophila* and mammals. Non-apoptotic functions of caspases are diverse and include processes like immunity, proliferation, and differentiation.

### 1.5.6. Caspase-8

Caspase-8 has roles in apoptosis, immunity, differentiation, and proliferation (Table 1.1)<sup>327</sup>. Caspase-8 was first identified by its association with the adapter protein FADD, and it was suggested that Caspase-8 is the most upstream enzymatic molecule in the cell death signaling cascade<sup>328,329</sup>.

*Caspase-8 as an apoptotic molecule:* Work with Caspase-8 knock-out mice and caspase-8 deficient cell lines indicated that Caspase-8 is required for apoptosis<sup>276,330,331</sup>. Similar to all other known caspases, Caspase-8 is synthesized as an inactive zymogen and is activated by the recruitment to a multimeric complex. Specifically, Caspase-8 is recruited by the adaptor protein FADD to complex II (see 1.3. TNF signaling pathway), which triggers the subsequent proximity induced dimerization and activation of Caspase-8<sup>169,181,191,332</sup>. Caspase-8 propagates the apoptotic signal either by direct cleavage of effector caspases like Caspase-3, -6, and -7, or by the cleavage of the pro-apoptotic B-cell lymphoma 2 (Bcl-2) family member Bid into tBid (Figure 1.9.)<sup>148,333-335</sup>. tBid interacts with other Bcl-2 family members on the mitochondria surface which results in mitochondrial outer membrane permeabilization<sup>333,334,336</sup>, the release of cytochrome c<sup>277,278,337</sup>, and subsequent activation of the Caspase-9 apoptosome<sup>186,279</sup>. Similar to Caspase-8, Caspase-9 also cleaves effector caspases<sup>280,282</sup>. Effector caspases also boost Caspase-8 activity and apoptotic signaling in a negative feedback loop<sup>282,338,339</sup>.

*Caspase-8 as a non-apoptotic molecule:* Caspase-8 mutant mice die in utero as an effect of defective development and proliferation<sup>276</sup>. Tissue specific knock-out experiments also indicated non-apoptotic functions for Caspase-8 in embryonic development, B and T-cell signaling, lymphocyte proliferation, natural killer cell activation, and NF- $\kappa$ B signaling<sup>276,300,305,307,340-342</sup>. In contrast to the apoptotic program, the requirements for Caspase-8 activation and function in the non-apoptotic processes appear different. For example, it has been suggested that Caspase-8 prodomain alone is sufficient to mediate Caspase-8 function in differentiation<sup>343</sup>. Also, overexpression of Caspase-8 triggers ectopic NF- $\kappa$ B activation, while depletion of Caspase-8 prevents NF- $\kappa$ B signaling in human cell

---

culture<sup>302</sup>. Caspase-8 dependent NF- $\kappa$ B activation appears independent of the caspase catalytic activity, and a prodomain only variant is sufficient to mediate NF- $\kappa$ B signaling<sup>344,345</sup>, suggesting that a fully processed and active Caspase-8 is not required for this process. The mechanisms underlying the diverse activities of Caspase-8 are still poorly understood.

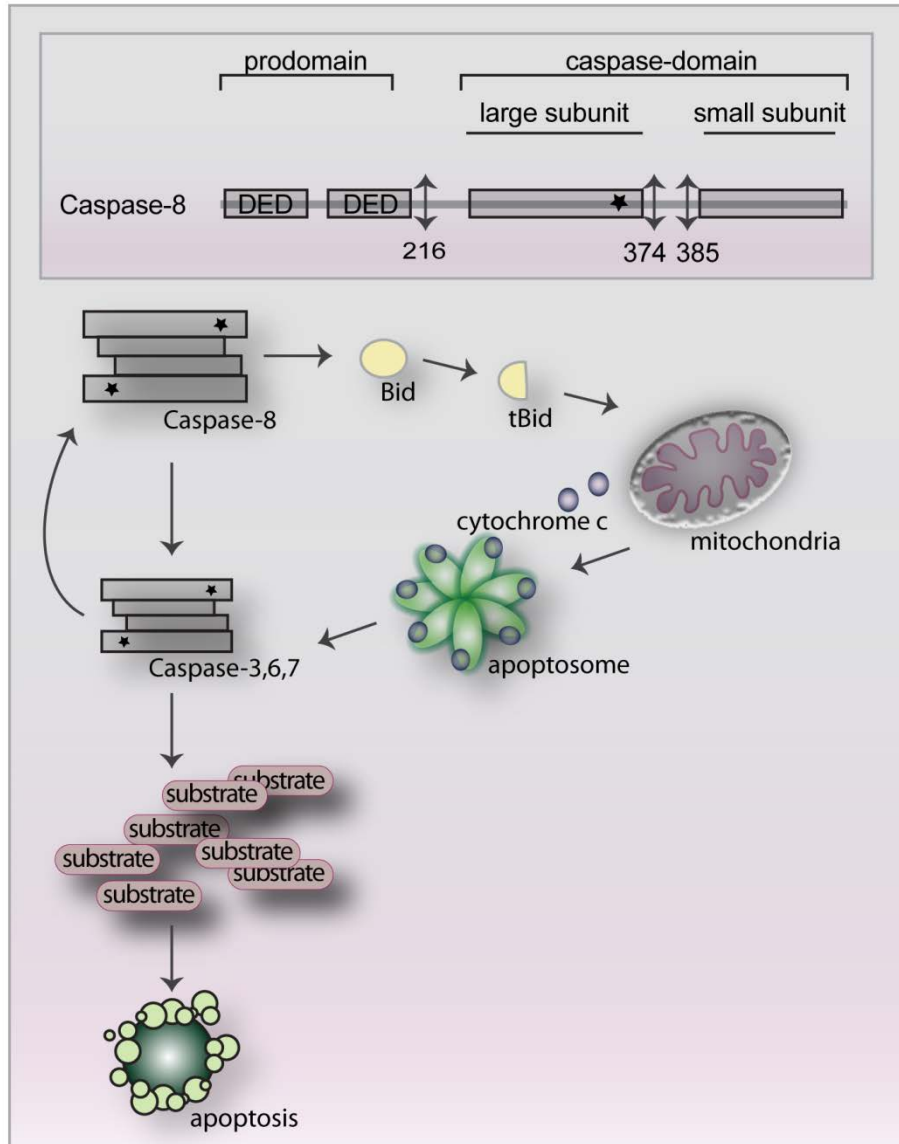


**Figure 1.9. Caspase-8 in apoptosis:** Caspase-8 induces apoptosis by the direct cleavage of effector caspases or indirectly by the cleavage of Bid into tBid. tBid triggers the release of cytochrome c from the mitochondria, thereby activating the Caspase-9 apoptosome. The apoptosome cleaves effector caspases and effector caspases then cleave downstream substrates that will push the cell towards apoptosis.

### 1.5.7. Dredd

*Dredd* was identified in a Blast search based on the *C.elegans* caspase *Ced-3* sequence (Figure 1.10.)<sup>129</sup>. Sequence analysis indicated that *Dredd* has structural hallmarks of initiator caspases with the greatest similarity to Caspase-8 family members. It possesses important residues, conserved among all caspases and that are essential for catalysis and stabilization between caspases and their substrates<sup>129,346</sup>. In addition, *Dredd* appears to possess DED-like structures (termed Death inducing domains (DID)) in the prodomain that were suggested to mediate protein-protein interactions<sup>115</sup>. In contrast to other caspases, *Dredd*'s catalytic site (QACQE) is unique among the caspases, bearing a glutamic acid in a position typically occupied by a glycine<sup>129</sup>.



*Dredd as an apoptotic molecule:* Initial studies to examine the molecular function of Dredd focused solely on a potential function during cell death. During development, *dredd* mRNA accumulates in embryonic cells that are designed to die in a RHG dependent manner<sup>129,347,348</sup>, indicating a potential role for Dredd during development. Dredd also induces ectopic apoptosis when expressed in HeLa cells<sup>115</sup>. However, *dredd* mutant animals are healthy and viable which is in contrast to the early death during development of *dronc* mutant animals<sup>349</sup>. Importantly, follow-up studies demonstrated the fundamental role of Dredd as a non-apoptotic molecule (see below).

*Dredd as a non-apoptotic molecule:* More recent reports described the involvement of Dredd in IMD signaling as an important regulator of the *Drosophila* immune response. Initially, it was reported that Dredd is required to resist gram-negative bacterial infection. It was shown that *dredd* loss-of-function flies are highly susceptible to infection with gram-negative bacteria and hence died quickly after an infection<sup>130</sup>. Afterwards, data demonstrated that Rel processing depends on Dredd, and that *dredd* mutant flies fail to express Rel-dependent genes upon infection<sup>125,126</sup>. Given that Rel is cleaved at a caspase consensus cleavage site and caspase inhibitors (like p35 and zVAD-FMK) block Rel cleavage, the model at the starting point of this study suggested that Dredd is required for the Imd/Rel response, where it proteolytically cleaves Rel (Figure 1.11.).

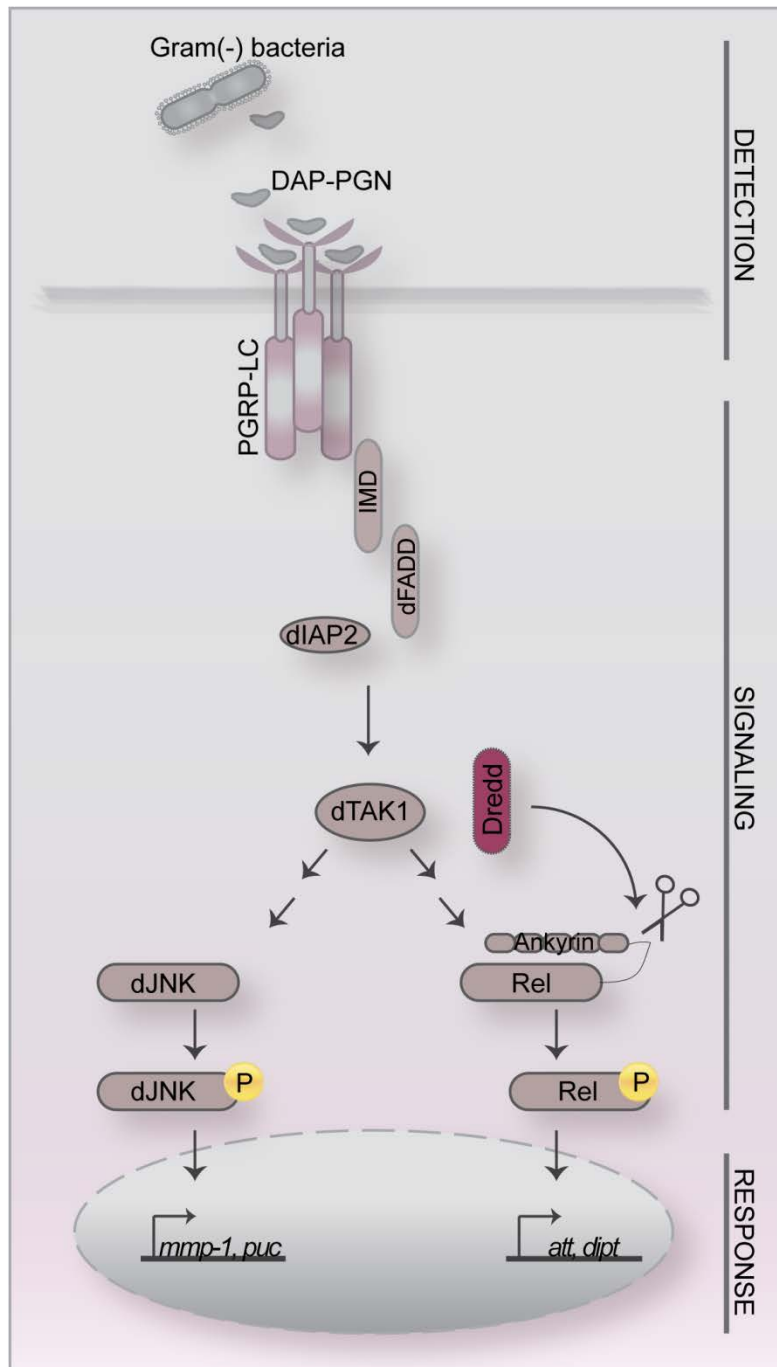


**Figure 1.11. Historical model of IMD signaling:** Illustration of the IMD signaling pathway at the starting point of this thesis (see text for more details).

While these data implicate Dredd in the IMD/Rel arm of the IMD response, more recent studies indicated a potential role for Dredd in the phosphorylation of dJNK<sup>113,146</sup>. Nevertheless, it was not known if Dredd is required for the induction of the IMD/dJNK response. I recently demonstrated that Dredd is essential for the full activation of IMD/dJNK signaling and I positioned Dredd upstream of dTAK1 as part of the signaling network<sup>350</sup>. My data are in line with the most recent work that demonstrated that Dredd cleaves Imd and that dIAP2 ubiquitinates Dredd<sup>114,273</sup>.

However, at the starting point of this study, the role for Dredd in the IMD pathway, other than in IMD/Rel signaling, was elusive and the position of Dredd and Dredd's interactions with the IMD signaling cascade were unknown. In addition, the molecular mechanism of Dredd activation and regulation was unclear.

## 1.6. Objectives

In this study, I examined the function of caspases in the *Drosophila* IMD signaling pathway (Figure 1.12.) with focus on the caspase Dredd. The experiments were designed to address the following main questions:

1. What are the functions of Dredd in IMD/Rel, IMD/dJNK, and apoptotic signaling?
2. What is the molecular basis of Dredd function in these signaling processes?
3. What is the contribution of caspases to IMD signaling?

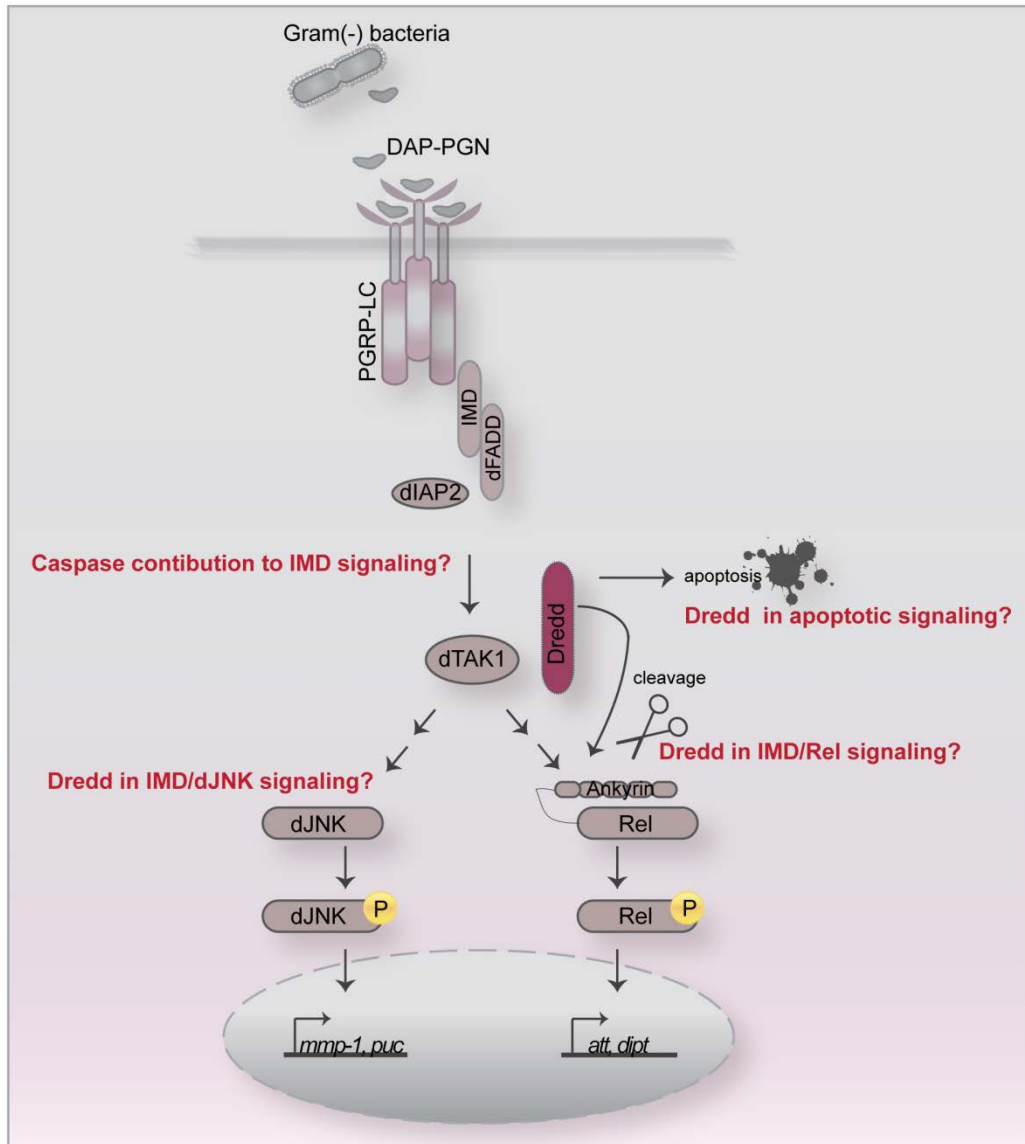


**Figure 1.12. Objectives:** Illustration of the IMD signaling pathway as described in the text. The main objectives, formulated as questions, that formed the path of this thesis are indicated in red.

## **Chapter 2. Materials and Methods**

## 2.1. Buffers and solutions

All buffers and solutions are listed below in alphabetical order. All solutions were prepared in Milli-Q ultrapure water unless indicated otherwise. v/v: volume per volume, w/v: weight per volume

### **DNA gel loading buffer (6x)**

30mM Tris, pH=7.5

36% glycerol (v/v)

0.15% bromophenol blue (w/v)

0.15% xylene cyanol (w/v)

### **DNA resuspension buffer for plasmid mini preparations**

1 $\mu$ l 10 mg/ml RNase A (Sigma)

200 $\mu$ l TE

### **EB elution buffer for QIAquick spin columns for PCR purification and gel extraction (Qiagen)**

10mM Tris, pH = 8.5

### **LB (Luria Bertani) bacterial growth medium (500 ml)**

5g tryptone (BD)

2.5g yeast extract (BD)

5g NaCl

7.5g Agar (Sigma) (*for culture plates*)

Autoclaved

### **Lysis buffer 1, lysis buffer for S2 cell culture for Western blotting**

50mM HEPES (pH 7.5)

10mM EDTA, pH=8.0

50mM KCL

50mM NaCl

1mM MgCl<sub>2</sub>

10% NP40 (v/v)

1mM PMSF

0.04% 1 protease inhibitor cocktail tablet/2 ml (Roche, 11873580001) (v/v)

**Lysis buffer 2, lysis buffer for HeLa cell culture for Western blotting**

20mM HEPES, pH=7.5

150mM NaCl

1% Triton X-100 (v/v)

10% glycerol (v/v)

1mM PMSF

0.04% 1 protease inhibitor cocktail tablet/2 ml (Roche, 11873580001)(v/v)

**P1 bacterial resuspension buffer for plasmid mini preparations/TE**

10mM Tris, pH=7.5

1mM EDTA, pH=8.0

**P1 bacterial resuspension buffer for plasmid midi preparations (Qiagen)**

50mM Tris, pH=8.0

10mM EDTA, pH=8.0

100µg/ml RNase A

**P2 bacterial lysis buffer for plasmid mini preparations**

200mM NaOH

1% SDS (w/v)

**P2 bacterial lysis buffer for plasmid midi preparations (Qiagen)**

200mM NaOH

1% SDS (w/v)

**P3 neutralization buffer for plasmid mini preparations**

3M potassium acetate, pH=5.5

**P3 neutralization buffer for plamid midi preparations (Qiagen)**

1M potassium acetate, pH=5.5

**PB DNA resuspension buffer for PCR purification (Qiagen)**

5M guanidine hydrochloride

30% isopropanol (v/v)

pH = 5.0

**PBS buffer (10X)**

1.4M NaCl

27mM KCl

100mM Na<sub>2</sub>HPO<sub>4</sub> - 7H<sub>2</sub>O

14mM KH<sub>2</sub>PO<sub>4</sub>

**PBT buffer**

0.1% Tween-20 (v/v)

in PBS

**PE wash buffer for QIAquick spin columns for PCR purification and gel extraction (Qiagen)**

10mM Tris, pH = 7.5

80% ethanol (v/v)

**QC wash buffer for QIAGEN-tips for plasmid midi preparations (Qiagen)**

1M NaCl

50mM MOPS, pH=7.0

15% isopropanol (v/v)

**QBT equilibration buffer for QIAGEN-tips for plasmid midi preparations (Qiagen)**

750mM NaCl

50mM MOPS, pH=7.0

15% isopropanol (v/v)  
0.15% Triton X-100 (v/v)

**QF elution buffer for QIAGEN-tips for plasmid midi preparations (Qiagen)**

1.25 M NaCl  
50mM Tris, pH=8.5  
15% isopropanol (v/v)

**QG agarose gel dissolution buffer for gel extraction (Qiagen)**

5.5M guanidine thiocyanate  
20mM Tris, pH = 6.6

**Sample buffer (2X)**

62.5mM Tris, pH=6.8  
10% glycerol (v/v)  
2% SDS (w/v)  
50mM  $\beta$ -mercaptoethanol (BioShop)  
0.00125% bromophenol blue (w/v)

**Sample buffer (2X) with urea for PARP1 Western blots**

62.5mM Tris, pH=6.8  
10% glycerol (v/v)  
2% SDS (w/v)  
50mM  $\beta$ -mercaptoethanol (BioShop)  
0.00125% bromophenol blue (w/v)  
8M urea

**SDS-PAGE resolving gel**

Table 2.1.

**SDS-PAGE stacking gel**

Table 2.1.

**SDS-PAGE running buffer (10x)**

250mM Tris

2M glycine

1% SDS (w/v)

**T7 5X transcription buffer**

400mM HEPES, pH 7.5

120mM MgCl<sub>2</sub>

10mM Spermidine

50mM DTT

**T7 dilution buffer**

5mM KHPO<sub>4</sub>, pH 8.0

50mM NaCl

0.05mM EDTA

0.5mM DTT

50% Glycerol

**TAE buffer (50X)**

2M Tris

500mM EDTA, pH = 8.0

5.71% glacial acetic acid (v/v)

**TE buffer**

10mM Tris, pH=7.4

1mM EDTA, pH=8.0

**Transformation solution 1 (2X) for the generation of competent cells**

200mM CaCl<sub>2</sub>

20mM MgCl<sub>2</sub>

10mM RuCl<sub>2</sub>

filter sterilized

**Transformation solution 2 for the generation of competent cells**

100mM CaCl<sub>2</sub>

10mM MgCl<sub>2</sub>

5mM RuCl<sub>2</sub>

10% glycerol (v/v)

filter sterilized

**Western blot transfer buffer**

25mM Tris

192mM glycine

0.37% SDS (m/v)

20% methanol (v/v)

**Molecular weight standards**

DNA standards

- 100bp DNA ladder (Invitrogen)
- 1kb DNA ladder (New England Biolabs)

Protein standards

- Precision Plus Protein Standard (Bio Rad)

component	resolving gel		stacking gel
	10% 20 - 70kDa	8% 40 - 100kDa	5%
H <sub>2</sub> O	1.3ml	1.8ml	1ml
30% acrylamide: bisacrylamide (Bio-Rad)	1.7ml	1.3ml	248µl
1M Tris (pH 8.8 for seperatin gel, pH 6.8 for stocking gel)	1.9ml	1.9ml	188µl
10% SDS	50 µl	50 µl	15µl
10% APS	50µl	50µl	15µl
TEMED (Sigma)	3µl	3µl	3µl

**Table 2.1. Components of the resolving and stacking SDS-polyacrylamide gel.**

## 2.2. DNA cloning

### 2.2.1. Expression constructs

The p35 expression plasmid has been described previously<sup>351</sup>. The pMT-HAdTAK1CA plasmid was generated by David Bond by amplifying the genomic region of dTAK1 lacking the kinase inhibitory domain with the primers specified in table 2.2. dTAK1 has been described previously<sup>113</sup>.

Caspase-8, dIAP2, dIAP2 $\Delta$ BIR1 (lacking the first 75 amino acid), dIAP2-BIR3 (amino acid 178-450 of dIAP2), dIAP2- $\Delta$ RING (lacking the last 36 amino acid), dFADD(\*), Dredd(\*), Dreddcasp-domain (lacking 103 amino acid that code for the caspase domain), Dreddprodomain (lacking 67 amino acid that code for the prodomain,\*), Imd(\*), and HAp35 expression plasmids were generated by cloning the respective coding regions into pENTR/D-TOPO (Invitrogen) with the specific primers listed in table 2.2.

DreddC408A (DreddCA) has been described previously<sup>352</sup>. The pENTR/D-TOPO Dredd vector was cloned based on the pMT-Flagdreddmyc vector (John M. Abrams) (\*). The pRK5-FlagDredd expression vector has been described previously<sup>115</sup>. The pRK5 control vector was a gift from Dr. Deborah Burshtyn.

Caspase-8C360A (Caspase-8CA), DroncC318S (DroncSC), dIAP2C472Y, dIAP2D92A, and dIAP2D100A were generated by site directed mutagenesis. More specifically, Caspase-8, Dronc, and dIAP2 pENTR/D-TOPO plasmids were amplified by a Pfx PCR reaction (2.2.2.) with primers designed with a Tm of at least 78°C that center the single amino acid change in the middle of the primer (table 2.2.). To eliminate the parental, non-mutated (methylated) plasmid DNA the newly synthesis non-methylated DNA product was digested with 1 $\mu$ l Dpn1 (20U/ $\mu$ l, New England Biolabs) for 1h at 37°C. 3 $\mu$ l of the final reaction was transformed into 50 $\mu$ l *Escherichia coli* DH5 $\alpha$  competent bacteria as described in 2.2.11.

The chimeric DC(\*) and CD were generated in a three step PCR (2.2.2.) with the primers specified in table 2.2. The reaction required primers (A and D) complementary to the start of the first target sequence and end of the second

target sequence (Figure 2.1.). In addition, two internal primers that anneal within the target sequence (B and C) and with a 3x Alanine overhang were used. During the first round of PCR, the AB fragment of the first target sequence and CD fragments of the second target sequence were created. These products were isolated from excised gel fragments (2.2.8.) and mixed for the second round of PCR using primers A and D. The complementary ends of the products hybridized in this second PCR to create the final product which contained a fusion of the two fragments of the original two sequences (Figure 2.1.).

All PCR products were analysed by agarose gel electrophoresis (2.2.7.) and purified by polymerase chain reaction (PCR) purification (2.2.8). The purified PCR fragments were cloned into the pENTR/D-TOPO plasmids (2.2.9.) and transformed into One Shot Competent *E. coli* (2.2.11.) for DNA preparation of bacterial mini culture (2.2.12.). All DNA constructs were confirmed by sequencing (2.2.16.). Oligonucleotides (table 2.2.) were designed with the Primer 3-Software (<http://frodo.wi.mit.edu/>) and synthesized by Intergraded DNA Technologies (IDT). (\*) = by Edan Foley

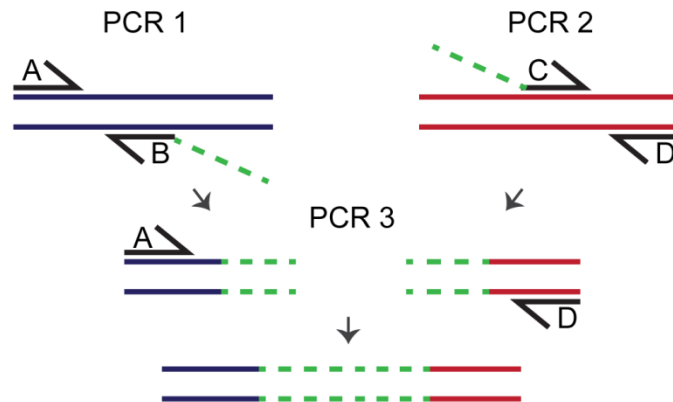


**Figure 2.1. Three step PCR to generate chimeric constructs:** The first DNA template is indicated in blue, the second DNA template in red, 3x Alanine overhang are indicated in green, and primers are indicated in black and termed A-D. See text for further explanations.

NAME	PRIMER SEQUENCE
<i>Caspase-8 forward</i>	5'-CACCATGGACTTCAGCAGAAATC-3'
<i>Caspase-8 reverse</i>	5'-TCAATCAGAAGGGAAGAC -3'
<i>Caspase-8C360A forward</i>	5'-CCCAAAGTGTTTTTTATTCAGGCTGCTCAGGGGGATAAC-3'
<i>Caspase-8C360A reverse</i>	5'-GTTATCCCCCTGAGCAGCCTGAATAAAAAACACTTTGG-3'
<i>CD A forward</i>	5'-CACCATGGACTTCAGCAGAAATC-3'
<i>CD B reverse</i>	5'-TGC GGC CGC ATC CTG TTC TCT TGG -3'
<i>CD C forward</i>	5'-GCGGCCGCGAGTGGATAA GAACGACTAATC G -3'
<i>CD D reverse</i>	5'- TCACAGACGAGGTGG-3'
<i>DC A forward</i>	5'-CACCATGTCAGCGAGTGCAATTTATCG-3'
<i>DC B reverse</i>	5'-TGCGGCCGCGATCCGTGCCATCCCGTCTACGC-3'
<i>DC C forward</i>	5'-GCGGCCGCAAGTGAATCACAGACTTTGGAC-3'
<i>DC D reverse</i>	5'-TCAATCAGAAGGGAAGAC-3'
<i>dIAP2 forward</i>	5'-CACCATGACGGAGCTGGGCATGGAG-3'
<i>dIAP2 reverse</i>	5'-TCACGAAAGGAACGTGCGC-3'
<i>dIAP2 reverse (no STOP)</i>	5'-CGAAAGGAACGTGCGCACGAATCCC-3'
<i>dIAP2BIR3 forward</i>	5'-CACCATGCAAATGGGCCCCCTTATAGAG-3'
<i>dIAP2 BIR3 reverse</i>	5'-TCATAAGCGTGTCATCCTTTAG -3'

**Table 2.2. List of primer sequences for PCR assays:** Primer sequences in alphabetical order.

NAME	PRIMER SEQUENCE
<i>dlAP2D92A forward</i>	5'-CCCAGGAGCCAGGAGAGCGCCAACGAGGGAAACAGCG-3'
<i>dlAP2D92A reverse</i>	5'-CGCTGTTTCCCTCGTTGGCGCTCTCCTGGCTCCTGGG-3'
<i>dlAP2D100A forward</i>	5'-CGAGGAAACAGCGTAGTGGCCAGCCCGGAGTCCTGC-3'
<i>dlAP2D100A reverse</i>	5'-GCAGGACTCCGGGCTGGCCACTACGCTGTTTCCCTCG-3'
<i>dlAP2C466Y forward</i>	5'-GGCGTAGTGTTCCCTGCCCTATGGCCACTTGGCCACCTGC-3'
<i>dlAP2 C466Y reverse</i>	5'-GCAGGTGGCCAAGTGGCCATAGGGCAGGAACACTACGCC-3'
<i>dlAP2 ΔBIR1 reverse</i>	5'- TCACGAAAGGAACGTGCGC-3'
<i>dlAP2ΔRING forward</i>	5'- CACCATGACGGAGCTGGG-3'
<i>dlAP2 ΔRING reverse</i>	5'-TCATAAGCGTGCATCCTTTAG -3'
<i>Dredd forward</i>	5'-CACCATGTCAGCGAGTGCAATTTATCG-3'
<i>Dredd reverse</i>	5'-TCACAGACGAGGTGG-3'
<i>Dreddcasp-domain forward</i>	5'-CACCGTGGATAAAGAACGACTAATCG-3'
<i>Dreddcasp-domain reverse</i>	5'-TCACAGACGAGGTGG-3'
<i>Dreddprodomain forward</i>	5'-CACCATGTCAGCGAGTGC-3'
<i>Dreddprodomain reverse</i>	5'-TCAATCCGTGCCATCCCG-3'
<i>Dronc forward</i>	5'-CACCATGCAGCCGCCGGA-3'
<i>Dronc reverse</i>	5'-CTATTCGTTGAAAACCCGGGATTG-3'

**Table 2.2. Continued list of primer sequences for PCR assays:** Primer sequences in alphabetical order.

NAME	PRIMER SEQUENCE
<i>Dronc318S forward</i>	5'-GGTGCTTATGTTTCCCTTTTCCC GCGGCGATGAATATG-3'
<i>DronC318S reverse</i>	5'-CATATTCATCGCCGCGGGAAAAGGGAAACATAAGCACC-3'
<i>dTAK1 forward</i>	5'-CACCGAATTCATGGCCACAGCATCGC-3'
<i>dTAK1 reverse</i>	5'-TTAATCTAGACTACGTGTATTCCAGG-3'
<i>lmd forward</i>	5'-CACCATGTCAAAGCTCAGGAACC-3'
<i>lmd reverse</i>	5'-CTAGCTGTTTGTCTTGCG-3'
<i>lmdcl forward</i>	5'-CACCGCAGCTCCCGTGGACGAC-3'
<i>lmdcl reverse</i>	5'-CTAGCTGTTTGTCTTGCG-3'
<i>p35 forward</i>	5'-CCCAGACGGTTATTGAGA-3'
<i>p35 reverse</i>	5'GCCCCAGTTCGATTCTGTAG3'

**Table 2.2. Continued list of primer sequences for PCR assays:** Primer sequences in alphabetical order.

### 2.2.2. Polymerase chain reaction (PCR) with Pfx polymerase

All PCR reactions were performed according to manufacturer's recommendations (Invitrogen). DNA templates were amplified according to the following protocol:

- 5.0µl 10X Pfx amplification buffer (Invitrogen)
- 1.0µl 50 mM MgSO<sub>4</sub> (Invitrogen)
- 1.5µl 10 mM dNTP mixture (Invitrogen)
- 1.0µl 200 ng DNA template
- 1.5µl 10 mM forward primer (table 2.2)
- 1.5µl 10 mM reverse primer (table 2.2)
- 0.5µl Platinum Pfx DNA polymerase (Invitrogen)
- 38.0 l nuclease-free water (HyClone)

Transcript amplification was performed in an Eppendorf PCR machine (Eppendorf, Mastercycler ep gradient S) with the following program: 1 cycle of 95°C for 2min, 40 cycles of 95°C for 1min, 55°C for 1min and 68°C for 1min per kb of DNA template, 1 cycle of 68°C for 10min, hold at 4°C.

### 2.2.3. Polymerase chain reaction (PCR) with Taq polymerase

All PCR reactions were performed according to manufacturer's recommendations (Invitrogen). DNA templates were amplified according to the following protocol:

- 2.5µl 10X ThermoPol reaction buffer (New England Biolabs)
- 0.5µl 10 mM dNTP mixture (Invitrogen)
- 1.0µl 200 ng DNA template
- 0.5µl 10 mM forward primer (table 2.2.)
- 0.5µl 10 mM reverse primer (table 2.2.)
- 0.125µl Taq DNA polymerase (New England Biolabs)

20.875µl nuclease-free water (HyClone)

Transcript amplification was performed in an Eppendorf PCR machine (Eppendorf, Mastercycler ep gradient S) with the following program: 1 cycle of 95°C for 30sec, 40 cycles of 95°C for 30sec, 55°C for 1min and 72°C for 1min per kb of DNA template, 1 cycle of 72°C for 10min, hold at 4°C. Samples were then analysed on a 1-1.5% agarose gel (2.2.6.).

#### **2.2.4. Reverse transcription polymerase chain reaction (RT-PCR)**

For RT-PCR, total RNA was isolated from  $1 \times 10^6$  S2 cells or 10 flies using Trizol (Invitrogen) according to manufacturer's recommendations (see 2.9.1.). To eliminate DNA residues, RNA was treated with DNase I (Invitrogen). Superscript III (Invitrogen) was used to generate cDNA using 3µg (S2 cells) or 5µg (flies) RNA and random primers (Invitrogen), according to the manufacturer's instructions. Transcript amplification was performed in an Eppendorf PCR machine using Taq DNA polymerase (Biolabs) (2.2.3.) and p35 primers (table 2.2.). Samples were then analysed on a 1-1.5% agarose gel (2.2.6.).

#### **2.2.5. Polymerase chain reaction (PCR) purification**

PCR reactions were purified according to the manufacturer's instructions with the QIAquick PCR Purification Kit (Qiagen). Samples were then analysed on a 1-1.5% agarose gel.

#### **2.2.6. Agarose gel electrophoresis**

For all experiments DNA/RNA was analysed by 1-1.5% agarose gels. 1-1.5g (w/v) of agarose (Invitrogen) was dissolved in TAE by heating the solution in a microwave until the agarose was completely dissolved. The liquid was poured into an agarose gel chamber holding a comb to generate loading pockets and 0.5 µg/ml ethidium bromide (Sigma) was added. After polymerisation the gel was

transferred to a running chamber that was filled with TAE. The samples were mixed in 6X DNA gel loading buffer and loaded into the pockets of the gel. The 1kb (New England Biolabs) or 100bp (Invitrogen) DNA size marker were loaded on each gel to determine the size of DNA/RNA. The gel was run at 100Volts for approximately 30min and the gel was visualized with an Image Quant 300UV light box with a digital camera (GE).

### **2.2.7. DNA isolation from excised gel fragments**

DNA were separated by agarose gel electrophoresis (2.2.6.) and excised under an Image Quant 300UV light box (GE). DNA/gel fragments were dissolved in 600µl Buffer QG and prepared according to the QIAquick gel extraction Kit (Qiagen) manufacturer's instructions. Samples were then analysed on a 1-1.5% agarose gel (2.2.6.).

### **2.2.8. TOPO TA cloning and recombination (Gateway recombination cloning technology)**

To generate DNA fragments for TOPO cloning DNA was amplified with primers specified in table 2.1. by a Pfx PCR reaction as described above (2.2.2.). The TOPO reaction was set up as followed:

- 0.5 – 4µl fresh PCR product (~1-5ng of a 1kb PCR product)
- 1.0µl salt solution (Invitrogen)
- 1.0µl TOPO vector (Invitrogen)
- Sterile water for a final volume of 6µl

The reaction was incubated for 20-30min at room temperature and 2µl of the reaction were transformed into One Shot Competent *E. coli*. according to the manufacturer's instructions (Invitrogen TOP10 Chemically Competent *E.coli*). 250µl LB medium was added and placed on a shaker for 1h at 37°C. 50µl of the bacterial culture were spread on a pre-warmed LB agar plate containing 30µg/ml

kanamycin (Sigma), and incubated overnight at 37°C. On the next day DNA was prepared as described in 2.2.12. - 2.2.16.

The Gateway entry clone for each construct was then recombined with a Gateway destination clone (table 2.3.) following the manufacturer's recommendations in a Gateway LR clonase reaction (Invitrogen). The reaction was set up as followed:

75ng entry clone (Invitrogen)

75ng destination vector

2.0µl 5X LR Clonase reaction buffer (Invitrogen)

TE (pH 8.0) for a final volume of 8µl

The reaction was incubated at room temperature for ~4h and transformed into *Escherichia coli* DH5α competent bacteria as described in 2.2.10. 200µl of the bacterial culture were spread on a pre-warmed LB agar plate containing 50µg/ml ampicillin (Sigma), and incubated overnight at 37°C. On the next day DNA was prepared as described in 2.2.12. - 2.2.16.

NAME	TAG	PROMOTOR	TAG DESCRIPTION
pAHW	3xHA	Actin5C	N-terminal 3x HA epitopes
pAMW	6xMyc	Actin5C	N-terminal 6x Myc epitopes
pAWM	6xMyc	Actin5C	C-terminal 6x Myc epitopes
pTHW	6xMyc	UASt	N-terminal 3x HA epitopes; GAL4-driven somatic expression <i>in vivo</i>
pTW	none	UASt	GAL4-driven somatic expression <i>in vivo</i>

**Table 2.3. List of Gateway destination clones used in Gateway LR clonase assays:** Gateway vector list in alphabetical order.

### 2.2.9. Generation of chemically competent bacteria

To generate chemically competent bacteria *Escherichia coli* DH5 $\alpha$  were grown over night in LB culture medium on a horizontal shaker at 250rpm at 37°C. 300 $\mu$ l of the bacterial overnight culture was inoculated with 30ml of fresh LB culture medium and incubated on a horizontal shaker at 250rpm at 37°C until the solution turned visibly cloudy. The bacterial culture was placed on ice for 10min and centrifuged at 3000 x g for 5min at 4°C (Eppendorf, 5810R). The bacterial pellet was resuspended in 15ml of transformation solution 1 and incubated on ice for 1h. The bacterial culture was again centrifuged at 1000 x g for 5min at 4°C and gently resuspended in 2ml transformation solution 2. The culture was incubated in the solution overnight on ice. On the next day 50 $\mu$ l of chemically competent bacteria were aliquoted into pre-chilled 1.5ml microfuge tubes and quickly transferred to -80°C for long time storage.

### 2.2.10. Transformation of bacteria

50 $\mu$ l *Escherichia coli* DH5 $\alpha$  competent bacteria were thawed on ice and mixed with 2 $\mu$ l plasmid DNA (DNA concentration of 500 $\mu$ g/ml). The mixture was incubated on ice for 5min and heat-shocked for 1min in a 42°C water bath. The bacterial plasmid mixture was put back on ice for another 5min and after the addition of 1ml of LB culture medium it was placed on a horizontal shaker at 250rpm and 37°C for 1h. For starter cultures that were anticipated to grow on culture plates 200 $\mu$ l of the culture was spread on a pre-warmed LB agar plate containing the appropriate selection antibiotic and incubated upside down at 37°C overnight. The starter culture that was intended for a plasmid midi preparation was transferred into 200ml LB culture medium with the appropriate selection antibiotic and incubated in a glass Erlenmeyer flask overnight in a horizontal shaker at 250rpm and 37°C.

### **2.2.11. Analytical polymerase chain reaction (PCR) from bacterial colonies**

To check bacterial colonies for the desired DNA a sterile tip was first dipped into the bacterial colony from a culture plate and transferred to a PCR mixture (2.2.3.). The same tip was then used to inoculate 2ml sterile LB culture medium in a glass test tube that contained the appropriate selection antibiotic. The culture was set up overnight on a horizontal shaker at 250rpm and 37°C for plasmid mini preparation (2.2.2.).

### **2.2.12. DNA preparation of bacterial mini cultures from bacterial colonies**

A sterile tip was dipped into a single bacterial colony and inoculated in a sterile glass test tube in 2ml LB culture medium with the appropriate selective antibiotic and incubated in a horizontal shaker at 250rpm and 37°C overnight. On the next day the bacterial culture was transferred into a 1.5ml microcentrifuge tube and spun in a benchtop centrifuge (Eppendorf 5415R) for 1min at maximum speed. The bacterial pellet was completely resuspended in 100µl resuspension buffer P1. 100µl lysis buffer P2 was added and incubated at room temperature for no more than 5min. 100µl neutralizing buffer P3 was added and the lysate was spun for 3min at maximum speed in a benchtop centrifuge. The supernatant was transferred to a new microcentrifuge tube and 250µl Tris-buffered phenol (Invitrogen) was added. The sample was mixed and spun for 3min at maximum speed in a benchtop centrifuge. The upper aqueous phase was transferred into a new 1.5ml microcentrifuge tube and 500µl of 100% EtOH were added and mixed. The sample was spun for 10min at max speed at 4°C. After removing the supernatant 100µl 70% EtOH was added and re-spun for 1min max speed at 4°C. The supernatant was removed and the DNA pellet was dried for 5-10min. The pellet was resuspended in 20µl DNA resuspension buffer. Samples were then analysed by an analytical restriction digest (2.2.4.).

### 2.2.13. DNA preparation of bacterial midi cultures from mini cultures

The plasmid midi preparation was performed with Qiagen Plasmid Midi Kit (Qiagen). The overnight bacterial culture was transferred into a 250ml screw cap centrifuge bottle and spun for 30min at 5,000rpm at 4°C in a high performance centrifuge (Sorvall, RC5C with GSA rotor). The bacterial pellet was resuspended and lysed according to the manufacturer's instructions. Samples were resuspended in 100µl nuclease-free water (HyClone) and analysed by an analytical restriction digest (2.2.4.).

### 2.2.14. Measurement of DNA concentration and purity

To determine the concentration of DNA in solution, the DNA was diluted 1:100 in water and measured at the absorbance of 260nm (A260) and 280nm (A280) in a spectrophotometer (Jenway, Genova). Water was used as a reference. The DNA concentration [DNA] was calculated with the following formula:

$$[\text{DNA}] (\mu\text{g/ml}) = A_{260} \times \text{dilution factor (here: 100)} \times 50\mu\text{g/ml}$$

The purity of the DNA (DNA<sub>p</sub>) was determined by the following calculation:

$$\text{DNA}_p = A_{260} / A_{280}$$

A ratio of ~1.8 is generally accepted as "pure" for DNA. All plasmid DNA was diluted to a final concentration of 500µg/ml for long time storage at -20°C.

### 2.2.15. Analytical restriction digest

All plasmid DNA generated by mini- or midi preparations (2.2.12. - 2.2.13) were analysed by analytical restriction digest in the following reaction:

2.0µl DNA

2.0µl 10X NEBuffer (New England Biolabs)

2.0µl 10X BSA solution (New England Biolabs), enzyme dependent

0.5µl restriction enzyme (New England Biolabs)

13.5µl nuclease-free water (HyClone)

The reaction was incubated in a 37°C water bath for 1h and analysed by agarose gel electrophoresis (2.2.6.).

### **2.2.16. Preparation of DNA samples for sequencing**

All generated DNA plasmids were analysed in a sequencing reaction. The BigDye Terminator v3.1 Cycle Sequencing Kit was used (Applied Biosystem) according to the manufacturer's instructions. Sequencing primers were designed for approximately every 500bp fragment of the sequence of interest.

The sequencing reaction was set up as followed:

0.5µl DNA (50-400ng)

1.5µl 5X dilution buffer (Applied Biosystem)

0.5µl 5 µM sequencing primer

1.0µl DYEnamic ET reagent mix (Applied Biosystem)

6.5µl nuclease-free water (HyClone)

The reaction was performed in a thermocycler (Eppendorf, Mastercycler ep gradient S) with the following program: 25 cycles of 96°C for 30s, 50°C for 15s, and 60°C for 2min, followed by a hold at 4°C. The reaction was transferred to a new 1.5ml microcentrifuge tube and 2µl 1.5M ammonium acetate and 80µl 95% EtOH were added to the reaction. The reaction was incubated on ice for 15min and spun in a bench top centrifuge (Eppendorf, 5415R) for 15min at 12,000rpm and 4°C. The pellet was washed with 500µl 70% EtOH and spun for 5min max speed. The sample was air-dried for 5min and stored at -20°C. The reaction was run on a Sanger DNA sequencer (Applied Biosystems, 3730) by the Sequencing Service of the Molecular Biology Service Unit at the University of Alberta.

### **2.2.17. Preparation of glycerol stocks and set up of bacterial cultures from a glycerol stock**

For long time storage of important DNA constructs, bacterial cultures were stored as a glycerol stocks at  $-80^{\circ}\text{C}$ . Plasmid DNA was transformed into *Escherichia coli* DH5 $\alpha$  competent bacteria (2.2.10.) and inoculated overnight in a horizontal shaker at 250rpm and  $37^{\circ}\text{C}$ . 250 $\mu\text{l}$  of the bacterial culture were mixed with 250 $\mu\text{l}$  sterile 80% glycerol solution in water. To recover the plasmid DNA from glycerol stocks the surface of the glycerol/bacterial mixture was scraped with a sterile tip and streaked on a pre-warmed LB agar plate containing the appropriate selection antibiotic and incubated upside down at  $37^{\circ}\text{C}$  overnight. On the next day colonies were prepared as described in 2.2.12.

## **2.3. Generation of dsRNA**

### **2.3.1. De novo synthesis of dsRNA**

Gene specific primers for amplification of genomic DNA were designed with a 5' anchor sequence GGGCGGT. DNA templates were amplified according to the following protocol:

- 5.0 $\mu\text{l}$  10X ThermoPol reaction buffer (New England Biolabs)
- 0.5 $\mu\text{l}$  25 mM dNTP mixture (Invitrogen)
- 1.0 $\mu\text{l}$  200 ng DNA template
- 10.0 $\mu\text{l}$  1  $\mu\text{M}$  primer mix (table 2.2.)
- 0.5 $\mu\text{l}$  *Taq* DNA polymerase (New England Biolabs)
- 33.0 $\mu\text{l}$  nuclease-free water (HyClone)

Transcript amplification was performed in an Eppendorf PCR machine (Eppendorf, Mastercycler ep gradient S) with the following program: 1 cycle of  $95^{\circ}\text{C}$  for 2min, 34 cycles of  $95^{\circ}\text{C}$  for 30sec,  $50^{\circ}\text{C}$  for 45sec and  $72^{\circ}\text{C}$  for 1min, 1 cycle of  $72^{\circ}\text{C}$  for 10min, hold at  $4^{\circ}\text{C}$ .

The generated template DNA was amplified in a second round of PCR with a primer that contained the RNA polymerase promotor sequence (TAATACGACTCACTATAGGGAGACCAC) and an anchor sequence (GGGCGGGT). The DNA templates were amplified according to the following protocol:

- 5.0µl 10X ThermoPol reaction buffer (New England Biolabs)
- 0.5µl 10 mM dNTP mixture (Invitrogen)
- 10.0µl DNA template
- 2.0µl 10 mM T7 primer (table 2.1.)
- 0.5µl *Taq* DNA polymerase (New England Biolabs)
- 32.0µl nuclease-free water (HyClone)

Transcript amplification was performed in an Eppendorf PCR machine (Eppendorf, Mastercycler ep gradient S) with the following program: 1 cycle of 95°C for 2min, 4 cycles of 95°C for 30sec, 42°C for 30sec and 72°C for 1min, 29 cycle of 94°C for 30sec, 60°C for 30sec, 1 cycle of 72°C for 1min, 1 cycle of 72°C for 10min, hold at 4°C.

### **2.3.2. Amplification of T7 tagged DNA**

Template DNA was amplified according to the following protocol:

- 5.0µl 10X ThermoPol reaction buffer (New England Biolabs)
- 0.5µl 25 mM dNTP mixture (Invitrogen)
- 2.0µl DNA template
- 2.0µl 10 mM T7 primer (table 2.2.)
- 0.5µl *Taq* DNA polymerase (New England Biolabs)
- 40.0µl nuclease-free water (HyClone)

Transcript amplification was performed in an Eppendorf PCR machine (Eppendorf, Mastercycler ep gradient S) with the following program: 1 cycle of

95°C for 2min, 40 cycles of 95°C for 15sec, 55°C for 15sec and 72°C for 1min, 1 cycle of 72°C for 5min, hold at 4 °C.

### **2.3.3. Generation of dsRNA**

T7 tagged DNA was amplified with a purified T7 RNA polymerase according to the following protocol:

- 2.5µl 5X T7 transcription buffer
- 3.125µl 25 mM rNTP mixture (Invitrogen)
- 5.0µl DNA template
- 1.25µl T7 in T7 dilution buffer (1/7 dilution of T7 enzyme)

Transcript amplification was performed in an Eppendorf PCR machine (Eppendorf, Mastercycler ep gradient S) with the following program: 1 cycle of 37°C for 6h, 1 cycle of cooling from 90°C to 30°C at 1°C/min. dsRNAs were analysed on a 1.5% agarose gel (2.2.6.).

NAME	PRIMER SEQUENCE
<i>damm forward</i>	5'-GGGCGGGTGACCGAAAAGAGAAAATCTTGG-3'
<i>damm reverse</i>	5'-GGGCGGGTTGTCATAGTTGACCTTCGTTTCG-3'
<i>dcp-1 forward</i>	5'-GGGCGGGTACTTCTCCTGGCGCAACAT-3'
<i>dcp-1 reverse</i>	5'-GGGCGGGTGGGTTTTCTATTGGCAAGGTC-3'
<i>decay forward</i>	5'-GGGCGGGTAAAACGAATGCTTTGTGTTGG-3'
<i>decay reverse</i>	5'-GGGCGGGTGTCGAATGTGGAGTAGAAGACG-3'
<i>dredd forward</i>	5'-GGGCGGGTATTCAATCTCTTGCTTGACTION-3'
<i>dredd reverse</i>	5'-GGGCGGGTCATGACACGATCAGACTTCCC-3'
<i>drice forward</i>	5'-GGGCGGGTCAAACCTTCTGGATGTACCAGC-3'
<i>drice reverse</i>	5'-GGGCGGGTGCCTGTATGAAGAACAACCTTGG-3'
<i>dronc#1 forward</i>	5'-GGGCGGGTATCGAAAAAGATACATGGTGGG-3'
<i>dronc#1 reverse</i>	5'-GGGCGGGTCAAACCTTCTGGATGTACCAGC-3'
<i>dronc#2 forward</i>	5'-GGGCGGTGCCGCCACTGGACATTTTATCATT-3'
<i>dronc#2 reverse</i>	5'-GGGCGGTCTGGAACCTCTGTATTATAATTTGTAG-3'
<i>T7 primer</i>	5'-TAATACGCTCACTATAGGGAGACCACCACGGGCGGGT-3'

**Table 2.4. List of primer sequences for generating dsRNA in a PCR reactions:** Primer sequences in alphabetical order.

## 2.4. Cell lines and cell culture

The *Drosophila* S2 cell line was received from the *Drosophila* Genomics Resource Center (DGRC). S2 cells are phagocytic cells with many features of a macrophage-like lineage. The S2 cell line is derived from a primary culture of *Drosophila* embryos and it is commonly used to examine molecular processes of a cell.

The HeLa cell line was received from Dr. James Smiley. HeLa cells are an immortal human cervical carcinoma cell line. The cell line was derived from cervical cancer cells that were taken from Henriette Lacks and that have had an indescribable influence on scientific investigations.

### 2.4.1. *Drosophila* cell line culture

The *Drosophila* embryonic macrophage-like S2 cell line was cultured at 25°C in HyQ TNM-FH medium (HyClone) supplemented with 10% heat-inactivated fetal bovine serum (GIBCO), 50U/ml penicillin and 50µg/ml streptomycin (GIBCO). Serum-free S2 cells were cultured in SFX-INSECT medium (HyClone) supplemented with 50U/ml penicillin and 50µg/ml streptomycin (GIBCO). Cells were cultured in 75cm<sup>2</sup> canted neck flask with vent cup (Corning) and cells were passaged every three to four days in a 1:5 dilution into fresh media. Serum free cells were detached with cell scrapers. Cells were plated into six, twelve, or twenty-four well plates (Corning Costar) corresponding to the experimental set-up. Overnight cultures were plated at 1x10<sup>6</sup>cells/ml while cell cultured incubated for three days (for RNAi treatments) were plated at 0.8x10<sup>6</sup>cells/ml. Plated cells were incubated at 25°C (TriTech Research, DigiTherm).

### 2.4.2. Human cell line culture

The HeLa cell line was cultured at 37°C and 5% CO<sub>2</sub> in a water jacketed CO<sub>2</sub> incubator (Thermo Electron Corporation, Forma Series II) in Dulbecco's Modified Eagle Medium with 4.5g/l D-glucose and L-glutamine and sodium bicarbonate

(Sigma, D5796) supplemented with 10% (v/v) fetal bovine serum (GIBCO), 50U/ml penicillin and 50µg/ml streptomycin (GIBCO). Cells were cultured in 150cm<sup>2</sup> canted neck flask with vent cup (Corning) and cells were passaged every three to four days. Cells were washed in 10ml sterile PBS and detached with 3ml of 0.25% Trypsin-EDTA (GIBCO) incubated for 5 to 10min at 37°C. 5ml culture medium was added and the cells were spun 2min at 1,000 x g and room temperature in a 15ml centrifuge tube (Corning). The cell pellet was resuspended in 5ml fresh culture medium and diluted 1:15 into fresh media. Cells were plated into six, twelve, or twenty-four well plates (Corning Costar) corresponding to the experimental set-up. Overnight cultures were plated at 2x10<sup>5</sup>cells/ml while cell cultures incubated for three days (for siRNA treatments) were plated at 1 x10<sup>5</sup>cells/ml. Plated cells were incubated at 37°C and 5% CO<sub>2</sub>.

#### **2.4.3. Determination of the concentration of viable cells in a cell suspension**

To determine the concentration of viable cell in a cell suspension 10µl of cell suspension were diluted in 90µl Trypan Blue (GIBCO). 10µl of the Trypan Blue/cell mixture was pipetted on a Neubauer hemacytometer covered by a coverslip (Hausser Scientific, Bright Line Counting Chamber). Cells in two squares of the 9 square grids were determined under a light microscope (Zeiss, Axiovert 40C) in two separate chambers. The sum was calculated and the concentration of cells was determined by multiplying the average number of viable cells by the hemocytometer constant (1x10<sup>4</sup>cells/ml) and the dilution factor (here 10).

## **2.5. Cell treatments**

### **2.5.1. S2 cell treatments**

Cells were treated with 5µg/ml PGN (InvivoGen) to induce the IMD pathway. To inhibit caspase function S2 cells were incubated with 100µM of the general caspase inhibitor zVAD-FMK in DMSO (R&D Systems) for 3h. For the proteasomal inhibition studies cells were incubated with 50 µM MG132 in DMSO (Sigma) for 3h. 2.5µg/ml cycloheximide (CHX) in DMSO (Sigma) was used to block translation in S2 cells for 0 - 8h before lysis of the cells. To induce apoptosis S2 cells, cells were incubated with 10µg/ml *diap1* dsRNA overnight or with 25µg/ml cycloheximide in DMSO for 8h.

### **2.5.2. Determination of the apoptotic index**

To determine the apoptotic index, approximately 200 S2 cells were counted under a light microscope (Zeiss, Axiovert 40C) and viable cells were distinguished from apoptotic cells by visible membrane blebbing of apoptotic cells. The apoptotic index was then calculated by dividing the number of apoptotic cells in the cell population by the total number of cells.

### **2.5.3. HeLa cell treatments**

Cells were treated with 20ng/ml tumor necrosis factor alpha (TNF-α) (Roche) and 5µg/ml cycloheximide (CHX) (Sigma) for 8h to induce apoptosis.

## **2.6. DNA transfection in cell culture**

### **2.6.1. DNA transfection in S2 cell culture**

For transient transfections, S2 cells were seeded at  $1 \times 10^6$  cells/ml and on the next day  $2 \mu\text{g}$  plasmid DNA per ml of cells was delivered into the cells with Cellfectin II (Invitrogen) following the manufacturer's recommendations. Briefly,  $2 \mu\text{g}$  DNA were mixed with  $100 \mu\text{l}$  SFX-INSECT medium (HyClone) in a microcentrifuge tube. In a second tube  $9 \mu\text{l}$  Cellfectin II were mixed with  $100 \mu\text{l}$  SFX-INSECT medium. Both tubes were incubated for 5 min at room temperature and then mixed together. After 20 min incubation at  $25^\circ\text{C}$  the DNA/transfection mixture was added drop wise to the cells. The cells were carefully mixed and cells were incubated overnight at  $25^\circ\text{C}$ , and analyzed the next day. For stable cell transfections, 3 ml of S2 cells ( $3 \times 10^6$  cells/ml) were co-transfected with plasmid DNA and a hygromycin B resistance selection plasmid (pCoHygro, Invitrogen) at a ratio of 19:1. After 3 days, transfection medium was replaced with fresh medium containing hygromycin B ( $300 \mu\text{g/ml}$ , Sigma). The process was repeated over a period of three weeks for selection of stable transfected cell lines. Cells transfected only with a hygromycin B resistance selection plasmid were used as a control cell line where indicated. Copper-sulphate ( $\text{CuSO}_4$ , pMT)-dependent plasmids were induced by the addition of  $500 \mu\text{M}$   $\text{CuSO}_4$  and incubated at  $25^\circ\text{C}$  for the indicated times. Cells treated with the  $\text{CuSO}_4$  solvent ddH<sub>2</sub>O were used as a control where indicated.

### **2.6.2. DNA transfection in HeLa cell culture**

For transient transfections, HeLa cells were seeded at  $2 \times 10^5$  cells/ml and on the next day  $1 \mu\text{g}$  plasmid DNA was delivered into the cells with Lipofectamin 2000 (Invitrogen) following the manufacturer's recommendations. Briefly,  $1 \mu\text{g}$  DNA were mixed with  $125 \mu\text{l}$  OptiMEM (GIBCO) in a microcentrifuge tube. In a second tube  $2 \mu\text{l}$  Lipofectamin 2000 were mixed with  $125 \mu\text{l}$  OptiMEM. Both tubes were incubated for 5 min at room temperature and then mixed and incubated

together for 15min at room temperature. In the meantime, the cells were washed with 1ml PBS and 250  $\mu$ l OptiMEM was added. After the 15min incubation, the DNA/transfection mixture was added drop wise to the cells. The cells were carefully mixed and incubated for 3. 500 $\mu$ l antibiotic-free culture medium (Sigma, D5796) with 20% FBS (GIBCO) were added and the cells were incubated overnight at 25°C and analysed at the next day.

## **2.7. RNAi treatment**

RNAi allows the inhibition of translation and the subsequent functional analysis of the loss-of-function phenotype. The ablation of a gene of interest is the result of the exposure of cells to dsRNA, which target a specific gene for degradation.

### **2.7.1. dsRNA in S2 cell culture**

The dsRNAs have been described before and are part of the double stranded RNAi library established by Dr. Foley and Prof. O'Farrell in collaboration with the labs of Dr. Davis and Dr. Vale at the University of California, San Francisco. For follow-up analysis dsRNA was generated as described in 2.3.

For targeted gene knock-out S2 cells were seeded at  $0.8 \times 10^6$  cells/ml and incubated with 10 $\mu$ g/ml dsRNAs at 25°C for three days before analysis unless cells were intended to be transiently transfected. In that case, cells were transfected after two days of incubation with dsRNA and placed at 25°C for another day.

Stable cell lines were transfected with 10 $\mu$ g/ml dsRNAs with the Cellfectin II Reagent (Invitrogen) according to the manufacturer's recommendations.

### **2.7.2. siRNA in HeLa cell culture**

siRNA transfections was performed with Dharmafect 1 (Dharmacon) following the manufacturer's recommendations. Briefly, 100µl of 50mM siRNA prediluted in sterile nuclease-free water (HyClone) were added to a well in a 12 well plate. 150µl OptiMEM (GIBCO) were mixed with 2µl Dharmafect 1 transfection reagent and incubated for 5min at room temperature. After the incubation the transfection mixture was added to the plate, carefully mixed with the siRNA, and incubated for another 30min at room temperature. In the meantime cells were counted and  $1 \times 10^5$  cells in 750µl antibiotic-free culture medium were added. The final siRNA concentration was 5nM. Cells were incubated for three days at 37°C and 5% CO<sub>2</sub> in a water jacketed CO<sub>2</sub> incubator.

TARGET GENE PRODUCT	siRNA ID#	TARGET SEQUENCE
non-silencing	negative control#1	proprietary
product caspase-8	Hs_CASP8_11_HP	AAGAGTCTGTGCC CAAATCAA

**Table 2.5. List of siRNAs:** siRNA against human gene product supplied by Qiagen.

## 2.8. Immunoprecipitation

For all immunoprecipitation assays  $1 \times 10^6$  S2 cells were transfected with the appropriate expression plasmids as described above (2.6.1.). On the next day cells were transferred into a 1.5ml microcentrifuge tube and placed in a centrifuge at  $1000 \times g$  for 3min. Cells were then lysed in 200 $\mu$ l lysis buffer (50mM HEPES (pH 7.5), 10mM EDTA (pH 8), 50mM KCl, 50mM NaCl, 1mM  $MgCl_2$ , 0.1% Nonidet P-40, protease inhibitors (Roche inhibitor cocktail tablets), phosphatase inhibitors (Sigma, phosphatase inhibitor cocktail) for 10 min at 4 °C. After clearing the sample of cell debris and cell wall residues by centrifugation at maximum speed for 10min at 4°C, rabbit anti-myc (Sigma, 1:500) or mouse anti-HA (Sigma, 1:500) was added to the supernatant and samples were rocked at 4°C overnight. On the next day, Protein G Sepharose (Amersham Biosciences) beads were added and incubated with the supernatant for 1h at 4°C. Beads were pelleted by centrifugation at  $300 \times g$  for 30sec and washed in lysis buffer three times. After discarding the supernatant, beads were resuspended in 2x sample buffer. Prior to analysis by Western blot, all samples were boiled for 5min at 95°C. 10 $\mu$ l of the input and immunoprecipitated sample were analysed on SDS-PAGE (2.10.).

## 2.9. Quantitative real-time PCR (qRT-PCR)

### 2.9.1. RNA purification

Total RNA was isolated from  $1 \times 10^6$  S2 cells or 10 flies using Trizol (Invitrogen) according to manufacturer's recommendations.  $1 \times 10^6$  S2 cells were transferred to a 1.5ml microcentrifuge tube and spun in a multi-purpose centrifuge (Eppendorf, 5810R) for 2min at  $1,000 \times g$  and room temperature. The supernatant was removed and 200 $\mu$ l Trizol was added and the mixed by pipetting up and down. After 5min of incubation the sample was spun in a bench top for 1 min at  $12,000 \times g$  and 4°C. The cleared homogenate was transferred to a new tube and the samples were mixed vigorously after the addition of 40 $\mu$ l chloroform (Fisher

Scientific). After a 3min incubation at room temperature the samples were spun in a bench top for 15min at 12,000 x g and 4°C. The upper aqueous upper phase was transferred into a new microcentrifuge tube and the RNA was precipitated by the addition of 100µl isopropanol. After mixing the samples the isopropanol/RNA mixture was incubated at room temperature for 10min and stored overnight at -20°C. On the next day the samples were spun for 10min at 12,000 x g and 4°C. The samples were washed once with 100µl 75% EtOH and re-spun for 5min at 7,500 x g and 4°C. The samples were air dried for 5min and dissolved in 2 µl nuclease-free water (HyClone). To eliminate DNA residues, RNA was treated with 0.5µl DNase I (Invitrogen) and incubated in a 37°C water bath for 1h.

To purify RNA from flies, 10 flies were mashed in 250µl Trizol. The next steps followed the same procedure as described for S2 cells. Volumes were adjusted accordingly.

### **2.9.2. Measurement of RNA concentration and purity**

To determine the unknown concentration of RNA in solution, the RNA was diluted 1:100 in water and measured at the absorbance of 260nm (A260) and 280 m (A280) in a spectrophotometer (Jenway, Genova). Water was used as a reference. The RNA concentration [RNA] was calculated with the following formula. A ratio of ~2.0 is generally accepted as “pure” for RNA.

$$[\text{RNA}] (\mu\text{g/ml}) = A260 \times \text{dilution factor (here: 100)} \times 40\mu\text{g/ml}$$

The purity of the RNA (RNA<sub>p</sub>) was determined by the following calculation:

$$\text{RNA}_p = A260 / A280$$

### **2.9.3. Synthesis of cDNA**

For cDNA synthesis 3µg RNA isolated from S2 cells or 5µg RNA isolated from flies were used to synthesis cDNA with qScript cDNA SuperMix (Quanta Biosciences) according to the manufacturer’s recommendations. 8µl of 5µg RNA diluted in nuclease-free water (HyClone) were mixed with 2µl 5x qScript cDNA

SuperMix (Quanta Biosciences) and incubated in a Mastercycler ep gradient S thermocycler (Eppendorf) under the following conditions: 25°C for 5min, 42°C for 30min, and 85°C for 5min, followed by a hold at 4°C.

#### 2.9.4. qRT-PCR with the SYBR green method

Transcript amplification was monitored with PerfeCTa SYBR Green FastMix (Quanta Biosciences) using an Eppendorf realplex 2 PCR machine and the primers indicated in table 2.5. Each reaction was set up in a well of a full-skirted 96-well PCR plate (twin.tec 0030132521; Eppendorf) that was covered with heat sealing film (Eppendorf, 30127854) with a heat sealer (Eppendorf, 951023078). The reaction was mixed and spun for 1min at 5,000 x g and 4°C. The reaction was set up as followed:

2.5µl diluted cDNA

2.5µl 1.6µM of forward and reverse primer (table 2.6.)

5.0µl 2X PerfeCTa SYBR Green FastMix (Quanta Biosciences)

Transcript amplification was performed with the following 2-step PCR program: 1 cycle 95°C for 2min, 40 cycles of 95°C for 15s and 60°C for 1min. Technical triplicates for the gene of interest and the housekeeping gene actin were measured. To quantify relative expression values, the mean of the technical triplicates was calculated and all samples were normalized to the reference gene expression level (here *actin*):

$$\Delta C_T (\text{sample}) = C_T \text{ target gene} - C_T \text{ reference gene}$$

$$\Delta C_T (\text{control}) = C_T \text{ target gene} - C_T \text{ reference gene}$$

The  $\Delta C_T$  values of each gene of interest were then normalized to the experimental control:

$$\Delta\Delta C_T = C_T (\text{sample}) - C_T (\text{control})$$

The normalized target gene expression level in sample were used to calculate the relative expression level of the gene of interest =  $2^{-\Delta\Delta C}$

NAME	PRIMER SEQUENCE
<i>actin</i> forward	5'-TGCCTCATCGCCGACATAA-3'
<i>actin</i> reverse	5'-CACGTCACCAGGGCGTAA-3'
<i>attacin</i> forward	5'-AGTCACAACCTGGCGGAAC-3'
<i>attacin</i> reverse	5'-TGTTGAATAAATTGGCATGG-3'
<i>dipteracin</i> forward	5'-ACCGCAGTACCCACTCAATC-3'
<i>dipteracin</i> reverse	5'-ACTTTCCAGCTCGGTTCTGA-3'
<i>puckered</i> forward	5'-GCCACATCAGAACATCAA-3'
<i>puckered</i> reverse	5'-CCGTTTTCCGTGCATCTT-3'
<i>mmp-1</i> forward	5'-ACGACTCCATCTGCAAGGAC-3'
<i>mmp-1</i> reverse	5'-GGAGATGAGCTGTGGGTA-3'
<i>dredd</i> forward	5'-CTCAAATGTTTTGGGCCTCTG-3'
<i>dredd</i> reverse	5'-CCGCCAGTGAACACATCGC-3'

**Table 2.6. List of qRT-PCR primer sequences used in qRT-PCR assays:**  
Primer sequences in alphabetical order.

### **2.9.5. Boxplots**

A boxplot presents data distribution, its central value and variability without making assumptions about their statistical significance. Specifically, boxplots show the most extreme values in a data set (maximum and minimum values), the lower and upper quartile and the median. The centerline indicating the median value in each data set and the top and bottom of the box represent the upper and lower quartiles, respectively. The top and bottom whiskers indicate the maximum and minimum values in a data set, respectively.

## **2.10. SDS-PAGE and Western blotting**

### **2.10.1. Sample preparation**

For protein analysis,  $1 \times 10^6$  S2 cells or 5 flies were lysed in 2x sample buffer (50 $\mu$ l for cells and 70 $\mu$ l for flies) and boiled for 5min at 95°C.  $2 \times 10^5$  HeLa cells were lysed in 100 $\mu$ l lysis buffer 2 for HeLa cells and 50 $\mu$ l 2x sample buffer was added before the samples were boiled for 5min at 95°C. Then samples were stored at -20°C.

### **2.10.2. SDS-PAGE**

All protein samples were analysed with sodium dodecyl sulphate-polyacrylamide gel electrophoresis (SDS-PAGE) using the Mini-PROTEAN 3 system (Bio-Rad). 5-10 $\mu$ l of the sample were analysed on a 1.00 mm 8-10% SDS-polyacrylamide gel corresponding to the expected protein size (table 2.1.). The Precision Plus Protein Standard (Bio Rad) was loaded on each gel as a molecular weights marker. The SDS-PAGE was run in a Mini-PROTEAN chamber filled with SDS-PAGE running buffer. The gel was run with a constant current of 25mA per gel till the bromophenol blue line run out the gel (~1.5h).

### **2.10.3. Transfer**

Each SDS-PAGE was transferred to a nitrocellulose membrane by semi-dry transfer in a Trans-Blot SD Semi-Dry Transfer Cell (Bio-Rad). The gel was soaked in western blot transfer buffer and placed on 3 sheets of chromatography paper (Fisherbrand), and one nitrocellulose membrane (pre-soaked in water). The gel was covered with another 3 sheets of chromatography paper and transferred for 20min (smaller proteins, >60kDa) to 25min (bigger proteins, <60kDa) at a constant voltage of 20V and a current of 0.4mA per gel. Maximal four gels were transferred in one transfer run.

### **2.10.4. Western blotting**

After the protein transfer, the nitrocellulose membrane was transferred into PBS and subsequently blocked in 4ml blocking buffer (LI-COR Biosciences, 1:1 in PBS) for 1h on an orbital shaker with gentle agitation. The membrane was probed with specific antibodies in blocking buffer and 0.1% Tween-20 (table 2.7.) overnight on an orbital shaker with gentle agitation at 4°C.

ANTIBODY	TYPE	SUPPLIER	CONCENTRATION
Caspase-8, 1C12	M, MC	Cell Signaling, #9746	1:1,000
Flag	R, MC	Cedarlane	1:1,000
HA	M, MC	Sigma, H9658	1:4,000
JNK	R, PC	Santa Cruz Biotechnology, sc-571	1:4,000
Myc	R, MC	Sigma, C3956	1:5,000
pan-actin	R, PC	Cell Signaling, #4968	1:1,000
PARP1, C2-10*	M, MC	Trevigen, #4338-MC-50	1:2,000
P-JNK	M, MC	Cell Signaling, 9255S	1:2,000
P-Relish	R, PC	Silverman, N. et al. 2009 (Proc Natl Acad Sci USA)	1:1,000
Relish	M, MC	DSHB	1:1,000
Tubulin, E7	M, MC	DSHB	1:1,000

**Table 2.7. List of primary antibodies used in Western blot assays:** Primary antibody list in alphabetical order. \*8M urea in sample buffer, M = mouse, R = rabbit, MC = monoclonal, PC = polyclonal, DSHB = Developmental Studies Hybridoma Bank

On the next day, the membrane was washed three times for 5min in PBT and then incubated with secondary antibodies conjugated to Alexa Fluor 750 or Alexa Fluor 680 (Invitrogen, 1:10000) in 3ml PBT with 1ml blocking buffer for 30min - 1h on an orbital shaker under gentle agitation. The membrane was washed three times in PBT for 5min and a final wash in PBS. The Proteins were visualised with a Licor Aeries automated infrared imaging system (LICOR Biosciences) and Aeries 1.0 software (LI-COR Biosciences). The membrane was scanned at 700nm for Alexa Fluor 680 conjugated secondary antibodies and at 800nm for Alexa Fluor 750 conjugated secondary antibodies at a resolution of 200 $\mu$ m, and the focus offset of 3.0mm (table 2.8.).

ANTIBODY	TYPE	SUPPLIER	CONCENTRATION
AlexaFluor 680 G anti-M IgG	G	Molecular Probes, A21057	1:10,000
AlexaFluor 680 G anti-R IgG	G	Molecular Probes, A21076	1:10,000
AlexaFluor 750 G anti-M IgG	G	Molecular Probes, A21037	1:10,000
AlexaFluor 750 G G anti-R IgG	G	Molecular Probes, A21039	1:10,000

**Table 2.8. List of secondary antibodies used in Western blot assays: G = goat, M = mouse, R = rabbit.**

### 2.10.5. In cell western

Plate-based quantitative analysis was carried out as described previously<sup>146,353</sup>. Briefly,  $1 \times 10^6$  cells/ml were plated in a 96well plate in a total volume of 150 $\mu$ l serum-free media. Cells were then fixed in 3.7% formaldehyde (Sigma) and solubilized in 0.1% Triton X-100. Rabbit anti-JNK and mouse anti-phospho-JNK primary antibodies were used to stain proteins, which were visualized with Alexa-fluor 750 or 680-coupled secondary antibodies using the Licor Aeries automated infrared imaging system (2.10.4.).

### 2.11. TMRE assay for the detection of the IMM potential

1.125 x 10<sup>5</sup> HeLa cells were plated into each well of a 12 well plate and transfected with siRNA as described in 2.2.6. After three day incubation with the siRNA apoptosis was induced with 20ng/ml TNF and 5 $\mu$ g/ml CHX for 8h. In the last hour of the TNF/CHX stimulation cells were incubated with 2 $\mu$ M tetramethylrhodamine ethyl ester (TMRE, Molecular Probes) in 500 $\mu$ l culture medium for 30min at 37°C and 5% CO<sub>2</sub> in a water jacketed CO<sub>2</sub> incubator. After incubation with TMRE, the culture medium containing the cells was collected into a 5ml round bottom tube (12 x 75mm, 352054; Fisherbrand). The remaining cells in the well were washed off with 500 $\mu$ l 37°C PBS and added to the same reaction tube. The attached cells in the well were detached with 250 $\mu$ l 37°C 0.25% Trypsin-EDTA incubated for 5 to 10min at 37°C. The mixture was added to the same tube and the cells were spun in a multi-purpose centrifuge (Eppendorf, 5810R) for 2min at 1,000 x g and room temperature. After removing the supernatant the pellet was washed in 1ml PBS, respun for 2min at 1,000 x g, and resuspended in 500 $\mu$ l PBS. Apoptotic cells were determined by flow cytometry (FACScan, Becton Dickinson) in the Faculty of Medicine and Dentistry Flow Cytometry Facility (University of Alberta). TMRE negative cells were used for calibration. The level of TMRE fluorescence was detected through the FL-2 channel equipped with a 585nm filter (42nm band pass). Data were acquired on

10,000 cells with fluorescence at logarithmic gain and analyzed with the CellQuest software (BD Biosciences).

## 2.12. Fly lines and fly husbandry

All *Drosophila* fly stocks were cultured on standard cornmeal medium (<http://flystocks.bio.indiana.edu/>) at 25°C (Table 2.9.). For caspase activity studies, *UASp35/CyO* flies were crossed to *yolkGAL4* flies and the progeny were separated by gender 3-5 days after hatching and analysed by qRT-PCR. For UASHADredd expression studies *UASHADredd* flies were crossed to *cgGAL4* or *dredd;cgGAL4* flies and the 3-5 day old progeny were lysed in 2x sample buffer for Western blotting. For the temperature sensitive induction of transgenes UAS-lines with the transgene(s) of interest were crossed to *cgGAL4;GAL80[ts]* or *dredd;cgGAL4;GAL80[ts]* flies. Temperature sensitive crosses were kept at 18°C. 3-5 days after hatching, male flies were transferred to 29°C for the desired time to induce transgene expression. Flies were analysed by qRT-PCT as described in 2.9.

*w<sup>1118</sup>*, *dredd<sup>B118</sup>*, *cgGAL4*, *dredd<sup>B118</sup>;P[dredd+]*, *cgGAL4;GAL80[ts]*, and *yolkGAL4* fly stocks have been described elsewhere<sup>108,130,354-356</sup>. *UASDredd*, *UASDreddCA*, *UASHADredd*, and *UASImdcl* transgenic lines were generated by Gateway LR clonase reaction (Invitrogen) of a Gateway entry clone for each construct with a Gateway destination clone (Table 2.3.) following the manufacturer's recommendations. The DNA construct were sent out to BestGene for the generation of individual stable transformants (BestGene Inc 2140 Grand Ave., Suite#205 Chino Hills, CA91709 U.S.A.).

FLY LINE	GENOTYPE	SOURCE
<i>cgGAL4</i>	<i>w,P{w[+mC]=cgGAL4.A};</i>	Kirst King-Jones
<i>cgGAL4;GAL80[ts]</i>	<i>w,P{w[+mC]=cgGAL4}; P{w[+mC]= tubPGAL80ts}</i>	homemade
<i>dredd<sup>B118</sup></i>	<i>y,w,dredd<sup>B118</sup>;;</i>	Bruno Lemaitre
<i>dredd<sup>B118</sup>,P[dredd+]</i>	<i>y,w,dredd<sup>B118</sup>,P{dredd+};;</i>	John M. Abrams
<i>UASDredd</i>	<i>w,P{w[+mC]=UASdredd};</i>	homemade (BestGene)
<i>UASDredd</i>	<i>w;;P{w[+mC]=UASdredd}</i>	homemade (BestGene)
<i>UASDreddCA</i>	<i>w,P{w[+mC]=UASdreddC408A};</i>	homemade (BestGene)
<i>UASDreddCA</i>	<i>w;;P{w[+mC]=UASdreddC408A}</i>	homemade (BestGene)
<i>UASHADredd</i>	<i>w;;P{w[+mC]=UASHAdredd}</i>	homemade (BestGene)
<i>UASImdcl</i>	<i>w;;P{w[+mC];UASimdcl};</i>	homemade (BestGene)
<i>UASp35</i>	<i>w;;P{w[+mC]=UASp35}/CyO;</i>	Bloomington stock center
<i>w<sup>1118</sup></i>	<i>w[1118];;</i>	Bloomington stock center
<i>yolkGAL4</i>	<i>y,w,P{w[+mC]=yolkGAL4};</i>	Jean Marc Reichhart

**Table 2.9. List of fly lines.** Genotype and source of fly lines in alphabetical order.

### **2.12.1. Septic injury**

For infection studies, flies were stabbed with a sharpened tungsten needle dipped in a pellet of an overnight *E. coli* DH5 $\alpha$  culture. Flies were then recovered at 25°C for the indicated times depending on the experimental approach before further analysis.

### **Chapter 3. The role of Dredd in *Drosophila* IMD signaling in cell culture**

**Results presented in this chapter are partially reflected in the following publication:**

**Guntermann, S.,** and Foley, E. The Protein Dredd Is an Essential Component of the c-Jun N-terminal Kinase Pathway in the *Drosophila* Immune Response. *J Biol Chem.* 2011 **286(35)**: 30284-94.

### 3.1. Background

The IMD pathway is an immune response pathway in flies activated by pathogen-associated molecules, such as PGN. Detection of bacterial PGN initiates Imd signaling and triggers the downstream activation of Rel-dependent and dJNK-dependent arms that induce the expression of immune response genes<sup>10</sup>. In contrast to the extensive molecular, genetic and cell biological studies of IMD/Rel activation, the IMD/dJNK arm remains relatively understudied. To advance our understanding of IMD/dJNK activation, our laboratory recently performed a whole-genome RNAi screen for IMD/dJNK modifiers in a *Drosophila* tissue culture cell line<sup>146</sup>. We found that depletion of *dredd* resulted in a loss of PGN-dependent phosphorylation of dJNK in cell culture. Our observations are in line with a previous tissue culture study that indicated a requirement for Dredd in the phosphorylation of dJNK through the IMD pathway<sup>113</sup>. These results suggest a general requirement for Dredd in the activation of the IMD/dJNK arm in the *Drosophila*. However, there are no data on the involvement of Dredd in the IMD/dJNK transcriptional response to PGN stimulation, the epistatic relationship of Dredd and additional IMD/dJNK members remains unexplored, and follow-up experiments to elucidate the mechanism of Dredd-mediated dJNK activation have not been performed.

To address these questions, I asked if Dredd is essential for IMD/dJNK activation in cell culture. In addition, I designed experiments to investigate where and how Dredd interferes with the IMD signaling cascade.

### 3.2. Dredd is an essential component of the IMD/dJNK pathway in cell culture

#### 3.2.1. Dredd is required for IMD/dJNK activation in cell culture

Recognition of PGN activates the *Drosophila* NF- $\kappa$ B protein Rel and the dJNK cascade<sup>10</sup>. dJNK activation is important for the induction of immune-induced genes, such as *mmp1*, *punch*, and *puckered*<sup>98,107,139,140</sup>. Activation of the dJNK

pathway can be monitored at different steps of the kinase cascade (Figure 3.1.A) for example the phosphorylation of dJNK or the induction of IMD/dJNK responsive gene transcripts. To investigate Dredd involvement in dJNK signaling I initially tested if the *Drosophila* macrophage-like S2 cell line reproduces the typical dynamics of dJNK/IMD activation (Figure 3.1.A). S2 cells are phagocytic cells with many features of a macrophage-like lineage. The S2 cell line is derived from a primary culture of *Drosophila* embryos and it is commonly used to examine molecular processes of a cell.

To follow the phosphorylation dynamics of S2 cells over time I monitored P-dJNK levels after stimulation with commercial preparations of PGN in a quantitative plate-based assay (Figure 3.1.B). I stimulated S2 cells with PGN for different times and probed the cells with P-dJNK and total dJNK specific antibodies. PGN triggered robust phosphorylation of dJNK after 10 min of stimulation. P-dJNK levels then declined over time and were close to levels seen in untreated cells by 120 min after stimulation. Quantifications of P-dJNK levels relative to total dJNK levels confirm a transient induction of P-dJNK over time. P-dJNK level peaked at 10 min after induction with a 7 fold increase in P-dJNK:dJNK relative to untreated cells (Figure 3.1.C). In addition, qRT-PCR analysis of S2 cell lysates that were stimulated with PGN showed a transient induction of the IMD/dJNK responsive transcripts *puc* and *mmp-1* (Figure 3.3.D and E). *puc* and *mmp-1* transcript levels peaked after 45 min of PGN stimulation and slowly declined to baseline-levels over a 6 h time period of PGN treatment. In conclusion, *Drosophila* S2 cells recapitulate two important features of IMD/dJNK activation, dJNK phosphorylation and induction of downstream transcripts. In addition, a recent publication by our lab established a quantitative plate-based assay to monitor dJNK phosphorylation events in S2 cells. Therefore I feel comfortable that S2 cells reflect the natural dynamics of IMD/dJNK activation in response to PGN and that they offer a suitable tool to investigate the molecular processes of IMD signaling.

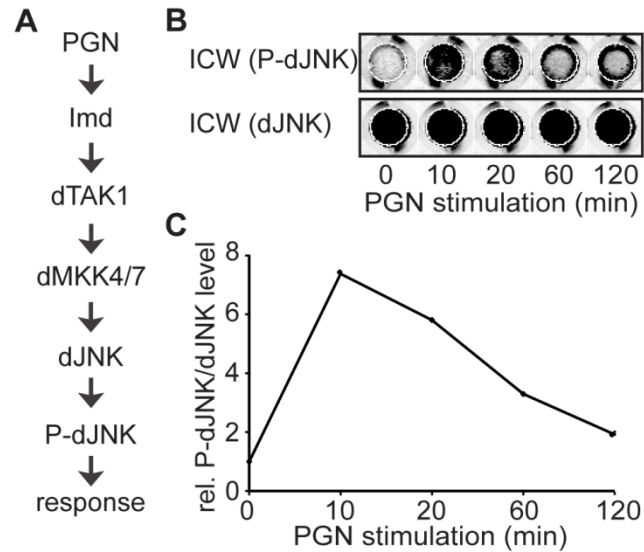


**Figure 3.1. PGN induces a transient Phospho-dJNK response in cell culture:** **A.** Flowchart of molecules activated in the IMD/dJNK signaling pathway after PGN stimulation. **B.** In Cell Western (ICW) analysis of S2 cells stimulated with PGN for the indicated times. Protein levels were visualised with P-dJNK (upper box) and total dJNK (lower box) specific antibodies. **C.** Relative quantification of P-dJNK levels visualized in A. The relative levels of P-dJNK protein for S2 cells at the indicated time points after stimulation with PGN are shown. The P-dJNK:total dJNK level at 0 min were assigned a value of 1 and all other levels are reported relative to this value. Stimulation with PGN induced a transient dJNK phosphorylation in S2 cells.

Several reports suggested that Dredd is required for proteolytic activation of Rel<sup>125,126,128</sup>. However, two recent studies in *Drosophila* tissue culture cells suggest a separate requirement for Dredd in the phosphorylation of dJNK through the IMD pathway<sup>113,146</sup>. To explore the requirements for Dredd in dJNK/IMD signaling, I analyzed how RNA interference (RNAi)-mediated depletion of *dredd* influences activation of dJNK in the S2 cell line.

RNAi is a powerful tool to investigate gene function by the specific inhibition of transcript expression and the subsequent functional analysis of the loss-of-function phenotype. The ablation of a protein of interest is the result of the exposure of cells to short dsRNA (typically >200 nt), which target a specific mRNA for degradation. S2 cells take up dsRNA through receptor-mediated endocytosis without a need for transfection<sup>357</sup>. To confirm the efficiency of *dredd* dsRNA I transfected S2 cells with Myc-tagged Imd, Dredd, or DreddCA expression constructs that were incubated with a control dsRNA or *dredd* dsRNA. The control dsRNA has been validated in a recently performed screen by our laboratory<sup>146</sup>. I analyzed S2 cell lysates of the transfected cells by Western blot (Figure 3.2.A). As expected incubation of S2 cells with *dredd* dsRNA did not have off-target effects towards Imd. Importantly, *dredd* dsRNA abolishes Dredd protein. Quantification of the protein levels relative to total dJNK levels showed about an 80% reduction of MycDredd, or MycDreddCA protein level compared to control cells (Figure 3.2.B).

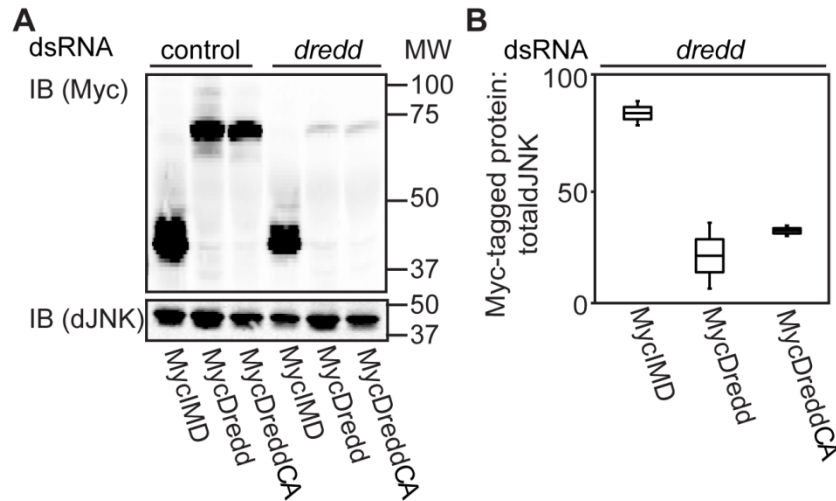


**Figure 3.2. RNAi-mediated depletion of *dredd* substantially eliminates Dredd protein:** **A.** Western blot analysis of lysates from S2 cells transfected with Myc-tagged expression constructs as indicated and incubated with control dsRNA (lanes 1-3) or *dredd* dsRNA (lanes 4-6). Lysates were probed with antibodies that detect Myc (upper panel) and total dJNK (lower panel) as a loading control. Molecular weights are indicated on the right of each panel. **B.** Relative quantification of protein levels visualized in A. The relative protein levels of Myc-tagged expression construct for S2 cells treated with control or *dredd* dsRNA are shown. The Myc-tagged protein:total dJNK level in control cells were assigned a value of 1 and levels in *dredd* depleted cells are reported relative to this value. Measurements illustrate the results of two independent experiments. *dredd* dsRNA depletes Dredd protein in S2 cells.

I next investigated if the depletion of *dredd* alters the activation of dJNK signaling. To activate the dJNK/IMD pathway, I incubated S2 cells with PGN (Figure 3.3.A). As expected, treatment of S2 cells with PGN resulted in Rel cleavage, Rel phosphorylation, and a transient phosphorylation of dJNK (Figure 3.3.B). In agreement with the requirement for Dredd in IMD/Rel activation, *dredd* depletion blocked Rel cleavage and Rel phosphorylation. In addition, *dredd* depletion from S2 cells fully inhibited phosphorylation of dJNK.

While these observations validate a general requirement for Dredd in PGN-mediated phosphorylation of dJNK, there are no data on the involvement of Dredd in the dJNK component of the IMD pathway transcriptional response to PGN. To address this question, I examined the expression of the dJNK-responsive transcripts *puc* and *mmp-1* in control S2 cells or S2 cells pre-treated with *dredd* dsRNA and incubated with PGN for various periods (Figure 3.3 C-F). Differences in passage numbers of my S2 cells caused minor variability in the relative induction of PGN-responsive transcripts in replicate assays. Nonetheless, each transcript showed a stereotypical and reproducible response to PGN. For example, stimulation of S2 cells with PGN repeatedly resulted in a gradual induction of the IMD/Rel-dependent AMP *att* and *dipt* (Figure 3.3.C-D). In contrast, IMD/dJNK activation resulted in a rapid and transient induction of *puc* and *mmp-1* (Figure 3.3.E-F). As expected, I detected a considerable drop in the PGN-mediated induction of *att* and *dipt* in S2 cells treated with *dredd* dsRNA (Figure 3.3.C-D). Likewise, depletion of *dredd* greatly decreased the expression of the dJNK-dependent transient response genes *puc* and *mmp-1* (Figure 3.3.E-F). Thus, my cell culture data confirm a role for Dredd in the activation of dJNK through the IMD pathway, and establish an essential role for Dredd in the dJNK arm of the IMD pathway transcriptional response.

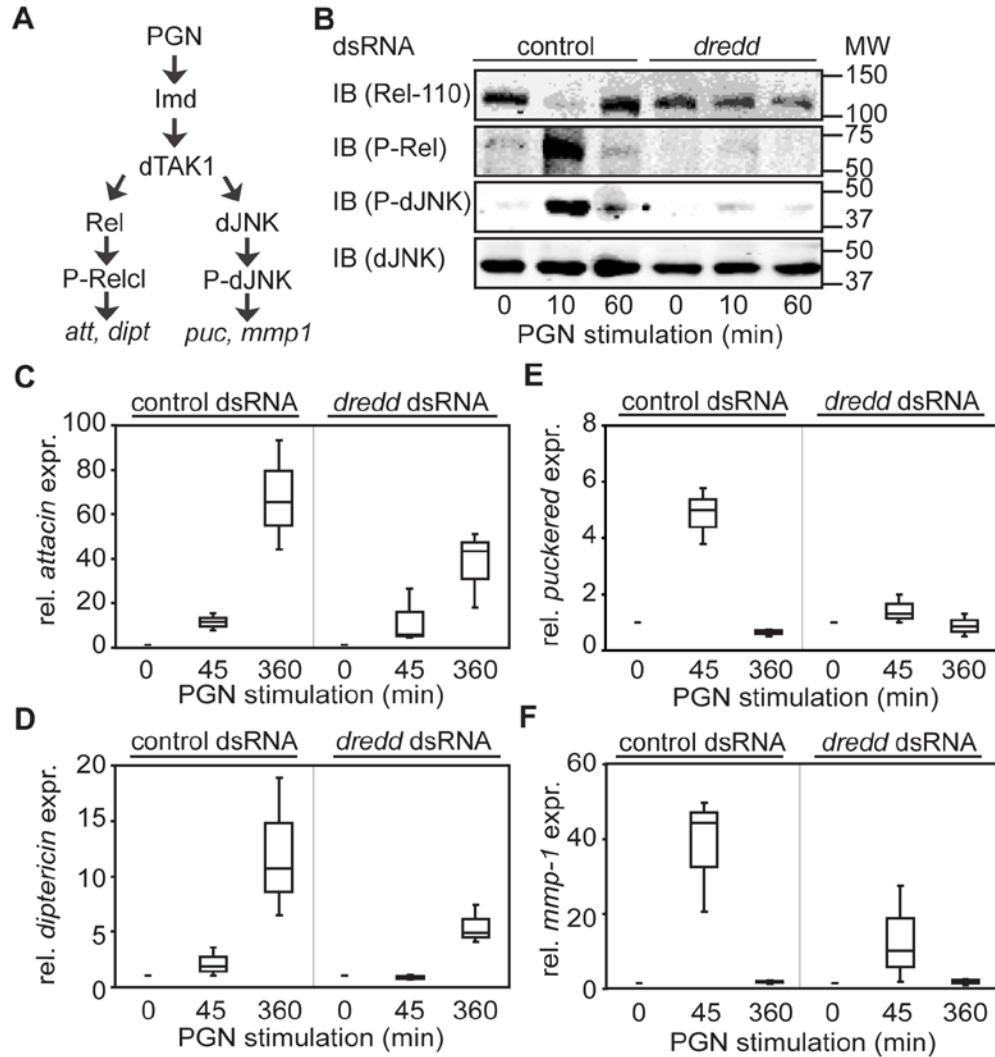


**Figure 3.3. Dredd is required for IMD/dJNK activation in cell culture: A.** Flowchart of molecules activated in IMD/Rel and IMD/dJNK signaling pathway after PGN stimulation. **B.** Western blot analysis of lysates from S2 cells incubated with control dsRNA (lanes 1-3) or *dredd* dsRNA (lanes 4-6) and stimulated with PGN for the indicated times. Lysates were probed with antibodies that detect Rel-110 (first panel), P-Rel (second panel), P-dJNK (third panel), and total dJNK (fourth panel) as a loading control. Molecular weights are indicated on the right of each panel. **C-F.** Quantitative real time PCR analysis of control cells and *dredd* depleted S2 cells, stimulated with PGN and recovered for the indicated times. The relative expression levels for *attacin*, *diptericin*, *puckered*, and *mmp-1* are standardized to *actin* levels. Values of control cells and *dredd* depleted cells at the indicated time points after PGN stimulation are reported relative to unstimulated control cells and *dredd* depleted cells, respectively. Measurements for each transcript are presented as a box plot to graphically illustrate the results of three independent experiments.

### 3.2.2. Baculovirus p35 inhibits Dredd-dependent activation of dJNK in cell culture

Dredd is the caspase molecule in IMD signaling essential to resist gram-negative bacterial infection in flies. More specifically, processing of the NF- $\kappa$ B molecule Rel depends on Dredd. In addition, Rel is cleaved at a consensus caspase cleavage site and Rel cleavage can be blocked with caspase specific inhibitors, such as the baculovirus pan-caspase inhibitor protein p35<sup>116</sup>. P35 is a cell survival protein found in several types of baculoviruses. Despite its natural inhibitory competence in the virus, p35 has been shown to specifically blocks endogenous caspase function in other species ranging from *C.elegans* to *H.sapiens*<sup>214</sup>.

As the molecular basis of Dredd-dependent dJNK activation is unclear, I asked if caspase activity is essential to induce dJNK-dependent immune responses. Specifically, I asked if the baculovirus pan-caspase inhibitor p35 blocks IMD/dJNK activation in cell culture.

To this end, I generated an S2 cell line that constitutively expresses p35 (Figure 3.4.A). I determined the extent to which p35 blocks PGN-mediated phosphorylation of dJNK in a quantitative plate-based assay. PGN-mediated phosphorylation of dJNK was markedly impaired in S2 cells that express p35 compared to control S2 cells (Figure 3.4.B). Quantifications of P-dJNK levels relative to total dJNK levels illustrate a robust reduction in dJNK phosphorylation in cells that express p35 (Figure 3.4.C). The residual phosphorylation of dJNK in cells that expressed p35 is likely a consequence of the fact that stable S2 cell lines are not clonal and the expression levels of transgenic constructs vary across cells in a given population. Western blot analysis showed a robust reduction in PGN-mediated phosphorylation of dJNK in p35 expressing cells compared to control cells (Figure 3.4.D).

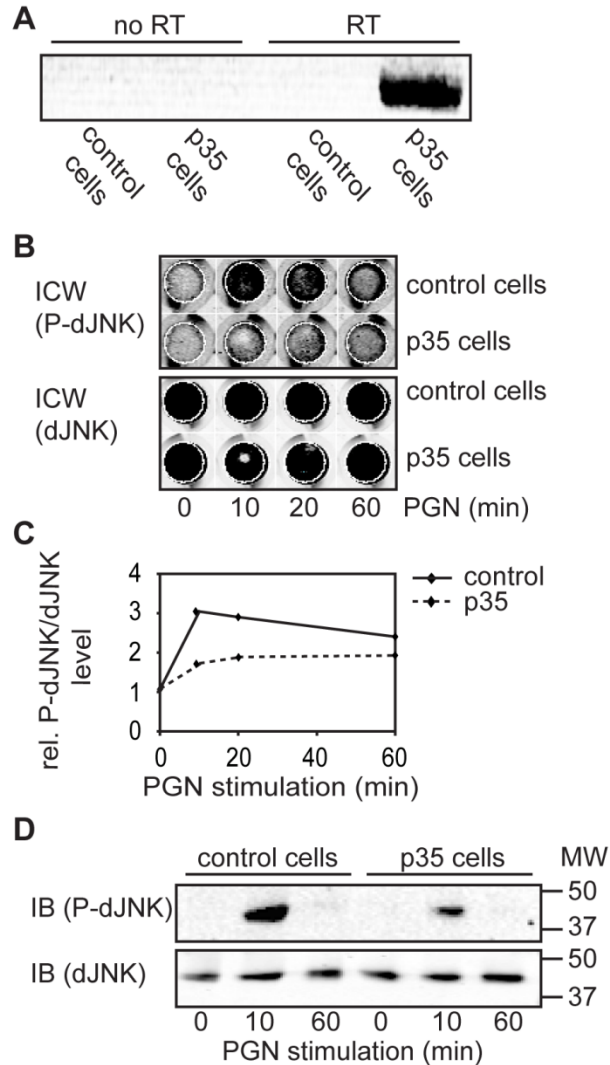


**Figure 3.4. Baculovirus p35 prevents Phospho-dJNK in cell culture: A.** Agarose gel electrophoresis of RT-PCR products amplified from RNA extracted from control S2 cells (lane 1 and 3) or S2 cells that were stably transfected with a Baculovirus *p35* expression plasmid (lane 2 and 4) using *p35* specific primers. cDNA was generated without (lane 1 and 2) or with (lane 3 and 4) adding reverse transcriptase (RT) enzyme. *P35* is only expressed in stably transfected cells. **B.** In Cell Western analysis of control cells (upper panel of each box) and cells stably transfected with a Baculovirus *p35* expression plasmid (lower panel of each box) and stimulated with PGN for the indicated times. Cells were stained with P-dJNK (upper box) and total dJNK (lower box) specific antibodies. **C.** Quantification of P-dJNK levels visualized in B. The relative levels of P-dJNK protein for control cells (upper row of each plate) and cells stably transfected with a Baculovirus *p35* expression plasmid (lower row of each plate) at the indicated time points after stimulation with PGN are shown. For control cells and *p35*-expressing cells the P-dJNK:total dJNK level at 0 min were assigned a value of 1

and all other levels are reported relative to this value. **D.** Western blot analysis of lysates from control cells (lane 1-3) and cells stably transfected with a Baculovirus *p35* expression plasmid (lane 4-6), and stimulated with PGN for the indicated times are shown. The membrane was probed with total dJNK (lower panel) and P-dJNK (upper panel) specific antibodies. Molecular weights are indicated on the right of each panel.

I expanded my studies to determine if p35 affects the IMD/dJNK-responsive transcriptional pathway. For these experiments, I generated an S2 cell line that constitutively expresses an HA-tagged p35 variant. I consistently found that PGN-dependent transcriptional levels of the Rel-responsive AMP *dipt* and *att* and the induction of dJNK-responsive transcripts *mmp-1* and *puc* were reduced in S2 cells that express HAp35 compared to control S2 cells (Figure 3.5.A-D).

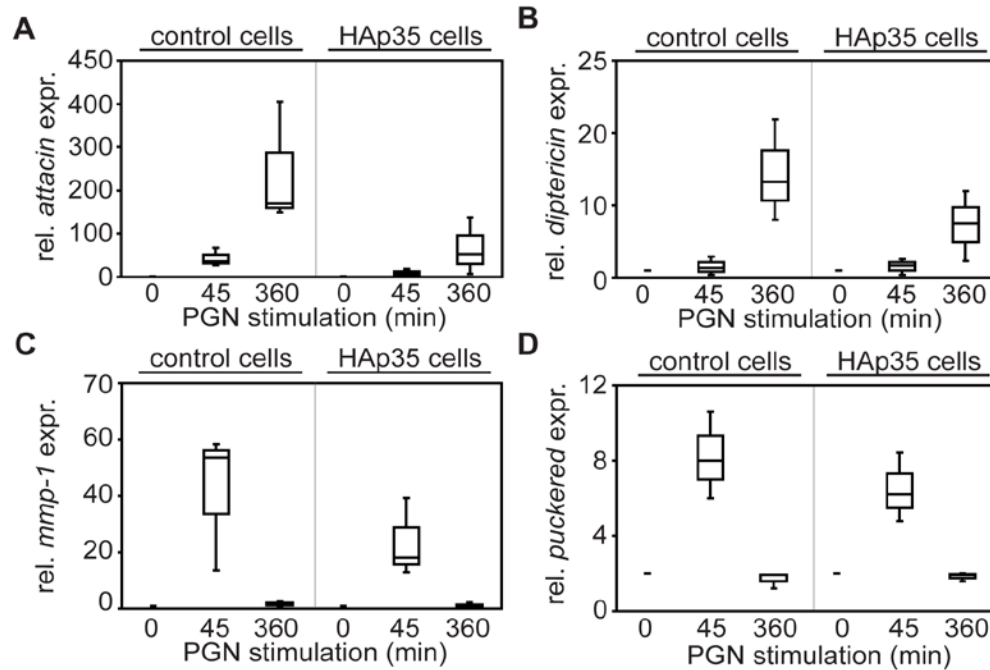


**Figure 3.5. Baculovirus p35 blocks transcriptional induction of dJNK-dependent transcripts in cell culture: A-D.** Quantitative real time PCR analysis of control cells and S2 cells stably transfected with a Baculovirus *p35* expression construct stimulated with PGN for the indicated times. The relative expression levels for *attacin* (A), *dipteracin* (B), *mmp-1* (C), and *puckered* (D) are standardized to *actin* levels. Values of control cells and *p35* expressing cells at the indicated time points after PGN stimulation are reported relative to unstimulated control cells and *p35* expressing cells, respectively. Measurements for each transcript are presented as a box blot to graphically illustrate the results of three independent experiments.

In line with my observations with untagged p35, I detected considerably less phosphorylation of dJNK in response to PGN in cells that stably express HAp35 compared to control cells (Figure 3.6.A, upper panel). Caspase inhibition by p35 requires the caspase-mediated cleavage of the p35 reactive site loop and the formation of a stable p35:caspase complex that consists of a 25 kDa cleavage product of p35 and a mature caspase<sup>214,224</sup>. In my assays, I did not detect processing of p35 to the 25 kDa product typically found in complex with inhibited caspases. This finding prompted me to ask if HAp35 and Dredd form a molecular complex. In co-immunoprecipitation assays I showed that immunoprecipitation of HAp35 co-precipitated MycDredd and to a lesser extent a proteolytically inactive MycDredd variant (Figure 3.6.B, lanes 9 and 10). The proteolytically inactive form of Dredd was generated by the introduction of a mutation in the active site cysteine of Dredd (MycDreddCA). In both cases, the co-purified caspase corresponded to the full-length variant. I consider these findings noteworthy, as p35 typically interacts with processed, mature caspases and the established paradigm for p35 action suggests that it acts as a suicide inhibitor of proteolytically active caspases.

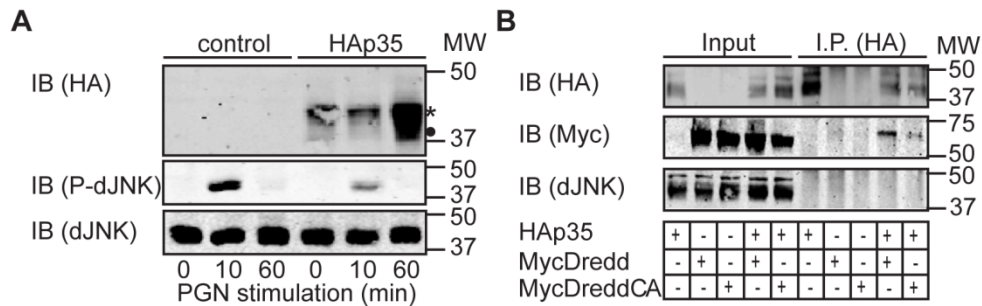


**Figure 3.6. Dredd interacts with Baculovirus p35 in cell culture:** **A.** Western blot analysis of lysates from control cells (lanes 1-3) and cells stably transfected with Baculovirus *p35* (lanes 4-6), and stimulated with PGN for the indicated times. Protein levels are visualised with HA (upper panel), P-dJNK (middle panel), and total dJNK (lower panel) specific antibodies. HAp35 is only detectable in cells stably transfected with the HAp35 expression construct (upper panel). The asterisk marks full-length HAp35 and the dot marks a potential truncated variant of HAp35. In contrast to control cells, stimulation with PGN induces lower levels of dJNK phosphorylation in *p35* expressing cells (middle panel). **B.** Western blot analysis of lysates from S2 cells transfected with HAp35, MycDredd, and MycDreddCA as indicated. Protein levels of input and immunoprecipitated samples were visualized with HA (upper panel), or with Myc (middle panel) specific antibodies. dJNK was visualized as a loading control (lower panel). Lanes 1-5 show lysates of the input samples, and lanes 6-10 show the same samples after immunoprecipitation with an HA specific antibody. For all Western Blots: molecular weights are indicated on the right of each panel.

*Drosophila* has seven caspases, where only Dredd is implicated in IMD signaling<sup>358</sup>. To investigate if Dredd is blocked by p35, I expanded my studies to test all *Drosophila* caspases for involvement in IMD/dJNK activation. To this end, I depleted each of the seven caspases from S2 cells individually and monitored subsequent IMD pathway responses to PGN exposure (Figure 3.7.). I analyzed whole cell lysates by Western blot analysis with Rel, P-dJNK and total dJNK specific antibodies. As anticipated, I detected Rel cleavage and dJNK phosphorylation in S2 cells or S2 cells treated with a control dsRNA in response to PGN treatment (Figure 3.7. upper and middle panel, lanes 1-3). Both events were fully blocked in cells depleted of *dredd* (Figure 3.7. lane 4). In contrast, I was unable to detect inhibition of either PGN-dependent Rel cleavage or dJNK phosphorylation in cells depleted of any other caspase (Figure 3.7. lanes 5-10). The results suggest that Dredd is the only caspase that influence the level of dJNK phosphorylation in IMD signaling.

My data demonstrate that Dredd is the essential caspase in the IMD pathway, that HAp35 interacts with Dredd in S2 cells, and that HAp35 blocks the PGN-dependent dJNK phosphorylation and transcriptional response.

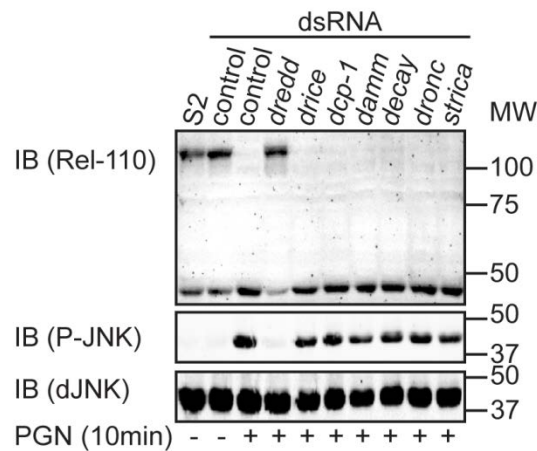


**Figure 3.7. Dredd is essential in IMD signaling:** Western blot analysis of lysates from S2 cells treated with the indicated dsRNAs, and stimulated with PGN for the indicated times. Protein levels are visualized with Rel-110 (upper panel), P-dJNK (middle panel), and total dJNK (lower panel) specific antibodies. PGN treatment of control cells (lane 1 and 2 of each panel) results in Rel cleavage, indicated by the loss of Rel-110 (lane 3, upper panel) and dJNK phosphorylation (lane 3, middle panel). In contrast to control cells, stimulation with PGN does not induce Rel cleavage or dJNK phosphorylation in *dredd* depleted cells (lane 4 of each panel). Molecular weights are indicated on the right of each panel.

### 3.3. Dredd interaction with the IMD pathway

#### 3.3.1. Dredd acts upstream of dTAK1 in dJNK phosphorylation in cell culture

A previous study indicated that Dredd acts upstream of dTAK1 in the phosphorylation of Rel<sup>113</sup>. However, this study did not describe the epistatic relationship of Dredd with dTAK1 in the activation of dJNK. To address this question, I generated an S2 cell line that inducibly expresses a constitutively active HA-tagged dTAK1 variant (pMT-HAdTAK1CA). dTAK1CA encodes a truncated dTAK1 protein that lacks the kinase inhibitory domain and therefore is considered constitutively active (Figure 3.8.A-B)<sup>113</sup>.

To validate the cell line, I initially tested HAdTAK1CA-expressing cells for key feature of dTAK1-dependent signaling activation (Figure 3.8.B). To do so, I induced the HAdTAK1CA expression construct in my stable transfected cells by adding CuSO<sub>4</sub>. I then monitored the expression of HAdTAK1 and induction of P-dJNK over time. I detected HAdTAK1CA protein within 100 min of induction (Figure 3.8.C, first panel). When I probed the same samples with a P-dJNK specific antibody, I detected dJNK phosphorylation at a similar time point (Figure 3.8.C, second panel). In addition, I detected a parallel induction of *puc* expression in the same experimental samples (Figure 3.8.D). Furthermore, simultaneous depletion of *dmkk4* and *dmkk7* from HAdTAK1CA-expressing cells resulted in a loss of PGN-dependent phosphorylation of dJNK (Figure 3.9.C, lanes 2 and 5). Thus, I am confident that my cell culture system reliably reproduces key features of dTAK1-dependent activation of dJNK in the IMD pathway.

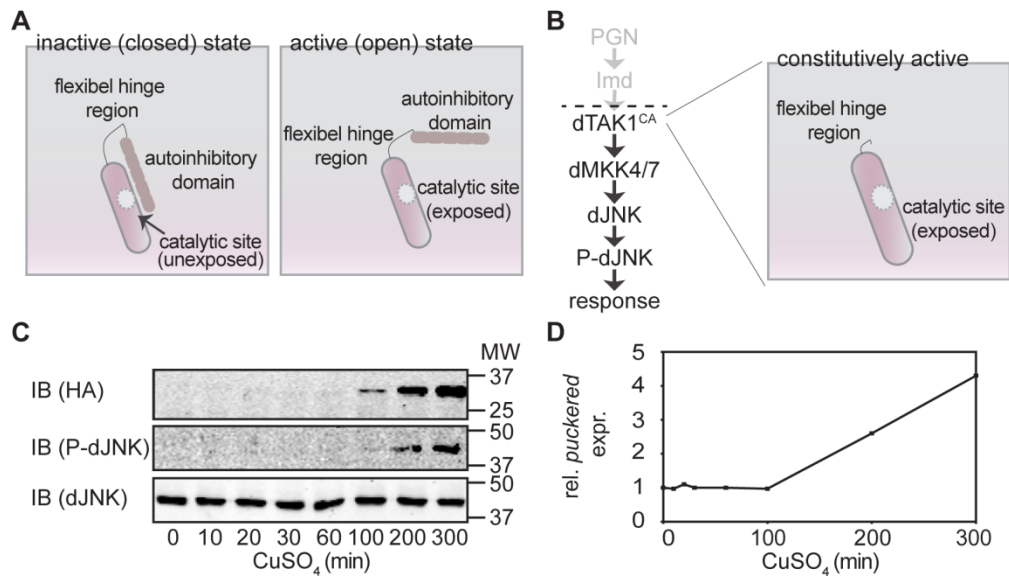


**Figure 3.8. Constitutively active dTAK1 cell line activates dJNK in the IMD pathway:** **A.** Simplified illustration of general kinase activation. In the absence of a cellular stimulus kinases are often found in the inactive (closed) state. When activated the autoinhibitory interaction with the inhibitory domain will be disrupted that triggers the exposure of the catalytic site of the kinase (open state). **B.** Flowchart of signal transduction through the IMD signaling pathway in a cell line that expresses a constitutively active dTAK1 cell line. Expression of a constitutively active dTAK1 activates downstream signaling (in black) independent of PGN-mediated IMD signaling (in grey). The blow-up on the right illustrates a constitutively active kinase. The truncation of the inhibitory domain renders the kinase permanently active. **C.** Western blot analysis of lysates from S2 cells that inducibly express a HATAK1CA and incubated with CuSO<sub>4</sub> for the indicated times. Protein levels are visualised with HA (first panel), P-dJNK (second panel), and total dJNK (third panel) specific antibodies. Induction of the pMT-HATAK1CA expression plasmid in response to CuSO<sub>4</sub> results in phosphorylation of dJNK protein. Molecular weights are indicated on the right of each panel. **D.** Quantitative real time PCR analysis of the same samples described in A. The relative expression levels for *puckered* were standardized to *actin* levels. Values of *puckered* expression at the indicated time points after CuSO<sub>4</sub> stimulation are reported relative to the unstimulated pMT-HATAK1CA sample.

I then asked if Dredd is required up- or downstream of dTAK1 for the activation of dJNK. To address this question, I depleted *dredd* by RNAi in HAdTAK1CA expressing cells and analysed whole cell lysates for P-dJNK by Western blot (Figure 3.9.A). In contrast to *dmkk4/dmkk7* depleted cells, I did not detect a change of dJNK phosphorylation when *dredd* was depleted (Figure 3.9.B, lane 3 and 6). Instead, P-dJNK levels remained at a level similar to control cells. Quantifications of P-dJNK levels relative to total dJNK levels confirmed a robust reduction in dJNK phosphorylation in cells depleted of *dmkk4/dmkk7* but not in *dredd* depleted cells (Figure 3.9.C)

These data indicate that Dredd acts upstream of dTAK1 and that Dredd is required for the transduction of a phospho-relay through the IMD pathway to dJNK.

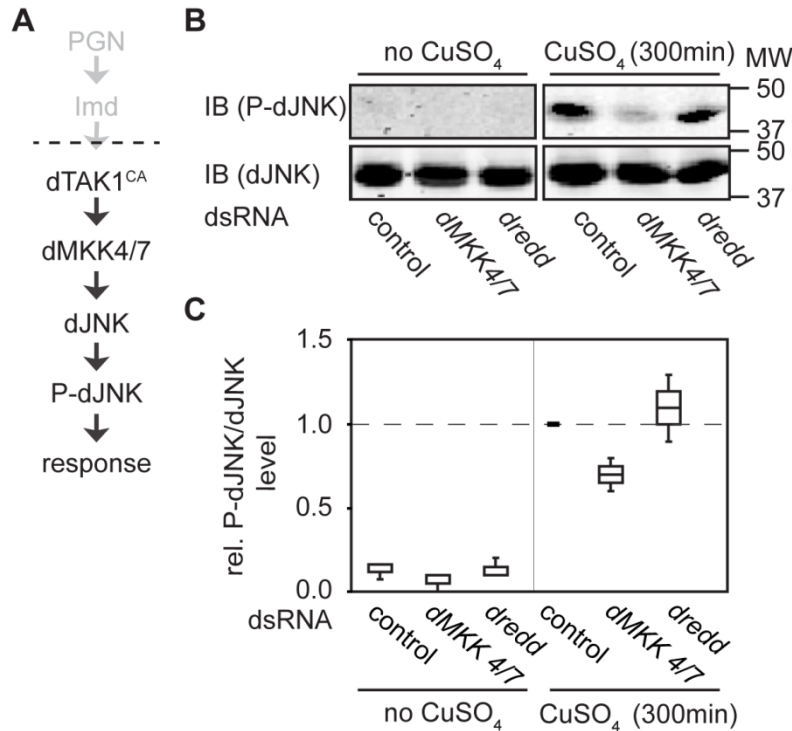


**Figure 3.9. Dredd acts upstream of dTAK1 in dJNK phosphorylation in the IMD pathway:** **A.** Flowchart of signal transduction through the IMD signaling pathway in a cell line that expresses a constitutively active dTAK1 cell line. Expression of a constitutively active dTAK1 (dTAK1CA) activates downstream signaling (in black) independent of PGN-mediated IMD signaling (in grey). **B.** Western blot analysis of lysates from S2 cells stably transfected with a pMT-HATAK1CA expression plasmid and treated with CuSO<sub>4</sub> as shown. Cells were incubated with identical amounts of control dsRNA (lanes 1 and 4), with *dMKK4/7* dsRNA (lanes 2 and 5), or with *dredd* dsRNA (lanes 3 and 6). Protein levels were visualised with P-dJNK (first panel), and total dJNK (second panel) specific antibodies. Molecular weights are indicated on the right of each panel. **C.** Quantification of P-dJNK levels visualized in A. The P-dJNK:total dJNK level of cells treated with control dsRNA and incubated with CuSO<sub>4</sub> for 300 min were assigned a value of 1 and all other levels are reported relative to this value. Measurements for each sample are presented as a box blot to graphically illustrate the results of three independent experiments.

### **3.3.2. Dredd interacts with early IMD pathway components**

My observation that Dredd acts upstream of dTAK1 in the IMD pathway suggests an interaction of Dredd with proximal IMD pathway members. To explore this possibility, I undertook a detailed examination of potential interactions between Dredd, Imd, dFADD and dIAP2. For these experiments, I generated Myc or HA tagged expression constructs for Imd, dFADD, dIAP2 and Dredd (Figure 3.10. A and B).

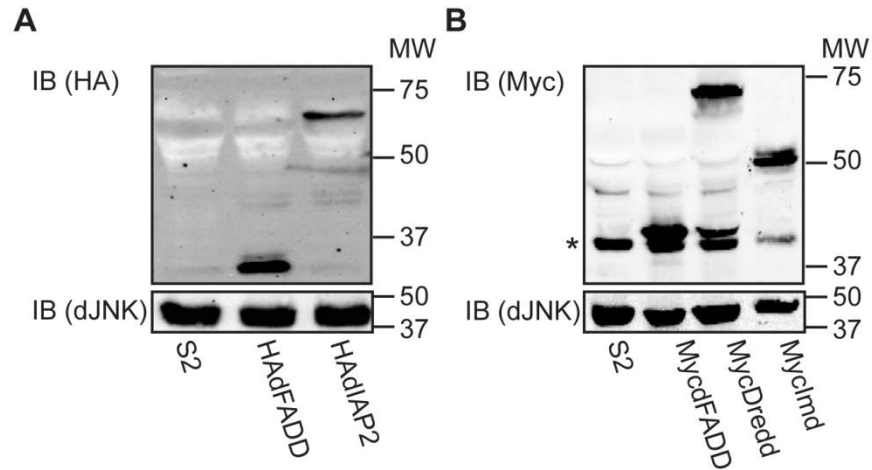


**Figure 3.10. Confirmation of HA- or Myc-tagged expression constructs in cell culture: A-B.** Western blot analysis of lysates from S2 cells transfected with the indicated HA (left panel) or Myc (right panel) tagged expression plasmids. Protein levels were visualised with HA (upper left panel), and Myc (upper right panel) specific antibodies. Control lysates from non-transfected S2 cells were loaded where indicated. dJNK was visualized as a loading control (lower left and right panel). Molecular weights are indicated on the right of each panel. \* marks an unspecific band.

I then probed potential protein-protein interactions in reciprocal co-immunoprecipitation assays performed in S2 cell lysates. I initially probed for a potential interaction between dFADD with Imd or dIAP2, respectively. For these studies, I performed anti-myc immunoprecipitations on whole cell lysates prepared from S2 cells that were co-transfected with MycdFADD and HAImd or HAIAP2 expression plasmids. As anticipated, I detected the reported interactions between Imd and dFADD (Figure 3.12.A-B)<sup>106</sup>. Also, I detected a robust co-precipitation of HAdIAP2 with MycdFADD (Figure 3.11.B, lane 6). In contrast, I did not observe precipitation of HAdIAP2 in the absence of MycdFADD (Figure 3.10.B, lane 4). In the reciprocal approach, I detected a specific co-precipitation of MycdFADD with HAdIAP2 (Figure 3.11.D, lane 6). These data indicate a molecular interaction between dIAP2 and dFADD.

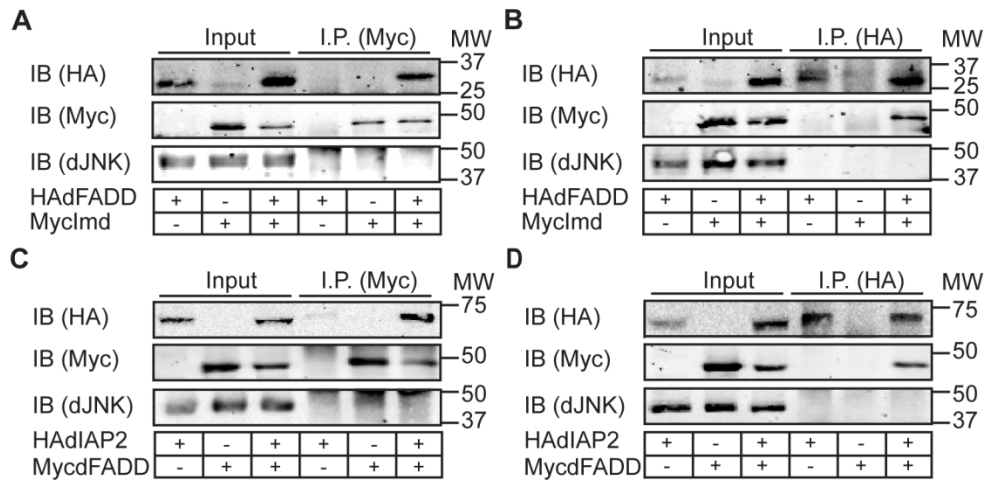


**Figure 3.11. dFADD interact with Imd and dIAP2 in cell culture: A-D.** Western blot analysis of lysates from S2 cells transfected with HAdFADD, Myclmd, HAdIAP2, and MycdfFADD as indicated. Protein levels of input and immunoprecipitated samples were visualised with HA (upper panel), or with Myc (middle panel) specific antibodies. dJNK was visualized as a loading control (lower panel). Lanes 1-3 show input samples of lysates, and lanes 4-6 show the same samples after immunoprecipitation with a Myc (A and C) or HA (B and D) specific antibody. Molecular weights are indicated on the right of each panel.

I then tested potential pairwise interactions between dFADD, dIAP2, and Dredd. I identified co-precipitations of dFADD with Dredd (Figure 3.12.A and B). In addition, I showed that Dredd co-precipitates with dIAP2 (Figure 3.12.C). I did not observe co-precipitations of Dredd or dIAP2 with Imd under our experimental conditions.

My interaction data are summarized in Figure 3.12.D and describe a robust network of physical interactions among proximal IMD pathway molecules. Importantly, these findings establish Dredd as a central element of the proximal signaling complex.

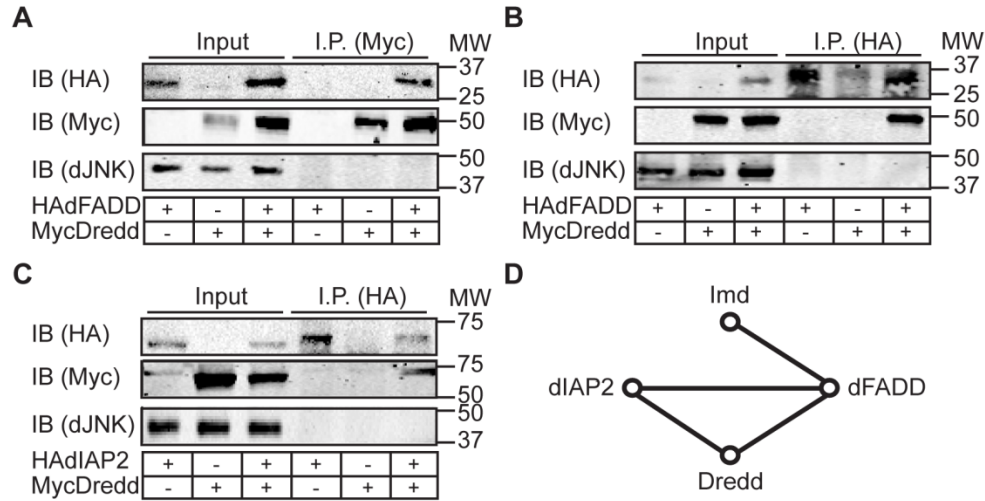


**Figure 3.12. Dredd interacts with dFADD and dIAP2 in cell culture: A-C.** Western blot analysis of lysates from S2 cells transfected with HAdFADD, MycDredd, and HAdIAP2 as indicated. Protein levels of input and immunoprecipitated samples were visualised with HA (upper panel), or with Myc (middle panel) specific antibodies. dJNK was visualized as a loading control (lower panel). Lanes 1-3 show input samples of lysates, and lanes 4-6 show the same samples after immunoprecipitation with a Myc (A) or an HA (B and C) specific antibody. Molecular weights are indicated on the right of each panel. **D.** Network of interactions between Dredd and additional early IMD signaling molecules based on data shown in Figure 3.11. and 3.12.

As immunoprecipitation of dIAP2 results in the co-purification of Dredd or dFADD in pairwise assays, I asked if Dredd competes with dFADD for interaction with dIAP2. For these studies, I followed the precipitation of MycdFADD by HAdIAP2 in the presence or absence of competing amounts of MycDredd. I found that immunoprecipitation of HAdIAP2 led to the purification of roughly equal amounts of MycdFADD in the absence (Figure 3.13. lanes 8-9) or presence of MycDredd (Figure 3.13. lane 10). These data suggest that Dredd does not compete with dFADD for binding to dIAP2.

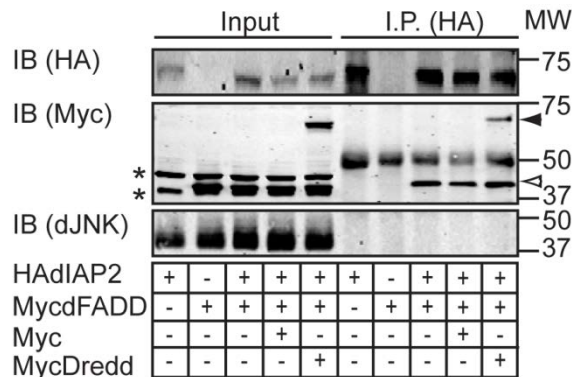


**Figure 3.13. Dredd does not compete with dFADD for binding with dIAP2 in cell culture:** Western blot analysis of lysates from S2 cells transfected with HAdIAP2, MycdFADD, Myc (empty destination vector), and MycDredd as indicated. Protein levels of input and immunoprecipitated samples were visualised with HA (upper panel), or with Myc (middle panel) specific antibodies. dJNK was visualized as a loading control (lower panel). Lanes 1-5 show lysates of the input samples, and lanes 6-10 show the same samples after immunoprecipitation with an HA specific antibody. Molecular weights are indicated on the right of each panel. Bands in immunoprecipitated samples that run at ~55 kDa correspond to the immunoglobulin heavy chain. \* marks unspecific bands, MycDredd is indicated with a closed arrowhead and MycdFADD is indicated with an open arrowhead.

I followed up on my initial finding of Dredd:dIAP2 binding and tested which of the protein domains of Dredd and dIAP2 are responsible for protein interaction. To do so, I generated a series of dIAP2 and Dredd truncation constructs and confirmed the expression of the corresponding proteins by Western blot (Figure 3.14.A-D). More specifically, I generated a construct that expresses only the prodomain or the caspase-domain of Dredd, respectively. In addition, I generated a dIAP2 construct that lacks the BIR1, the RING, or a combination of BIR1, BIR2, and RING domain. Visualisation of the tagged proteins with HA or Myc specific antibodies confirmed expression of the proteins at the expected molecular weight.

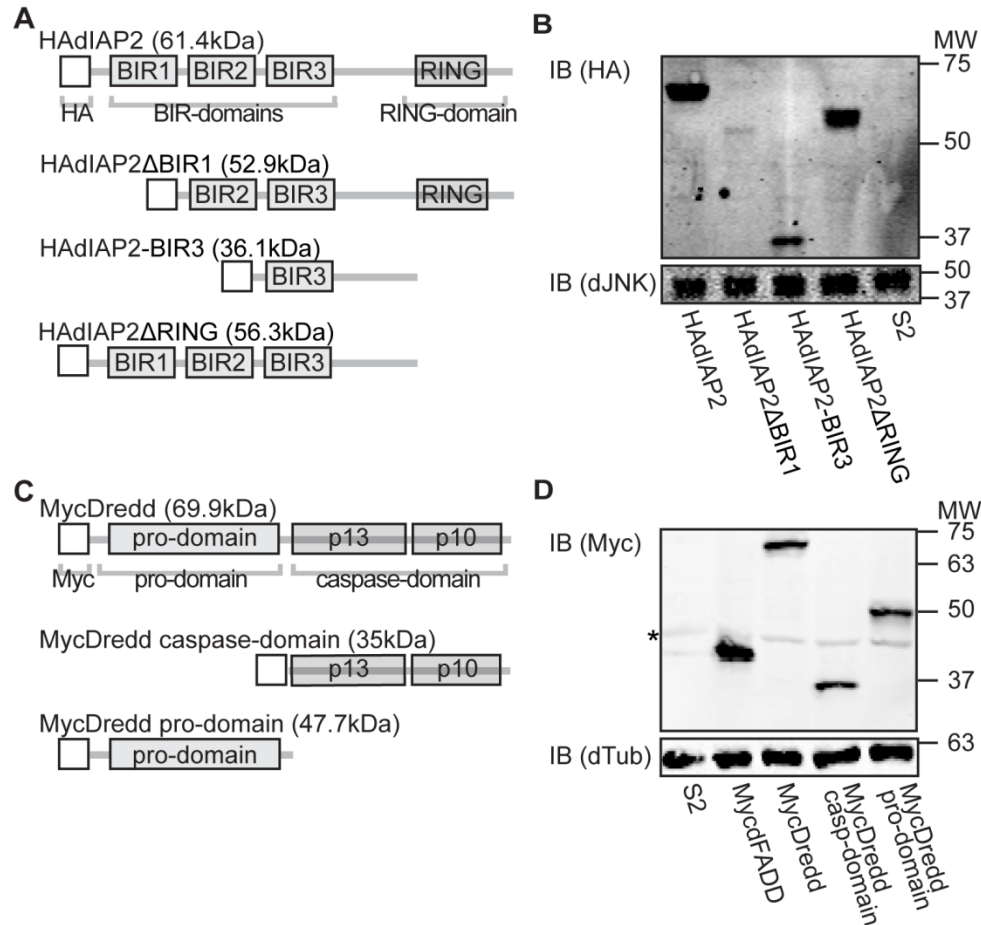


**Figure 3.14. Dredd and dIAP2 expression constructs for S2 cells: A-C.** Schematic illustration of HA-tagged dIAP2, dIAP2 $\Delta$ BIR1, dIAP2-BIR3, and dIAP2 $\Delta$ RING or Myc-tagged Dredd, Dredd caspase-domain, and Dredd prodomain expression constructs. Protein domains and molecular weights of the corresponding protein are indicated. **B- D.** Western blot analysis of lysates from S2 cells transfected with the indicated HA-tagged or Myc-tagged expression plasmids. Control lysates from non-transfected S2 cells were loaded where indicated. Protein levels were visualized with a HA or Myc specific antibody (upper panel). dJNK was visualized as a loading control (lower panel). Molecular weights are indicated on the right of each panel. \* marks an unspecific band.

I then probed potential protein-protein interactions in co-precipitation assays performed in S2 cell lysates. I initially tested the ability of full-length Dredd to co-precipitate the various dIAP2 deletion constructs. I performed anti-HA immunoprecipitations on whole cell lysates prepared from S2 cells that were co-transfected with MycDredd and HAdIAP2, HAdIAP2 $\Delta$ BIR1, HAdIAP2BIR3, and HAdIAP2 $\Delta$ RING expression plasmids. Analysis of the input controls showed the successful expression of all dIAP2 constructs alone or when co-expressed with MycDredd (Figure 3.15.A left panel, lane 1-9). I detected a co-precipitation of HAdIAP2, HAdIAP2 $\Delta$ BIR1, HAdIAP2BIR3, and HAdIAP2 $\Delta$ RING with MycDredd (Figure 3.15.A right panel, lane 6-9). In contrast, I did not observe precipitation of the HAdIAP2 variants in the absence of MycDredd (Figure 3.15.A right panel, lane 1-5). Only full-length HAdIAP2 robustly co-precipitated with MycDredd (Figure 3.15.A right panel, lane 6). The removal of the dIAP2 RING domain or the first two BIR domains did not block the precipitation by MycDredd but the protein appear to interact less efficiently with MycDredd (Figure 3.15.A right panel, lane 7-9). Since Dredd:dIAP2 binding is not disrupted by the deletion of RING, BIR1, or BIR2 domain it is unlikely that binding is mediated by one of the domains alone. The data indicate that Dredd:dIAP2 binding is mediated by the BIR3 domain which is in agreement with a recent report that demonstrated that the dIAP2 BIR3 domain mediates interaction with Dredd<sup>273</sup>.

I next tested which Dredd domain is required for binding to dIAP2. I performed anti-HA immunoprecipitations on whole cell lysates prepared from S2 cells that were co-transfected with full-length HAdIAP2 and MycDredd, MycDreddcasp-domain, MycDreddprodomain, and MycDreddCA (Figure 3.15.B). I identified a robust interaction between full-length HAdIAP2 and MycDredd, MycDreddcasp-domain, MycDreddprodomain, and MycDreddCA (Figure 3.15.B right panel, lane 6-9). My data show that dIAP2 interacts with either domain of Dredd, the pro- and caspase-domain and are summarized in Figure 3.15.C-D.

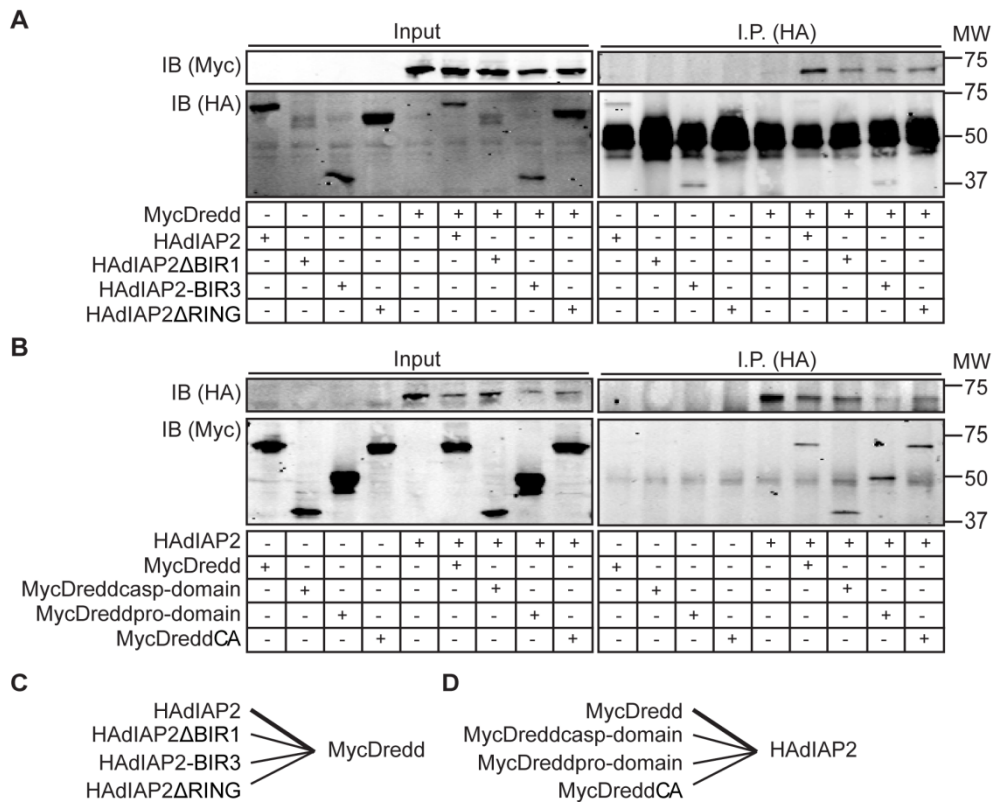


**Figure 3.15. Dredd:diAP2 interaction in cell culture: A-B.** Western blot analysis of lysates from S2 cells transfected with indicated expression constructs. Protein levels of input and immunoprecipitated samples were visualised with Myc (upper panel), or with HA (lower panel) specific antibodies. Lanes 1-9 show lysates of the input samples, and lanes 10-18 show the same samples immunoprecipitated with a HA specific antibody. For all Western Blots: bands in immunoprecipitated samples that run at ~55 kDa correspond to the immunoglobulin heavy chain. Molecular weights are indicated on the right of each panel. **C.** Schematic illustration of interactions between full-length MycDredd and HAdIAP2 constructs observe in Figure A. **D.** Schematic illustration of interactions between full-length HAdIAP2 and MycDredd constructs observe in Figure B.

### **3.4. Summary**

In this chapter, I present the results of the analysis of Dredd in the activation of IMD/dJNK in cell culture (Figure 3.16.). My initial cell culture assays demonstrated a fundamental requirement for Dredd in the activation of dJNK, including dJNK phosphorylation and the expression of dJNK-dependent target genes. I demonstrated a dependence of the IMD/dJNK arm on caspase activity in cell culture. My interaction experiments identified Dredd as a central component of a rich network of interactions among proximal IMD signal transduction molecules and placed Dredd upstream of dTAK1 in the activation of IMD/dJNK. My results establish the position of Dredd within the IMD/dJNK pathway and enhance our understanding of signal transduction events in the IMD response.

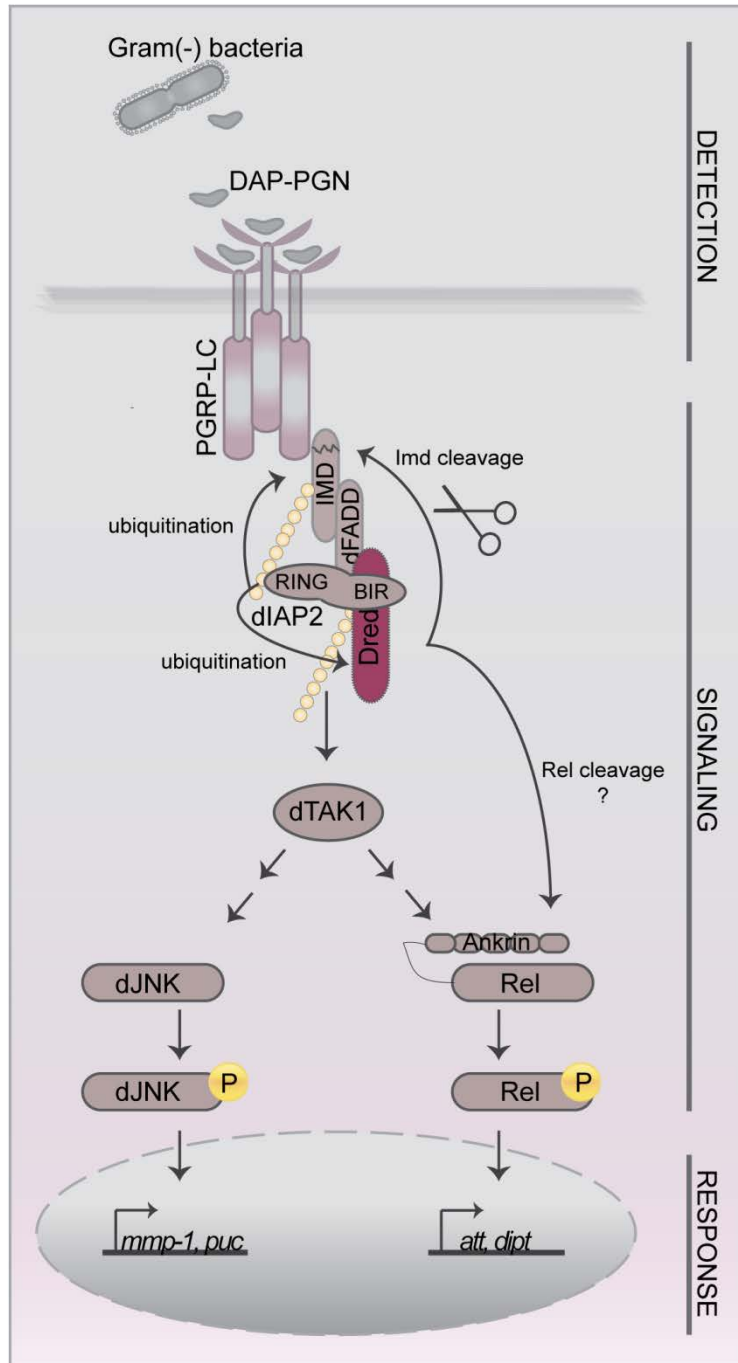


**Figure 3.16. Summary of section 3:** Illustration of the *Drosophila* IMD signaling pathway with the added changes that resulted from this study. In summary, my results demonstrated in chapter 3 establish the position of Dredd within the IMD/dJNK pathway upstream of dTAK1 where Dredd interacts with proximal IMD pathway members. In conclusion, the data enhance our understanding of signal transduction events in the IMD response.

**Chapter 4. The role of Dredd in *Drosophila* IMD signaling *in vivo***

**Results presented in this chapter are partially reflected in the following publication:**

**Guntermann, S., and Foley, E.** The Protein Dredd Is an Essential Component of the c-Jun N-terminal Kinase Pathway in the *Drosophila* Immune Response. *J Biol Chem.* 2011 **286(35)**: 30284-94.

#### 4.1. Background

A complete loss-of-function mutation in *dredd* (*dredd*<sup>B118</sup>) generated animals highly susceptible to gram-negative bacterial infection which correlated with a complete block of Rel-cleavage and downstream AMP expression<sup>130</sup>. In the *dredd* mutant line, *dredd*<sup>B118</sup> encodes a truncated Dredd protein that replaces arginine 127 with a stop codon and is considered a null allele<sup>129</sup>. Given that Rel is cleaved at a caspase consensus cleavage site and caspase inhibitors block Rel cleavage, the current model suggests that Dredd directly cleave Rel and therefore enables the induction of AMP such as *attacin* and *diptericin*<sup>125,126,128</sup>.

I recently demonstrated a fundamental requirement for Dredd in IMD/dJNK activation in cell culture and that Dredd interacts with early IMD pathway members upstream of dTAK1 (Chapter 3)<sup>350</sup>. These findings reposition Dredd in IMD signaling (Figure 3.16.). However, an involvement of Dredd in the dJNK/IMD response in a whole animal setting has not been addressed. In agreement with my data that placed Dredd in the early IMD signaling cascade, a recent report suggested a role for Dredd in the cleavage of Imd<sup>114</sup>. Therefore, it is possible that Dredd is not responsible for Rel cleavage and instead acts earlier in the IMD cascade.

To address these questions I initially analyzed Dredd involvement in the dJNK/IMD pathway *in vivo*. I then investigated if Dredd is necessary and sufficient for Rel activation *in vivo*. The fly strains that were used in this section are listed in Table 4.1.

## 4.2. Dredd is an essential component of the IMD/dJNK pathway *in vivo*

### 4.2.1. Baculovirus p35 inhibits dJNK activation *in vivo*

To date, the involvement of Dredd in IMD/dJNK activation is unexplored *in vivo*. IMD pathway activity is typically monitored *in vivo* by following the immune responses of flies that were pierced with a sterile needle dipped in pellets of gram-negative bacteria. In this system, the fat body is a major site of AMP expression<sup>31,32</sup>. Consistent with a requirement for Dredd in IMD/Rel activation, expression of the caspase inhibitor p35 blocks the challenge-dependent induction of *dipt* in adult fat bodies<sup>116</sup>. I used the GAL4-UAS binary expression system to monitor the effects of p35 on the IMD/dJNK pathway (Figure 4.1.A)<sup>359</sup>. The fly lines that were used in this study are listed in Table 4.1.

Specifically, I crossed *yolkGAL4* transgenic flies with *UASp35* transgenic flies to generate *yolkGAL4/UASp35* progeny. As *yolkGAL4* expression is restricted to female fat bodies, p35 expression is likewise restricted to the fat bodies of female *yolkGAL4/UASp35* flies. The use of a female specific driver enabled me to use male flies as isogenic controls in all my experiments. I initially examined the expression of p35 in male and female flies by RT-PCR analysis (Figure 4.1.B). As expected, female flies expressed p35 at a very high level, while male flies showed a weak expression of p35 that likely resulted from leaky expression from the UAS elements.

GENOTYPE	ABBREVIATION	DESCRIPTION	EXPECTED PHENOTYPE
<i>w<sup>1118</sup></i>	<i>w<sup>1118</sup></i>	wild type; flies have white eyes due to deletion in white gene but are otherwise considered wild type	wild type activation of the IMD response after infection
<i>dredd<sup>B118</sup></i>	<i>dredd<sup>B118</sup></i>	Arg127 mutation generates a premature stop in <i>dredd</i> : null allele for <i>dredd</i>	no activation of the IMD response after infection
<i>yolkGAL4</i>	<i>yolkGAL4</i>	female fat-body specific expression of <i>GAL4</i>	wild type activation of the IMD response after infection
<i>UASp35;yolkGAL4</i>	<i>UASp35;yolkGAL4</i>	<i>GAL4</i> -dependent expression of caspase inhibitor <i>p35</i> transgene in the female fat-body	inefficient activation of the Rel arm after infection; induction of the dJNK arm = ?

**Table 4.1: Fly strains for section 4.2.:** A brief description of the fly lines and the expected phenotypes in section 4.2. For more information on the fly lines see Materials and Methods (Chapter 2).

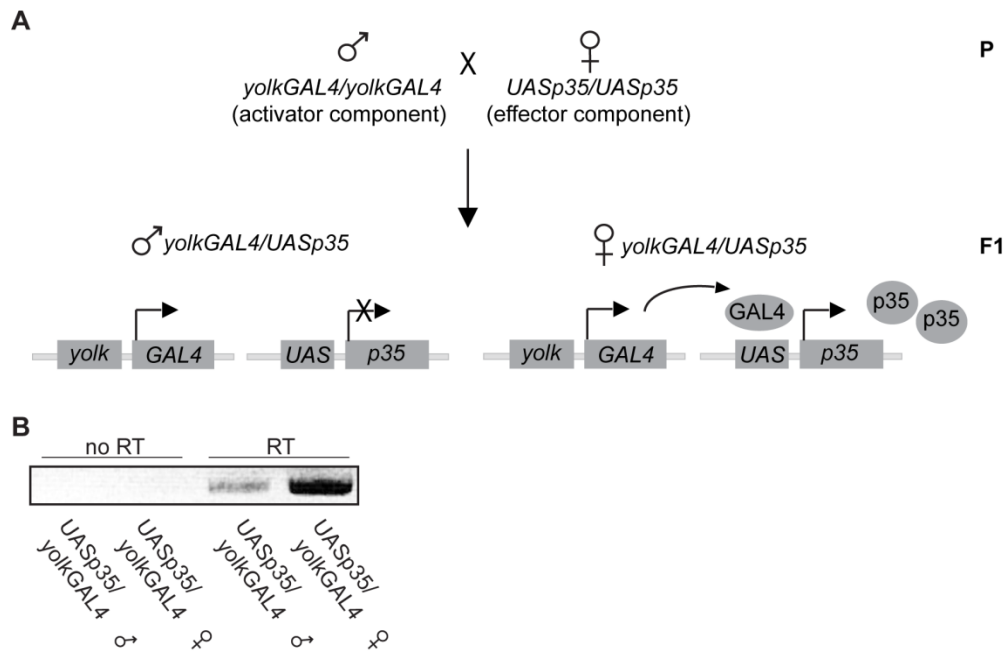


**Figure 4.1. Confirmation of baculovirus p35 expression *in vivo*:** **A.** Schematic representation of the binary UAS/GAL4 system for transgene expression in flies. Crossing a transgenic activator line (*yolkGAL4*) to a transgenic effector line (*UASp35*) allows the directed expression of a gene of interest (*p35*). The *yolk* promoter triggers the female fatbody specific expression of the GAL4 transcription factor. GAL4 binds the UAS sequences upstream of *p35* and induces transcriptional expression of *p35* in the female fat body. **B.** Agarose gel electrophoresis of RT-PCR products amplified from RNA extracted from *UASp35/yolkGAL4* male flies (lanes 1 and 3) or *UASp35/yolkGAL4* female flies (lanes 2 and 4) using *p35* specific primers. RT-PCR reaction was performed without (lanes 1 and 2) or with (lanes 3 and 4) reverse transcriptase (RT) enzyme.

I then monitored the infection-dependent phosphorylation of dJNK in male and female *yolkGAL4/UASp35* flies. Male flies showed a transient increase in P-dJNK levels in response to bacterial challenge. In contrast, the relative levels of dJNK phosphorylation remained unchanged in female flies (Figure 4.2.A). These data strongly hint at a requirement for caspase activity in the activation of IMD/dJNK *in vivo*.

To explore the impact of p35 on IMD/dJNK activation further, I determined if the expression of p35 in the fly blocks the infection-mediated induction of dJNK-dependent transcripts. Initially, I confirmed that the expression of GAL4 in female fat bodies alone does not have an appreciable impact on IMD pathway responses, as *yolkGAL4* females express *dipt* and *puc* at levels comparable to *yolkGAL4* males upon bacterial challenge (Figure 4.2.B-C).

I then analyzed the transcriptional response of *yolkGAL4,UASp35* male and female flies after immune challenge. Despite a minor variability between replicates, likely a reflection of the efficacy of my bacterial delivery between replicates, each transcript showed a clear and reproducible trend throughout the experiments (Figure 4.2.D-G). For example in my control experiment, quantification of the Rel-dependent AMP *att* and *dipt* repeatedly demonstrated a gradual increase in peptide levels after infection of *yolkGAL4/UASp35* males (Figure 4.2.D-E). Likewise, bacterial challenges of *yolkGAL4/UASp35* males always resulted in a transient induction of the dJNK-dependent transcripts *puc* and *mmp-1* (Figure 4.2.F-G). In contrast, I observed a greatly diminished induction of *att* and *dipt* in infected *yolkGAL4/UASp35* female flies (Figure 4.2.D-E). Most importantly, I also observed a markedly impaired induction of the dJNK-dependent transcripts *puc* and *mmp-1* in infected *yolkGAL4/UASp35* female flies (Figure 4.2.F-G). In summary, my *in vivo* observations recapitulate my cell culture data and establish a requirement for caspase activity in the activation of IMD/dJNK and the attendant induction of dJNK-responsive transcripts in adult *Drosophila*.

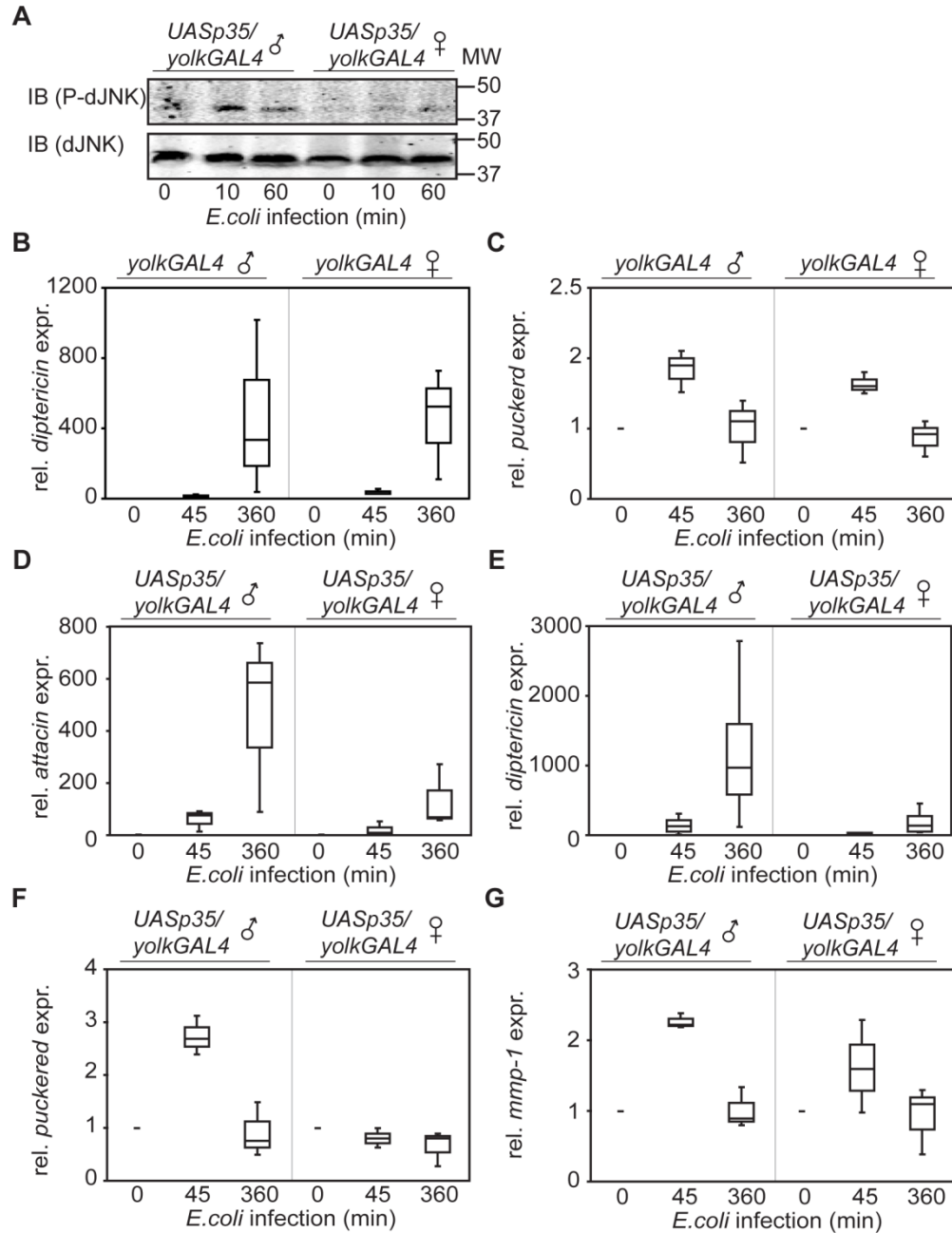


**Figure 4.2. Baculovirus p35 inhibits dJNK activation *in vivo*:** **A.** Western blot analysis of lysates from *UASp35/yolkGAL4* male (lanes 1-3) and *UASp35/yolkGAL4* female (lanes 4-6) flies, infected with *E. coli* for the indicated times. Protein levels are visualised with total dJNK (lower panel) and P-dJNK (upper panel) specific antibodies. Molecular weights are indicated on the right of each panel. **B-C.** Quantitative real time PCR analysis of *yolkGAL4* male flies (as indicated on the left side of each box plot) and *yolkGAL4* female flies (as indicated on the right side of each box plot), infected with *E. coli* for the indicated times. The relative expression levels for *dipteracin* (B), and *puckerd* (C) are

standardized to *actin* levels. The expression levels for *yolkGAL4* male and *yolkGAL4* female flies at the indicated time points after infection are reported relative to uninfected *yolkGAL4* male or *yolkGAL4* female flies, respectively. **D-G.** Quantitative real time PCR analysis of *UASp35/yolkGAL4* male flies (left side of each box plot) and *UASp35/yolkGAL4* female flies (right side of each box plot), infected with *E.coli* and recovered for the indicated times. The relative expression levels for *attacin* (D), *dipthericin* (E), *puckered* (F), and *mmp-1* (G) are standardized to *actin* levels. The expression levels for *UASp35/yolkGAL4* male and *UASp35/yolkGAL4* female flies at the indicated time points after infection are reported relative to uninfected *UASp35/yolkGAL4* male or *UASp35/yolkGAL4* female flies. The measurements for each transcript (B–G) are presented as a box blot to graphically illustrate the results of three independent experiments.

#### 4.2.2. Dredd is required for dJNK activation in IMD signaling *in vivo*

My cell culture analyses strongly suggest that Dredd is required for IMD/dJNK activation and the expression of IMD/dJNK-responsive transcripts, and my *in vivo* data demonstrate a requirement for caspase activity in the IMD/dJNK module. The simplest explanation for these findings is that Dredd is required for IMD/dJNK activation *in vivo*. To test this hypothesis, I analysed *dredd*<sup>B118</sup> mutant flies for their ability to activate the IMD/dJNK pathway in response to infection with *E.coli*. I initially asked if bacterial challenge induces the phosphorylation of dJNK in *dredd*<sup>B118</sup> flies. To do so, I performed a Western blot analysis of P-dJNK levels in immune challenged control and *dredd*<sup>B118</sup> flies. Compared to control flies, *dredd*<sup>B118</sup> mutant flies were clearly impaired in their ability to induce dJNK phosphorylation upon infection (Figure 4.3.A).

I next asked if *dredd*<sup>B118</sup> flies induce dJNK-responsive transcripts after infection. Despite a minor variability between replicates, each transcript showed a clear and reproducible trend throughout the experiments. I repeatedly observed induction of *att* and *dipt* in immune challenged wild-type flies. As anticipated, we did not detect an infection-dependent increase in *att* or *dipt* expression levels in *dredd*<sup>B118</sup> flies (Figure 4.3.B-C). I then followed the infection-mediated induction of *puc* and *mmp-1*. I consistently found that induction of both transcripts was greatly impaired in *dredd*<sup>B118</sup> mutant flies compared to wild-type control flies (Figure 4.3.D-E).

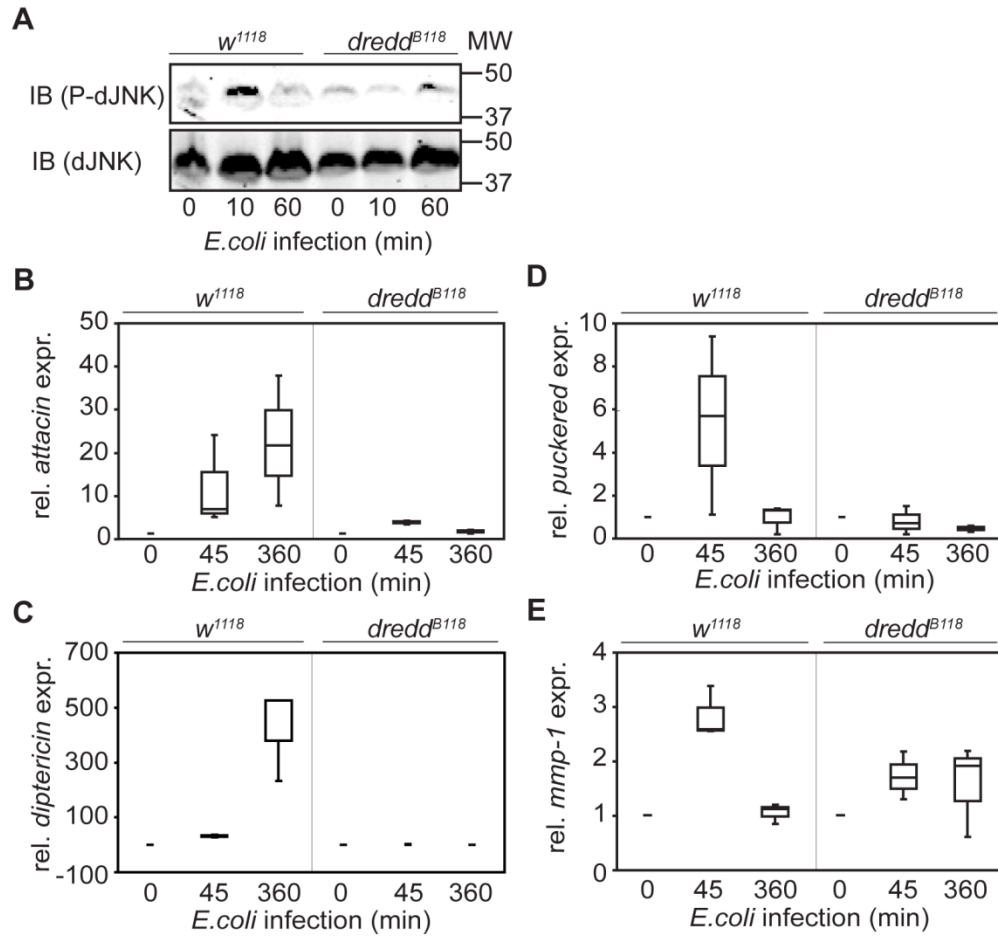


**Figure 4.3. Dredd is required for dJNK activation in IMD signaling *in vivo*: A.** Western blot analysis of lysates from *w<sup>1118</sup>* (lanes 1-3) and *dredd<sup>B118</sup>* (lanes 4-6) flies, infected with *E. coli* and recovered for the indicated times. Protein levels are visualised with total dJNK (lower panel) and P-dJNK (upper panel) specific antibodies. Molecular weights are indicated on the right of each panel. **B-E.** Quantitative real time PCR analysis of *w<sup>1118</sup>* flies (left side of each box plot) and *dredd<sup>B118</sup>* flies (right side of each box plot), infected with *E. coli* and recovered for the indicated times. The relative expression levels for *attacin* (B), *diptericin* (C), *puckered* (D), and *mmp1* (E) were standardized to *actin* levels. The expression levels for *w<sup>1118</sup>* and *dredd<sup>B118</sup>* flies at the indicated time points after infection are reported relative to uninfected *w<sup>1118</sup>* or *dredd<sup>B118</sup>* flies. Measurements for each transcript are presented as a box blot to graphically illustrate the results of three independent experiments.

Combined, my data demonstrate that the two hallmarks of IMD/dJNK activation, phosphorylation of dJNK and the transcriptional induction of *puc* and *mmp-1*, are completely absent in *dredd*<sup>B118</sup> mutant flies. The failure of dJNK activation in *dredd* mutant flies is phenocopied by the observed reduction of P-dJNK and dJNK-dependent transcripts in my p35 experiments. These data are in agreement with my observations in cell culture assays (chapter 3) and argue that Dredd is essential for the activation of an IMD/dJNK response to infection in *Drosophila*.

### **4.3. Dredd is an essential component in IMD/Rel signaling downstream of Imd activation *in vivo***

#### **4.3.1. Dredd is required downstream of Imd activation**

The pan caspase inhibitor z-VAD-FMK blocks Rel processing in S2 cells and overexpression of Dredd in S2 cells triggers cleavage of Rel<sup>123,126</sup>. Hence, the current model suggests that Dredd is the protease responsible for Rel cleavage. However, overexpression of a catalytically inactive Dredd construct in S2 cells still triggers Rel cleavage and the demonstration of Dredd dependent cleavage of Rel in an *in vitro* assay has been challenging<sup>125,126,128</sup>. In addition, my work and the work of others propose a role for Dredd early in the IMD cascade<sup>114,273,350</sup>. Therefore Rel activation might be Dredd independent.

To clarify if Dredd is involved in activation of Rel, I investigated if Dredd is necessary and sufficient for Rel activation. The current data suggest that Dredd mediates N-terminal cleavage of the Imd protein which results in the subsequently exposure of an IAP-binding motif (IBM) in Imd. The IBM assists with the association of Imd with dIAP2 which mediates K63-linked polyubiquitination essential for IMD/Rel activation (Figure 4.4. left panel)<sup>114</sup>. Given the proposed model where Dredd is required for the N-terminal cleavage of Imd, the expression of a truncated version of Imd (*imdcl*) should activate the IMD/Rel arm independently of Dredd's role in the early IMD cascade. If Dredd is not required for the proteolytic cleavage of Rel, the IMD/Rel signaling arm should

be activated in response to the expression of a constitutive active Imd in a *dredd* mutant background (Figure 4.4. middle panel). In contrast, if Dredd is necessary for Rel cleavage, loss of *dredd* should block the IMD/Rel arm in a constitutive active Imd fly line (Figure 4.4. right panel). The fly strains that were used in this section are listed in Table 4.2.

GENOTYPE	ABBREVIATION	DESCRIPTION	EXPECTED PHENOTYPE
<i>cgGAL4/+;GAL80ts/+</i>	<i>GAL4[ts]</i>	temperature sensitive fat-body specific expression of <i>GAL4</i> (no expression at 18°C but at 29°C)	no activation of the IMD response after a heatshift to 29°C
<i>dreddB118;cgGAL4/+;GAL80ts/+</i>	<i>dredd;GAL4[ts]</i>	<i>GAL4[ts]</i> transgene and null for <i>dredd</i>	no activation of the IMD response after a heatshift to 29°C
<i>cgGAL4/UASImdcl;GAL80ts/+</i>	<i>Imdcl[ts]</i>	<i>Imdcl</i> transgene (constitutive active IMD) driven by <i>GAL4[ts]</i>	?
<i>dreddB118;cgGAL4/UASImdcl;GAL80ts/+</i>	<i>dredd;Imdcl[ts]</i>	<i>Imdcl</i> transgene driven by <i>GAL4[ts]</i> and null for <i>dredd</i>	?
<i>dreddB118,P[dredd+];cgGAL4/UASImdcl;GAL80ts/+</i>	<i>dredd,P[dredd+];Imdcl[ts]</i>	<i>Imdcl</i> transgene driven by <i>GAL4[ts]</i> with a genomic Dredd and null for <i>dredd</i>	?

**Table 4.2: Fly strains for section 4.3.1.:** A brief description of the fly lines and the expected phenotypes in section 4.3.1. For more information on the fly lines see Materials and Methods (Chapter 2).

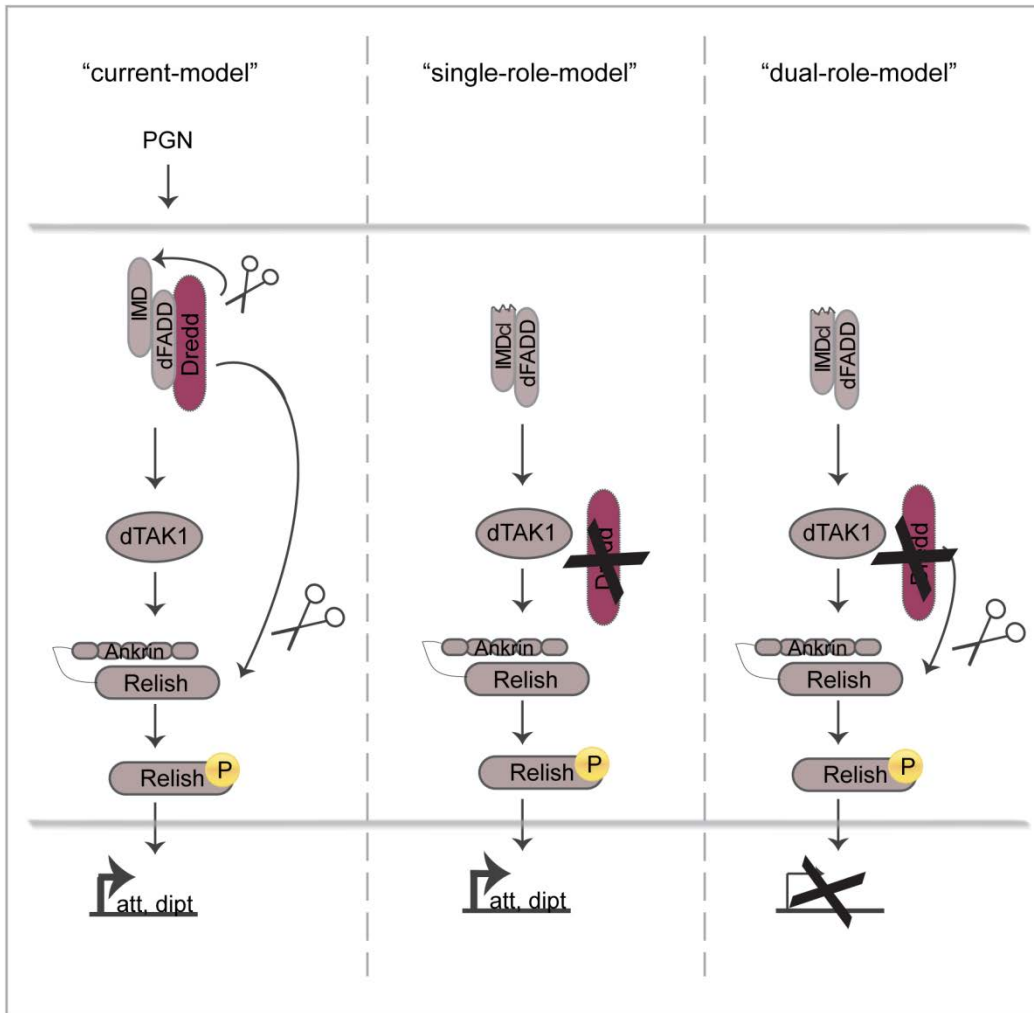


**Figure 4.4. Dredd in IMD signaling:** Schematic representation of the current view of IMD pathway activation. It is suggested that Dredd is required for Imd and Rel cleavage (left panel). Schematic representation of the hypothetical single-role-model for Dredd (middle panel). Dredd is not required for Rel cleavage and therefore a constitutive Imd induces AMP expression if Dredd is lost. Schematic representation of the hypothetical dual-role-model for Dredd (right panel). Dredd is required for Rel cleavage and therefore a constitutive Imd does not induces AMP expression if Dredd is lost.

To mimic Dredd-dependent activation of Imd, I established a fly line that expresses an N-terminal truncated construct of Imd (Imdcl). More specifically, I generated a construct with a 73 amino acids truncation of the N-terminus that maintained the sequence motifs necessary for nucleation of a signaling complex at the PGRP-LC receptor. I initially tested if Imdcl expressing flies constitutively activate IMD/Rel.

To test for constitutively activation of the IMD/Rel arm I tested if the expression of Imdcl induces IMD/Rel specific AMP expression by qRT-PCR. In flies, the fat body is a major site of AMP expression. Therefore I generated flies that express Imdcl under the control of a fat-body specific driver TARGET system (*cgGAL4; GAL80[ts]*) (Figure 4.5.). The temperature sensitive mutant allele of GAL80 (*GAL80[ts]*) blocks GAL4-dependant expression of UAS-bearing transgenes at permissive temperatures (< 25°C), but not at restrictive temperatures (> 29°C). This system allows for a controlled expression of the Imdcl transgene. More precisely, Imdcl is not expressed at 18°C while incubation of flies to 29°C induces transgene expression. I kept all fly-crosses at 18°C. Three to four days after flies eclosed I shifted the flies to 29°C for 0-6 hours depending on the experimental approach.

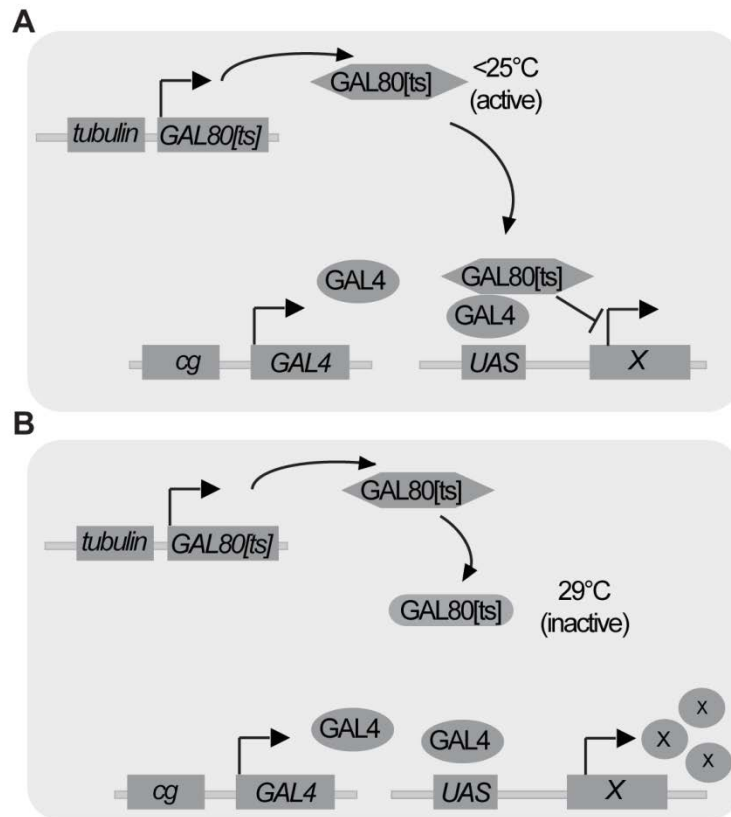


**Figure 4.5. UAS/GAL4 GAL80[ts] TARGET system:** A. Schematic representation of the GAL4-based system for transgene expression (Figure 4.1.B). The addition of the GAL80[ts] TARGET system allows temporal regulation of the expression of a transgene. Incubated at the permissive temperature ( $< 25^{\circ}\text{C}$ ) prevents the *cg*GAL4-driven expression of the transgene X while transgene expression is induced at the restrictive temperature ( $29^{\circ}\text{C}$ ).

To analyze the effect of *Imdcl* transgene expression I monitored the IMD/Rel dependent transcripts *att* and *dipt* by qRT-PCR. I predicted that *Imdcl* transgene expression will induce *att* and *dipt* expression independent of PGN stimulation (Figure 4.6.A). In control flies (*GAL4[ts]*) that do not drive *Imdcl* transgene the AMP levels did not increase over time (Figure 4.6.B-C, left side of each blot). Similar, the *cgGAL4*-driven induction of the *Imdcl* transgene over 6 h resulted in no changes of AMP levels (*Imdcl[ts]*). In contrast, the expression levels of *dipt* and *att* increased dramatically after 24h in flies that express *Imdcl* transgene (Figure 4.6.B-C, right side of each blot). I conclude that *Imdcl* transgene expression in flies induces the Rel-responsive transcripts *dipt* and *att* in the absence of an exogenous microbial challenge.

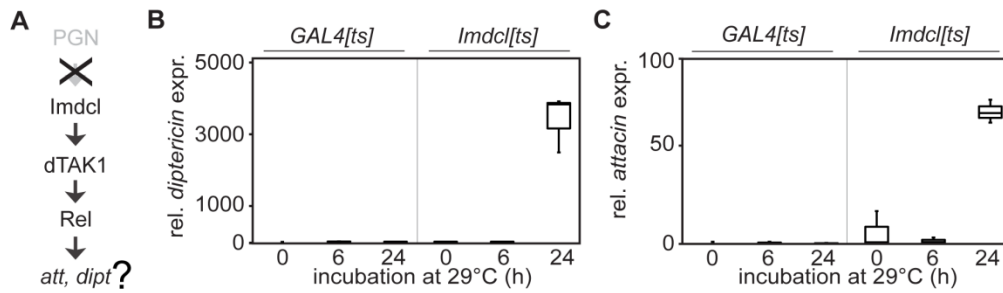


**Figure 4.6. Expression of Imdcl induces an antimicrobial response *in vivo*:**

**A.** Flowchart of signal transduction through the IMD signaling pathway in a fly line that expresses a constitutively active Imd (Imdcl). Expression of Imdcl is predicted to induce downstream signaling (in black) independent of PGN stimulation (in grey). **B-C.** Quantitative real time PCR analysis of control flies (*GAL4[ts]*) and Imdcl (*Imdcl[ts]*) flies incubated at the restrictive temperature (29°C) for the indicated times. The relative expression levels for *attacin* (A) and *dipteracin* (B) were standardized to *actin* levels. The expression levels for control and Imdcl flies at the indicated time points after heat shift are reported relative to uninduced control flies.

I next asked if the loss of *dredd* blocks AMP expression in *Imdcl* flies (Figure 4.7.A). To do so, I induced *Imdcl* transgene expression in WT or *dredd* mutant flies by heat-shifting the flies from 18°C to 29°C over 24h. I then analyzed relative AMP expression by qRT-PCR (Figure 4.7. B-C).

In control flies that lack the *Imdcl* transgene (*GAL4[ts]* and *dredd;GAL4[ts]*, respectively) showed no increase in *att* or *dipt* expression after heatshift (Figure 4.7.B-C). WT flies that express *Imdcl* showed a strong induction of AMP expression. In contrast to WT flies, expression of the *Imdcl* transgene in *dredd*<sup>B118</sup> mutant flies failed to induce AMP expression. Instead *att* or *dipt* levels remained close to uninduced samples. These data indicate that Dredd is required downstream of *Imd* cleavage and are consistent with a requirement for Dredd in *Rel* cleavage.

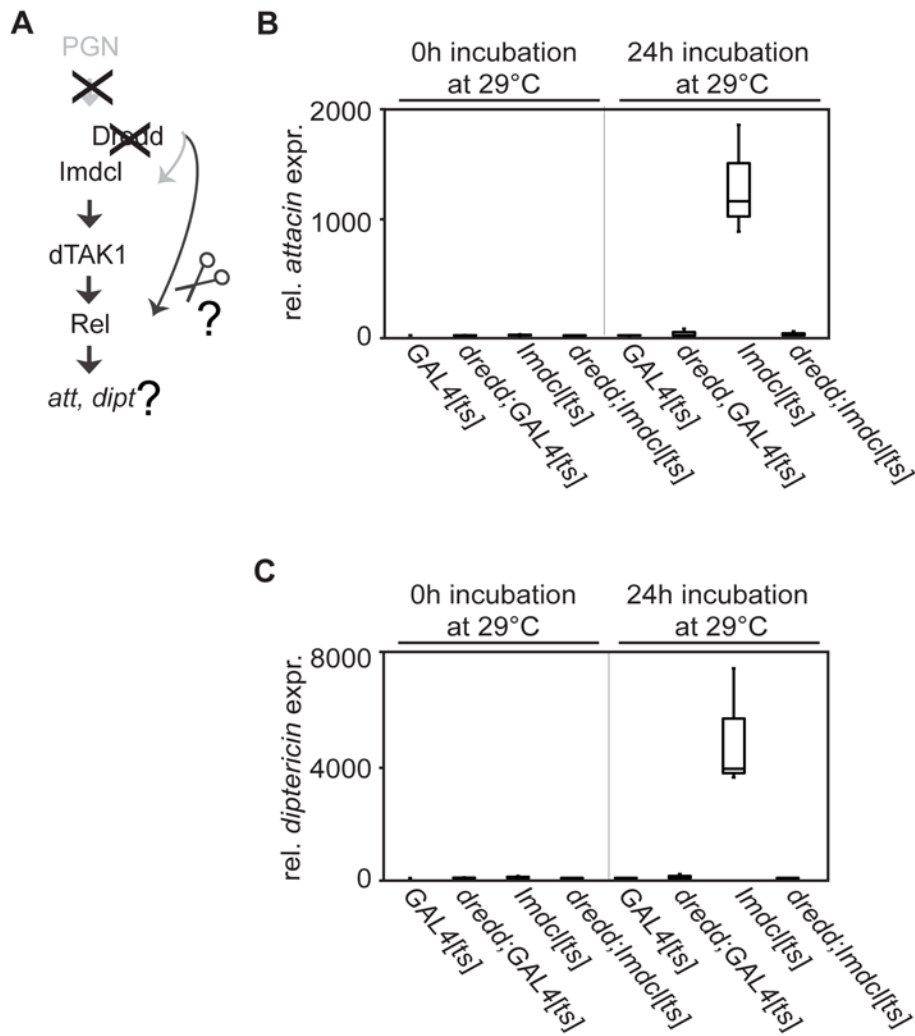


**Figure 4.7. Dredd functions downstream of or parallel to cleaved Imd (Imdcl) *in vivo*:** **A.** Flowchart of signal transduction through the IMD signaling pathway of a *dredd* mutant fly line that expresses a constitutively active Imd. These flies circumvent PGN-mediated Imd cleavage and allow to address the requirement for Dredd in IMD/Rel signaling. If Dredd is required downstream of Imd cleavage in the IMD/Rel arm *dredd;Imdcl* flies will fail to induce AMP expression. **B-C.** Quantitative real time PCR analysis of *GAL4[ts]*, *dredd;GAL4[ts]*, *Imdcl[ts]*, and *dredd;Imdcl[ts]* flies incubated at the restrictive temperature (29°C) for indicated times. The relative expression levels for *attacin* (A) and *diptericin* (B) were standardized to *actin* levels. The expression levels for *dredd;GAL4[ts]*, *Imdcl[ts]*, and *dredd;Imdcl[ts]* flies are reported relative to uninduced *GAL4[ts]* control flies. Measurements for each transcript are presented as a box blot to graphically illustrate the results of three independent experiments.

To test if the insufficiency of AMP induction in *dredd*<sup>B118</sup> null mutant flies that express *Imdcl* is specific to the *dredd*<sup>B118</sup> mutation I asked if a genomic Dredd construct rescues AMP expression in *dredd*<sup>B118</sup> mutant flies (Figure 4.8.A)<sup>129</sup>. The genomic *dredd* construct (*P[dredd+]*) is a P element insertion that contains 7.6 kb of genomic DNA that includes only the *dredd* locus. *dredd*<sup>B118</sup> mutant flies that carry *P[dredd+]* show a rescue of IMD/Rel-dependent AMP expression, Rel cleavage and survival after bacterial infection<sup>112</sup>.

I tested *P[dredd+]* flies for their ability to induce the expression of *dipt* and *att* expression in *dredd;Imdcl[ts]* flies. Compared to uninduced flies and in agreement with earlier results, flies that express *Imdcl* showed a strong induction of *att* and *dipt* (Figure 4.3.B-C). While the *dredd*<sup>B118</sup> mutation fully blocked AMP expression in *Imdcl* flies, expression of *Imdcl* in flies that carry the genomic Dredd in the *dredd*<sup>B118</sup> mutant background rescued *att* and *dipt* expression levels (Figure 4.7.B-C). The result shows that genomic Dredd rescues AMP expression in *dredd*<sup>B118</sup> null mutant flies and validate that the observed phenotype in *dredd*<sup>B118</sup> mutant flies is specific to the loss-of-function of the *dredd* gene.

Combined my data demonstrate an essential role for Dredd in the IMD/Rel activation downstream of *Imd* cleavage and therefore establish a dual requirement for Dredd in IMD-signaling.

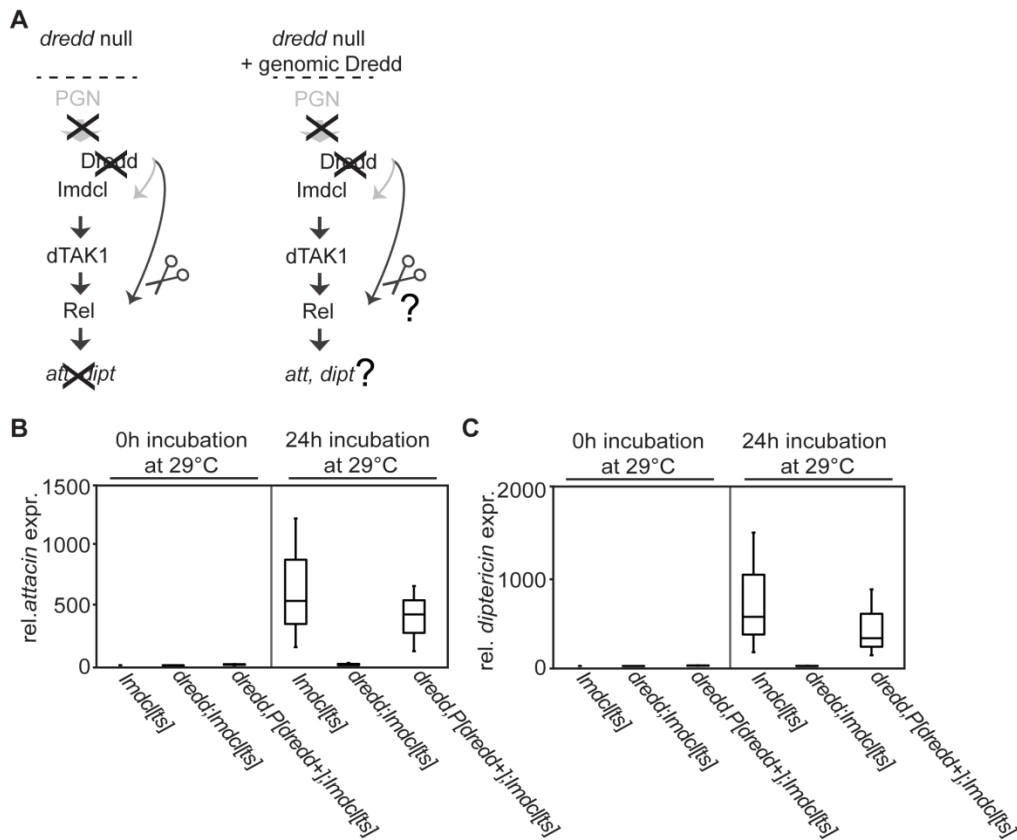


**Figure 4.8. P[dredd+] rescues the *dredd*<sup>B118</sup> mutation in *Imdcl* flies:** **A.** Flowchart of signal transduction through the IMD signaling pathway of a *dredd* mutant fly line that expresses a constitutively active *Imd*. If Dredd is required downstream of *Imd* cleavage in the IMD/Rel arm a genomic Dredd will restore AMP expression in *dredd.Imdcl* flies. **B-C.** Quantitative real time PCR analysis of *Imdcl[ts]*, *dredd;Imdcl[ts]*, and *dredd,P[dredd+];Imdcl[ts]* flies incubated at the restrictive temperature (29°C) for 0h or 24h. The relative expression levels for *attacin* (A) and *dipericin* (B) were standardized to *actin* levels. The expression levels for *dredd;Imdcl[ts]* and *dredd,P[dredd+];Imdcl[ts]* flies are reported relative to uninduced *Imdcl[ts]* flies. Measurements for each transcript are presented as a box blot to graphically illustrate the results of three independent experiments.

#### 4.3.2. Dredd does not rescue the *dredd*<sup>B118</sup> mutation

To investigate if Dredd proteolytic activity is required for IMD/Rel signaling I generated UASDredd (UASDredd) and UASDreddCA (UASDreddCA) transgenic fly lines. The fly strains that were used in this section are listed in Table 4.3.

UASDredd and UASDreddCA fly lines express the  $\gamma$  isoform of the Dredd transcript that has been described before<sup>129</sup>. In the UASDreddCA expression construct the catalytic site is mutated from a cysteine to an alanine to render Dredd catalytic dead<sup>352</sup>. If the catalytic activity of Dredd is required in IMD/Rel signaling UASDredd flies but not UASDreddCA should rescue AMP expression in *dredd;Imdcl[ts]* flies (Figure 4.9.A). I expressed both constructs in *dredd;Imdcl[ts]* flies and followed IMD/Rel activation in flies by monitoring *att* and *dipt* expression by qRT-PCR analysis (Figure 4.8.B-C). More specifically, *Imdcl* flies induced AMP expression that was blocked by the loss of *dredd* (*dredd;Imdcl[ts]*). Co-expression of *Imdcl* with UASDredd or UASDreddCA induces similar levels of IMD/Rel response genes as *Imdcl* by itself. In contrast, the *dredd*<sup>B118</sup> mutation blocked *att* and *dipt* expression in flies that co-express *Imdcl* with UASDredd or UASDreddCA. The data are in contrast to my previous result that showed rescue of the *dredd*<sup>B118</sup> mutation by a genomic Dredd and the result indicate that the fat body specific expression of UASDredd or UASDreddCA does not restore *att* or *dipt* expression in *dredd;Imdcl[ts]* flies.

GENOTYPE	ABBREVIATION	DESCRIPTION	EXPECTED PHENOTYPE
cgGAL4	GAL4	fat-body specific expression of <i>GAL4</i>	no activation of the IMD response after a heatshift to 29°C
cgGAL4/UAS <i>Imdcl</i> ; GAL80ts/+	<i>Imdcl</i> [ts]	<i>Imdcl</i> transgene (constitutive active IMD) driven by GAL4[ts]	activation of the IMD response after a heatshift to 29°C
dreddB118;cgGAL4/ UAS <i>Imdcl</i> ; GAL80ts/+	dredd; <i>Imdcl</i> [ts]	<i>Imdcl</i> transgene driven by GAL4[ts] and null for <i>dredd</i>	no activation of the IMD response after a heatshift to 29°C
cgGAL4/UAS <i>Imdcl</i> ; UAS <i>Dredd</i> /GAL80ts	<i>Imdcl</i> [ts]; <i>Dredd</i> [ts]	<i>Imdcl</i> and <i>UASDredd</i> transgenes driven by GAL4[ts]	?
dreddB118;cgGAL4/ UAS <i>Imdcl</i> ; UAS <i>Dredd</i> /GAL80ts	dredd; <i>Imdcl</i> [ts]; <i>Dredd</i> [ts]	<i>Imdcl</i> and <i>UASDredd</i> transgenes driven by GAL4[ts] and null for <i>dredd</i>	?
cgGAL4/UAS <i>Imdcl</i> ; UAS <i>DreddCA</i> / GAL80ts	<i>Imdcl</i> [ts]; <i>DreddCA</i> [ts]	<i>Imdcl</i> and <i>UASDreddCA</i> transgenes driven by GAL4[ts]	?
dreddB118;cgGAL4/ UAS <i>Imdcl</i> ; UAS <i>DreddCA</i> /GAL80ts	dredd; <i>Imdcl</i> [ts]; <i>DreddCA</i> [ts]	<i>Imdcl</i> and <i>UASDreddCA</i> transgenes driven by GAL4[ts] and null for <i>dredd</i>	?
dreddB118,P[ <i>dredd+</i> ]; cgGAL4/+	dredd,P[ <i>dredd+</i> ]	GAL4 transgene with a genomic <i>Dredd</i>	wild type activation of the IMD response after infection
cgGAL4/UAS <i>Dredd</i>	<i>UASDredd</i>	<i>UASDredd</i> transgene driven by GAL4	?
dreddB118;cgGAL4/ UAS <i>Dredd</i>	dredd; <i>UASDredd</i>	<i>UASDredd</i> transgene driven by GAL4 and null for <i>dredd</i>	
cgGAL4/UAS <i>DreddCA</i>	<i>UASDreddCA</i>	<i>UASDreddCA</i> transgene driven by GAL4	?
dreddB118;cgGAL4/ UAS <i>DreddCA</i>	dredd; <i>UASDreddCA</i>	<i>UASDreddCA</i> transgene driven by GAL4 and null for <i>dredd</i>	?

**Table 4.3: Fly strains for section 4.3.2.:** A brief description of the fly lines and the expected phenotypes in section 4.3.2. For more information on the fly lines see Materials and Methods (Chapter 2).

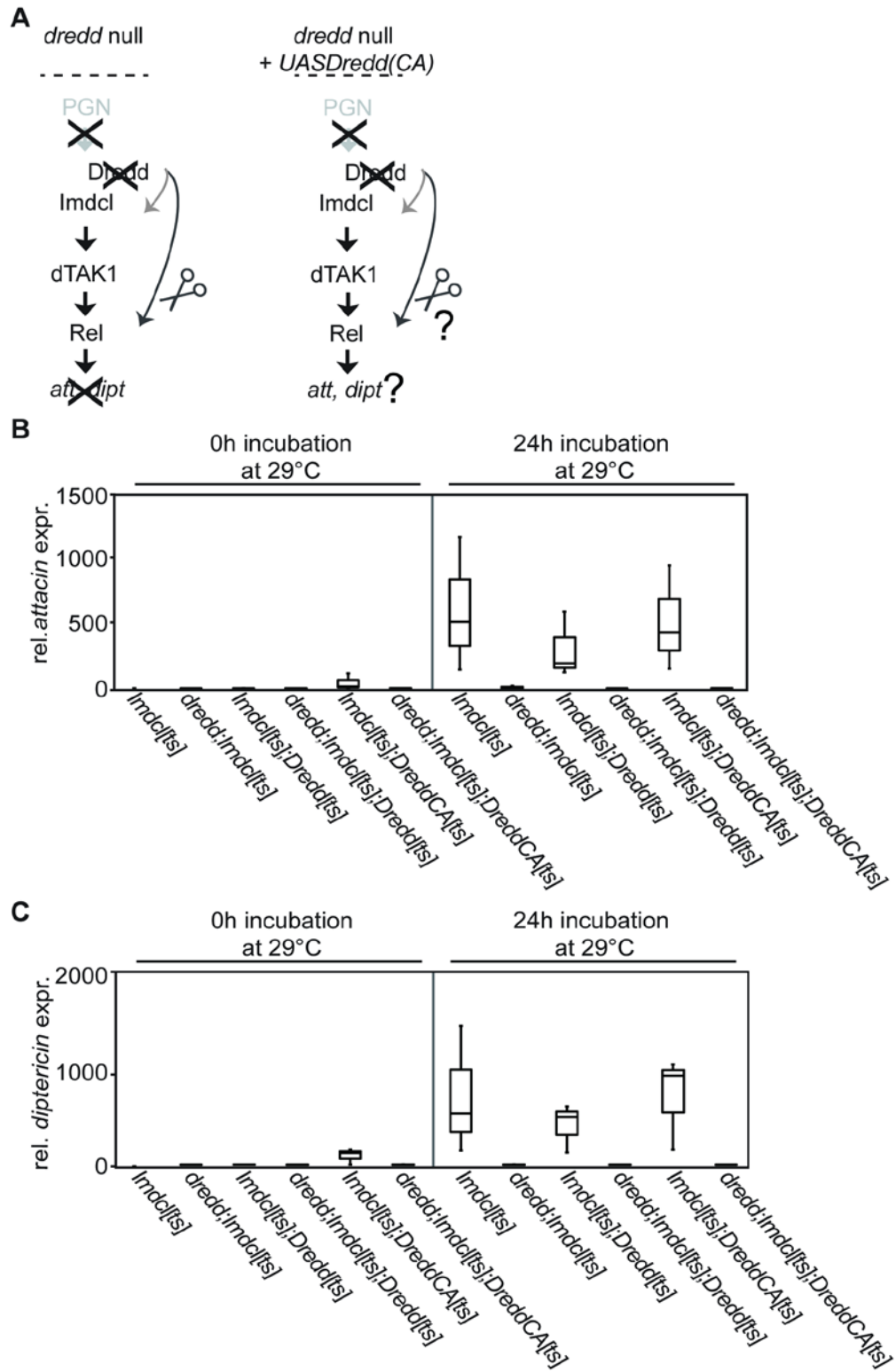


**Figure 4.9. Dredd does not rescue the *dredd*<sup>B118</sup> mutation in *Imdcl* flies: A.** Flowchart of signal transduction through the IMD signaling pathway of a *dredd* mutant fly line that expresses a constitutively active Imd. If a catalytically active Dredd is required downstream of Imd cleavage in the IMD/Rel arm expression of a Dredd transgene will restore AMP expression in *dredd,Imdcl* flies while expression of DreddCA will not. **B-C.** Quantitative real time PCR analysis of *Imdcl[ts]*, *dredd;Imdcl[ts]*, *Imdcl[ts]; UASDredd*, *dredd;Imdcl[ts]*, and *UASDreddCA* flies incubated at the restrictive temperature (29°C) for 0h or 24h. The relative expression levels for *attacin* (A) and *diptericin* (B) were standardized to *actin* levels. The expression levels for each sample are reported relative to uninduced *Imdcl[ts]* flies. Measurements for each transcript are presented as a box blot to graphically illustrate the results of three independent experiments.

To further evaluate the  $\gamma$  variant of Dredd in IMD/Rel signaling I next analyzed if UASDredd and UASDreddCA flies can restore AMP expression in *dredd*<sup>B118</sup> mutant flies after bacterial infection (Figure 4.10.A). As a positive control I included *P[dredd+]* flies that are known to rescue the *dredd*<sup>B118</sup> mutation. I initially confirmed the expression of both Dredd expression constructs by qRT-PCR (Figure 4.10.B). In contrast to control flies (*GAL4*), *dredd* is expressed in UASDredd and UASDreddCA flies. Insertion of the UASDredd and UASDreddCA transgenes into different regions of a genome (*position effect*) probably caused the variation of expression seen for either transcript.

I next tested if expression of one of the Dredd variants restores AMP induction in *dredd*<sup>B118</sup> mutant flies (Figure 4.10.C-D). Expression of UASDredd or UASDreddCA in a WT background showed an induction of AMP expression at levels similar to control flies (*GAL4*) after bacterial challenge. In contrast to *P[dredd+]* flies that restore AMP expression after bacterial challenge, expression of UASDredd or UASDreddCA did not restore *att* or *dipt* expression in *dredd*<sup>B118</sup> flies.

The data indicate that the Dreddy variant is insufficient to rescue the *dredd*<sup>B118</sup> mutation and suggests a requirement for different Dredd isoform(s) in the regulation of AMP expression in IMD/Rel signaling.

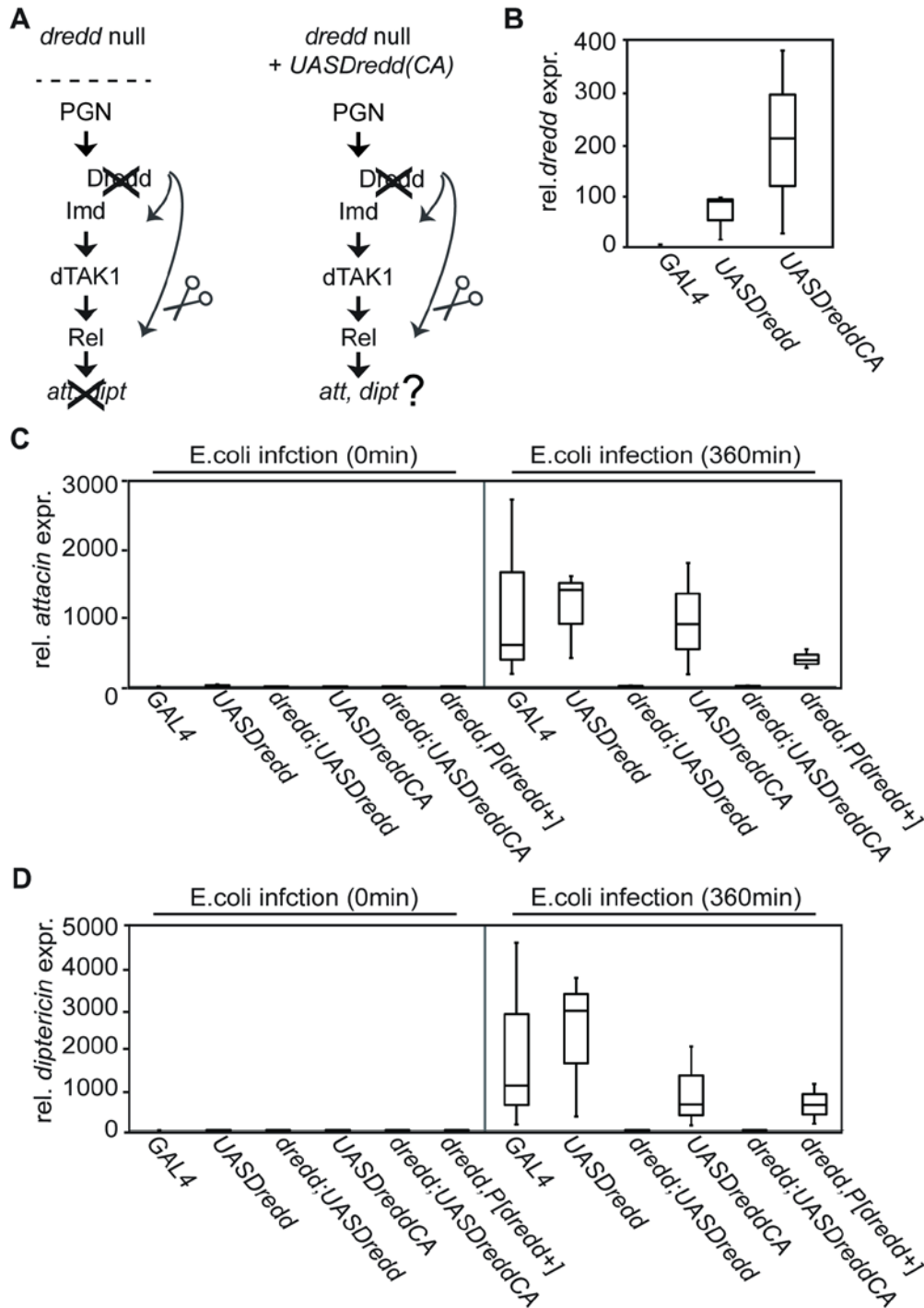


**Figure 4.10. Dredd does not rescue the *dredd*<sup>B118</sup> mutation:** **A.** Flowchart of signal transduction through the IMD signaling pathway of a *dredd* mutant fly line. If Dreddy is sufficient to mediate signaling in the IMD pathway, expression of a Dreddy transgene will restore AMP expression in *dredd*<sup>B118</sup> flies while expression

of DreddyCA will not. **B.** Quantitative real time PCR analysis of *cgGAL4*, *UASDredd*, and *UASDreddCA* flies, infected with *E.coli* and recovered for the indicated times. The relative expression level for *dredd* was standardized to *actin* levels. The expression levels for *UASDredd* and *UASDreddCA* flies at the indicated time points after infection are reported relative to *cgGAL4* flies. Measurements for each transcript are presented as a box blot to graphically illustrate the results of three independent experiments. **C-D.** Quantitative real time PCR analysis of *cgGAL4*, *UASDredd*, *UASDreddCA*, and *dredd,P[dredd+]*, infected with *E.coli* and recovered for the indicated times. The relative expression levels for *attacin* (A) and *diptericin* (B) were standardized to *actin* levels. The expression levels for each sample are reported relative to uninduced *cgGAL4*. Measurements for each transcript are presented as a box blot to graphically illustrate the results of three independent experiments.

#### 4.4. Summary

The genetically tractable model system *Drosophila* allows us to test cell culture observations in a more physiologically relevant *in vivo* context. I exploited this advantage to explore a requirement for Dredd in IMD/dJNK and IMD/Rel activation in a whole animal setting. My studies clearly demonstrated a direct requirement for Dredd in IMD/dJNK and IMD/Rel activation *in vivo* (Figure 4.11.). Specifically, I showed that loss of Dredd blocks infection-responsive phosphorylation of dJNK and prevents a bacterial challenge-dependent induction of dJNK-dependent target genes *in vivo*. In addition, I showed that Dredd is essential downstream of Imd cleavage to facilitate the appropriate activation of the IMD/Rel arm. Dredd therefore fulfills a dual function in IMD signaling: as an essential proximal element of a phospho-relay in the activation of IMD/dJNK, and separately in the expression of IMD/Rel-dependent transcripts.

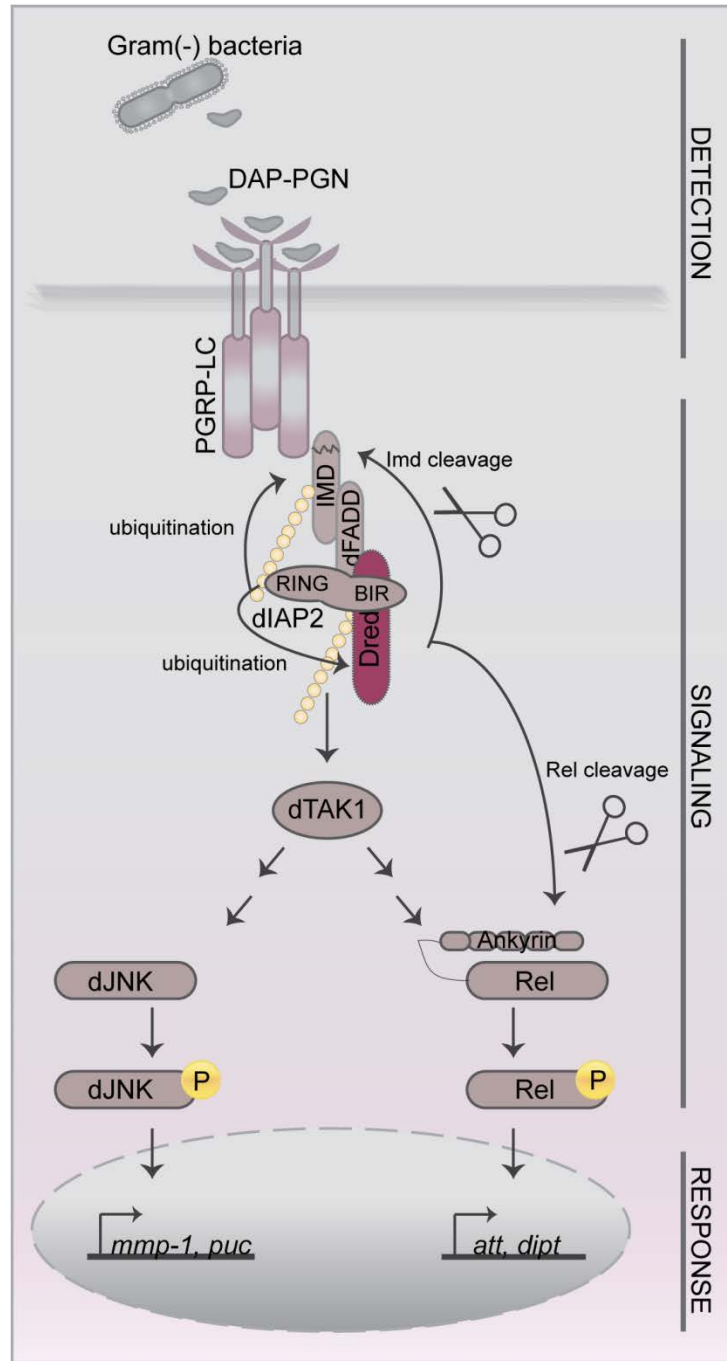


**Figure 4.11. Summary of section 4:** Illustration of the *Drosophila* IMD signaling pathway with the added changes that resulted from this study. In summary, my results demonstrated in chapter 4 establish Dredd as an essential proximal element of the IMD pathway that is required for full activation of both, the IMD/dJNK and the IMD/Rel signaling arm *in vivo*.

## **Chapter 5. Caspase function in *Drosophila* IMD signaling**

## 5.1. Background

In general, initiator caspases are activated through proximity induced dimerization that mediates autoproteolytic cleavage of the caspase linker regions and release of a mature and stable caspase<sup>184</sup>. Once initiator caspases are activated, they catalytically cleave effector caspases, driving the cell towards apoptosis<sup>184</sup>. IAP proteins provide an additional step of caspase regulation by the specific inhibition of caspases through BIR domain mediated binding or by targeting the caspase for proteasomal degradation via RING mediated E3 ubiquitin activity<sup>360</sup>. Although best known to inhibit apoptosis at the caspase level, IAPs also affect the decision between apoptosis and cell survival by influencing the ubiquitin-dependent pathways that modulate innate immune signaling. For example a recent report in *Drosophila* showed that dIAP2 mediated ubiquitination of Imd and Dredd is required for proper downstream signaling in the IMD pathway<sup>114,273</sup>. Dredd is considered the *Drosophila* ortholog of Caspase-8 based on broad similarities to the Caspase-8 sequence (percent sequence identity: 21%)<sup>129</sup>. However, disruption of the *caspase-8* gene causes embryonic lethality, while *dredd* mutant flies are healthy and fertile and do not show defects associated with abortive apoptosis<sup>129,276,340</sup>. In contrast to the extensive analysis of Caspase-8 activation during apoptosis, Dredd activation is unclear. Thus, the molecular basis of Dredd activation in IMD signaling remain to be defined.

I initially examined the structural and functional similarities and differences between Dredd and Caspase-8 to elucidate the degree of conservation between the caspase modules and their activation. In my second set of experiments I analysed if there is a further requirement for caspase function in IMD signaling at the level of dIAP2. The fly strains that were used in this section are listed in Table 5.1.

GENOTYPE	ABBREVIATION	DESCRIPTION
<i>cgGAL4/+</i>	<i>GAL4</i>	fat-body specific expression of <i>GAL4</i>
<i>dreddB118;cgGAL4/+</i>	<i>dredd;GAL4</i>	<i>GAL4</i> transgene and null for <i>dredd</i>
<i>cgGAL4/+;</i> <i>UASHADredd/+</i>	<i>HADredd</i>	<i>UASHADredd</i> transgene driven by <i>GAL4</i>
<i>dreddB118;cgGAL4/;</i> <i>UASHADredd/+</i>	<i>dredd;HADredd</i>	<i>UASHADredd</i> transgene driven by <i>GAL4</i> and null for <i>dredd</i>

**Table 5.1. Fly strains for section 5.2.1.:** A brief description of the fly lines and the expected phenotypes in section 5.2.1. For more information on the fly lines see Materials and Methods (Chapter 2).

## **5.2. Dredd structure and activation is distinct from Caspase-8 in cell culture**

### **5.2.1. Dredd forms homodimers in S2 cells**

A key feature of caspase activation is the initial dimerization and subsequent auto-processing of the caspase molecules<sup>184</sup>. To examine the functional similarity between Dredd and Caspase-8, and to further explore functional domains of Dredd in IMD signaling, I initially tested if Dredd homodimerizes in S2 cells. I performed anti-HA immunoprecipitations on whole cell lysates prepared from S2 cells that were co-transfected with HADredd and MycDredd full-length expression plasmids (Figure 5.1.A). I detected a co-precipitation of MycDredd with HADredd (Figure 5.1.A, lane 6 middle panel). In contrast, I did not observe precipitation of MycDredd in the absence of HADredd (Figure 5.1.A, lane 4 middle panel). The result indicate that Dredd homodimerizes in S2 cells.

To identify the domains required for Dredd dimerization I analysed Dredd deletion construct for their ability to precipitate full-length HA-tagged Dredd (Figure 5.1.B). To this end, I transfected S2 cells with a HADredd expression construct, and co-transfected either with a Myc-tagged construct that expresses the caspase domain (MycDreddcasp-domain) or the prodomain (MycDredd-prodomain) of Dredd. I immunoprecipitated HADredd protein with a HA specific antibody and analysed the S2 cell lysates by Western blot. I identified a co-immunoprecipitation of both, MycDreddcasp-domain and MycDreddprodomain, with full-length HADredd, indicating that both domains independently interact with full-length Dredd. The data confirm homodimerization that is mediated by the pro- and caspase domain of Dredd.

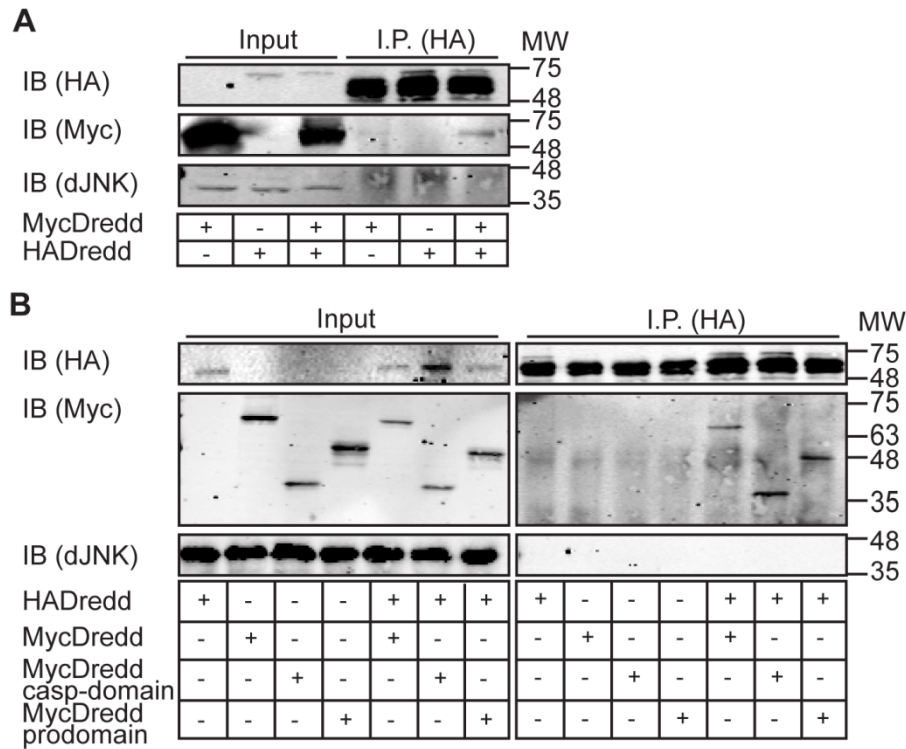


**Figure 5.1. Dredd forms homodimers in S2 cells: A-B.** Western blot analysis of lysates from S2 cells transfected with the indicated expression constructs. Protein levels of input and immunoprecipitated samples were visualised with HA (upper panel), or with Myc (middle panel) specific antibodies. dJNK was visualized as a loading control (lower panel). Lysates of the input samples, and the same samples after immunoprecipitation with an HA specific antibody are indicated. For all Western Blots: bands in immunoprecipitated samples that run at ~55 kDa correspond to the immunoglobulin heavy chain. Molecular weights are indicated on the right of each panel. HADredd co-precipitates MycDredd, MycDreddcasp-domain, and MycDreddprodomain.

### 5.2.2. Dredd and Caspase-8 have distinct proteolytic activities

A typical feature of caspase activation is dimerization and subsequent proximity induced processing of the caspase molecules<sup>184</sup>. Surprisingly, I did not detect lower molecular bands that indicate auto-processing of Dredd in S2 cells (Figure 5.1.B; second lane of the Myc-blot on the left). To elucidate similarities and differences in Caspase-8 and Dredd proteolytic activities I generated a tagged Caspase-8 expression construct that allows the endogenous expression of Caspase-8 in S2 cells. In addition, I cloned chimeric expression constructs that contains the prodomain of human Caspase-8 and the caspase domain of *Drosophila* Dredd (CD) and a second chimeric construct that contains the prodomain of Dredd and the caspase domain of Caspase-8 (DC) (Figure 5.2.A). I confirmed expression of all constructs by Western blot (Figure 5.2.B). In agreement with my earlier results I did not detected lower molecular bands in S2 cell lysates that were transfected with a MycDredd expression construct. Likewise, samples of cells transfected with either chimeric constructs did not show lower molecular bands. In contrast, expression of a tagged Caspase-8 construct revealed two lower molecular weight bands that suggest proteolytic cleavage of Caspase-8 at the prodomain and the large subunit.

Since Dredd is part of the IMD signaling cascade it is possible that the pathway requires activation prior to Dredd processing. Therefore, I asked if activation of IMD signaling induces processing of Dredd. To address this question I transfected S2 cells with expression constructs for Dredd, CD, DC, and Caspase-8, and activated the IMD pathway by PGN treatment (Figure 5.2.C). Western blot analysis of S2 cell lysates transfected with a control MycdFADD expression plasmid showed no changes in MycdFADD protein levels in response to PGN. Similarly, PGN did not alter the appearance of MycDredd, MycCD, MycDC, or MycCaspase-8 cleavage products compared to non-treated cells. In line with earlier results (Figure 5.2.A) MycCaspase-8 cleavage products were easily detectable and were unaffected by PGN treatment. The result suggests that Dredd processing is not induced by PGN.

Next, I used the GAL4-UAS binary expression system to monitor Dredd cleavage in flies. Specifically, I crossed *cg-GAL4* transgenic flies with *UASHADredd* transgenic flies to generate flies that express HA-tagged Dredd in the fat body (*HADredd*). I visualised HADredd with a HA specific antibody by Western blot. To exclude possible interference with endogenous Dredd I also generated *cg-GAL4/UASHADredd* flies that are *dredd* null (*dredd;HADredd*), and therefore lack endogenous Dredd (Figure 5.2.D). While I easily detected full-length Dredd, I was unable to visual detect lower molecular weight bands in samples of *UASHADredd* flies. The data are in line with my cell culture data and suggest that Dredd is not auto-processed in *Drosophila*.

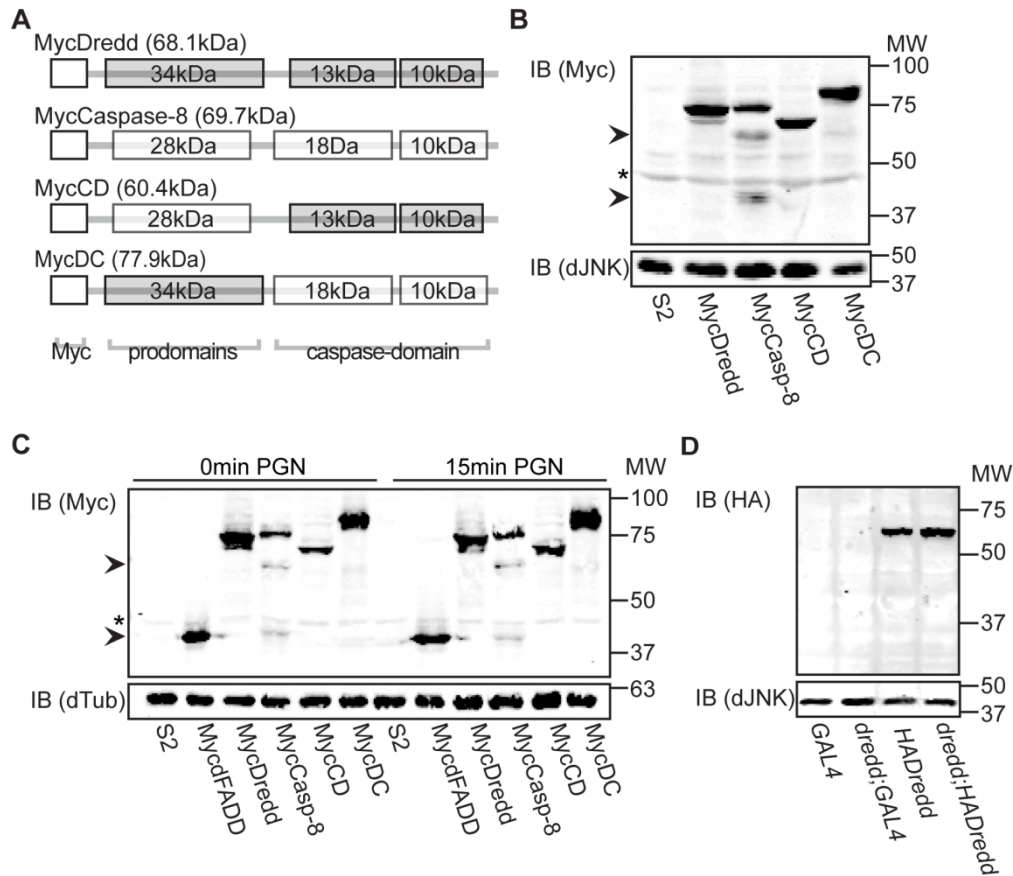


**Figure 5.2. Examination of caspase expression constructs in S2 cells and flies:** **A.** Schematic illustration of Myc-tagged Dredd, Caspase-8 (Casp-8), and Dredd/Caspase-8 chimeric (CD and DC, respectively) expression constructs. Protein domains and the molecular weights of the corresponding proteins are indicated. **B.** Western blot analysis of lysates from S2 cells transfected with the indicated Myc-tagged expression plasmids. Protein levels were visualized with a Myc (upper panel) specific antibody. dJNK (lower panel) was visualized as a loading control. **C.** Western blot analysis of lysates from S2 cells transfected with the indicated Myc-tagged expression plasmids and stimulated with PGN for the indicated times. Lysates were probed with a Myc specific antibody (upper panel). Tubulin was visualized as a loading control (lower panel). **D.** Western blot analysis of lysates from *cgGAL4* male (lane 1), *dredd;GAL4* male (lanes 2), *cgGAL4;UASHADredd* male (lane 3), and *dredd;HADredd* male (lane 4) flies. Protein levels were visualized with HA (upper panel) and total dJNK (lower panel) specific antibodies. For all Western blots: control lysates from non-transfected S2 cells were loaded where indicated. Molecular weights are indicated on the right of each panel, \* marks an unspecific band, and ► marks truncation products.

As mentioned above (Figure 5.2.B), Western blot analysis of a tagged Caspase-8 expression construct in S2 cells revealed three distinct protein bands. While the upper band corresponds to full-length Caspase-8, the two lower bands are in agreement with fragments of processed Caspase-8 after the prodomain and the p18 subunit. Next, I tested if the inhibition of caspase activity with zVAD-FMK prevents the appearance of the observed cleavage fragments (Figure 5.3.A). As a control I included the Caspase-9 ortholog Dronc and as expected, zVAD-FMK blocked Dronc processing in S2 cells. Likewise, in Caspase-8 transfected cell lysates, caspase inhibition by zVAD-FMK greatly diminished the appearance of the lower molecular weight fragments while the full-length Caspase-8 band appeared stronger. The data confirm that Caspase-8 is processed in S2 cells and suggest that caspase activity is required for processing of Caspase-8.

My initial data prompted me to ask if catalytic activity of Caspase-8 is required for Caspase-8 processing in S2 cells. To do so, I introduced a point mutation in the active site of Caspase-8 that renders Caspase-8 proteolytically inactive (Figure 5.3.B). More specifically, I converted the Caspase-8 active site Cysteine 360 to Alanine (Caspase-8CA). In line with zVAD-FMK data, I found that an inactive Caspase-8 variant is not processed in S2 cells. In summary, Caspase-8 is processed in S2 cells and processing can be blocked by zVAD-FMK or by mutating the active site of Caspase-8. These findings indicate that Caspase-8 is auto-processed in S2 cell culture.

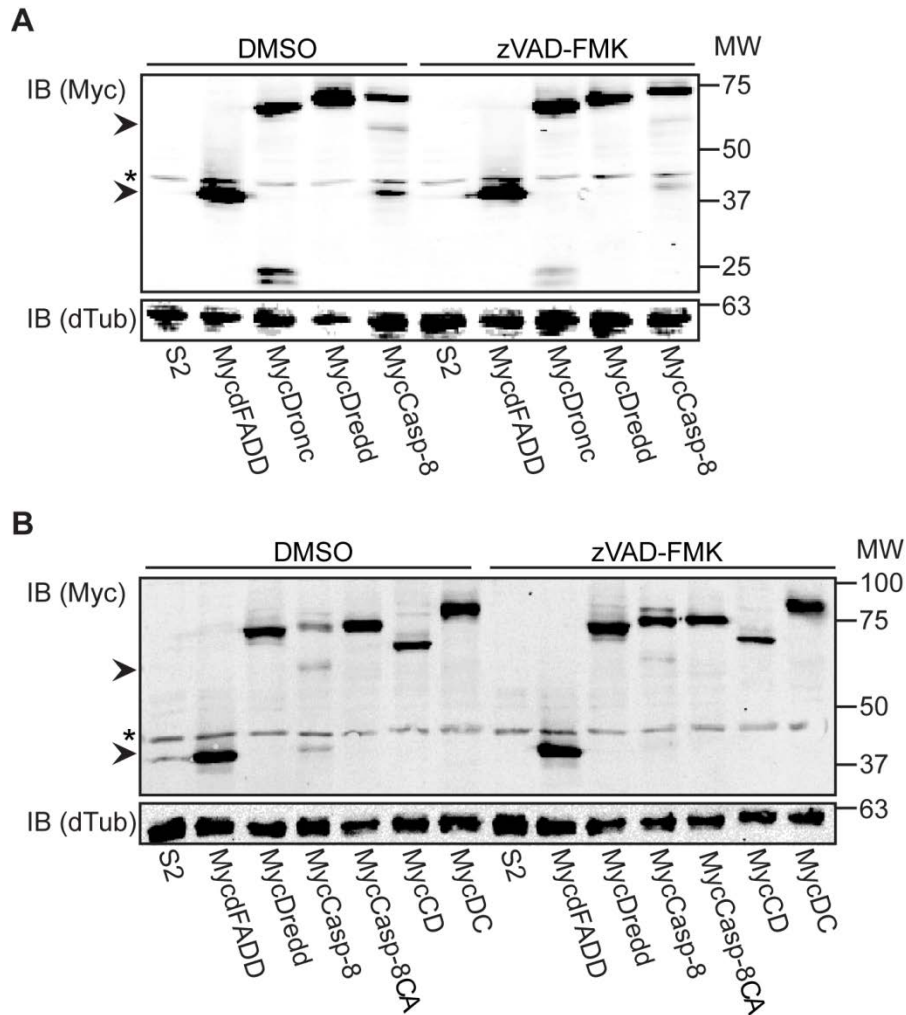


**Figure 5.3. Caspase-8 is processed in a zVAD-FMK dependent manner in cell culture: A-B.** Western blot analysis of lysates from S2 cells transfected with the indicated Myc-tagged expression plasmids and incubated with DMSO or zVAD-FMK for 3 h. For all Western blots: control lysates from non-transfected S2 cells were loaded where indicated. Lysates were probed with Myc (first panel) and tubulin (lower panel) specific antibodies. Molecular weights are indicated on the right of each panel, \* marks an unspecific band, and > marks truncation products.

zVAD-FMK blocks Dredd dependent Rel cleavage in IMD signaling<sup>126</sup>. Therefore it is possible that exogenous Caspase-8 dimerizes with endogenous Dredd and triggers Caspase-8 processing. To investigate if Caspase-8 is auto-processed or processed by Dredd I initially asked if Caspase-8 and Dredd interact in S2 cells. To probe for a potential interaction between Caspase-8 and Dredd I performed a co-immunoprecipitation assay in S2 cell lysates. To reveal domains required for a potential Dredd:Caspase-8 interaction, I tested if a HACaspase-8 expression construct co-immunoprecipitates MycDredd, MycCD or MycDC (Figure 5.4.A). I found that Dredd interacts with both chimeric Dredd/Caspase-8 variants. In addition, HADredd binds weakly Caspase-8 in S2 cells. The data confirm the independent interactions between the Dredd pro- and caspase-domains and suggest a mild interaction of Dredd with Caspase-8.

My initial data raised the possibility that Caspase-8 processing is a result of heterodimerization between Dredd and Caspase-8 that might result in trans-processing. In line, Dredd and Caspase-8 interact in S2 cells. Therefore I analyzed how RNAi-mediated depletion of *dredd* affects Caspase-8 processing in S2 cells (Figure 5.4.B). I incubated cells with control or *dredd* dsRNA and transfected the same cells with MycdFADD, MycDredd, and MycCaspase-8 expression constructs. I used MycdFADD as a control since it is not a caspase substrate. I then monitored protein levels by Western blot. MycdFADD protein levels were unaffected by control and *dredd* dsRNA. As expected, incubation of MycDredd transfected cells with *dredd* dsRNA completely eliminated MycDredd protein. In contrast, MycCaspase-8 protein levels were unaffected by *dredd* dsRNA and depletion of *dredd* did not block MycCaspase-8 processing (Figure 5.4.B, Myc blot lane 4 and 8). These data demonstrate that Caspase-8 processing is independent of Dredd in S2 cells.



I detected a lower molecular band below the full-length Dredd in lysates from S2 cells that co-expressed Dredd with Caspase-8. Since my previous result indicated that Caspase-8 is proteolytic active in S2 cells it is intriguing to speculate that Caspase-8 binds Dredd to trigger processing. To check if Caspase-8 processes Dredd I transfected S2 cells with Myc-tagged Dredd, DreddCA, CD, or CD expression constructs and co-transfected either with HACaspase-8 or with HACaspase-8CA expression construct (Figure 5.5.A). While co-expression of control plasmid MycdFADD with HACaspase-8 did not alter MycdFADD protein levels, co-expression of HACaspase-8 with MycDredd, MycDreddCA, MycCD, or MycDC triggered the appearance of lower molecular weight bands for all constructs. S2 cell lysates that co-expressed the catalytic inactive Caspase-8 variant do not display truncation products. The results indicate that human Caspase-8 processes Dredd, DreddCA, MycCD, or MycDC in S2 cells. In line, MycDreddCA protein is cleaved in cells that express HACaspase-8 indicating that proteolysis is mediated by Caspase-8 and not Dredd.

To address if processing of Dredd is mediated specifically by Caspase-8 I co-expressed MycDredd with HADronc or HACaspase-8 in S2 cells and incubated the transfected cells either with the control solvent DMSO or with zVAD-FMK to block caspase activity (Figure 5.5.B). Expression of MycDredd alone generated a protein of the appropriate molecular weight of full-length Dredd. In contrast, a lower molecular weight band appeared in cell lysates that co-express MycDredd and HACaspase-8 but not HADronc. The size of the lower molecular weight band indicates a cleavage event in the Dredd prodomain. The appearance of the cleavage product is blocked by zVAD-FMK. The data demonstrate that Caspase-8 processes MycDredd in S2 cells.

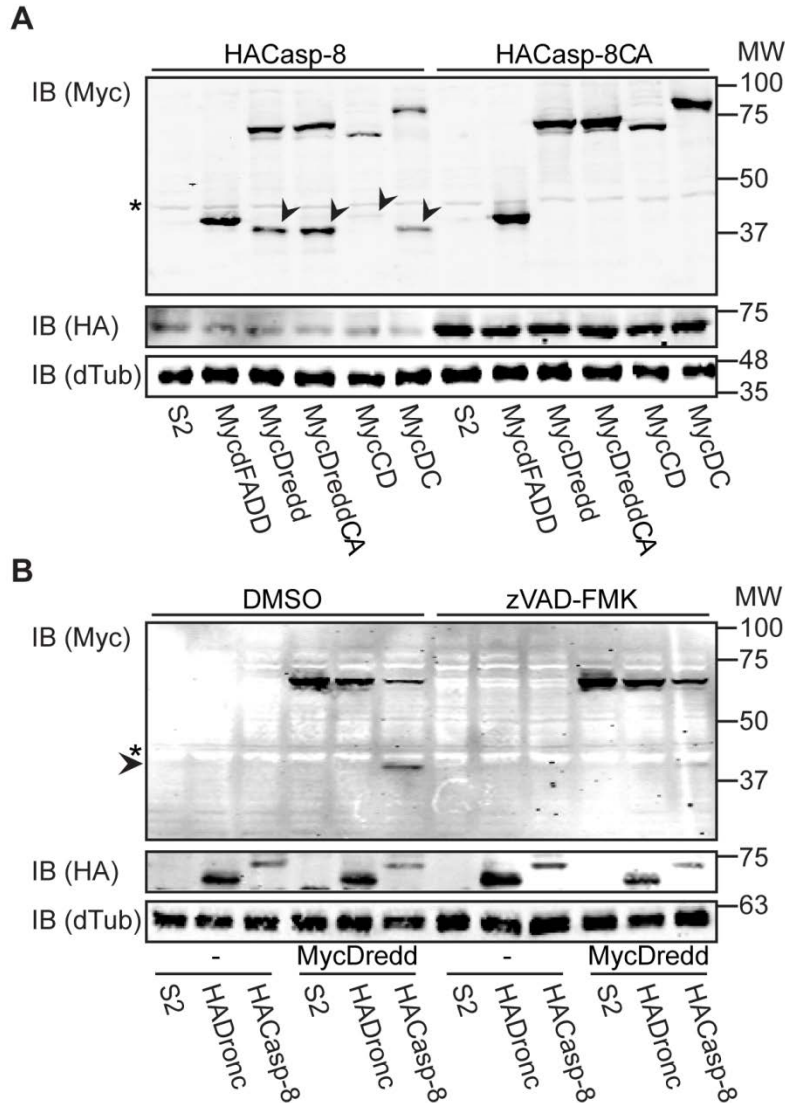


**Figure 5.5. Caspase-8 induces Dredd processing in cell culture: A.** Western blot analysis of lysates from S2 cells transfected with Myc-tagged expression constructs and co-transfected with HACasp-8 (lanes 1-6) or HACasp-8CA (lanes 7-12) expression plasmid as indicated. **B.** Western blot analysis of lysates from S2 cells transfected with HA-tagged expression constructs and co-transfected with Myc-tagged Dredd expression plasmid (lanes 4-6, and 10-12) as indicated. Samples were incubated with DMSO or zVAD-FMK for 3 h. For all Western blots: control lysates from non-transfected S2 cells were loaded where indicated. Lysates were probed with antibodies that detect Myc (upper panel), HA (middle panel), and tubulin (lower panel). Molecular weights are indicated on the right of each panel, \* marks an unspecific band, and ▶ marks truncation products. Dredd processing by Caspase-8 is zVAD-FMK dependent and is specific to Caspase-8.

My data showed auto-processing of Caspase-8 and Caspase-8 processes Dredd in S2 cells. These results suggest that Caspase-8 is proteolytically active in S2 cells. Therefore I asked if the expression of a proteolytic active Caspase-8 activates the IMD pathway. To determine the impact of Caspase-8 expression on the IMD signaling pathway I expressed MycdFADD, MycDredd and MycCaspase-8 constructs in S2 cells and stimulated the cells with DMSO as a control, with zVAD-FMK to block caspase activity, or with PGN to induce IMD signaling. I visualized Rel cleavage and phosphorylation of dJNK to follow the PGN-dependent activation of the IMD pathway (Figure 5.6.). As expected, incubation with zVAD-FMK blocked PGN-induced Rel cleavage and dJNK phosphorylation. I found that PGN-dependent phosphorylation of dJNK and Rel-cleavage were unaffected by the expression of Caspase-8 suggesting that the expression of Caspase-8 does not interfere with IMD signaling in S2 cells.

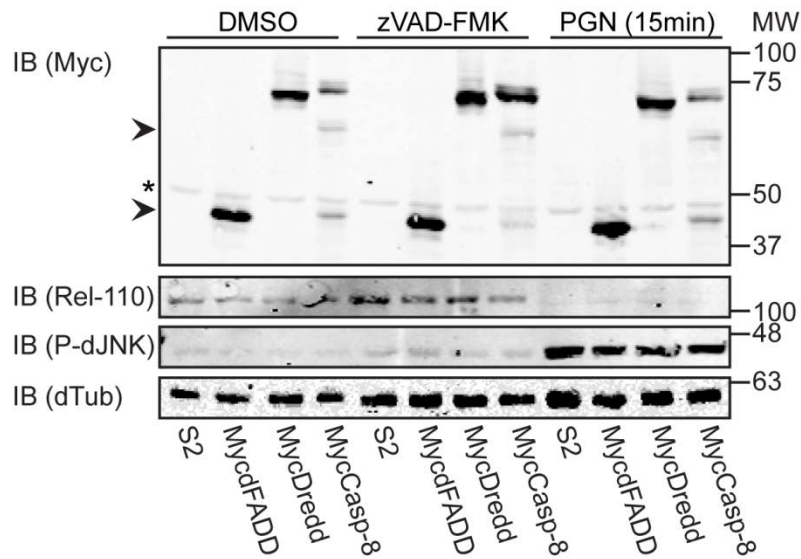


**Figure 5.6. Processing of Caspase-8 does not influence IMD signaling:**

Western blot analysis of lysates from S2 cells transfected with Myc-tagged expression constructs and incubated with DMSO (3 h), zVAD-FMK (3 h), or PGN (15 min) as indicated. Lysates were probed with antibodies that detect Myc (first panel), Rel-110 (second panel), P-dJNK (third panel), and tubulin (fourth panel). Control lysates from non-transfected S2 cells were loaded where indicated. Molecular weights are indicated on the right of each panel, \* marks an unspecific band, and  $\blacktriangleright$  marks proteolytic products.

Over-expression studies in HeLa cells initially implicated Dredd in apoptosis<sup>115</sup>. However, our data show that Dredd is not processed in S2 cells unless co-expressed with human Caspase-8 and Dredd lacks an apoptotic phenotype. Based on the experiments in S2 and HeLa cells I propose that endogenous Caspase-8 binds Dredd in HeLa cells which results in the clustering and concomitant autoproteolytic activation of Caspase-8. In this model, apoptotic signaling is mediated exclusively by Caspase-8 catalytic activity and Dredd serves as an assembly platform for caspase dimerization. To test this hypothesis, I investigated if Dredd functionally substitute for Caspase-8 in HeLa cells.

Initially, I confirmed the induction of apoptosis in HeLa cells in response to expression of FlagDredd (Figure 5.7.A). Dredd expression led to PARP cleavage, a common marker for apoptosis. I next tested if *caspase-8* siRNA specifically decreases Caspase-8 and not FlagDredd protein levels in HeLa cells (Figure 5.7.B). Protein analysis by Western blot demonstrated a strong reduction of Caspase-8 protein levels after *caspase-8* siRNA treatment while FlagDredd protein levels remained constant compared to cells treated with a control non-silencing siRNA. I next depleted *caspase-8* in HeLa cells to test for the ability of Dredd to substitute for Caspase-8 in the induction of apoptosis (Figure 5.7.C). In agreement with previous results FlagDredd induced apoptosis. However, *caspase-8* depletion in cells that expressed FlagDredd resulted in significantly lower levels of apoptosis induction. The results indicate that Dredd does not substitute for Caspase-8 pro-apoptotic functions in HeLa cells.

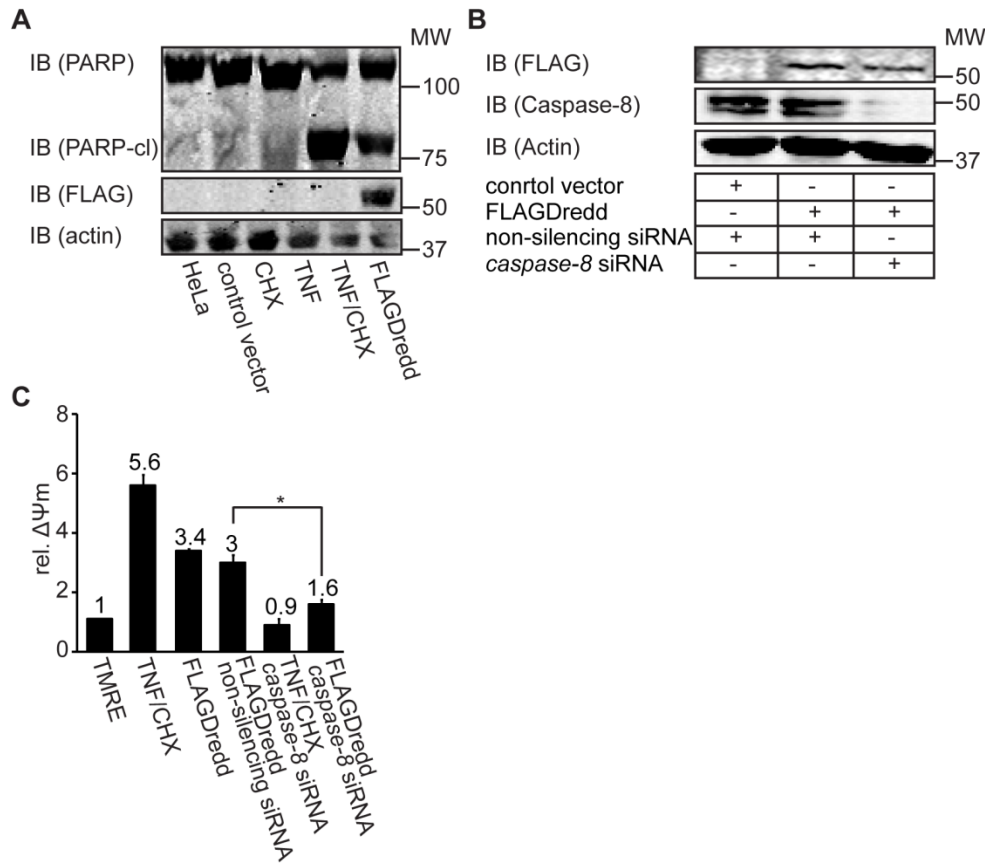


**Figure 5.7. Dredd does not substitute for Caspase-8 during apoptosis in HeLa cells:** **A.** Western blot analysis of lysates from HeLa cells transfected with a control or a FLAG-tagged Dredd expression plasmid as indicated. Cells are stimulated with cyclohexamide (CHX), TNF, or a combination of both. Protein levels were visualized with PARP (upper panel), FLAG (middle panel), and total actin (lower panel) specific antibodies. **B.** Western blot analysis of lysates from HeLa cells incubated with control non-silencing siRNA (lanes 1-2) or *caspase-8* siRNA (lanes 3) and transfected with control or FLAG-tagged Dredd expression plasmids as indicated. Lysates were probed with antibodies that detect FLAG (upper panel), endogenous Caspase-8 (middle panel), and total actin (lower panel). For all Western blots: molecular weights are indicated on the right of each panel. **C.** TMRE assay for the cell mitochondrial transmembrane potential following treatment with TNF/CHX or transfection with FLAGDredd expression construct as indicated. Cells are treated with a non-silencing control siRNA or with *caspase-8* siRNA. All values are presented relative to TMRE negative cells in a cell population. Each measurement graphically illustrates the result of three independent experiments. \* marks  $p$ -value  $< 0.05$ .

### 5.2.3. Dredd and Caspase-8 have distinct interaction profiles

Human Caspase-8 activation requires homodimerization and formation of a higher molecular weight complex composed of the adaptor molecules FADD, TRADD, TRAF2 and RIP1. The protein-protein interactions are mediated by tandem Death Domains (DD) and Death Effector Domains (DED)<sup>184</sup>. In contrast it has been suggested that Dredd interacts with dFADD through Death Inducing Domains (DID)<sup>115</sup>. In addition, Dredd also interacts with dIAP2 in S2 cells<sup>350</sup>. To investigate if Dredd and Caspase-8 have similar interaction profiles in S2 cells I checked if Caspase-8 interacts with dFADD in S2 cells.

I probed for potential protein-protein interactions in co-immunoprecipitation assays performed in S2 cell lysates. Specifically, I tested if HAdFADD co-immunoprecipitated with MycDredd, MycCaspase-8, MycCD, or MycDC. I did not detect precipitation of MycDredd, MycCaspase-8, MycCD, and MycDC in the absence of HAdFADD (Figure 5.8.A right panel, lane 1-5). In contrast, I observed co-precipitation of MycDredd and MycDC with HAdFADD (Figure 5.8.A right panel, lane 6 and 9). I did not detect a co-precipitation of MycCaspase-8 or MycCD with HAdFADD (Figure 5.8.A right panel, lane 7-8). The data show that Dredd interacts with dFADD through the prodomain while Caspase-8 fail to interact with dFADD.

I then asked if Caspase-8 binds dIAP2. Analysis of the input controls showed the successful expression of all expression constructs alone or when co-expressed with HAdIAP2 (Figure 5.8.B left panel, lane 1-9). I detected a co-precipitation of MycdFADD, MycCaspase-8, MycCD, and MycDC by HAdIAP2 (Figure 5.8.B right panel, lane 6, 8, and 9). In contrast, I did not observe precipitation of MycCaspase-8 with HAdIAP2 (Figure 5.8.B right panel, lane 7). Therefore I conclude that MycCD and MycDC bind to dIAP2 through the Dredd casp- and prodomain while Caspase-8 fails to interact with dIAP2. The data are in line with interactions of the Dredd pro- and caspase domains with dIAP2 (Chapter 3, Figure 3.16.B).

In summary, my data demonstrate distinctions between the proteolytic and interaction profiles of Caspase-8 and Dredd.

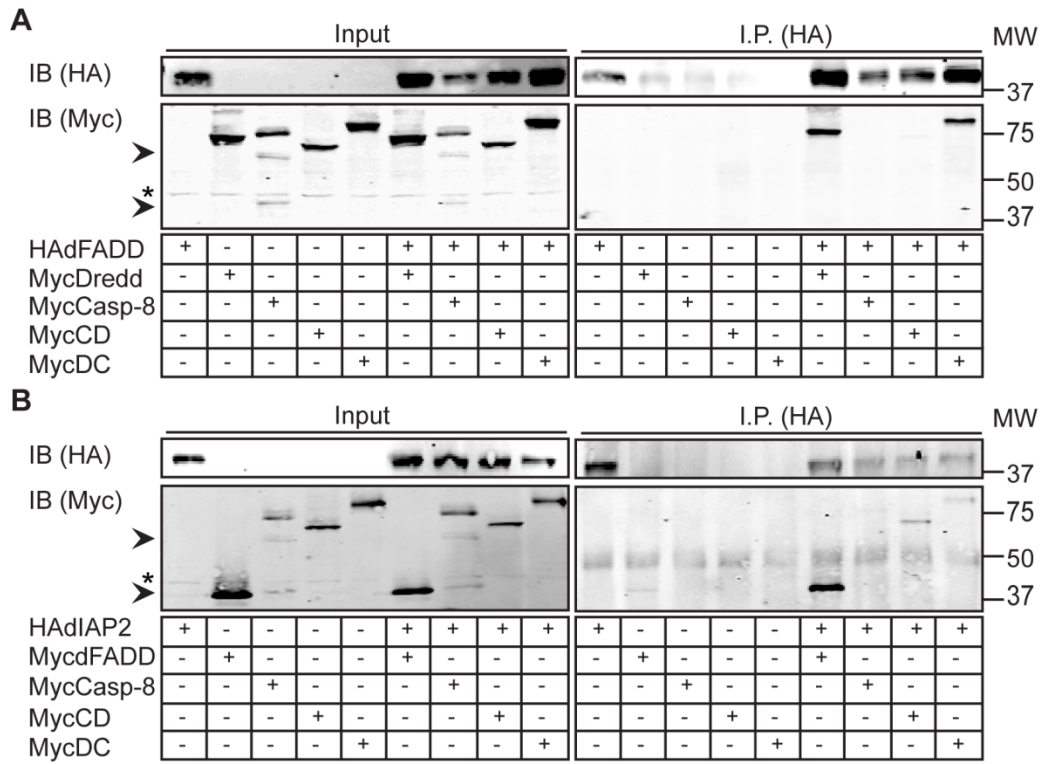


**Figure 5.8. Dredd and Caspase-8 have distinct interaction profiles: A-B.** Western blot analysis of lysates from S2 cells transfected with indicated expression constructs. Protein levels of input and immunoprecipitated samples were visualised with HA (upper panel), or with Myc (lower panel) specific antibodies. Lanes 1-9 show lysates of the input samples, and lanes 10-18 show the same samples after immunoprecipitation with an HA specific antibody. Molecular weights are indicated on the right of each panel, \* marks an unspecific band, and > marks truncation products.

### 5.3. Dronc regulates dIAP2 protein levels in cell culture

#### 5.3.1. N-terminal processing of dIAP2 is distinct from RING-dependent turnover of the full-length protein

IAP proteins are an important part of the apoptotic machinery where they regulate caspase activity. However, recent research demonstrated the important role of IAPs in other processes like immunity. Members of the IAP family typically contain two specific protein domains required for their function: the BIR domain that mediates binding to their target protein and a ubiquitin-ligase RING domain that mediates the addition of ubiquitin to target proteins. *Drosophila* has two IAP proteins, dIAP1 and dIAP2<sup>360</sup>. While dIAP1 is an important part in apoptosis prevention in the fly, dIAP2 seems to play no role in apoptosis<sup>111,112,269-271</sup>. Instead dIAP2 is required to fight gram-negative bacterial infections in a RING domain dependent manner<sup>114</sup>.

Interestingly, I consistently detected a lower molecular weight band upon expression of Myc-tagged dIAP2 in S2 cells, suggesting N-terminal processing of dIAP2 (Figure 5.9.B; third lane). I initially asked if the lower molecular weight band corresponds to processed version of dIAP2. To address this question, I cloned a C-terminal Myc-tagged full-length dIAP2 expression construct (dIAP2Myc) and an N-terminal truncated version of dIAP2 (MycdIAP2 $\Delta$ BIR1) that lacks the first 75 amino acids. To check if the dIAP2 RING domain is involved in dIAP2 proteolysis I additionally generated a dIAP2 expression construct with an inactive RING domain. More specifically, I introduced a Cysteine to Tyrosine mutation that renders the RING domain inactive (MycdIAP2C472Y). I expressed the different constructs in S2 cells and visualized the tagged-dIAP2 proteins by Western blot (Figure 5.9.A-B). Similar to MycdIAP2, I detected a lower molecular weight band for dIAP2Myc, MycdIAP2 $\Delta$ BIR1, and MycdIAP2C472Y. In each case the molecular weight band correlates with cleavage at the N-terminus of dIAP2. The RING mutation in dIAP2 increased full-length dIAP2 levels compared to WT dIAP2 (Figure 5.9.A, fourth lane) but it did not prevent the appearance of

truncation fragments. The data indicate that dIAP2 is N-terminally cleaved and that proteolysis is independent of the RING domain.

To visualize the relative stability of MycdIAP2, MycdIAP2 $\Delta$ BIR1, or MycdIAP2C472Y I blocked de novo protein synthesis with the translation inhibitor cycloheximide (CHX), and monitored the protein levels over time (Figure 5.9.C-E). Protein levels of the control dFADD remained stable during the treatment period with cycloheximide (CHX). In contrast, I was unable to detect full-length dIAP2 and dIAP2 $\Delta$ BIR1 within 120 min of cycloheximide treatment. Inactivation of the RING domain (MycdIAP2 C472Y) delayed the disappearance of the full-length protein but again did not block processing of dIAP2.

The results indicate that dIAP2 stability is determined by the RING domain and by proteolytic cleavage of dIAP2.

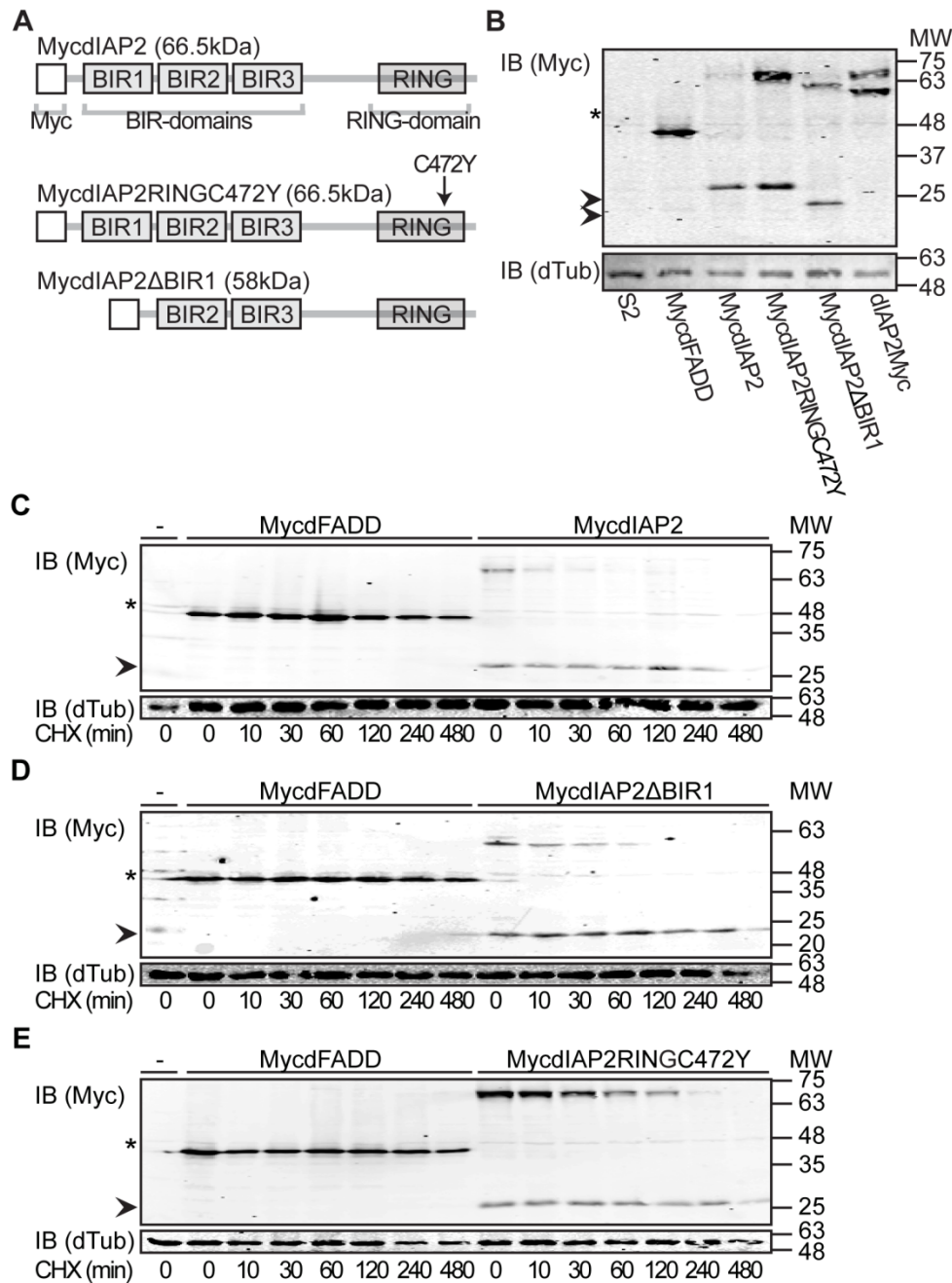


**Figure 5.9. N-terminal processing of dIAP2 is distinct from a RING-dependent turnover of a full-length protein: A.** Schematic illustration of Myc-tagged expression constructs. Protein domains and their corresponding molecular weights are indicated. C472Y indicates a point-mutation in the dIAP2 RING domain. **B.** Western blot analysis of lysates from S2 cells transfected with the indicated Myc-tagged expression plasmids. Control lysates from non-transfected S2 cells were loaded where indicated. Protein levels were visualized with a Myc-specific antibody (upper panel). Tubulin was visualized as a loading

control (lower panel). **C-E.** Western blot analysis of lysates from cells transfected with the indicated expression constructs that were incubated with CHX for the indicated times. For all Western blots: control lysates from non-transfected S2 cells were loaded where indicated. Lysates were probed with antibodies that detect Myc (upper panel), and tubulin (lower panel). Molecular weights are indicated on the right of each panel, \* marks an unspecific band, and ► marks truncation products.

Caspases often regulate protein activity and function by proteolytic processing. Since Dredd is the only caspase known to be involved in the IMD pathway, it is tempting to speculate that Dredd processes dIAP2 at the N-terminus. To address this possibility I initially asked if N-terminal processing of dIAP2 requires caspase activity (Figure 5.10.). Western blot analysis revealed significant increases in the levels of full-length MycdIAP2, MycdIAP2C472Y, Myc $\Delta$ BIR1 and dIAP2Myc when caspase activity was blocked by zVAD-FMK. Detectable protein levels of the control expression construct MycdFADD did not change in response to zVAD-FMK treatment. The data indicate that caspase activity is required for the proteolytic processing of dIAP2.

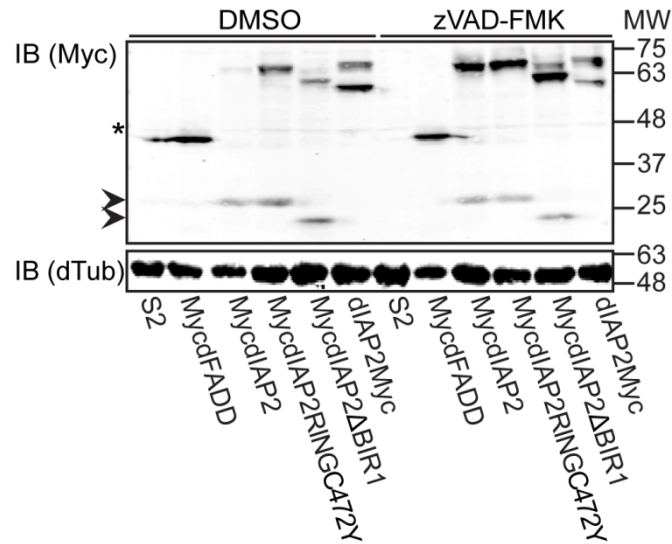


**Figure 5.10. N-terminal processing of dIAP2 is impaired by zVAD-FMK treatment:** Western blot analysis of lysates from S2 cells transfected with the indicated Myc-tagged expression plasmids and incubated with DMSO or zVAD-FMK for 3 h. Lysates were probed with Myc (first panel) and tubulin (lower panel) specific antibodies. Control lysates from non-transfected S2 cells were loaded where indicated. Molecular weights are indicated on the right of each panel. \* marks an unspecific band, ➤ marks lower molecular weight bands.

To validate my results I followed the turnover of MycdFADD, MycdIAP2, dIAP2Myc, MycdIAP2 $\Delta$ BIR1, and MycdIAP2C472Y after inhibiting caspase activity by zVAD-FMK treatment (Figure 5.11.A-E). I detected increasing amounts of full-length MycdIAP2, dIAP2Myc, MycdIAP2 $\Delta$ BIR1, and MycdIAP2C472Y and a corresponding decrease of the lower molecular truncation product upon incubation with zVAD-FMK. Based on my findings I conclude that N-terminal processing of dIAP2 depends on caspase activity.

Combined, my results uncover two distinct proteolytic controls of dIAP2 stability – regulation by the RING domain and regulation by caspase-mediated N-terminal cleavage.

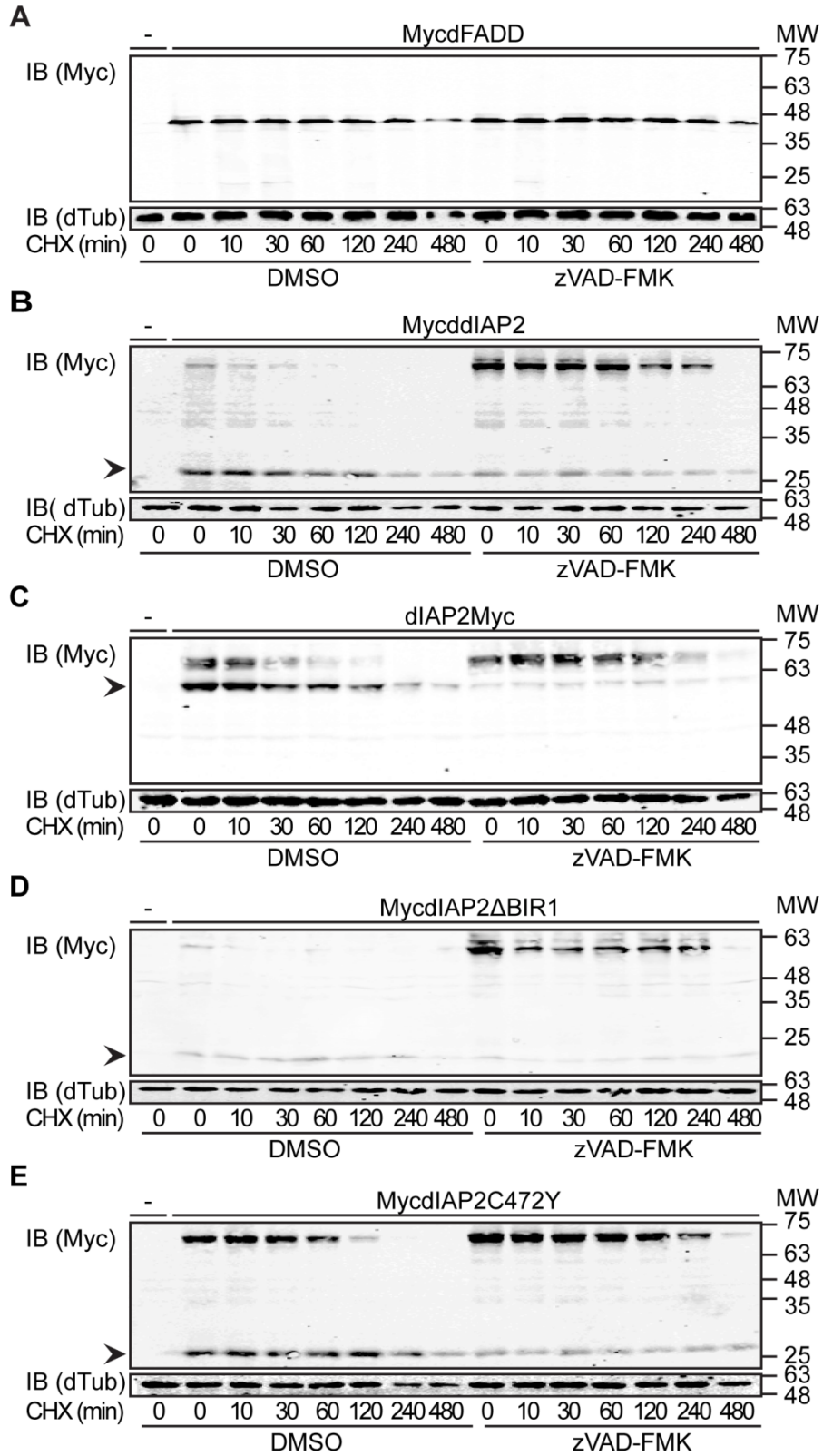


**Figure 5.11. zVAD-FMK stabilizes MycdIAP2 protein: A-E.** Western blot analysis of S2 cell lysates that were treated with z-VAD, CHX and DMSO as shown and transfected with expression constructs for MycdFADD (A), MycdIAP2 (B), dIAP2Myc (C), MycdIAP2 $\Delta$ BIR1 (D), and MycdIAP2C472Y (E). For all Western blots: protein levels are visualized with Myc (upper panel) and tubulin (lower panel) specific antibodies. Control lysates from non-transfected S2 cells were loaded where indicated, molecular weights are indicated on the right of each panel, \* marks an unspecific band, and ► marks truncation products.

### 5.3.2. Dronc is required for dIAP2 cleavage

In the context of apoptosis a recent study showed that Drice cleaves dIAP2<sup>267</sup>. However the study did not consider the involvement of other caspases in the regulation of dIAP2. To determine which of the seven *Drosophila* caspases is involved in the processing of dIAP2 I performed a RNAi-mediated knock-down of each of the caspases in S2 cells. I then transfected the cells with Myc-tagged dFADD or dIAP2 expression constructs and monitored the protein levels by Western blot (Figure 5.12.A and B). As expected, depletion of any of the seven caspases did not alter MycdFADD protein levels. Likewise, *dredd*, *strica*, *dcp-1*, *decay*, and *damm* depletion did not cause significant changes in MycdIAP2 protein levels and did not prevent dIAP2 processing. Surprisingly, knock-down of *drice* did not significantly block dIAP2 processing while depletion of the initiator caspase *dronc* resulted in a robust inhibition of dIAP2 cleavage. The data suggest that Dronc inhibits dIAP2 cleavage in S2 cells.

To date, Dredd is the only known caspase involved in IMD signaling and Dredd binds dIAP2<sup>350</sup>. To confirm that Dredd is not involved in dIAP2 cleavage I depleted *dredd* from S2 cells by RNAi (Figure 5.12.C). While control cells showed phosphorylation of dJNK in response to PGN treatment, dJNK/IMD signaling was blocked in *dredd* depleted cells. The lack of dJNK phosphorylation confirms the efficiency of the *dredd* dsRNA. I next checked if the loss of *dredd* interferes with dIAP2 cleavage (Figure 5.12.D). In agreement with my initial results, *dredd* depletion did not block dIAP2 cleavage while in a similar experiment treatment with *dronc* dsRNA greatly inhibited dIAP2 processing.

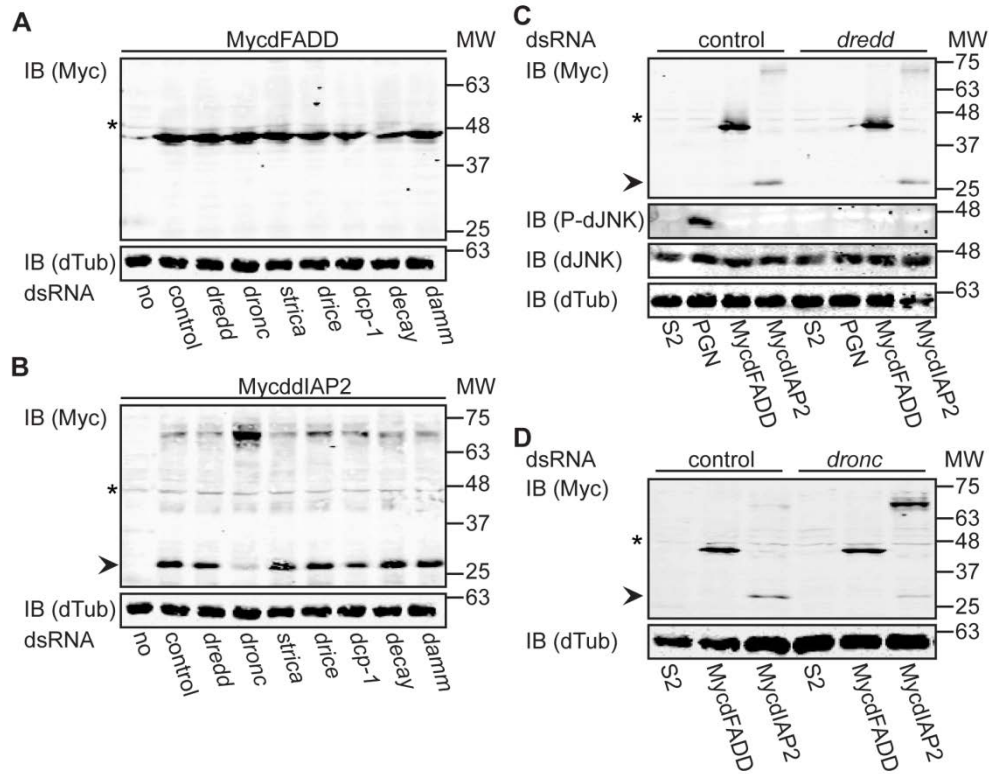


**Figure 5.12. Dronc influences N-terminal processing of dIAP2: A-D.** Western blot analysis of lysates from S2 cells transfected with the indicated expression plasmids and treated with the indicated dsRNAs. In C. S2 cells were stimulated with PGN as indicated. For all Western Blots: Protein levels for all Western blots were visualized with Myc (A-D, upper panel), P-dJNK (C, middle panel), and tubulin (A-D, lower panel) specific antibodies. Control lysates from non-transfected S2 cells were loaded where indicated. Molecular weights are indicated on the right of each panel, \* marks an unspecific band, and > marks truncation products.

To confirm my finding that Dronc cleaves dIAP2 I initially tested *dronc* dsRNA efficiency. Dronc is a major component in the process of apoptosis and removal of Dronc blocks the induction of apoptosis<sup>349</sup>. Therefore, I incubated S2 cells with control or *dronc* dsRNA and induced apoptosis with toxic doses of cycloheximide (Figure 5.13.A). Incubation of S2 cells with cycloheximide for eight hours resulted in robust membrane blebbing, a morphological marker of apoptosis. Approximately 55% of S2 cells showed signs of membrane blebbing eight hours after exposure to cycloheximide while cells depleted of *dronc* greatly inhibited induction of membrane blebbing (Figure 5.13.B). The data confirm that *dronc* dsRNA induces a loss of function phenotype. To avoid potential off-target effects I next generated a second *dronc* dsRNA that targets a different area of the *dronc* transcript. I tested both dsRNA by analysing S2 cells transfected with a Myc-tagged dFADD or Dronc expression construct (Figure 5.13.C). MycdFADD protein levels stayed constant in control and *dronc* depleted cells. In contrast, MycDronc protein levels were no longer detectable in *dronc* depleted cells compared to control samples. I conclude that both *dronc* dsRNA efficiently deplete Dronc protein from S2 cells.

To validate an involvement of Dronc in dIAP2 processing I depleted *dronc* with the two non-overlapping dsRNAs and followed dIAP2 processing by transfecting a N- or a C-terminal tagged dIAP2 expression construct into S2 cells. I used cells transfected with MycdFADD as a control (Figure 5.13.D-E). Consistent with my previous results, MycdFADD levels were unaffected by control or *dronc* dsRNA. In contrast, both *dronc* dsRNAs independently blocked MycdIAP2 and dIAP2Myc processing. I conclude that dIAP2 processing is Dronc dependent.

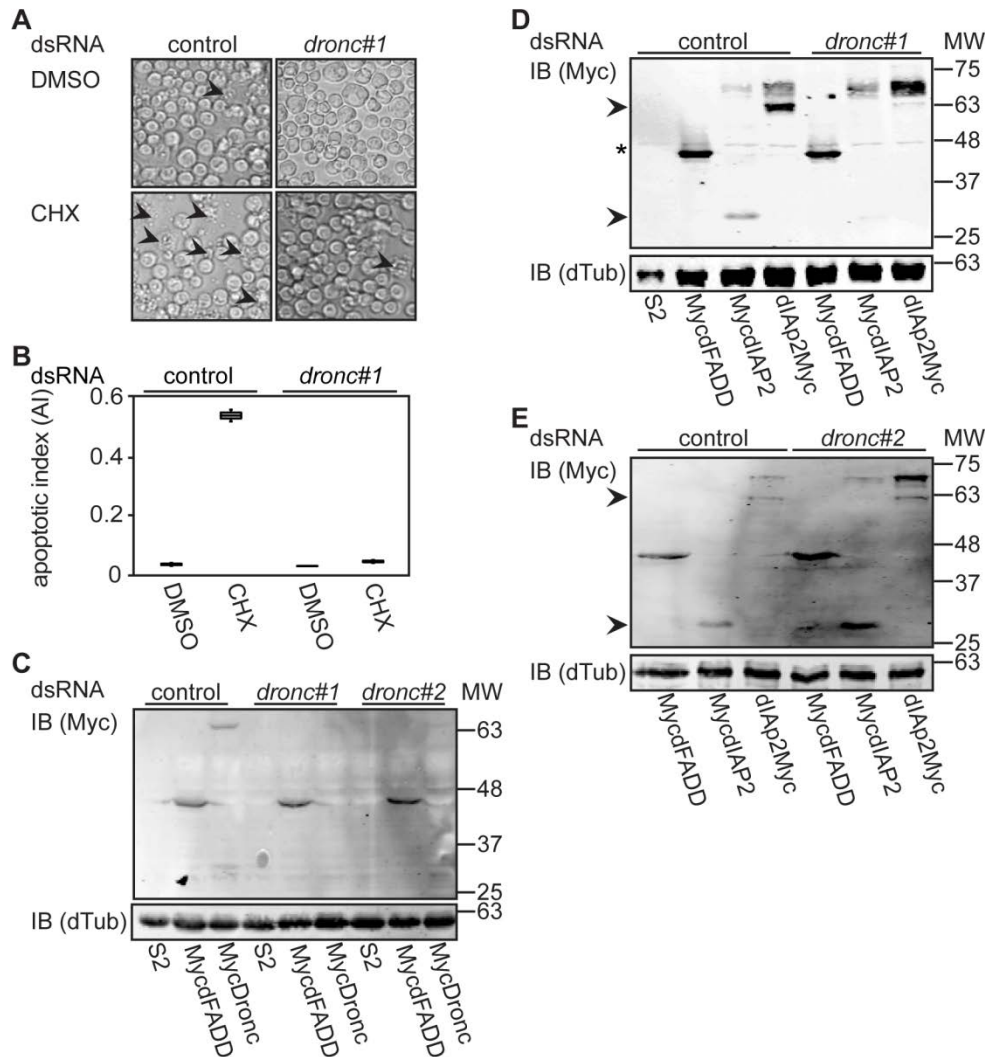


**Figure 5.13. Dronc is required for dIAP2 protein cleavage:** **A.** Bright field microscopy of S2 cells incubated with control dsRNA (lower panels) or *dronc* dsRNA#1 (upper panel). Cells were treated with DMSO (left panels) or CHX (right panels) for 4 h.  $\blacktriangleright$  marks apoptotic cells. **B.** Quantification of the apoptotic index of S2 cells in A, incubated with the indicated dsRNA before (columns 1,3) or after exposure to toxic doses of CHX (columns 2,4). Measurements for each sample are presented as a box blot to graphically illustrate the results of three independent experiments. **C-E.** Western blot analysis of lysates from S2 cells transfected with the indicated expression constructs and incubated with the indicated dsRNA). For all Western blots control lysates from non-transfected S2 cells were loaded where indicated. Lysates were probed with antibodies that detect Myc (upper panel) and tubulin (lower panel) as indicated. Molecular weights are indicated on the right of each panel. \* marks an unspecific band, and  $\blacktriangleright$  marks truncation products.

Dronc is an initiator caspase in *Drosophila* that processes downstream effector caspases<sup>349</sup>. Therefore I wanted to investigate if Dronc proteolytic activity is necessary for dIAP2 cleavage. I co-expressed HADronc with MycdFADD or MycdIAP2 and analysed the cell lysates by Western blot (Figure 5.14.A). Co-expression of HADronc did not alter MycdFADD protein levels. In contrast, simultaneous expression of HADronc and MycdIAP2 triggered an enhanced cleavage of MycdIAP2. I then co-expressed WT HADronc or a point mutant HADronc (DroncCS) that has a proteolytic inactive caspase domain with MycdFADD, MycdIAP2, dIAP2Myc, or MycdIAP2RINGC472Y (Figure 5.14.B). In line with my previous result, co-expression of wildtype HADronc showed greater cleavage of MycdIAP2, dIAP2Myc, and MycdIAP2RINGC472Y. In contrast, HADroncCS did not accelerate MycdIAP2 cleavage. Instead HADroncCS co-expression appeared to reduce the amount of cleaved MycdIAP2 compared to S2 cells that only express a MycdIAP2 expression constructs alone. I conclude that Dronc catalytic activity is required for dIAP2 cleavage.

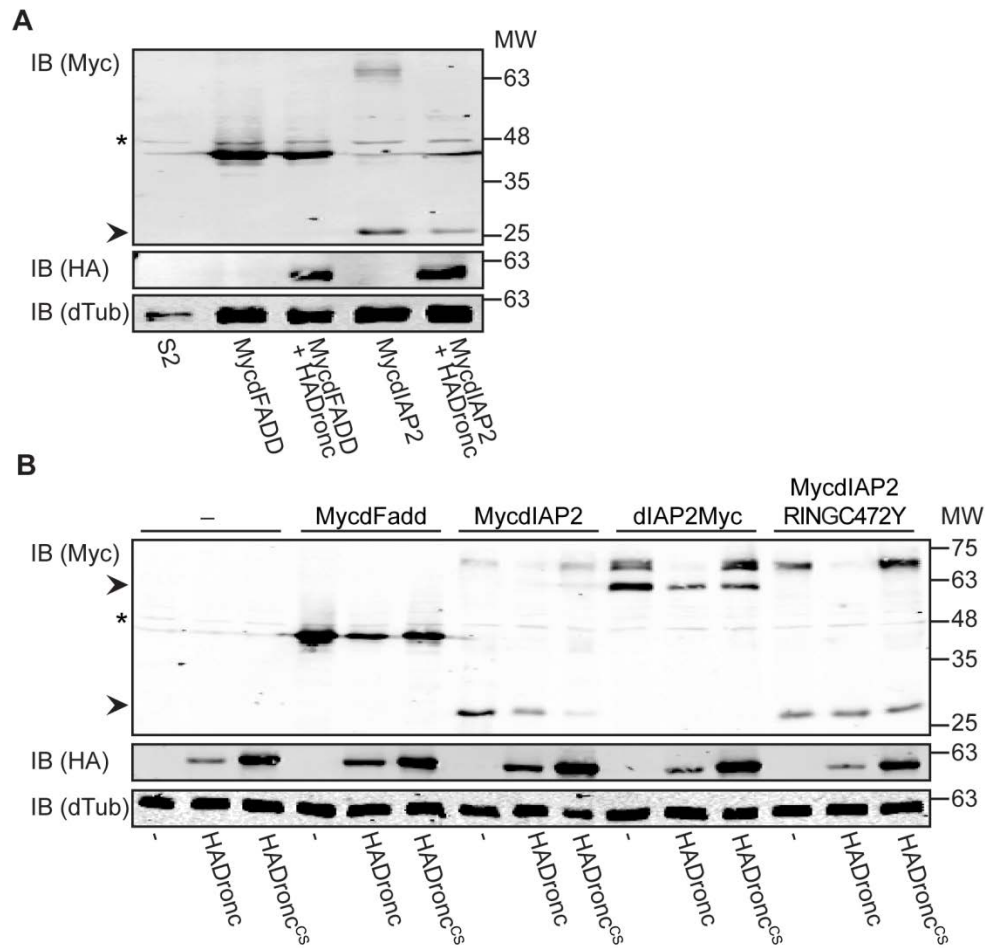


**Figure 5.14. Dronc catalytic activity is required for dIAP2 cleavage: A.** Western blot analysis of lysates from S2 cells transfected with Myc-tagged expression constructs and co-transfected with HADronc as indicated. **B.** Western blot analysis of lysates from S2 cells transfected with Myc-tagged expression constructs and co-transfected with HADronc or HADroncCA as indicated. For all Western blots control lysates from non-transfected S2 cells were loaded where indicated. Lysates were probed with antibodies that detect Myc (upper panel), HA (middle panel), and tubulin (lower panel) as indicated. Molecular weights are indicated on the right of each panel. \* marks an unspecific band, and > marks truncation products.

My results suggest that dIAP2 protein is regulated by two distinct processes - proteasomal degradation and caspase-mediated cleavage. In this model, blocking the proteasome and parallel inhibition of Dronc activity should fully restore full-length dIAP2 protein levels.

To check for a dual regulation of dIAP2 I depleted *dronc* with dsRNA and followed dIAP2 processing by transfecting a tagged dIAP2 expression construct into S2 cells. In addition, I inhibited the proteasome with the cell-permeable proteasome inhibitor MG132 which blocks the proteolytic activity of the 26S proteasome complex (Figure 5.15.A). In samples treated with a control dsRNA, MG132 treatment partially stabilized full-length MycdIAP2 and to greater extent the N-terminal cleavage product. In agreement with earlier results, *dronc* depletion inhibited MycdIAP2 cleavage in samples treated with the DMSO solvent alone. Importantly, in *dronc* depleted cells that were treated with MG132 showed greatly increased levels of full-length dIAP2 compared to DMSO treated control cells.

Co-expression of dIAP2 with Dronc accelerated dIAP2 processing. In contrast, a catalytically inactive Dronc blocked dIAP2 cleavage in S2 cells. Therefore I tested if blocking dIAP2 processing by DroncCS overexpression in combination with MG132 treatment increases the levels of full-length dIAP2 (Figure 5.15.B). In DMSO treated cells, co-expression of MycdIAP2 and MycDronc triggered accelerated cleavage of dIAP2 while co-expression of catalytically inactive Dronc blocked dIAP2 cleavage. Expression of a catalytically inactive Dronc in cells treated with MG132 greatly enhanced the stability of MycdIAP2 compared to all other treatments.

The results are in agreement with a model where full-length dIAP2 protein stability is mediated by two distinct processes, degradation by the proteasome and processing by Dronc.

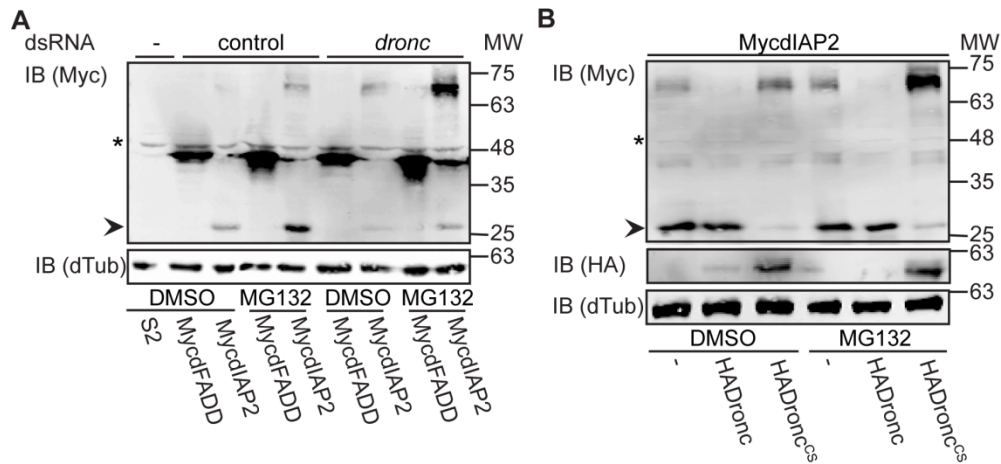


**Figure 5.15. dIAP2 protein stability:** **A.** Western blot analysis of lysates from S2 cells transfected with Myc-tagged expression constructs and incubated with control dsRNA (lanes 1-5) or *dronc* dsRNA (lanes 6-9). Cells were treated with DMSO or MG132 for 3 h to block proteasomal activity. **B.** Western blot analysis of lysates from S2 cells transfected with a Myc-dIAP2 expression construct and co-transfected with HADronc (lanes 2 and 5) or HADroncCS (lanes 3 and 6). Cells were treated with DMSO or MG132 for 3 h to block proteasomal activity. For all Western blots control lysates from non-transfected S2 cells were loaded where indicated. Lysates were probed with antibodies that detect Myc (A-B, upper panel), HA (B, middle panel), and tubulin (A-B, lower panel) as indicated. Molecular weights are indicated on the right of each panel. \* marks an unspecific band, and ➤ marks truncation products.

While my initial results did not implicate Drice in the process of dIAP2 cleavage, a recent report suggested dIAP2-mediated regulation of Drice in the context of apoptosis<sup>267</sup>. I therefore asked if *drice* dsRNA has a similar effect on dIAP2 cleavage as described for *dronc* dsRNA. I initially tested the efficiency of *dronc* and *drice* dsRNAs to block apoptosis. I incubated S2 cells with control, *dronc*, or *drice* dsRNA and induced apoptosis by an overnight incubation with *dIAP1* dsRNA that is known to induce apoptosis in S2 cells (Figure 5.16.A-B)<sup>361</sup>. *dIAP1* dsRNA incubation caused death in approximately 60% of S2 cells with extensive membrane blebbing, an indication for apoptosis. In contrast, cells depleted of *dronc* or *drice* greatly inhibited induction of membrane blebbing. The data confirm that *dronc* and *drice* dsRNA induce a loss of function phenotype. To address Dronc and Drice contribution to dIAP2 cleavage I performed a double knock-down experiment (Figure 5.16.C). As a control, I incubated cells with control dsRNA or with a combination of control dsRNA with *drice* or *dronc* dsRNA. Finally, I depleted cells of both *dronc* and *drice* and I followed dIAP2 cleavage by Western blot. In line with my previous result only *dronc* dsRNA blocked dIAP2 cleavage. Visually, the simultaneous knock-down of *dronc* and *drice* might stabilize full length dIAP2 a bit more effectively than *dronc* dsRNA by itself. However, in contrast to *dronc* dsRNA, *drice* dsRNA alone did not restore full length dIAP2 which indicates that Dronc and not Drice is the main contributor to dIAP2 cleavage.

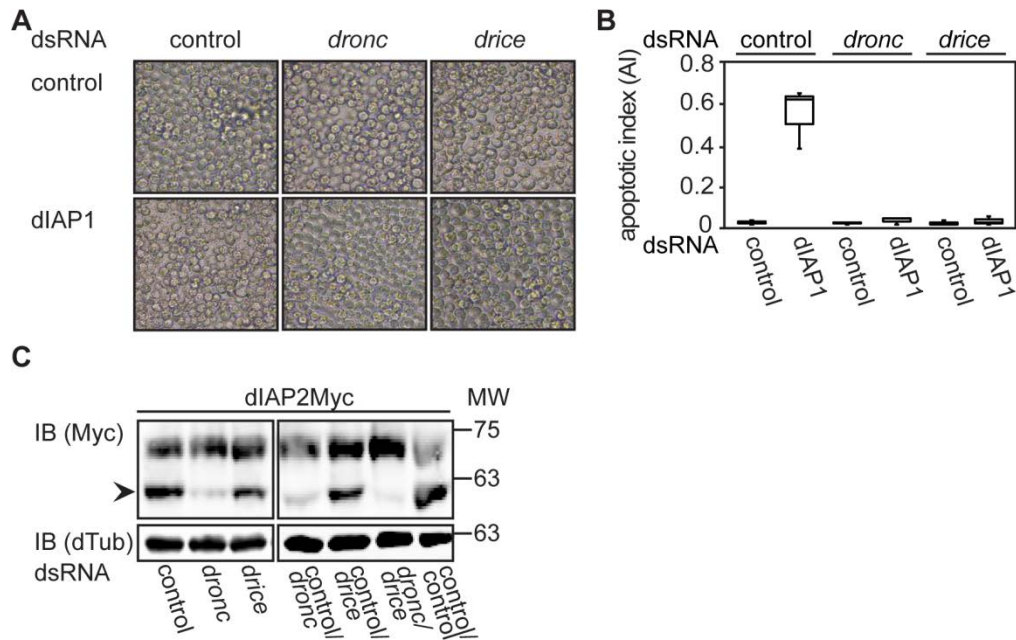


**Figure 5.16. Dronc and not Drice cleaves dIAP2:** **A.** Bright field microscopy of S2 cells incubated with control dsRNA (upper panels), *dronc* dsRNA (middle panel), or *drice* dsRNA (lower panel). Cells were treated with a control dsRNA (upper panels) or *dIAP1* dsRNA (lower panels) for 4 h. **B.** Quantification of the apoptotic index of S2 cells in A. Measurements for each sample are presented as a box plot to graphically illustrate the results of three independent experiments. **C.** Western blot analysis of lysates from S2 cells transfected with Myc- or HA-tagged expression constructs and incubated with the indicated dsRNAs. For all Western blots control lysates from non-transfected S2 cells were loaded where indicated. Lysates were probed with antibodies that detect Myc (upper panel), tubulin (lower panel) as indicated. Molecular weights are indicated on the right of each panel. ➤ marks truncation products.

### 5.3.3. Identification of dIAP2 cleavage site

The observed cleavage products of dIAP2 indicated processing between BIR1 and BIR2. There are two potential caspase cleavage sites at aspartate 92 and aspartate 100 (Figure 5.17.A). To check if dIAP2 is cleaved at either site I introduced aspartate (D) to alanine (A) point mutation at D92 (dIAP2D91A), D100 (dIAP2D100A), or in both sites (dIAP2D92A/D100A) and analysed protein expression by Western Blot. Rendering D92 uncleavable enhanced dIAP2 cleavage while the D100 mutation in dIAP2 appeared to slightly stabilize full-length dIAP2. In contrast, point mutation in both potential cleavage sites - D92 and D100 – blocked dIAP2 cleavage. Inhibition of cleavage at D100 in dIAP2 still generated a cleavage product. The examination of the cleavage product of dIAP2D100A indicates a size (Figure 5.17.B, lane six) similar to the WT dIAP2 cleavage product (Figure 5.17.B, lane three) which indicates that the preferred cleavage site for Dronc is at D92.

Dronc is known for its essential role in apoptosis. Therefore I asked if induction of apoptosis increases dIAP2 cleavage. I expressed MycdFADD, dIAP2Myc, and MycdIAP2D92A/D100A in S2 cells and monitored the protein upon toxic doses of cycloheximide (CHX) (Figure 5.17.B). The control protein dFADD was unaffected by the cycloheximide treatment while dIAP2 cleavage was greatly enhanced upon incubation with cycloheximide. In contrast to WT dIAP2, aspartate to alanine mutations in both putative cleavage sites renders dIAP2 uncleavable to cycloheximide treatment. I then asked if cycloheximide-induced apoptosis alters the PGN induced IMD response. To do so, I expressed MycdFADD, dIAP2Myc constructs, induced apoptosis by cycloheximide, and stimulated IMD signaling by PGN treatment in S2 cells. The control protein dFADD again remained unaffected by cycloheximide and as expected control samples (MycdFADD) showed phosphorylation of dJNK in response to PGN. Cycloheximide treatment enhanced dIAP2Myc cleavage and did not change P-dJNK levels in samples treated with PGN. The data indicate that cycloheximide-mediated apoptosis and subsequently enhanced dIAP2 cleavage do not interfere with IMD signaling in response to PGN.

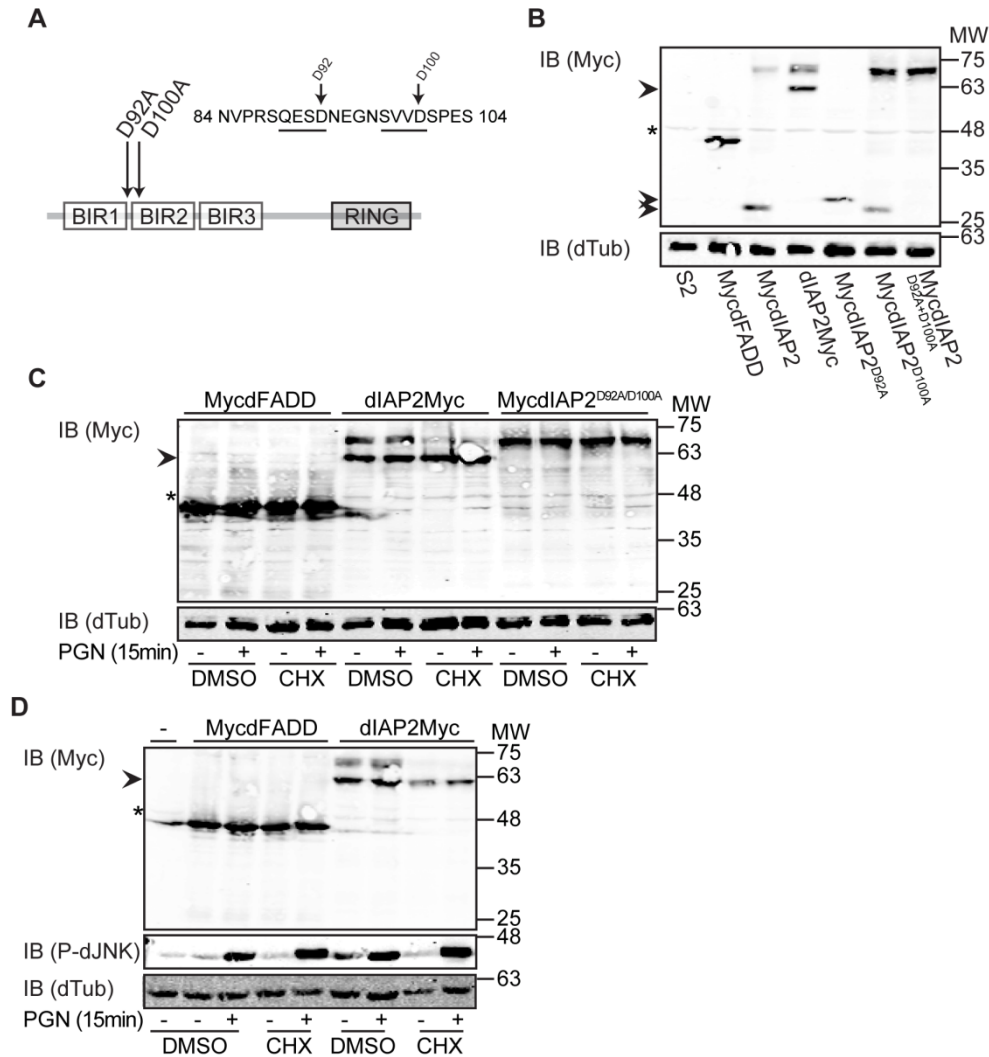


**Figure 5.17. Dronc cleaves dIAP2 at two specific Aps residues:** **A.** Schematic illustration of dIAP2. The primary structure of residues 84 to 104 is shown in single amino acid code with two putative caspase cleavage sites underlined. The locations of the respective aspartates relative to the BIR domains are also indicated. **B.** Western blot analysis of lysates from S2 cells transfected with the indicated Myc-tagged expression plasmids. **C.** Western blot analysis of lysates from S2 cells transfected with the indicated Myc-tagged expression plasmids and stimulated with PGN as indicated. Cells were treated with DMSO or CHX for 8 h. **D.** Western blot analysis of lysates from S2 cells transfected with the indicated Myc-tagged expression plasmids and stimulated with PGN as indicated. Cells were treated with DMSO or CHX for 8 h.

#### **5.3.4. Loss of *dronc* activity alters the IMD pathway response in S2 cells**

To understand the contributions of Dronc-mediated dIAP2 cleavage to IMD signaling I investigated if the depletion of *dronc* alters the immune response through the IMD/Rel arm. I incubated S2 cells with a control dsRNA or a *dronc* specific dsRNA and monitored *att* levels after 0 or 6 h of PGN incubation by qRT-PCR (Figure 5.18.). My preliminary results indicated that *att* expression was diminished in *dronc* depleted cells indicating a potential requirement for *dronc* in the full-activation of the IMD/Rel transcriptional response.

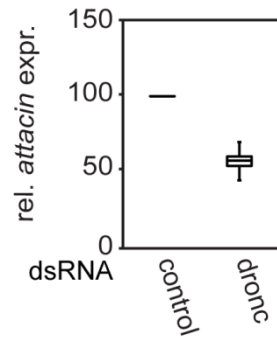


**Figure 5.18. Loss of *dronc* alters the IMD pathway response in cell culture:** Quantitative real time PCR analysis of control cells and *dronc* depleted S2 cells, stimulated with PGN and recovered for 360min. The relative expression levels for *attacin* are standardized to *actin* levels. Values of control cells and *dronc* depleted cells after PGN stimulation are reported relative to unstimulated control cells. Measurements are presented as a box blot to graphically illustrate the results of three independent experiments.

#### **5.4. Summary**

In this chapter, I investigated the contribution of caspases to the IMD response (Figure 5.19.). Specifically, I examined the molecular basis of Dredd activation and I revealed fundamental proteolytic and structural differences between Dredd and Caspase-8. In addition, I found indications for an involvement of the caspase Dronc in IMD signaling and I identified two separate regulation of dIAP2 stability by RING-mediated degradation and by Dronc-mediated N-terminal cleavage. The data reveal new insights of caspase regulation and contribution to the IMD response.

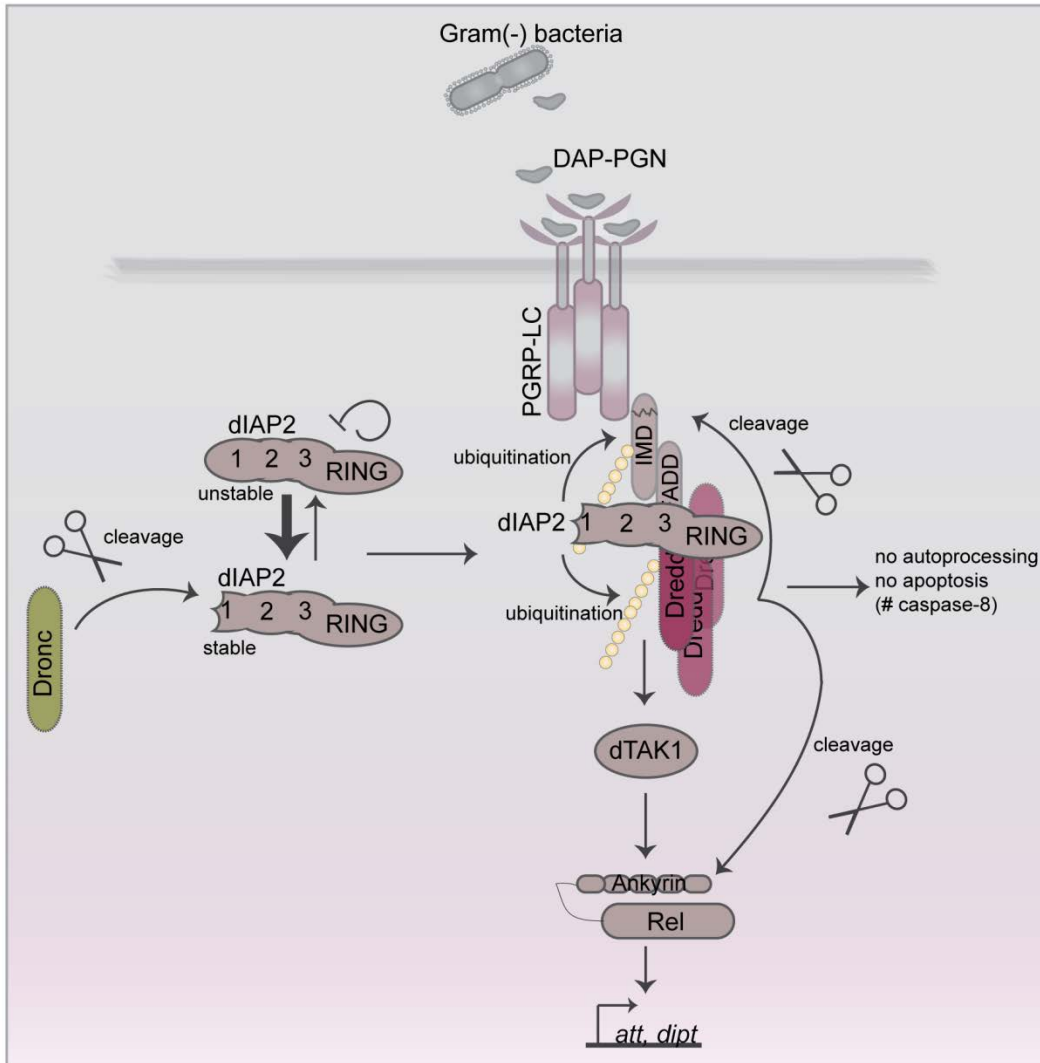


**Figure 5.19. Summary of section 5:** Illustration of the *Drosophila* IMD signaling pathway with the added changes that resulted from this study. In summary, my results in chapter 5 demonstrated that Dredd homodimerization but that Dredd is not processed in S2 cells. The structural differences between Dredd and Caspase-8 suggest that Dredd and Caspase-8 activation and function are distinct from each other. In addition, the data presented in this chapter established a dual mechanism for dIAP2 regulation where dIAP2 stability is regulated in a RING-dependent manner and by Dronc N-terminal cleavage.

## **Chapter 6. Discussion**

## **6.1. Background - The role of Dredd in *Drosophila* IMD signaling in cell culture**

All multicellular organisms rely on their innate immune system to induce defense responses against microbial invaders. *Drosophila* responds to gram-negative bacterial challenges through the IMD pathway. Signal transduction through the IMD pathway requires NF- $\kappa$ B, caspase, and JNK modules to induce appropriate antimicrobial responses<sup>10</sup>. The only caspase implicated in the IMD pathway thus far is Dredd. *dredd* null mutant flies are greatly impaired in their ability to mount comprehensive immune responses to bacterial challenges<sup>130</sup>. More specifically, Rel cleavage and induction of IMD/Rel responsive transcripts is compromised in *dredd* mutant flies<sup>125,126,130</sup>. Therefore, Dredd is an indispensable element of the IMD pathway and the current model positions Dredd in the IMD/Rel arm of IMD signaling.

More recent data indicated a requirement for Dredd in the phosphorylation of dJNK in tissue culture assays<sup>113,146</sup>. However, the precise involvement of Dredd in the dJNK arm of the IMD pathway was unexplored. In particular, there were no data on the degree to which Dredd contributes to the IMD/dJNK transcriptional response and the molecular basis for Dredd-mediated activation of dJNK were unknown. My initial analysis established an essential role for Dredd in the IMD/dJNK pathway. These observations let me to ask where Dredd interacts with the IMD signaling cascade.

In chapter 3.2. and 3.3. I presented results that establish Dredd as an essential component in the IMD/dJNK arm and I deciphered a network of interactions between Dredd and early IMD signaling components upstream of dTAK1. The results are discussed below.

### **6.1.1. Dredd is an essential component of the IMD/dJNK pathway in cell culture**

In my initial set of experiments, I investigated the role of Dredd in IMD/dJNK signaling (chapter 3.2.). PGN-mediated activation of dJNK signaling is a

transient process and measurements of downstream transcript levels are not as vigorous as seen for the IMD/Rel arm. However, RNAi-mediated depletion of *dredd* showed a robust reduction in *puc* and *mmp-1* transcript levels and cells depleted of *dredd* failed to phosphorylate dJNK. My results indicate a requirement for Dredd in IMD/dJNK signaling. As the molecular basis of Dredd-dependent dJNK activation is unclear, I next asked if caspase activity is essential to induce dJNK-dependent immune responses. Specifically, I asked if the caspase inhibitor p35 blocks IMD/dJNK activation in cell culture. I found that p35 attenuates signal transduction through the IMD/Rel and IMD/dJNK cassettes. These observations agree with established requirements for Dredd in the IMD/Rel arm and support a general requirement for caspase activity in the IMD/dJNK arm. p35 is a viral caspase “suicide substrate” that is proteolytically cleaved by caspases to generate 25kDa and 10kDa products. The 25kDa product forms a stable complex with the corresponding caspase, rendering the bound caspase proteolytically inactive<sup>214,224</sup>. I note that key features of my p35-Dredd data are not consistent with the suicide inhibitor model described above. For example, I detected interactions between p35 and a proteolytically inactive Dredd, and the molecular weights of the individual members of the p35/Dredd complex were not consistent with p35 cleavage by a mature caspase.

Despite these caveats, I believe that p35 acts directly on Dredd, potentially as a competitive inhibitor, as I demonstrated a physical interaction of p35 with Dredd in S2 cells. In agreement with a model where p35 binds to the active site of a caspase, proteolytically inactive Dredd co-precipitates less efficiently with p35 than WT Dredd. In addition, my RNAi experiments indicate that Dredd is the sole caspase required for the phosphorylation of dJNK. However, given the atypical nature of the p35-Dredd interactions, I cannot definitively conclude that p35 prevents the induction of IMD/dJNK responses by inhibiting the caspase activity of Dredd. I did not examine the efficiency of the generated dsRNAs and therefore I cannot conclude that each one of the tested caspases was depleted to comparably levels. In addition, redundancies among the respective caspases might mask the RNAi-phenotype of individual caspases. Therefore I cannot currently exclude the possibility that additional caspases are required for dJNK

or Rel activation in the IMD pathway. Nonetheless, my results demonstrate that Dredd is essential for the activation of the IMD/dJNK arm.

### 6.1.2. Dredd interacts with early IMD pathway components

In my next set of experiments I investigated interaction between early IMD signaling components and Dredd (chapter 3.3.). Caspase-dependent signal transduction often proceeds through multiprotein complexes formed through homotypic interactions. For example, human Caspase-8 interacts with FADD through death-effector domains (DED). The DED domains are a subclass of protein motifs known as the death fold that contains 6 alpha helices that mediate protein interactions<sup>184,362,363</sup>. Previous analysis of the Dredd sequence indicated only minor similarities between Dredd prodomain and any DED-containing proteins using BLAST or SMART and therefore the domain in Dredd was termed "death-inducing domains" (DID)<sup>129</sup>.

Independent of the nature of the N-terminal domains in dFADD and Dredd, mis-expressed Dredd interacts with mis-expressed dFADD in the HeLa cell line<sup>115</sup>. This led me to ask if Dredd interacts with dFADD in a more physiologically relevant *Drosophila* tissue culture line. I demonstrated an interaction between Dredd and dFADD in S2 cells. As dFADD is a proximal signal transduction element in the IMD pathway, I elaborated my studies to probe interactions among dFADD, Dredd and additional IMD pathway members. I showed for the first time that Dredd forms a molecular complex with dIAP2 and that dFADD and dIAP2 interact in S2 cells. Previous results from our laboratory that Dredd, dFADD, and Imd are essential for PGN-mediated phosphorylation of dJNK support the molecular interactions described in this study<sup>146</sup>. Somewhat surprisingly, addition of PGN did not visibly alter interactions in my assays. It is possible that the discovered interaction exist independent of PGN stimulation. Interaction of PGN with the receptor may be required to initiate oligomerization and formation of a multimeric complex at the receptor that is required for signal transduction. Intriguingly, Imd is mostly localized in the nucleus and translocates to the plasma membrane only after pathway stimulation<sup>364</sup>. The cellular

localisation of the described interactions is unclear and it is possible that pathway activation is required to enable the cellular relocalisation of signaling-molecules to the receptor to allow signal transduction.

In my interaction studies, I failed to detect the reported interaction between Imd and dIAP2<sup>114</sup>. On this note, a recent report suggested that Imd requires N-terminal cleavage in order to interact with dIAP2. Since my immunoprecipitation experiments were performed with an N-terminal Myc-tag it is possible that I was unable to detect the reported interaction between cleaved Imd and dIAP2.

My initial finding of an interaction between Dredd and dIAP2 prompted me to further decipher the molecular basis of Dredd:dIAP2 interactions. My data suggested the involvement of the dIAP2 BIR3 domain in Dredd binding. These results are in agreement with a recent study that showed that BIR 2 and 3 of dIAP2 interact with Dredd<sup>273</sup>. In contrast to this study, I demonstrated that the prodomain and the caspase-domain of Dredd individually interact with dIAP2. Variances in the experimental set-up or the expression constructs used might explain the discrepancy in both studies. For example, the full-length Dredd described by Meinander et al.<sup>273</sup> has a molecular mass lower than the predicted 56kDa and might illustrate a different isoform of Dredd. Unfortunately, the commercial available Caspase-8 antibody does not detect Dredd on Western blots and we have made two unsuccessful attempts to generate a Dredd antibody. However, we are now in the possession of different Dredd isoform expression constructs and therefore able to test if the inconsistencies in the two studies are the result of different Dredd variants.

My interaction studies prompted me to explore the relative position of Dredd in the IMD/dJNK pathway. Given the extensive interactions among Dredd and early IMD pathway members, I speculated that Dredd acts at an early stage of IMD/dJNK activation. My epistasis analysis confirmed that dMKK4/7 acts downstream of dTAK1 in the activation of dJNK<sup>138</sup>. In contrast, I demonstrated for the first time that Dredd acts upstream of dTAK1 in the IMD/dJNK arm. As a caveat, these epistatic data require confirmation in an *in vivo* model. I note that my data overlap with previous studies that proposed a role for Dredd upstream of dTAK1 in the activation of the IMD/Rel pathway. These observations lead me

to propose that Dredd is an essential part of the phospho-relay in the IMD pathway that diverges downstream of dTAK1 and is required for the full activation of the IMD/Rel and IMD/dJNK immune responses.

In summary, the results described in chapter 3. establish the position of Dredd within the IMD/dJNK pathway and enhance our understanding of signal transduction events in the IMD response. More specifically, my interaction studies revealed a rich network of protein:protein interactions among early IMD signaling molecules and identified Dredd as a vital part of this interaction network.

## 6.2. Background - The role of Dredd in *Drosophila* IMD signaling *in vivo*

The high degree of conservation, the accessibility of the complete genome sequences, the enormous collection of mutants, and the ease of genetic manipulation make *Drosophila* an excellent model system to study the mechanisms that regulate essential biological processes at the molecular level<sup>30,365,366</sup>. Most importantly, *Drosophila* allows us to test cell culture observations in a more physiologically relevant, *in vivo* context. For example, while initial cell culture assays indicated a tentative role for Dredd in the apoptotic machinery of the fly, the generation of a null mutation in the *Drosophila* Dredd locus demonstrate Dredd's essential and probably only role in immunity<sup>129,130</sup>. More specifically, *dredd*<sup>B118</sup> mutant flies do not display an apoptotic phenotype but fail to cope with gram-negative bacterial infections<sup>130</sup>. On a molecular level the data are in agreement with findings that *dredd*<sup>B118</sup> mutant flies fail to induce Rel cleavage or the expression of IMD/Rel dependent transcripts<sup>125,126</sup>. However, experiments to show proteolytic cleavage of Rel by Dredd have been challenging<sup>125,126,128</sup>. My cell culture experiments in chapter 4 established a position for Dredd in the IMD/dJNK arm upstream of dTAK1. Therefore, the role of Dredd in IMD signaling and specifically in Rel cleavage required clarification. In addition, there was no evidence for the requirement of a caspase or specifically for Dredd in IMD/dJNK activation *in vivo*.

In chapter 4.2. and 4.3. I presented results that establish Dredd as an essential component in the IMD/dJNK arm *in vivo* and I gave evidence for a second role for Dredd in IMD/Rel signaling. The results are discussed below.

### **6.2.1. Dredd is an essential component of the IMD/dJNK pathway *in vivo***

To address an involvement of Dredd in IMD/dJNK signaling *in vivo* I initially tested for the general requirement of caspase activity in the IMD/dJNK arm (chapter 4.2.). In agreement with my cell culture data, I demonstrated for the first time that p35 blocks dJNK phosphorylation and the induction of dJNK-dependent genes *in vivo* after bacterial challenge. Given my interaction and epistasis data, I consider it likely that Dredd cleaves a proximal IMD pathway member upstream of dTAK1 to activate dJNK. In this context, it is particularly noteworthy that Imd is cleaved at a caspase consensus cleavage site and that Imd cleavage requires the proteolytic activity of Dredd<sup>114</sup>. I suggest that p35 competes with Imd for Dredd binding which inhibits Dredd-dependent cleavage of Imd. This scenario implicates inhibition of the Dredd-dependent phospho-relay and consequently blocks IMD/dJNK and IMD/Rel activation. I note that I did not detect a physical interaction between Imd and Dredd. However, caspase cleavage generally occurs rapidly and it is possible that Dredd binds and cleaves Imd and then quickly dissociates from the active Imd molecule to facilitate the activation of IMD/Rel and IMD/dJNK.

At the time of these studies there was no evidence of a requirement for Dredd in IMD/dJNK activation *in vivo*. Therefore, I explored a requirement for Dredd in IMD/dJNK activation in a whole animal setting. My studies clearly demonstrated a requirement for Dredd in IMD/dJNK activation *in vivo*. I showed that loss of Dredd blocks infection-responsive phosphorylation of dJNK and prevents a bacterial challenge-dependent induction of dJNK-dependent target genes *in vivo*. In my Western blot analysis, I noticed a basal amount of P-dJNK in samples from adult flies, which probably reflects a broad requirement for dJNK activity in the adult. Bacterial infection always resulted in a brief increase of P-dJNK levels that paralleled IMD/dJNK pathway activation and I did not

observe such an increase in *dredd*<sup>B118</sup> mutant flies. I believe that the ability of Dredd to modify dJNK is likely specific to the IMD pathway, as *dredd*<sup>B118</sup> null mutants do not display the traditional dorsal closure phenotype of dJNK pathway mutants. In summary, my data demonstrate that Dredd is essential for the activation of the IMD/dJNK response *in vivo*. The failure of dJNK activation in *dredd*<sup>B118</sup> mutant flies is phenocopied by the observed reduction of P-dJNK and dJNK-dependent transcripts in my p35 experiments. My *in vivo* data are entirely in agreement with my cell culture data and both approaches demonstrate that loss of Dredd causes a failure to activate IMD/dJNK.

### **6.2.2. Dredd is an essential component in IMD/Rel signaling downstream of Imd activation *in vivo***

My data that position Dredd upstream of dTAK1 agree with a recent study that suggests Dredd dependent cleavage of Imd<sup>114</sup> and indicate a proximal requirement for Dredd in the IMD response. Previous data recognized a role for Dredd in Rel cleavage at a later point of the IMD pathway and therefore the combined data suggest distinct roles for Dredd in the IMD pathway. To address Dredd's role(s) in IMD signaling I re-examined the involvement of Dredd in the IMD/Rel downstream of Imd cleavage (chapter 3.3.). I found that the expression of an N-terminal truncated Imd construct (Imdcl) induced AMP expression *in vivo*, that the *dredd*<sup>B118</sup> mutation blocks AMP expression in Imdcl flies, and that a genomic Dredd rescues AMP expression in the *dredd*<sup>B118</sup> mutant Imdcl flies. Based on these data, I propose that Dredd-mediated activation of the IMD/Rel arm downstream of Imd cleavage is an event distinct of Dredd's role upstream of Imd.

Recent studies suggested that dIAP2 dependent ubiquitination of Dredd is required for Dredd function in IMD signaling<sup>273</sup>. However, it is not clear if ubiquitination of Dredd is required for the activation of Dredd and therefore also required for cleavage of Rel. Further investigations are necessary to clarify the mechanism of Dredd activation and to appreciate how Dredd mediates the sequential cleavage of Imd and Rel. If ubiquitination is required to activate and

enable Dredd to proteolytically cleave substrates like Imd and Rel, I would predict that Dredd needs to be ubiquitinated downstream of Imd cleavage. To address this question one could test if Dredd is ubiquitinated in Imdcl flies. Also, the loss-of-function *dreddD44* fly line carries a missense mutation (G120R) that blocks signal-dependent cleavage of Imd and AMP expression. A recent group suggested that the G120R mutation disrupts ubiquitination of Dredd by dIAP2 and therefore blocks Dredd-mediated cleavage of Imd and consequently inhibits induction of AMP<sup>273</sup>. If ubiquitination is necessary for Dredd activation I would expect that the expression of Imdcl in *DreddD44* flies will not restore the induction of AMP. Alternatively, ubiquitination of Dredd might be not essential for Dredd-dependent Rel cleavage and therefore expression of Imdcl in *DreddD44* flies might restore the induction of AMP.

Previous reports suggested the existence of four Dredd isoforms<sup>129</sup>. In contrast to the  $\alpha$ ,  $\gamma$ , and  $\delta$  isoforms, the  $\beta$  isoform retains intron two and as a result has a premature stop codon. The  $\alpha$  isoform appears to be a truncated version of the  $\delta$  type transcript. The  $\gamma$  and  $\delta$  isoforms are the most similar variants and differ only due to an alternative splicing event at the second intron that adds an additional six amino acid at the end of the prodomain in the  $\delta$  variant. Unfortunately, further analyses of the different isoforms and how they are involved in signaling in *Drosophila* have not been performed.

I confirmed the expression of the UASDreddy transgene by qRT-PCR. I found that the fat body specific expression of the Dreddy isoform does not restore AMP levels in Imdcl flies that are *dredd*<sup>B118</sup> null and does not restore AMP levels in *dredd*<sup>B118</sup> mutant flies after bacterial challenge. This is in contrast to a genomic Dredd that re-establishes AMP levels after bacterial infection. I suggest that the Dreddy isoform is not the functional variant in the fat body-driven expression of AMP. As a caveat of this study I did not test if the UASDreddy transgene is expressed at appropriate physiological levels. In addition, I examined the UASDreddy transgene expression only in the fat body. While the fat body is the major source of AMP in response to infection other cells like hemocytes also synthesize AMP. It is possible that Dredd is required elsewhere than the fat body to generate full humoral responses to PGN.

As my initial experiments demonstrated the efficient interaction of Dreddy with known IMD pathway molecules, it is tempting to speculate about the requirement of Dredd isoforms in the regulation of the IMD pathway. Since Dredd performs dual function in IMD signaling, it is possible that different isoforms influence the IMD cascade at different levels, just as at the point of Imd or Rel cleavage. Further experiments are required to analyse the involvement of Dredd isoforms in the immune response of *Drosophila*. Since the Dredd $\beta$  isoform contains a premature stop after the prodomain, I find it unlikely that it will generate a functional protein. However, multiple Caspase-8 isoforms have been described to date and a recent report showed that the prodomain-only polypeptide of Caspase-8 can activate NF- $\kappa$ B<sup>345</sup>. It would be interesting to assess the physiological function of the Dredd $\beta$  isoform to test whether a similar mechanism exists in the fly. While Dreddy and Dredd $\delta$  differ in only six amino acids it is possible that it confers different structures to the protein and therefore might establish unique functions for each isoform. Our laboratory possesses Dreddy and Dredd $\delta$  variants. It will be informative to generate S2 cells- and fly-expression constructs that contain either isoform and decipher their contribution to Imd and Rel cleavage as well as IMD/Rel and IMD/dJNK signaling in general.

In summary, my *in vivo* results described in chapter 4. agree with my cell culture data described in chapter 3. and establish Dredd as an essential component of the IMD/dJNK pathway. In addition, the data demonstrate a distinct second role for Dredd in IMD/Rel signaling downstream of Imd cleavage. I propose that Imd recruits a proximal signaling complex that contains Dredd. Complex-mediated activation of Dredd triggers the Dredd specific cleavage of Imd and Rel. Cleaved Imd recruits dIAP2 to initiate a phospho-relay cascade that culminates in the phosphorylation of Rel. Finally, phosphorylated and cleaved Rel translocates to the nucleus where it then starts transcription of IMD specific gene products.

### 6.3. Background – Caspase function in *Drosophila* IMD signaling

Caspases are cysteinyl aspartate proteases with essential developmental and homeostatic roles in programmed cell death and immunity. The *Drosophila* caspase Dredd is considered an evolutionary relative of Caspase-8<sup>129</sup>. The degree of conservation between Dredd and Caspase-8 is unclear, as Dredd displays several structural features that are unusual for established Caspase-8 orthologs. For example, recent papers suggested that Dredd lacks of *bona fide* N-terminal Death Effector Domains (DED) and that the active site pentamer of Dredd (QACQE) is different to that found in other Caspase-8 orthologs (QACQG)<sup>115,129</sup>. Most importantly, Dredd does not appear to perform apoptotic roles *in vivo*<sup>130</sup>. While the molecular basis of Caspase-8 activation in TNF signaling is well understood, surprisingly little is known for Dredd in IMD signaling. Given the atypical nature of the Dredd sequence compared to Caspase-8, I examined the structural and functional basis of Dredd activation in IMD signaling.

In a second set of experiments, I investigated the requirement for caspases in IMD signaling. Dredd is the only described caspase in IMD signaling. In the IMD signaling pathway Dredd appears to cleavage Imd and Rel<sup>114,125,126</sup>. Previously I demonstrated an interaction between dIAP2 and Dredd and a recent report suggested dIAP2-mediated ubiquitination and activation of Dredd upstream of Imd cleavage. Interaction between caspases and IAP molecules often requires proteolytic cleavage of both. I found that dIAP2 is readily processed in unstimulated S2 cells and that full-length dIAP2 is an unstable protein. Since the regulation of dIAP2 stability and the potential involvement of dIAP2 cleavage in IMD signaling were unknown, I decided to investigate the caspase-dependent mechanism of dIAP2 stability.

In section 5.2. and 5.3. I presented results that establish structural and functional differences between the proteolytic activities of Dredd and Caspase-8 as well as in the interaction profile for Dredd and Caspase-8. In addition, I demonstrated a requirement for the RING domain of dIAP2 in the regulation of dIAP2 stability and a second, distinct requirement for a caspase in the cleavage

of dIAP2. Specifically, I showed that Dronc cleaves dIAP2. The results are discussed below.

### **6.3.1. Dredd structure and activation is distinct from Caspase-8 in cell culture**

To enhance our understanding of Dredd activation I looked at the relationship between Dredd and Caspase-8 from several perspectives (chapter 5.2.). In my initial set of experiments, I investigated structural similarities and differences between Dredd and Caspase-8.

Mammalian Caspase-8 homodimerizes and forms a complex with Fadd that initiate proximity-induced auto-processing and subsequent activation of Caspase-8<sup>184</sup>. I found that Caspase-8 is readily processed in S2 cells. Processing is specific to Caspase-8 activity, since zVAD-FMK treatment or expression of a proteolitically inactive Caspase-8 blocks Caspase-8 processing. On that note, Caspase-8 did not appear to induce apoptosis in S2 cells. This might indicate that S2 cells lack the requirements for Caspase-8-mediated apoptosis.

I also found that Dredd and Caspase-8 form heterodimers in S2 cells. However, I find it unlikely that heterodimerization leads to Dredd-mediated processing of Caspase-8 since a catalytically inactive Caspase-8 is not processed in S2 cells and *dredd* depletion doesn't block Caspase-8 processing.

Similar to Caspase-8, I showed that Dredd binds dFADD and homodimerizes. Since dFADD interacts with Dredd and Dredd interacts with dIAP2, I speculated that dFADD recruits Dredd and dIAP2 to form a higher molecular weight complex that enables auto-processing of Dredd. Unexpectedly, I was unable to detect processing of Dredd in S2 cells or in flies. I find it unlikely that I was unable to detect cleavage of Dredd based on the instability of the Dredd cleavage products since I readily detected cleavage products for Dredd in cells that co-expressed Caspase-8. In contrast to my findings, an earlier study indicated that overexpressed Dredd is cleaved in S2 cells<sup>273</sup>. It is possible that overexpression of Dredd at sufficiently high levels causes artificial processing or alternatively that differences in the proteolytic processing of various Dredd isoforms exist. Also,

another protease could be responsible for the cleavage of overexpressed Dredd in S2 cells, which would be in line with a recent report that showed processing of a catalytically inactive Dredd. Unfortunately, I was unable to assess endogenous Dredd protein in my assays as no available antibody for Dredd exists and attempts by both our laboratory and others to generate a Dredd-specific antibody have been unsuccessful.

Similarly to full-length MycDredd, MycDreddCA and MycDC co-expressed with Caspase-8 generated cleavage products that are smaller in size than a putative prodomain that terminates at aspartate 309. The cleavage product for Dredd, DreddCA, and DC correspond in size to a fragment produced when cleaved in the prodomain. There are three potential cleavage sites in the Dredd prodomain that will generate a protein close to the estimated size (LLKD234, IESD260, or TQID269). While IESD matches the preferred cleavage site for Caspase-8 (IEXD), LLKD and IESD both fall into predicted  $\alpha$ -helices that are important for dimerization. At the moment, it is not clear where Caspase-8 cleaves Dredd or if Caspase-8 only cleaves Dredd at one site. Mutations of the aspartate in the potential cleavage sites will clarify which site(s) of Dredd is processed by Caspase-8. The data presented suggest that Caspase-8 fulfills two hallmarks of caspase activation in S2 cells: autoproteolytic processing and processing of a substrate (Dredd).

Caspase-8 most likely recognizes a cleavage site in Dredd that is not recognized by endogenous caspases. Alternatively, there might be endogenous inhibitors that act on Dredd but are ineffective against Caspase-8. It would be surprising if processing of Dredd is required for IMD signaling and that a putative Dredd inhibitor is removed in response to pathway activation, since I did not detect cleavage of Dredd after PGN stimulation. I cannot exclude that Dredd is processed since my studies focused on a tagged Dredd construct. It is possible that Dredd processing is facilitated under certain conditions or in certain tissues not examined under my experimental conditions. However, my data argue against auto-processing of Dredd in response to PGN-mediated IMD activation in S2 cells. It is possible that Dredd fails to recognize potential cleavage sites and consequently lacks auto-processing. Therefore, I predict that the alteration of the

cleavage sites to the optimal Dredd cleavage site (LEXD) may induce auto-processing of Dredd.

If Caspase-8 is active in S2 cells, I speculated that replacement of the catalytic-domain of Dredd with the corresponding Caspase-8 domain would lead to auto-processing. I found that replacement of the pro- or caspase-domain of Dredd with the corresponding Caspase-8 domain blocked the appearance of cleavage products. The results show that the Dredd domains can't functionally substitute the corresponding domains in Caspase-8. I hypothesize that transactivation of Caspase-8 is only mediated by Caspase-8 homodimers. Active Caspase-8 cleaves substrates like Dredd. In contrast, replacement of the pro- or caspase-domain with the corresponding Dredd domain prevents the formation of the required platform for Caspase-8 transactivation and therefore renders the chimera inactive.

I also observed differences between the interactions of Caspase-8 and Dredd with the p35 caspase inhibitor. Inhibition of caspases, including Caspase-8 by p35 requires cleavage of p35 by the active caspase followed by the formation of a covalent bond with the caspase<sup>214</sup>. My data demonstrated that p35 interacts with Dredd and inhibits Dredd-mediated IMD/dJNK signaling. In contrast to Caspase-8/p35 inhibition, I readily detected p35 binding with a catalytic inactive Dredd as well as with a full-length Dredd. In addition, I did not detect the expected p35 processing products for a typical suicide inhibitor. The result indicates that Dredd is a major exception from the general mechanism of p35-dependent caspase inhibition. Combined, the data suggest that Dredd and Caspase-8 have distinct substrate specificities. In addition, Dredd lacks autoproteolytic properties and interacts differently with p35 compared to Caspase-8. The findings also indicate a mechanism independent of auto-processing may exist to generate a fully active and stable caspase. Notably, auto-processing supports but is not essential for Dronc mediated apoptosis<sup>203,204</sup>. Similar to Dronc, my data suggest that Dredd is active in its unprocessed form. In contrast to Dronc, it appears that Dredd remains exclusively unprocessed. In addition, recent reports uncovered non-apoptotic functions of Caspase-8 in NF- $\kappa$ B activation that appear independent of auto-processing<sup>367,368</sup>.

Based on my structural data, I suggest that in IMD signaling Dredd remains in its full-length form and that Dredd does not require autoproteolytic processing in order to become active. Therefore I propose that Dredd activation circumvents the typical hallmarks of caspase activation. It is noteworthy that active Dredd and active Caspase-8 have opposed functions. While Dredd is a component of a robust pro-survival response, Caspase-8 is a critical initiator of programmed cell death. It is intriguing to speculate that the physiological differences in survival and apoptosis between Dredd and Caspase-8 are caused by the differences in the molecular basis for processing.

While Dredd interacts with dFADD and dIAP2, Caspase-8 failed to interact with dFADD or dIAP2. In contrast, Dredd and Caspase-8 interact with each other. The findings suggest that Caspase-8 orthologs retained homodimeric interaction motifs during evolution while heterotypic interaction divergently evolved (such as interactions with dIAP2). I speculate that Dredd and Caspase-8 have different binding capabilities and that the rearrangement of interaction partners supports distinct functions for Caspase-8. Combined, the variations in binding partners with the development of auto-processing in Caspase-8 might have established novel, pro-apoptotic functions for Caspase-8. Future experiments that investigate the interaction of Dredd with human FADD and cIAP1 in HeLa cells will give additional understandings of the similarities and differences in the binding capabilities of Dredd and Caspase-8. In addition, further analyses are required to understand how the folding and structure of Dredd and Caspase-8 confer their specific binding properties and molecular functions.

The structural differences between Dredd and Caspase-8 prompted me to ask if Dredd and Caspase-8 are functionally similar. Preliminary reports implicated Dredd as an ancillary contributor to developmental apoptosis. Expression of the apoptotic activators *reaper*, *grim* and *hid* triggered an enrichment of *dredd* mRNA and heterozygosity at the Dredd locus suppresses *reaper* induced cell death in the eye<sup>129</sup>. Subsequent studies of Dredd mutant animals clarified that Dredd is dispensable for all forms of apoptosis and established Dredd as a critical regulator of the IMD response<sup>125,126,130</sup>.

Intriguingly, overexpression of Dredd induced Dredd processing and apoptosis in HeLa cells<sup>115</sup>. The apparent conflict between the *dredd* mutant fly phenotypes and the Dredd overexpression data in human cells prompted me to investigate Dredd's role during apoptosis in HeLa cells. I showed that Dredd does not substitute for Caspase-8 apoptotic activity and that Dredd alone does not induce apoptosis in HeLa cells. Instead, my data suggest that Dredd acts as an assembly platform that enables Caspase-8 dependent autoproteolytic activation with subsequent Caspase-8-mediated cell death.

Examination of Caspase-8 and Dredd proteolytic activity and binding affinities in HeLa cells will give further insights into their molecular function. For example, the catalytic site of Dredd (QACGE) is different to the conserved site (QACAG) of other Caspase-8 orthologs<sup>129</sup>. The exchange of the catalytic domain of Dredd with the corresponding Caspase-8 domain or a mutation of the catalytic site in Dredd might turn Dredd apoptotic in HeLa cells.

In mammals, inhibition of NF- $\kappa$ B results in the induction of apoptosis upon engagement of the TNF receptor. A previous paper demonstrated that overexpression of Imd induces apoptosis in adult *Drosophila*<sup>116</sup>. However, it is not clear if the IMD pathway induces apoptosis. We therefore asked if the inhibition of the IMD/Rel arm prevents Dredd-mediated induction of apoptosis in the IMD pathway (by Edan Foley, supplementary Figure 1.). Depletion of IMD/Rel signaling molecules blocked the PGN-mediated expression of *att*. However, blocking IMD/Rel signaling failed to induce apoptosis in S2 cells exposed to PGN. Thus, I propose that the IMD pathway lacks a pro-apoptotic equivalent to the Caspase-8 mediated apoptotic arm in TNF signaling.

Since Dredd enhances but does not substitute the physiological function of Caspase-8 in apoptosis, I wondered if Caspase-8 interferes with the physiological role of Dredd in IMD signaling. I demonstrated that Caspase-8 is active in S2 cells and therefore I asked if an active Caspase-8 influences Rel cleavage or dJNK phosphorylation. My result showed that expression of Caspase-8 in S2 cells does not interfere with IMD signaling. Independent of pathway activation, Caspase-8 expression in S2 cells did not alter Rel cleavage or phosphorylation of dJNK. In addition, exogenous expression of Caspase-8 does not appear to

induce apoptosis in S2 cells or in flies. Given this, I suggest that flies do not support the full activation of Caspase-8 and/or that flies lack the required molecular backbone for Caspase-8 mediated signaling. Based on my current data I suggest that Caspase-8 does not substitute for Dredd which might be explained by the lack of Caspase-8 interaction with dFADD and dIAP2. Also, it is not clear if Caspase-8 has the proper specificity to cleave Imd or Rel.

Combined, the data indicate fundamental differences between Dredd and Caspase-8 in auto-processing, binding-partners interactions, and substrate recognition. The structural distinction between Dredd and Caspase-8 may explain the differences between Dredd and Caspase-8 function in TNF and IMD signaling. Activation of the TNF-mediated apoptotic response requires the internalization of the receptor and formation of complex II that is observed approximately two hours after stimulation. The formation of complex II enables the recruitment of Fadd and Caspase-8 that is necessary for Caspase-8 activation. Caspase-8 requires autoproteolytic activation, remodeling of the subunits and maturation due to release from the prodomain. The released caspase is stable and active, thus the caspase optimally binds and processes downstream substrates<sup>73</sup>. This process is relatively slow compared to the quickly activated NF- $\kappa$ B response. Similar to the NF- $\kappa$ B response, activation of the pro-survival IMD response relies on the fast signal transduction to mediate rapid responses. In addition, it is important to also effectively terminate the immune response once the threat is cleared. I propose that activation of the IMD pathway mediates the formation of a molecular complex that induces Dredd activity in the absence of the molecular hallmarks of Caspase-8 activation. I speculate further that sidestepping the proteolytic activation of Dredd assists in the fast activation and termination of the response. Negative regulations are in place to counteract a prolonged immune response and probably mediate a quick deactivation of Dredd. For example, in a recent study I showed that the RING finger containing Defense repressor 1 (Dnr1) negatively regulates Dredd in IMD signaling and a recent publication confirmed the importance of Dnr1 to avoid prolonged activation of the immune response<sup>352,369</sup>.

To further decipher similarities and differences between Dredd and Caspase-8 I asked how Dredd is related to other caspases at the sequence level. The prodomain of initiator caspases contain protein interaction motifs such as DED and CARD domains that are part of the death domain superfamily<sup>363</sup>. While the sequence similarity across death domains is quite low (~25%), they often possess similar structure. For example the DED and CARD domains both display a similar backbone of six  $\alpha$ -helices.

While recent reports suggested a lack of DED in Dredd and dFADD, our sequence (by Bart Hazes) analysis of Dredd and Caspase-8 indicated 20% sequence identity over 88% of the prodomain sequence, including both DED domains. The data indicate that the prodomains of Dredd and Caspase-8 have diverged from a common ancestor.

A recent report indicated that residues important for binding and catalysis in the catalytic domain of Dredd are conserved compared to other caspases with the exception of the catalytic site (QACQE) that is unique among the caspases<sup>129,346</sup>. While these similarities indicate that the overall structure of the catalytic domain of Dredd is probably similar to other caspase, we observed that the inter-subunit linker amongst Caspase-8 orthologs vary in length. Our initial examinations of the Dredd sequence indicated that Dredd lacks caspase cleavage sites in the linker sequence between the caspase-domain subunits (by Bart Hazes, supplementary Figure 2.). Caspase-8 is cleaved at two sites in the inter-subunit linker sequence (VETD and LEMD)<sup>194</sup>. While two cleavage sites within the linker appear to be typical for caspases of higher species, lower species display at most one potential cleavage site. Sequence alignments of the linker region between Caspase-8 and *Drosophila* Caspase-8 orthologs showed that Dredd lacks a typical caspase consensus site and instead displays only one aspartate at a site composed of FRID. This site is different to known caspase cleavage sites. Most importantly the FRID sequence does not match the LEXD consensus sequence for Dredd and it appears that this site is not present in some *Drosophila* species altogether. The data suggest that Dredd and other *Drosophila* Caspase-8 orthologs may not be autoproteolytically cleaved as a result of a lack of the supporting structural features at the linker region.

I propose that the caspase inter-subunit linker sequence of different species changed over time and consequently altered the specific requirements for their activation. Some caspases might require auto-processing to be fully active while others might function without the requirement for processing. If the functional differences between Dredd and Caspase-8 are the result of the structural differences one could predict that the introduction of a Dredd-specific cleavage site (as seen in Imd and Rel) into the Dredd sequence will turn Dredd into a protein capable of autoproteolytic activation, leading to the cleavage of effector caspases such as Drice and Dcp-1, and the induction of apoptosis. In addition, if cleavage of Dredd is not required to activate and stabilize Dredd, I would predict that the aspartate in the FRID motif of the Dredd linker region is non-essential for Dredd signaling. Therefore, a point mutation of the aspartate in the FRID motif would not interfere with Dredd function.

At the moment I cannot exclude that Dredd is never processed. As mentioned earlier, my analysis only looked at overexpressed Dredd and specifically at the Dreddy isoform. One could speculate that different isoforms display differences in auto-processing and therefore mediate the diverse functions of Dredd in Imd and Rel cleavage, respectively. However, based on the sequence data that indicate a lack for cleavage sites in the Dredd linker sequence, I find it unlikely that any Dredd isoform is processed in *Drosophila*. Expression analysis of Dredd variants will clarify potential differences between Dredd isoforms.

The sequence analysis of the Dredd linker region is in line with the initial finding that Dredd lacks auto-processing in S2 cells and flies. The difference in auto-processing might be an explanation for the functional differences in life and death decisions between Dredd and Caspase-8. On that note, cFLIP<sub>L</sub> (inactive Caspase-8 paralog) inhibits the Caspase-8 apoptotic activity by forming a heterodimer with the Caspase-8 zymogen<sup>91</sup>. Intriguingly, although Caspase-8 is not processed in the heterodimer it has proteolytic activity<sup>92-94</sup>. However, the proteolytic activity is decreased compared to Caspase-8 homodimers since only the processed and released Caspase-8 homodimer activates effector caspases<sup>95</sup>. In the Caspase-8/cFLIP<sub>L</sub> heterodimer Caspase-8 cleaves cFLIP<sub>L</sub> which recruits other components like TRAF2 and RIPK1 resulting in NF-κB

signaling<sup>370,371</sup>. Therefore cFLIP<sub>L</sub> restricts Caspase-8 activity towards non-apoptotic functions.

In flies, Dredd interactions with dFADD and dIAP2 enable the attachment of ubiquitin to Dredd and Imd<sup>114,273</sup>. The ubiquitin-scaffold assists with the recruitment of other signaling components. Within that local environment Imd and Rel are probably easily accessible for proteolytic cleavage by Dredd. However, the lack of auto-processing of Dredd might block the accessibility of other substrates like effector caspases and therefore might explain why Dredd contributes solely to the survival response.

### 6.3.2. Dronc regulates dIAP2 protein levels in cell culture

Indications for an involvement for dIAP2 in apoptosis resulted from overexpression studies where dIAP2 appears to lower Drice activity<sup>267,268</sup>. However, dIAP2 does not play a substantial role in apoptosis since dIAP2 mutant animals are viable and healthy, and respond to a number of apoptotic stresses that are also tolerated by WT flies. In contrast, dIAP2 is essential for the IMD-mediated immune response to gram-negative bacteria<sup>109-112,114,273</sup>. dIAP2 interacts with Dredd, dFADD, and Imd and dIAP2 mediates signaling through a series of ubiquitination events<sup>114,350</sup>. My initial experiments with a tagged dIAP2 expression construct indicated low protein stability for full-length dIAP2 and revealed N-terminal cleavage. Since the regulatory mechanism of dIAP2 stability or the potential requirement for dIAP2 cleavage in IMD signaling is unknown, I investigated how both processes are realized for dIAP2 and how that might modify the IMD signaling pathway (chapter 5.3).

Recent studies demonstrated that the dIAP2 RING domain is required for IMD signaling and are consistent with the current model where dIAP2 ubiquitinates Dredd and Imd<sup>114,273</sup>. My data demonstrated that the RING domain also controls dIAP2 stability. I propose that dIAP2 targets Dredd, Imd and itself for ubiquitination and by that contributes to the balance of pathway activation and inhibition. I speculate that the attachment of ubiquitin (probably K48-linked) to dIAP2 mediates constant degradation of dIAP2 to avoid unwanted signaling

pathway activation. Pathway activation might initiate the stabilization of dIAP2 possibly through protein modification or incorporation into a higher protein complex. Stabilized dIAP2 then ubiquitinates Imd and Dredd that enables further signal transduction.

The lack of a functional RING domain did not block dIAP2 cleavage and therefore indicates that the RING domain does not regulate dIAP2 cleavage. In contrast, cleavage is mediated by a caspase since the appearance of the truncation products were greatly diminished after blocking caspase activity. So far, Dredd is the only caspase with an established role in IMD signaling. Surprisingly, my data indicated Dronc as the caspase responsible for dIAP2 cleavage. At the moment I cannot exclude the involvement of additional caspases in dIAP2 processing due to inefficient depletion of the caspases by RNAi. In addition, redundancies among caspases might mask the involvement of another caspase in dIAP2 cleavage. Further evaluations of all the *Drosophila* caspases are required to confirm my initial results. However, my data strongly indicate that Dronc and not Dredd or Drice is essential for dIAP2 cleavage and that RING mediated degradation and Dronc-mediate cleavage of dIAP2 are two distinct processes. In addition, it appears that an N-terminal truncated dIAP2 has increased stability. I propose a model where activation of PGRP-LC triggers the formation of a high molecular weight complex that contains Imd, dFADD, Dredd and dIAP2. Imd and dFADD interact through DD; dFADD and Dredd form homotypic interaction through DED; and dIAP2 and Dredd through BIR 2 and 3 motifs and the caspase-and prodomain of Dredd. In this model, the first 92 amino acids at the N-terminus of dIAP2 are dispensable. Therefore, I propose that N-terminal cleavage of dIAP2 by Dronc generates a more stable protein that effectively binds and activates Dredd and Imd.

Interestingly, my preliminary data indicated a reduction of *att* expression in *dronc* depleted cells. A recently performed screen in our laboratory indicated an increase in dJNK activity due to RNAi-mediated depletion of *dronc*<sup>146</sup>. Since the IMD/Rel arm negatively regulates the IMD/dJNK arm I propose that depletion of *dronc* lowers IMD/Rel activity and by that increases IMD/dJNK activity. The data suggest a requirement for Dronc in the full activation of the IMD/Rel antimicrobial

response. However, further analyses are necessary (for example measurements of other IMD/Rel and IMD/dJNK responsive transcripts) to confirm my initial result and to further understand Dronc involvement in IMD/dJNK and IMD/Rel signaling.

So far I cannot conclude that the loss of Dronc substantially impairs the ability of flies to combat bacterial challenges. Since the RNAi-mediated knock-down of *dronc* did not fully block *att* expression it is unclear if the loss of *dronc* renders flies inefficient to fight off bacterial infection. *dronc* mutant flies are homozygous lethal making it impossible to evaluate the immune phenotype of null mutants<sup>349</sup>. The targeted gene knock-down of *dronc* may elucidate the role of Dronc in the IMD pathway after bacterial encounter *in vivo*. In addition, DroncCS acts as a dominant negative in S2 cells. The generation of a DroncCS transgenic fly line will help to decipher Dronc's contribution to the IMD signaling pathway.

Recent reports that indicated potential links between apoptosis and IMD signaling have generated conflicting results. For example, bacterial infection triggers AMP expression but not apoptosis while UV radiation induces apoptosis but not AMP expression<sup>116</sup>. In contrast, overexpression of Imd induces apoptosis and dIAP1 depletion induces mild AMP expression<sup>116,349</sup>. In addition, situations where one molecule is shared by the apoptotic arm and the immune arms are not uncommon. As an example, Dnr1 inhibits Dronc's apoptotic capabilities and Dredd's immunological capacities<sup>352,372</sup>.

While my results suggest that the PGN-mediated IMD response does not support apoptosis, my data also indicate that the pro- and anti-apoptotic responses are not completely separated from each other and that Dronc might represent a point of convergence between pushing a cell towards death or survival.

Intriguingly, a recent report demonstrated that depletion of *diap1* triggered induction of *dipt* expression that is blocked by the simultaneous depletion of *diap2*<sup>111</sup>. The data indicate that Dronc activation (by *dIAP1* depletion) triggers IMD activation in a dIAP2-dependent manner. These data are in line with the proposed function of Dronc in IMD signaling at the level of dIAP2. If this model holds true I suggest that PGN stabilizes dIAP2, that cleaved dIAP2 preferably binds Dredd and Imd, and that inhibition of the apoptotic arm downstream of

Dronc causes increased AMP levels after PGN stimulation. In addition, the uncleavable dIAP2 variant should be less efficient compared to a WT dIAP2 to substitute endogenous dIAP2 after signal induction. Finally, the examination of dIAP1 and Dronc RNAi lines and dIAP2 transgenic lines (e.g. uncleavable dIAP2) will help to decipher the impact of Dronc on dIAP2-dependent IMD signaling.

In support of Dronc function in non-apoptotic processes, recent studies demonstrated that Dronc coordinates the execution of cell death and compensatory proliferation<sup>318,320</sup>. Little is known how Dronc mediates compensatory proliferation but it is suggested that Dronc activation induces extra division of surrounding cells. The mechanisms how caspases accomplish such divergent function in cell death and cell survival are not well understood, but some studies suggest that caspase activation is not necessarily an all-or-nothing process<sup>373-375</sup>. Therefore, low levels of caspase activity can be beneficial for the survival and it is suggested that cellular lethality is only accomplished when caspase activity reaches a critical threshold. Below that threshold the cell fails to induce apoptosis.

I speculate that Dronc functions as a sensor that helps to boost the immune response under moderate stress levels, while Dronc induces apoptosis beyond a certain threshold. The fine-tuned level of Dronc activation might be the important factor that differentiates between life and death decisions. How this is accomplished on a molecular level requires further investigations and considering the fine-balance struck between apoptotic and survival responses it will not be surprising that the differences in timing (e.g. development ) and localization (e.g. tissue) will add more complexity on how caspases are regulated in their distinct functions.

In summary, in section 5. I demonstrated data that revealed differences between Dredd and Caspase-8 activation that might explain the functional differences of the two proteins in immunity and apoptosis. In addition, the data give indications for a distinct regulatory mechanism of dIAP2 where dIAP2 is regulated by RING domain mediated destruction and Dronc mediated cleavage.

An emerging body of literature discovered that caspases are not exclusively inducers of apoptosis and instead caspase activation can have the exact

opposing effect and be vital for a cell. The activation mechanism (e.g. non-processed caspase versus processed caspase) and the activation level (e.g. low versus high caspase activity) of caspases might establish the necessary distinction required to functions in such profoundly different processes of apoptosis or immunity. During evolution caspases probably acquired multiple and distinct activation mechanisms to facilitate their unique roles in both apoptotic and non-apoptotic applications.

#### **6.4. Model**

I propose that activation of PGRP-LC by PGN initiates the formation of a higher molecular weight complex that incorporates Imd, dFADD, Dredd and dIAP2. Imd is likely the most proximal protein recruited to the receptor that engages dFADD through DD binding. dFADD recruits Dredd to the receptor complex through homotypic interactions between the DED. Dronc generates a stable, N-terminal processed dIAP2 that effectively binds Dredd through dIAP2 BIR 2 and 3 motifs. The formation of the proximal complex enables the ubiquitination and activation of Dredd that now proteolytically cleaves Imd. Cleaved Imd generates a docking site for dIAP2 at the IBM motif. dIAP2 further ubiquitinates the complex by the attachment of ubiquitin to Imd. The polyubiquitin chains function as a scaffold to recruit and activate the downstream complexes of dTAB2/dTAK1 and IKK. At the same time the scaffold generates the required proximity between Dredd and Rel to enable proteolytic cleavage of Rel by Dredd. Combined, the molecular processes ensure the proper induction of IMD/Rel and IMD/dJNK dependent immune responses (Figure 6.1.).

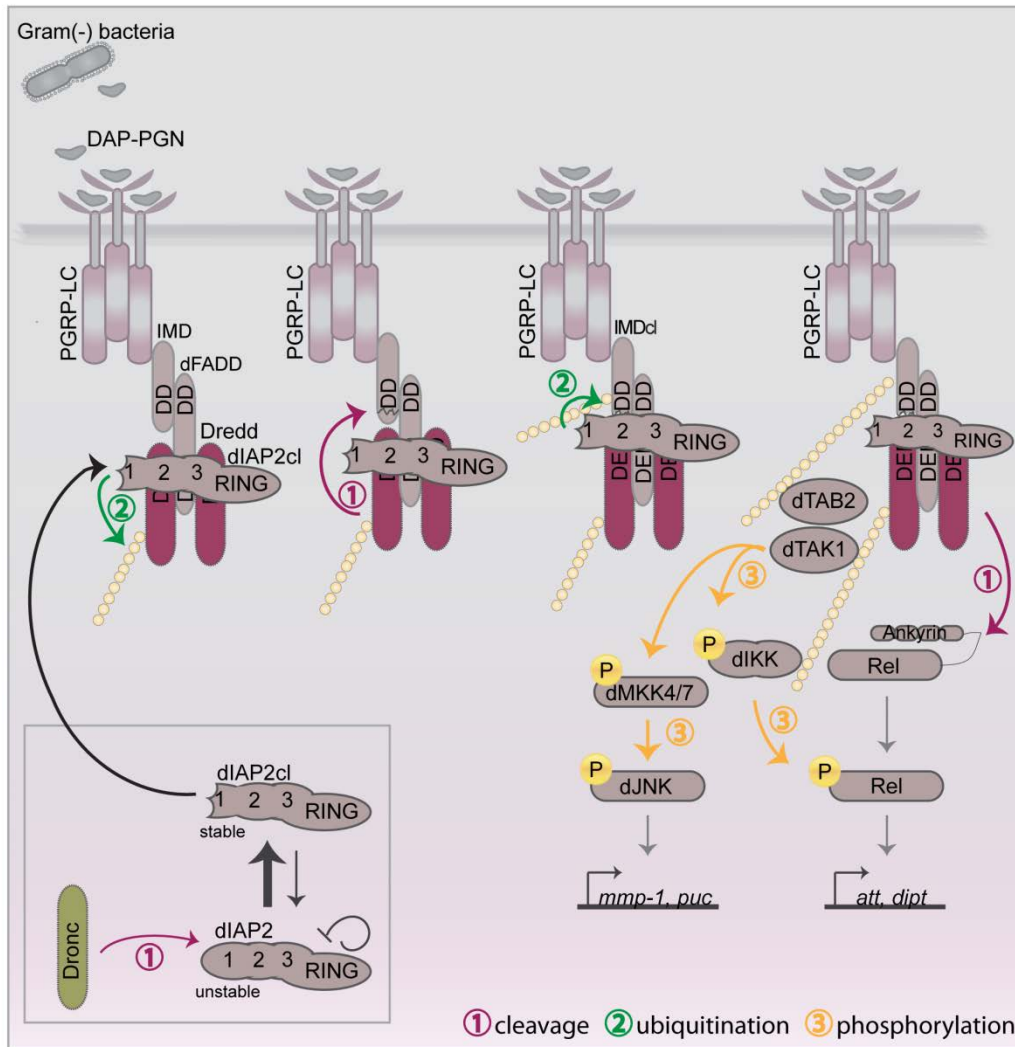


**Figure 6.1. Proposed model:** Sequential steps of the IMD signaling cascade after receptor activation by PGN are indicated from right to left. Proteolytic cleavage of components are indicated in purple and with the number one, ubiquitination steps are indicated in green and number two, and phosphorylation events are marked in yellow and number three. DD = Death Domain, DED = Death Effector Domain, P = phospho-, *Imdcl* = cleaved *Imd*, *diAP2cl* = cleaved *diAP2*, numbers 2-3 in *diAP2* = BIR1-3 domain, RING = RING domain.

## 6.5. Significance

The vast majority of metazoans rely solely on innate immunity to counter an innumerable variety of invading microorganisms demonstrating the remarkable potency of the innate immune system. Since innate immunity represents such a powerful tool to ensure health and fitness of most organisms it is not a surprise that evolution conserved the pathways and signaling molecules of the innate immune system in as widely separated species of human and flies. Scientists have made remarkable contributions towards our understanding of the processes in immunity by acquiring information from comparative biology across species.

*Drosophila* as a model system is no exception and analysis of the fly immune system have been a profound contributor to our current view on immune signaling pathways. The availability of the complete genome sequences, the large collection of mutants, and the ease of genetic manipulation make *Drosophila* an outstanding model system to study the underlying mechanisms that regulate essential biological processes in life and death decisions. One priceless advantage of flies is the prospect to validate cell culture observations in a physiologically relevant *in vivo* context.

The pathway that I have been interested in throughout the path of my thesis is the *Drosophila* IMD signaling pathway. The IMD pathway is one of the major players in fly immunity and essential to counteract gram negative bacterial infections. While excellent work has elucidated key players within the IMD signaling cascade, many fundamental questions of the molecular mechanisms in IMD signaling remained. In particular the early signaling steps, sequential activation of signaling molecules, and the molecular mechanism of activation of important mediators were still elusive.

Throughout my thesis I addressed several outstanding questions about the molecular concepts in the IMD signaling cascade with the specific focus on the caspase Dredd. Although caspases have been described as major contributors to apoptosis, recent years have accumulated mounting evidence that caspases also have vital function. Dredd is a remarkable example for a caspase with a pro-survival function in the IMD-mediated immune response demonstrated by the

early death of immune challenged flies that are mutant for *dredd*. Likewise, the human ortholog of Dredd - Caspase-8 - is well described for its role in apoptosis but Caspase-8 has also essential implications in non-apoptotic processes. It is suggested that Caspase-8 mediates pro-survival functions without the need of auto-processing. However, the underlying mechanism of caspase activation in non-apoptotic function is still not very well understood.

In my effort to address the molecular basis of Dredd activity and function I demonstrated dual functions for Dredd in the IMD signaling cascade, where Dredd is required in a proximal signaling complex for the early transduction of a phospho-relay to Rel and dJNK as well as for the subsequent activation of Rel. The activation mechanism for Dredd appears to be independent of auto-processing and distinct from the typical activation mechanism of apoptotic caspases. The differences might be the basis for Dredd's sole function in pro-survival responses. More specifically, the interaction with the early proximal signaling complex and the subsequent lack of auto-processing might retain Dredd in a non-apoptotic configuration.

My data also implicated Dronc in the IMD signaling pathway at the level of dIAP2 regulation. The exact molecular mechanism how Dronc mediates pro- and anti-survival functions is not clear at the moment. It is possible that differences in the activation level of Dronc distinguish between the two opposing functions and that low level of Dronc activity restricts Dronc towards non-apoptotic tasks.

Caspases most likely acquired different strategies to regulate their activity to control their unique roles in life and death decisions throughout evolution. The activation mechanism and the activation level may be key for the life and death decisions of caspases. Combined the findings underline the importance and complexity of non-apoptotic roles of caspases. The continuous effort to understand signaling processes in diverse species is most promising to elucidate more and profounder details of the molecular mechanism of caspase activation in life and death decisions.

## Chapter 7. Bibliography

- 1 Medzhitov, R. & Janeway, C. A., Jr. Decoding the patterns of self and nonself by the innate immune system. *Science* **296**, 298-300, doi:10.1126/science.1068883 (2002).
- 2 Janeway, C. A., Jr. & Medzhitov, R. Innate immune recognition. *Annual review of immunology* **20**, 197-216 (2002).
- 3 Chaplin, D. D. 1. Overview of the human immune response. *The Journal of allergy and clinical immunology* **117**, S430-435 (2006).
- 4 Janeway, C. A., Jr. How the immune system protects the host from infection. *Microbes and infection / Institut Pasteur* **3**, 1167-1171 (2001).
- 5 Medzhitov, R. & Janeway, C., Jr. Innate immune recognition: mechanisms and pathways. *Immunological reviews* **173**, 89-97 (2000).
- 6 Kimbrell, D. A. & Beutler, B. The evolution and genetics of innate immunity. *Nature reviews. Genetics* **2**, 256-267, doi:10.1038/35066006 (2001).
- 7 Beutler, B. Innate immunity: an overview. *Molecular immunology* **40**, 845-859 (2004).
- 8 Akira, S., Uematsu, S. & Takeuchi, O. Pathogen recognition and innate immunity. *Cell* **124**, 783-801, doi:10.1016/j.cell.2006.02.015 (2006).
- 9 Heine, H. & Lien, E. Toll-like receptors and their function in innate and adaptive immunity. *International archives of allergy and immunology* **130**, 180-192, doi:69517 (2003).
- 10 Lemaitre, B. & Hoffmann, J. The host defense of *Drosophila melanogaster*. *Annual review of immunology* **25**, 697-743, doi:10.1146/annurev.immunol.25.022106.141615 (2007).
- 11 Scully, L. R. & Bidochka, M. J. Developing insect models for the study of current and emerging human pathogens. *FEMS microbiology letters* **263**, 1-9, doi:10.1111/j.1574-6968.2006.00388.x (2006).
- 12 Anderson, K. V., Jurgens, G. & Nusslein-Volhard, C. Establishment of dorsal-ventral polarity in the *Drosophila* embryo: genetic studies on the role of the Toll gene product. *Cell* **42**, 779-789 (1985).
- 13 Medzhitov, R., Preston-Hurlburt, P. & Janeway, C. A., Jr. A human homologue of the *Drosophila* Toll protein signals activation of adaptive immunity. *Nature* **388**, 394-397, doi:10.1038/41131 (1997).
- 14 Rock, F. L., Hardiman, G., Timans, J. C., Kastelein, R. A. & Bazan, J. F. A family of human receptors structurally related to *Drosophila* Toll. *Proc Natl Acad Sci U S A* **95**, 588-593 (1998).
- 15 Anderson, K. V., Bokla, L. & Nusslein-Volhard, C. Establishment of dorsal-ventral polarity in the *Drosophila* embryo: the induction of polarity by the Toll gene product. *Cell* **42**, 791-798 (1985).
- 16 Lemaitre, B. *et al.* Functional analysis and regulation of nuclear import of dorsal during the immune response in *Drosophila*. *EMBO J* **14**, 536-545 (1995).
- 17 Lemaitre, B., Nicolas, E., Michaut, L., Reichhart, J. M. & Hoffmann, J. A. The dorsoventral regulatory gene cassette *spatzle/Toll/cactus* controls the potent antifungal response in *Drosophila* adults. *Cell* **86**, 973-983 (1996).
- 18 Nusslein-Volhard, C., Frohnhofer, H. G. & Lehmann, R. Determination of anteroposterior polarity in *Drosophila*. *Science* **238**, 1675-1681 (1987).

- 19 Akira, S., Takeda, K. & Kaisho, T. Toll-like receptors: critical proteins linking innate and acquired immunity. *Nature immunology* **2**, 675-680 (2001).
- 20 Lemaitre, B. *et al.* A recessive mutation, immune deficiency (imd), defines two distinct control pathways in the *Drosophila* host defense. *Proc Natl Acad Sci U S A* **92**, 9465-9469 (1995).
- 21 Hoffmann, J. A., Kafatos, F. C., Janeway, C. A. & Ezekowitz, R. A. Phylogenetic perspectives in innate immunity. *Science* **284**, 1313-1318 (1999).
- 22 Hoffmann, J. A. The immune response of *Drosophila*. *Nature* **426**, 33-38, doi:10.1038/nature02021 (2003).
- 23 Rubin, G. M. *et al.* Comparative genomics of the eukaryotes. *Science* **287**, 2204-2215 (2000).
- 24 Sondergaard, L. Homology between the mammalian liver and the *Drosophila* fat body. *Trends in genetics : TIG* **9**, 193 (1993).
- 25 Kounatidis, I. & Ligoxygakis, P. *Drosophila* as a model system to unravel the layers of innate immunity to infection. *Open biology* **2**, 120075, doi:10.1098/rsob.120075 (2012).
- 26 Vallet-Gely, I., Lemaitre, B. & Boccard, F. Bacterial strategies to overcome insect defences. *Nature reviews. Microbiology* **6**, 302-313, doi:10.1038/nrmicro1870 (2008).
- 27 Hetru, C., Troxler, L. & Hoffmann, J. A. *Drosophila melanogaster* antimicrobial defense. *The Journal of infectious diseases* **187 Suppl 2**, S327-334, doi:10.1086/374758 (2003).
- 28 De Gregorio, E., Spellman, P. T., Rubin, G. M. & Lemaitre, B. Genome-wide analysis of the *Drosophila* immune response by using oligonucleotide microarrays. *Proc Natl Acad Sci U S A* **98**, 12590-12595, doi:10.1073/pnas.221458698 (2001).
- 29 De Gregorio, E., Spellman, P. T., Tzou, P., Rubin, G. M. & Lemaitre, B. The Toll and Imd pathways are the major regulators of the immune response in *Drosophila*. *EMBO J* **21**, 2568-2579, doi:10.1093/emboj/21.11.2568 (2002).
- 30 Pandey, U. B. & Nichols, C. D. Human disease models in *Drosophila melanogaster* and the role of the fly in therapeutic drug discovery. *Pharmacological reviews* **63**, 411-436, doi:10.1124/pr.110.003293 (2011).
- 31 Brogden, K. A. Antimicrobial peptides: pore formers or metabolic inhibitors in bacteria? *Nature reviews. Microbiology* **3**, 238-250, doi:10.1038/nrmicro1098 (2005).
- 32 Ganz, T. The role of antimicrobial peptides in innate immunity. *Integrative and comparative biology* **43**, 300-304, doi:10.1093/icb/43.2.300 (2003).
- 33 Dimarcq, J. L. *et al.* Characterization and transcriptional profiles of a *Drosophila* gene encoding an insect defensin. A study in insect immunity. *European journal of biochemistry / FEBS* **221**, 201-209 (1994).
- 34 Fehlbaum, P. *et al.* Insect immunity. Septic injury of *Drosophila* induces the synthesis of a potent antifungal peptide with sequence homology to plant antifungal peptides. *J Biol Chem* **269**, 33159-33163 (1994).

- 35 Levashina, E. A. *et al.* Metchnikowin, a novel immune-inducible proline-rich peptide from *Drosophila* with antibacterial and antifungal properties. *European journal of biochemistry / FEBS* **233**, 694-700 (1995).
- 36 Imler, J. L. & Bulet, P. Antimicrobial peptides in *Drosophila*: structures, activities and gene regulation. *Chemical immunology and allergy* **86**, 1-21, doi:10.1159/000086648 (2005).
- 37 Asling, B., Dushay, M. S. & Hultmark, D. Identification of early genes in the *Drosophila* immune response by PCR-based differential display: the Attacin A gene and the evolution of attacin-like proteins. *Insect biochemistry and molecular biology* **25**, 511-518 (1995).
- 38 Wicker, C. *et al.* Insect immunity. Characterization of a *Drosophila* cDNA encoding a novel member of the dipterecin family of immune peptides. *J Biol Chem* **265**, 22493-22498 (1990).
- 39 Bulet, P. *et al.* A novel inducible antibacterial peptide of *Drosophila* carries an O-glycosylated substitution. *J Biol Chem* **268**, 14893-14897 (1993).
- 40 Kylsten, P., Samakovlis, C. & Hultmark, D. The cecropin locus in *Drosophila*; a compact gene cluster involved in the response to infection. *EMBO J* **9**, 217-224 (1990).
- 41 Locksley, R. M., Killeen, N. & Lenardo, M. J. The TNF and TNF receptor superfamilies: integrating mammalian biology. *Cell* **104**, 487-501 (2001).
- 42 Aggarwal, B. B. Signalling pathways of the TNF superfamily: a double-edged sword. *Nature reviews. Immunology* **3**, 745-756, doi:10.1038/nri1184 (2003).
- 43 Nathan, C. Points of control in inflammation. *Nature* **420**, 846-852, doi:10.1038/nature01320 (2002).
- 44 Nathan, C. & Ding, A. Nonresolving inflammation. *Cell* **140**, 871-882, doi:10.1016/j.cell.2010.02.029 (2010).
- 45 Medzhitov, R. Inflammation 2010: new adventures of an old flame. *Cell* **140**, 771-776, doi:10.1016/j.cell.2010.03.006 (2010).
- 46 Suryaprasad, A. G. & Prindiville, T. The biology of TNF blockade. *Autoimmunity reviews* **2**, 346-357 (2003).
- 47 Hsu, H., Shu, H. B., Pan, M. G. & Goeddel, D. V. TRADD-TRAF2 and TRADD-FADD interactions define two distinct TNF receptor 1 signal transduction pathways. *Cell* **84**, 299-308 (1996).
- 48 Hsu, H., Xiong, J. & Goeddel, D. V. The TNF receptor 1-associated protein TRADD signals cell death and NF-kappa B activation. *Cell* **81**, 495-504 (1995).
- 49 Wajant, H., Pfizenmaier, K. & Scheurich, P. Tumor necrosis factor signaling. *Cell death and differentiation* **10**, 45-65, doi:10.1038/sj.cdd.4401189 (2003).
- 50 Yang, J. *et al.* The essential role of MEKK3 in TNF-induced NF-kappaB activation. *Nature immunology* **2**, 620-624, doi:10.1038/89769 (2001).
- 51 Schmidt, C. *et al.* Mechanisms of proinflammatory cytokine-induced biphasic NF-kappaB activation. *Mol Cell* **12**, 1287-1300 (2003).
- 52 Luo, J. L., Kamata, H. & Karin, M. IKK/NF-kappaB signaling: balancing life and death--a new approach to cancer therapy. *The Journal of clinical investigation* **115**, 2625-2632, doi:10.1172/JCI26322 (2005).

- 53 Gaur, U. & Aggarwal, B. B. Regulation of proliferation, survival and apoptosis by members of the TNF superfamily. *Biochem Pharmacol* **66**, 1403-1408 (2003).
- 54 Hsu, H., Huang, J., Shu, H. B., Baichwal, V. & Goeddel, D. V. TNF-dependent recruitment of the protein kinase RIP to the TNF receptor-1 signaling complex. *Immunity* **4**, 387-396 (1996).
- 55 Tada, K. *et al.* Critical roles of TRAF2 and TRAF5 in tumor necrosis factor-induced NF-kappa B activation and protection from cell death. *J Biol Chem* **276**, 36530-36534, doi:10.1074/jbc.M104837200 (2001).
- 56 Varfolomeev, E. *et al.* c-IAP1 and c-IAP2 are critical mediators of tumor necrosis factor alpha (TNFalpha)-induced NF-kappaB activation. *J Biol Chem* **283**, 24295-24299, doi:10.1074/jbc.C800128200 (2008).
- 57 Silke, J. The regulation of TNF signalling: what a tangled web we weave. *Current opinion in immunology* **23**, 620-626, doi:10.1016/j.coi.2011.08.002 (2011).
- 58 Vince, J. E. *et al.* TRAF2 must bind to cellular inhibitors of apoptosis for tumor necrosis factor (tnf) to efficiently activate nf-{kappa}b and to prevent tnf-induced apoptosis. *J Biol Chem* **284**, 35906-35915, doi:10.1074/jbc.M109.072256 (2009).
- 59 Mace, P. D., Smits, C., Vaux, D. L., Silke, J. & Day, C. L. Asymmetric recruitment of cIAPs by TRAF2. *Journal of molecular biology* **400**, 8-15, doi:10.1016/j.jmb.2010.04.055 (2010).
- 60 Walczak, H. TNF and ubiquitin at the crossroads of gene activation, cell death, inflammation, and cancer. *Immunological reviews* **244**, 9-28, doi:10.1111/j.1600-065X.2011.01066.x (2011).
- 61 Bertrand, M. J. *et al.* cIAP1 and cIAP2 facilitate cancer cell survival by functioning as E3 ligases that promote RIP1 ubiquitination. *Mol Cell* **30**, 689-700, doi:10.1016/j.molcel.2008.05.014 (2008).
- 62 Dynek, J. N. *et al.* c-IAP1 and Ubch5 promote K11-linked polyubiquitination of RIP1 in TNF signalling. *EMBO J* **29**, 4198-4209, doi:10.1038/emboj.2010.300 (2010).
- 63 Ea, C. K., Deng, L., Xia, Z. P., Pineda, G. & Chen, Z. J. Activation of IKK by TNFalpha requires site-specific ubiquitination of RIP1 and polyubiquitin binding by NEMO. *Mol Cell* **22**, 245-257, doi:10.1016/j.molcel.2006.03.026 (2006).
- 64 Kanayama, A. *et al.* TAB2 and TAB3 activate the NF-kappaB pathway through binding to polyubiquitin chains. *Mol Cell* **15**, 535-548, doi:10.1016/j.molcel.2004.08.008 (2004).
- 65 Rahighi, S. *et al.* Specific recognition of linear ubiquitin chains by NEMO is important for NF-kappaB activation. *Cell* **136**, 1098-1109, doi:10.1016/j.cell.2009.03.007 (2009).
- 66 Lo, Y. C. *et al.* Structural basis for recognition of diubiquitins by NEMO. *Mol Cell* **33**, 602-615, doi:10.1016/j.molcel.2009.01.012 (2009).
- 67 Komander, D. *et al.* Molecular discrimination of structurally equivalent Lys 63-linked and linear polyubiquitin chains. *EMBO Rep* **10**, 466-473, doi:10.1038/embor.2009.55 (2009).
- 68 Wang, C. *et al.* TAK1 is a ubiquitin-dependent kinase of MKK and IKK. *Nature* **412**, 346-351, doi:10.1038/35085597 (2001).

- 69 Tian, B., Nowak, D. E., Jamaluddin, M., Wang, S. & Brasier, A. R. Identification of direct genomic targets downstream of the nuclear factor-kappaB transcription factor mediating tumor necrosis factor signaling. *J Biol Chem* **280**, 17435-17448, doi:10.1074/jbc.M500437200 (2005).
- 70 Hayden, M. S. & Ghosh, S. Shared principles in NF-kappaB signaling. *Cell* **132**, 344-362, doi:10.1016/j.cell.2008.01.020 (2008).
- 71 Lawrence, T. The nuclear factor NF-kappaB pathway in inflammation. *Cold Spring Harbor perspectives in biology* **1**, a001651, doi:10.1101/cshperspect.a001651 (2009).
- 72 Karin, M. & Lin, A. NF-kappaB at the crossroads of life and death. *Nature immunology* **3**, 221-227, doi:10.1038/ni0302-221 (2002).
- 73 Micheau, O. & Tschopp, J. Induction of TNF receptor I-mediated apoptosis via two sequential signaling complexes. *Cell* **114**, 181-190 (2003).
- 74 Kyriakis, J. M. & Avruch, J. Mammalian MAPK signal transduction pathways activated by stress and inflammation: a 10-year update. *Physiological reviews* **92**, 689-737, doi:10.1152/physrev.00028.2011 (2012).
- 75 Derijard, B. *et al.* Independent human MAP-kinase signal transduction pathways defined by MEK and MKK isoforms. *Science* **267**, 682-685 (1995).
- 76 Lu, X., Nemoto, S. & Lin, A. Identification of c-Jun NH2-terminal protein kinase (JNK)-activating kinase 2 as an activator of JNK but not p38. *J Biol Chem* **272**, 24751-24754 (1997).
- 77 Tournier, C., Whitmarsh, A. J., Cavanagh, J., Barrett, T. & Davis, R. J. Mitogen-activated protein kinase kinase 7 is an activator of the c-Jun NH2-terminal kinase. *Proc Natl Acad Sci U S A* **94**, 7337-7342 (1997).
- 78 Wu, Z., Wu, J., Jacinto, E. & Karin, M. Molecular cloning and characterization of human JNKK2, a novel Jun NH2-terminal kinase-specific kinase. *Molecular and cellular biology* **17**, 7407-7416 (1997).
- 79 Karin, M. & Gallagher, E. From JNK to pay dirt: jun kinases, their biochemistry, physiology and clinical importance. *IUBMB life* **57**, 283-295, doi:10.1080/15216540500097111 (2005).
- 80 Shaulian, E. & Karin, M. AP-1 as a regulator of cell life and death. *Nat Cell Biol* **4**, E131-136, doi:10.1038/ncb0502-e131 (2002).
- 81 Van Antwerp, D. J., Martin, S. J., Kafri, T., Green, D. R. & Verma, I. M. Suppression of TNF-alpha-induced apoptosis by NF-kappaB. *Science* **274**, 787-789 (1996).
- 82 Schneider-Brachert, W. *et al.* Compartmentalization of TNF receptor 1 signaling: internalized TNF receptors as death signaling vesicles. *Immunity* **21**, 415-428, doi:10.1016/j.immuni.2004.08.017 (2004).
- 83 Tchikov, V., Bertsch, U., Fritsch, J., Edelmann, B. & Schutze, S. Subcellular compartmentalization of TNF receptor-1 and CD95 signaling pathways. *European journal of cell biology* **90**, 467-475, doi:10.1016/j.ejcb.2010.11.002 (2011).
- 84 Muzio, M., Stockwell, B. R., Stennicke, H. R., Salvesen, G. S. & Dixit, V. M. An induced proximity model for caspase-8 activation. *J Biol Chem* **273**, 2926-2930 (1998).

- 85 Donepudi, M., Mac Sweeney, A., Briand, C. & Grutter, M. G. Insights into the regulatory mechanism for caspase-8 activation. *Mol Cell* **11**, 543-549 (2003).
- 86 Chowdhury, I., Tharakan, B. & Bhat, G. K. Caspases - an update. *Comparative biochemistry and physiology. Part B, Biochemistry & molecular biology* **151**, 10-27, doi:10.1016/j.cbpb.2008.05.010 (2008).
- 87 Fan, T. J., Han, L. H., Cong, R. S. & Liang, J. Caspase family proteases and apoptosis. *Acta biochimica et biophysica Sinica* **37**, 719-727 (2005).
- 88 Micheau, O., Lens, S., Gaide, O., Alevizopoulos, K. & Tschopp, J. NF-kappaB signals induce the expression of c-FLIP. *Molecular and cellular biology* **21**, 5299-5305, doi:10.1128/MCB.21.16.5299-5305.2001 (2001).
- 89 Thome, M. & Tschopp, J. Regulation of lymphocyte proliferation and death by FLIP. *Nature reviews. Immunology* **1**, 50-58, doi:10.1038/35095508 (2001).
- 90 Irmeler, M. *et al.* Inhibition of death receptor signals by cellular FLIP. *Nature* **388**, 190-195, doi:10.1038/40657 (1997).
- 91 Pop, C. *et al.* FLIP(L) induces caspase 8 activity in the absence of interdomain caspase 8 cleavage and alters substrate specificity. *The Biochemical journal* **433**, 447-457, doi:10.1042/BJ20101738 (2011).
- 92 Micheau, O. *et al.* The long form of FLIP is an activator of caspase-8 at the Fas death-inducing signaling complex. *J Biol Chem* **277**, 45162-45171, doi:10.1074/jbc.M206882200 (2002).
- 93 Boatright, K. M., Deis, C., Denault, J. B., Sutherlin, D. P. & Salvesen, G. S. Activation of caspases-8 and -10 by FLIP(L). *The Biochemical journal* **382**, 651-657, doi:10.1042/BJ20040809 (2004).
- 94 Peter, M. E. The flip side of FLIP. *The Biochemical journal* **382**, e1-3, doi:10.1042/BJ20041143 (2004).
- 95 Kang, T. B. *et al.* Mutation of a self-processing site in caspase-8 compromises its apoptotic but not its nonapoptotic functions in bacterial artificial chromosome-transgenic mice. *Journal of immunology* **181**, 2522-2532 (2008).
- 96 Hoffmann, J. A. & Reichhart, J. M. *Drosophila* innate immunity: an evolutionary perspective. *Nature immunology* **3**, 121-126, doi:10.1038/ni0202-121 (2002).
- 97 Silverman, N. & Maniatis, T. NF-kappaB signaling pathways in mammalian and insect innate immunity. *Genes Dev* **15**, 2321-2342, doi:10.1101/gad.909001 (2001).
- 98 Boutros, M., Agaisse, H. & Perrimon, N. Sequential activation of signaling pathways during innate immune responses in *Drosophila*. *Dev Cell* **3**, 711-722 (2002).
- 99 Kaneko, T. *et al.* Monomeric and polymeric gram-negative peptidoglycan but not purified LPS stimulate the *Drosophila* IMD pathway. *Immunity* **20**, 637-649 (2004).
- 100 Kaneko, T. *et al.* PGRP-LC and PGRP-LE have essential yet distinct functions in the *drosophila* immune response to monomeric DAP-type peptidoglycan. *Nature immunology* **7**, 715-723, doi:10.1038/ni1356 (2006).

- 101 Takehana, A. *et al.* Overexpression of a pattern-recognition receptor, peptidoglycan-recognition protein-LE, activates imd/relish-mediated antibacterial defense and the prophenoloxidase cascade in *Drosophila* larvae. *Proc Natl Acad Sci U S A* **99**, 13705-13710, doi:10.1073/pnas.212301199 (2002).
- 102 Takehana, A. *et al.* Peptidoglycan recognition protein (PGRP)-LE and PGRP-LC act synergistically in *Drosophila* immunity. *EMBO J* **23**, 4690-4700, doi:10.1038/sj.emboj.7600466 (2004).
- 103 Werner, T., Borge-Renberg, K., Mellroth, P., Steiner, H. & Hultmark, D. Functional diversity of the *Drosophila* PGRP-LC gene cluster in the response to lipopolysaccharide and peptidoglycan. *J Biol Chem* **278**, 26319-26322, doi:10.1074/jbc.C300184200 (2003).
- 104 Stenbak, C. R. *et al.* Peptidoglycan molecular requirements allowing detection by the *Drosophila* immune deficiency pathway. *Journal of immunology* **173**, 7339-7348 (2004).
- 105 Leulier, F., Vidal, S., Saigo, K., Ueda, R. & Lemaitre, B. Inducible expression of double-stranded RNA reveals a role for dFADD in the regulation of the antibacterial response in *Drosophila* adults. *Curr Biol* **12**, 996-1000 (2002).
- 106 Naitza, S. *et al.* The *Drosophila* immune defense against gram-negative infection requires the death protein dFADD. *Immunity* **17**, 575-581 (2002).
- 107 Silverman, N. *et al.* Immune activation of NF-kappaB and JNK requires *Drosophila* TAK1. *J Biol Chem* **278**, 48928-48934, doi:10.1074/jbc.M304802200 (2003).
- 108 Vidal, S. *et al.* Mutations in the *Drosophila* dTAK1 gene reveal a conserved function for MAPKKKs in the control of rel/NF-kappaB-dependent innate immune responses. *Genes Dev* **15**, 1900-1912, doi:10.1101/gad.203301 (2001).
- 109 Gesellchen, V., Kutenkeuler, D., Steckel, M., Pelte, N. & Boutros, M. An RNA interference screen identifies Inhibitor of Apoptosis Protein 2 as a regulator of innate immune signalling in *Drosophila*. *EMBO Rep* **6**, 979-984, doi:10.1038/sj.embor.7400530 (2005).
- 110 Kleino, A. *et al.* Inhibitor of apoptosis 2 and TAK1-binding protein are components of the *Drosophila* Imd pathway. *EMBO J* **24**, 3423-3434, doi:10.1038/sj.emboj.7600807 (2005).
- 111 Huh, J. R. *et al.* The *Drosophila* inhibitor of apoptosis (IAP) DIAP2 is dispensable for cell survival, required for the innate immune response to gram-negative bacterial infection, and can be negatively regulated by the reaper/hid/grim family of IAP-binding apoptosis inducers. *J Biol Chem* **282**, 2056-2068, doi:10.1074/jbc.M608051200 (2007).
- 112 Leulier, F., Lhocine, N., Lemaitre, B. & Meier, P. The *Drosophila* inhibitor of apoptosis protein DIAP2 functions in innate immunity and is essential to resist gram-negative bacterial infection. *Molecular and cellular biology* **26**, 7821-7831, doi:10.1128/MCB.00548-06 (2006).
- 113 Zhou, R. *et al.* The role of ubiquitination in *Drosophila* innate immunity. *J Biol Chem* **280**, 34048-34055 (2005).

- 114 Paquette, N. *et al.* Caspase-mediated cleavage, IAP binding, and ubiquitination: linking three mechanisms crucial for *Drosophila* NF-kappaB signaling. *Mol Cell* **37**, 172-182, doi:10.1016/j.molcel.2009.12.036 (2010).
- 115 Hu, S. & Yang, X. dFADD, a novel death domain-containing adapter protein for the *Drosophila* caspase DREDD. *J Biol Chem* **275**, 30761-30764 (2000).
- 116 Georgel, P. *et al.* *Drosophila* immune deficiency (IMD) is a death domain protein that activates antibacterial defense and can promote apoptosis. *Dev Cell* **1**, 503-514 (2001).
- 117 Choe, K. M., Lee, H. & Anderson, K. V. *Drosophila* peptidoglycan recognition protein LC (PGRP-LC) acts as a signal-transducing innate immune receptor. *Proc Natl Acad Sci U S A* **102**, 1122-1126, doi:10.1073/pnas.0404952102 (2005).
- 118 Lu, Y., Wu, L. P. & Anderson, K. V. The antibacterial arm of the *drosophila* innate immune response requires an IkappaB kinase. *Genes Dev* **15**, 104-110 (2001).
- 119 Rutschmann, S. *et al.* Role of *Drosophila* IKK gamma in a toll-independent antibacterial immune response. *Nature immunology* **1**, 342-347, doi:10.1038/79801 (2000).
- 120 Zhuang, Z. H. *et al.* *Drosophila* TAB2 is required for the immune activation of JNK and NF-kappaB. *Cell Signal* **18**, 964-970, doi:10.1016/j.cellsig.2005.08.020 (2006).
- 121 Silverman, N. *et al.* A *Drosophila* IkappaB kinase complex required for Relish cleavage and antibacterial immunity. *Genes Dev* **14**, 2461-2471 (2000).
- 122 Wu, L. P. & Anderson, K. V. Regulated nuclear import of Rel proteins in the *Drosophila* immune response. *Nature* **392**, 93-97 (1998).
- 123 Hedengren, M. *et al.* Relish, a central factor in the control of humoral but not cellular immunity in *Drosophila*. *Mol Cell* **4**, 827-837 (1999).
- 124 Dushay, M. S., Asling, B. & Hultmark, D. Origins of immunity: Relish, a compound Rel-like gene in the antibacterial defense of *Drosophila*. *Proc Natl Acad Sci U S A* **93**, 10343-10347 (1996).
- 125 Stoven, S., Ando, I., Kadalayil, L., Engstrom, Y. & Hultmark, D. Activation of the *Drosophila* NF-kappaB factor Relish by rapid endoproteolytic cleavage. *EMBO Rep* **1**, 347-352, doi:10.1093/embo-reports/kvd072 (2000).
- 126 Stoven, S. *et al.* Caspase-mediated processing of the *Drosophila* NF-kappaB factor Relish. *Proc Natl Acad Sci U S A* **100**, 5991-5996, doi:10.1073/pnas.1035902100 (2003).
- 127 Wiklund, M. L., Steinert, S., Junell, A., Hultmark, D. & Stoven, S. The N-terminal half of the *Drosophila* Rel/NF-kappaB factor Relish, REL-68, constitutively activates transcription of specific Relish target genes. *Developmental and comparative immunology* **33**, 690-696, doi:10.1016/j.dci.2008.12.002 (2009).
- 128 Erturk-Hasdemir, D. *et al.* Two roles for the *Drosophila* IKK complex in the activation of Relish and the induction of antimicrobial peptide genes. *Proc Natl Acad Sci U S A* **106**, 9779-9784, doi:10.1073/pnas.0812022106 (2009).

- 129 Chen, P., Rodriguez, A., Erskine, R., Thach, T. & Abrams, J. M. Dredd, a novel effector of the apoptosis activators reaper, grim, and hid in *Drosophila*. *Developmental biology* **201**, 202-216, doi:10.1006/dbio.1998.9000 (1998).
- 130 Leulier, F., Rodriguez, A., Khush, R. S., Abrams, J. M. & Lemaitre, B. The *Drosophila* caspase Dredd is required to resist gram-negative bacterial infection. *EMBO Rep* **1**, 353-358 (2000).
- 131 Elrod-Erickson, M., Mishra, S. & Schneider, D. Interactions between the cellular and humoral immune responses in *Drosophila*. *Curr Biol* **10**, 781-784 (2000).
- 132 Davis, R. J. Signal transduction by the JNK group of MAP kinases. *Cell* **103**, 239-252 (2000).
- 133 Riesgo-Escovar, J. R., Jenni, M., Fritz, A. & Hafen, E. The *Drosophila* Jun-N-terminal kinase is required for cell morphogenesis but not for DJun-dependent cell fate specification in the eye. *Genes Dev* **10**, 2759-2768 (1996).
- 134 Krishna, M. & Narang, H. The complexity of mitogen-activated protein kinases (MAPKs) made simple. *Cellular and molecular life sciences : CMLS* **65**, 3525-3544, doi:10.1007/s00018-008-8170-7 (2008).
- 135 Kim, E. K. & Choi, E. J. Pathological roles of MAPK signaling pathways in human diseases. *Biochimica et biophysica acta* **1802**, 396-405, doi:10.1016/j.bbadis.2009.12.009 (2010).
- 136 Sluss, H. K. *et al.* A JNK signal transduction pathway that mediates morphogenesis and an immune response in *Drosophila*. *Genes Dev* **10**, 2745-2758 (1996).
- 137 Park, J. M. *et al.* Targeting of TAK1 by the NF-kappa B protein Relish regulates the JNK-mediated immune response in *Drosophila*. *Genes Dev* **18**, 584-594, doi:10.1101/gad.1168104 (2004).
- 138 Geuking, P., Narasimamurthy, R., Lemaitre, B., Basler, K. & Leulier, F. A non-redundant role for *Drosophila* Mkk4 and hemipterous/Mkk7 in TAK1-mediated activation of JNK. *PLoS One* **4**, e7709, doi:10.1371/journal.pone.0007709 (2009).
- 139 Kockel, L., Homsy, J. G. & Bohmann, D. *Drosophila* AP-1: lessons from an invertebrate. *Oncogene* **20**, 2347-2364, doi:10.1038/sj.onc.1204300 (2001).
- 140 Johansson, K. C., Metzendorf, C. & Soderhall, K. Microarray analysis of immune challenged *Drosophila* hemocytes. *Experimental cell research* **305**, 145-155, doi:10.1016/j.yexcr.2004.12.018 (2005).
- 141 Martin-Blanco, E. *et al.* puckered encodes a phosphatase that mediates a feedback loop regulating JNK activity during dorsal closure in *Drosophila*. *Genes Dev* **12**, 557-570 (1998).
- 142 Martin-Blanco, E. Regulatory control of signal transduction during morphogenesis in *Drosophila*. *The International journal of developmental biology* **42**, 363-368 (1998).
- 143 Kallio, J. *et al.* Functional analysis of immune response genes in *Drosophila* identifies JNK pathway as a regulator of antimicrobial peptide gene expression in S2 cells. *Microbes and infection / Institut Pasteur* **7**, 811-819, doi:10.1016/j.micinf.2005.03.014 (2005).

- 144 Delaney, J. R. *et al.* Cooperative control of *Drosophila* immune responses by the JNK and NF-kappaB signaling pathways. *EMBO J* **25**, 3068-3077, doi:10.1038/sj.emboj.7601182 (2006).
- 145 Kim, T. *et al.* Downregulation of lipopolysaccharide response in *Drosophila* by negative crosstalk between the AP1 and NF-kappaB signaling modules. *Nature immunology* **6**, 211-218, doi:10.1038/ni1159 (2005).
- 146 Bond, D. & Foley, E. A quantitative RNAi screen for JNK modifiers identifies Pvr as a novel regulator of *Drosophila* immune signaling. *PLoS Pathog* **5**, e1000655, doi:10.1371/journal.ppat.1000655 (2009).
- 147 Thompson, C. B. Apoptosis in the pathogenesis and treatment of disease. *Science* **267**, 1456-1462 (1995).
- 148 Li, J. & Yuan, J. Caspases in apoptosis and beyond. *Oncogene* **27**, 6194-6206, doi:10.1038/onc.2008.297 (2008).
- 149 Hanahan, D. & Weinberg, R. A. The hallmarks of cancer. *Cell* **100**, 57-70 (2000).
- 150 Yuan, J., Shaham, S., Ledoux, S., Ellis, H. M. & Horvitz, H. R. The *C. elegans* cell death gene *ced-3* encodes a protein similar to mammalian interleukin-1 beta-converting enzyme. *Cell* **75**, 641-652 (1993).
- 151 Thornberry, N. A. & Lazebnik, Y. Caspases: enemies within. *Science* **281**, 1312-1316 (1998).
- 152 Cerretti, D. P. *et al.* Molecular cloning of the interleukin-1 beta converting enzyme. *Science* **256**, 97-100 (1992).
- 153 Thornberry, N. A. *et al.* A novel heterodimeric cysteine protease is required for interleukin-1 beta processing in monocytes. *Nature* **356**, 768-774, doi:10.1038/356768a0 (1992).
- 154 Yi, C. H. & Yuan, J. The Jekyll and Hyde functions of caspases. *Dev Cell* **16**, 21-34, doi:10.1016/j.devcel.2008.12.012 (2009).
- 155 Miura, M. Apoptotic and nonapoptotic caspase functions in animal development. *Cold Spring Harbor perspectives in biology* **4**, doi:10.1101/cshperspect.a008664 (2012).
- 156 Kuranaga, E. & Miura, M. Nonapoptotic functions of caspases: caspases as regulatory molecules for immunity and cell-fate determination. *Trends in cell biology* **17**, 135-144, doi:10.1016/j.tcb.2007.01.001 (2007).
- 157 Galluzzi, L., Kepp, O., Trojel-Hansen, C. & Kroemer, G. Non-apoptotic functions of apoptosis-regulatory proteins. *EMBO Rep* **13**, 322-330, doi:10.1038/embor.2012.19 (2012).
- 158 Earnshaw, W. C., Martins, L. M. & Kaufmann, S. H. Mammalian caspases: structure, activation, substrates, and functions during apoptosis. *Annual review of biochemistry* **68**, 383-424, doi:10.1146/annurev.biochem.68.1.383 (1999).
- 159 Fischer, U., Janicke, R. U. & Schulze-Osthoff, K. Many cuts to ruin: a comprehensive update of caspase substrates. *Cell death and differentiation* **10**, 76-100, doi:10.1038/sj.cdd.4401160 (2003).
- 160 Nicholson, D. W. Caspase structure, proteolytic substrates, and function during apoptotic cell death. *Cell death and differentiation* **6**, 1028-1042, doi:10.1038/sj.cdd.4400598 (1999).

- 161 Denault, J. B. & Salvesen, G. S. Caspases: keys in the ignition of cell death. *Chemical reviews* **102**, 4489-4500 (2002).
- 162 Cohen, G. M. Caspases: the executioners of apoptosis. *The Biochemical journal* **326 ( Pt 1)**, 1-16 (1997).
- 163 Nagata, S. Apoptotic DNA fragmentation. *Experimental cell research* **256**, 12-18, doi:10.1006/excr.2000.4834 (2000).
- 164 Eberstadt, M. *et al.* NMR structure and mutagenesis of the FADD (Mort1) death-effector domain. *Nature* **392**, 941-945, doi:10.1038/31972 (1998).
- 165 Tibbetts, M. D., Zheng, L. & Lenardo, M. J. The death effector domain protein family: regulators of cellular homeostasis. *Nature immunology* **4**, 404-409, doi:10.1038/ni0503-404 (2003).
- 166 Hofmann, K. The modular nature of apoptotic signaling proteins. *Cellular and molecular life sciences : CMLS* **55**, 1113-1128 (1999).
- 167 Hofmann, K., Bucher, P. & Tschopp, J. The CARD domain: a new apoptotic signalling motif. *Trends in biochemical sciences* **22**, 155-156 (1997).
- 168 Fesik, S. W. Insights into programmed cell death through structural biology. *Cell* **103**, 273-282 (2000).
- 169 Fuentes-Prior, P. & Salvesen, G. S. The protein structures that shape caspase activity, specificity, activation and inhibition. *The Biochemical journal* **384**, 201-232, doi:10.1042/BJ20041142 (2004).
- 170 Parrish, A. B., Freil, C. D. & Kornbluth, S. Cellular mechanisms controlling caspase activation and function. *Cold Spring Harbor perspectives in biology* **5**, doi:10.1101/cshperspect.a008672 (2013).
- 171 van Raam, B. J. & Salvesen, G. S. Proliferative versus apoptotic functions of caspase-8 Hetero or homo: the caspase-8 dimer controls cell fate. *Biochimica et biophysica acta* **1824**, 113-122, doi:10.1016/j.bbapap.2011.06.005 (2012).
- 172 Dorstyn, L., Colussi, P. A., Quinn, L. M., Richardson, H. & Kumar, S. DRONC, an ecdysone-inducible *Drosophila* caspase. *Proc Natl Acad Sci U S A* **96**, 4307-4312 (1999).
- 173 Fraser, A. G. & Evan, G. I. Identification of a *Drosophila melanogaster* ICE/CED-3-related protease, drICE. *EMBO J* **16**, 2805-2813, doi:10.1093/emboj/16.10.2805 (1997).
- 174 Song, Z., McCall, K. & Steller, H. DCP-1, a *Drosophila* cell death protease essential for development. *Science* **275**, 536-540 (1997).
- 175 Dorstyn, L., Read, S. H., Quinn, L. M., Richardson, H. & Kumar, S. DECAY, a novel *Drosophila* caspase related to mammalian caspase-3 and caspase-7. *J Biol Chem* **274**, 30778-30783 (1999).
- 176 Harvey, N. L. *et al.* Characterization of the *Drosophila* caspase, DAMM. *J Biol Chem* **276**, 25342-25350, doi:10.1074/jbc.M009444200 (2001).
- 177 Adrain, C. & Martin, S. J. Search for *Drosophila* caspases bears fruit: STRICA enters the fray. *Cell death and differentiation* **8**, 319-323, doi:10.1038/sj.cdd.4400869 (2001).
- 178 Doumanis, J., Quinn, L., Richardson, H. & Kumar, S. STRICA, a novel *Drosophila melanogaster* caspase with an unusual serine/threonine-rich prodomain, interacts with DIAP1 and DIAP2. *Cell death and differentiation* **8**, 387-394, doi:10.1038/sj.cdd.4400864 (2001).

- 179 Chai, J. *et al.* Crystal structure of a procaspase-7 zymogen: mechanisms of activation and substrate binding. *Cell* **107**, 399-407 (2001).
- 180 Riedl, S. J. *et al.* Structural basis for the activation of human procaspase-7. *Proc Natl Acad Sci U S A* **98**, 14790-14795, doi:10.1073/pnas.221580098 (2001).
- 181 Shi, Y. Mechanisms of caspase activation and inhibition during apoptosis. *Mol Cell* **9**, 459-470 (2002).
- 182 Srinivasula, S. M. *et al.* Generation of constitutively active recombinant caspases-3 and -6 by rearrangement of their subunits. *J Biol Chem* **273**, 10107-10111 (1998).
- 183 Martin, S. J. *et al.* The cytotoxic cell protease granzyme B initiates apoptosis in a cell-free system by proteolytic processing and activation of the ICE/CED-3 family protease, CPP32, via a novel two-step mechanism. *EMBO J* **15**, 2407-2416 (1996).
- 184 Pop, C. & Salvesen, G. S. Human caspases: activation, specificity, and regulation. *J Biol Chem* **284**, 21777-21781, doi:10.1074/jbc.R800084200 (2009).
- 185 Tinel, A. & Tschopp, J. The PIDDosome, a protein complex implicated in activation of caspase-2 in response to genotoxic stress. *Science* **304**, 843-846, doi:10.1126/science.1095432 (2004).
- 186 Acehan, D. *et al.* Three-dimensional structure of the apoptosome: implications for assembly, procaspase-9 binding, and activation. *Mol Cell* **9**, 423-432 (2002).
- 187 Medema, J. P. *et al.* FLICE is activated by association with the CD95 death-inducing signaling complex (DISC). *EMBO J* **16**, 2794-2804, doi:10.1093/emboj/16.10.2794 (1997).
- 188 Mace, P. D. & Riedl, S. J. Molecular cell death platforms and assemblies. *Current opinion in cell biology* **22**, 828-836, doi:10.1016/j.ceb.2010.08.004 (2010).
- 189 Park, H. H. *et al.* Death domain assembly mechanism revealed by crystal structure of the oligomeric PIDDosome core complex. *Cell* **128**, 533-546, doi:10.1016/j.cell.2007.01.019 (2007).
- 190 Donepudi, M. & Grutter, M. G. Structure and zymogen activation of caspases. *Biophysical chemistry* **101-102**, 145-153 (2002).
- 191 MacKenzie, S. H. & Clark, A. C. Death by caspase dimerization. *Advances in experimental medicine and biology* **747**, 55-73, doi:10.1007/978-1-4614-3229-6\_4 (2012).
- 192 Boatright, K. M. *et al.* A unified model for apical caspase activation. *Mol Cell* **11**, 529-541 (2003).
- 193 Pop, C., Timmer, J., Sperandio, S. & Salvesen, G. S. The apoptosome activates caspase-9 by dimerization. *Mol Cell* **22**, 269-275, doi:10.1016/j.molcel.2006.03.009 (2006).
- 194 Keller, N., Mares, J., Zerbe, O. & Grutter, M. G. Structural and biochemical studies on procaspase-8: new insights on initiator caspase activation. *Structure* **17**, 438-448, doi:10.1016/j.str.2008.12.019 (2009).
- 195 Oberst, A. *et al.* Inducible dimerization and inducible cleavage reveal a requirement for both processes in caspase-8 activation. *J Biol Chem* **285**, 16632-16642, doi:10.1074/jbc.M109.095083 (2010).

- 196 Keller, N., Grutter, M. G. & Zerbe, O. Studies of the molecular mechanism of caspase-8 activation by solution NMR. *Cell death and differentiation* **17**, 710-718, doi:10.1038/cdd.2009.155 (2010).
- 197 Chang, H. Y. & Yang, X. Proteases for cell suicide: functions and regulation of caspases. *Microbiology and molecular biology reviews : MMBR* **64**, 821-846 (2000).
- 198 Pop, C., Fitzgerald, P., Green, D. R. & Salvesen, G. S. Role of proteolysis in caspase-8 activation and stabilization. *Biochemistry* **46**, 4398-4407, doi:10.1021/bi602623b (2007).
- 199 Chang, D. W., Xing, Z., Capacio, V. L., Peter, M. E. & Yang, X. Interdimer processing mechanism of procaspase-8 activation. *EMBO J* **22**, 4132-4142, doi:10.1093/emboj/cdg414 (2003).
- 200 Chao, Y. *et al.* Engineering a dimeric caspase-9: a re-evaluation of the induced proximity model for caspase activation. *PLoS biology* **3**, e183, doi:10.1371/journal.pbio.0030183 (2005).
- 201 Yuan, S. *et al.* Structure of an apoptosome-procaspase-9 CARD complex. *Structure* **18**, 571-583, doi:10.1016/j.str.2010.04.001 (2010).
- 202 Stennicke, H. R. *et al.* Caspase-9 can be activated without proteolytic processing. *J Biol Chem* **274**, 8359-8362 (1999).
- 203 Dorstyn, L. & Kumar, S. A biochemical analysis of the activation of the Drosophila caspase DRONC. *Cell death and differentiation* **15**, 461-470, doi:10.1038/sj.cdd.4402288 (2008).
- 204 Snipas, S. J., Drag, M., Stennicke, H. R. & Salvesen, G. S. Activation mechanism and substrate specificity of the Drosophila initiator caspase DRONC. *Cell death and differentiation* **15**, 938-945, doi:10.1038/cdd.2008.23 (2008).
- 205 Timmer, J. C. & Salvesen, G. S. Caspase substrates. *Cell death and differentiation* **14**, 66-72, doi:10.1038/sj.cdd.4402059 (2007).
- 206 Kerr, J. F., Wyllie, A. H. & Currie, A. R. Apoptosis: a basic biological phenomenon with wide-ranging implications in tissue kinetics. *British journal of cancer* **26**, 239-257 (1972).
- 207 Taylor, R. C., Cullen, S. P. & Martin, S. J. Apoptosis: controlled demolition at the cellular level. *Nature reviews. Molecular cell biology* **9**, 231-241, doi:10.1038/nrm2312 (2008).
- 208 Callus, B. A. & Vaux, D. L. Caspase inhibitors: viral, cellular and chemical. *Cell death and differentiation* **14**, 73-78, doi:10.1038/sj.cdd.4402034 (2007).
- 209 Renatus, M. *et al.* Crystal structure of the apoptotic suppressor CrmA in its cleaved form. *Structure* **8**, 789-797 (2000).
- 210 Zhou, Q. *et al.* Target protease specificity of the viral serpin CrmA. Analysis of five caspases. *J Biol Chem* **272**, 7797-7800 (1997).
- 211 Zhou, Q. & Salvesen, G. S. Viral caspase inhibitors CrmA and p35. *Methods in enzymology* **322**, 143-154 (2000).
- 212 Annand, R. R. *et al.* Caspase-1 (interleukin-1beta-converting enzyme) is inhibited by the human serpin analogue proteinase inhibitor 9. *The Biochemical journal* **342 Pt 3**, 655-665 (1999).

- 213 Komiyama, T. *et al.* Inhibition of interleukin-1 beta converting enzyme by the cowpox virus serpin CrmA. An example of cross-class inhibition. *J Biol Chem* **269**, 19331-19337 (1994).
- 214 Xu, G. *et al.* Covalent inhibition revealed by the crystal structure of the caspase-8/p35 complex. *Nature* **410**, 494-497, doi:10.1038/35068604 (2001).
- 215 Riedl, S. J., Renatus, M., Snipas, S. J. & Salvesen, G. S. Mechanism-based inactivation of caspases by the apoptotic suppressor p35. *Biochemistry* **40**, 13274-13280 (2001).
- 216 Fisher, A. J., Cruz, W., Zoog, S. J., Schneider, C. L. & Friesen, P. D. Crystal structure of baculovirus P35: role of a novel reactive site loop in apoptotic caspase inhibition. *EMBO J* **18**, 2031-2039, doi:10.1093/emboj/18.8.2031 (1999).
- 217 Stennicke, H. R. & Salvesen, G. S. Properties of the caspases. *Biochimica et biophysica acta* **1387**, 17-31 (1998).
- 218 Wilson, K. P. *et al.* Structure and mechanism of interleukin-1 beta converting enzyme. *Nature* **370**, 270-275, doi:10.1038/370270a0 (1994).
- 219 Walsh, C. T. Suicide substrates, mechanism-based enzyme inactivators: recent developments. *Annual review of biochemistry* **53**, 493-535, doi:10.1146/annurev.bi.53.070184.002425 (1984).
- 220 Clem, R. J., Fechheimer, M. & Miller, L. K. Prevention of apoptosis by a baculovirus gene during infection of insect cells. *Science* **254**, 1388-1390 (1991).
- 221 Zhou, Q. *et al.* Interaction of the baculovirus anti-apoptotic protein p35 with caspases. Specificity, kinetics, and characterization of the caspase/p35 complex. *Biochemistry* **37**, 10757-10765, doi:10.1021/bi980893w (1998).
- 222 Bertin, J. *et al.* Apoptotic suppression by baculovirus P35 involves cleavage by and inhibition of a virus-induced CED-3/ICE-like protease. *Journal of virology* **70**, 6251-6259 (1996).
- 223 Bump, N. J. *et al.* Inhibition of ICE family proteases by baculovirus antiapoptotic protein p35. *Science* **269**, 1885-1888 (1995).
- 224 dela Cruz, W. P., Friesen, P. D. & Fisher, A. J. Crystal structure of baculovirus P35 reveals a novel conformational change in the reactive site loop after caspase cleavage. *J Biol Chem* **276**, 32933-32939, doi:10.1074/jbc.M103930200 (2001).
- 225 Garcia-Calvo, M. *et al.* Inhibition of human caspases by peptide-based and macromolecular inhibitors. *J Biol Chem* **273**, 32608-32613 (1998).
- 226 Nicholson, D. W. From bench to clinic with apoptosis-based therapeutic agents. *Nature* **407**, 810-816, doi:10.1038/35037747 (2000).
- 227 Hay, B. A., Wassarman, D. A. & Rubin, G. M. Drosophila homologs of baculovirus inhibitor of apoptosis proteins function to block cell death. *Cell* **83**, 1253-1262 (1995).
- 228 Duckett, C. S. *et al.* A conserved family of cellular genes related to the baculovirus iap gene and encoding apoptosis inhibitors. *EMBO J* **15**, 2685-2694 (1996).

- 229 Rothe, M., Pan, M. G., Henzel, W. J., Ayres, T. M. & Goeddel, D. V. The TNFR2-TRAF signaling complex contains two novel proteins related to baculoviral inhibitor of apoptosis proteins. *Cell* **83**, 1243-1252 (1995).
- 230 Crook, N. E., Clem, R. J. & Miller, L. K. An apoptosis-inhibiting baculovirus gene with a zinc finger-like motif. *Journal of virology* **67**, 2168-2174 (1993).
- 231 Roy, N., Deveraux, Q. L., Takahashi, R., Salvesen, G. S. & Reed, J. C. The c-IAP-1 and c-IAP-2 proteins are direct inhibitors of specific caspases. *EMBO J* **16**, 6914-6925, doi:10.1093/emboj/16.23.6914 (1997).
- 232 Birnbaum, M. J., Clem, R. J. & Miller, L. K. An apoptosis-inhibiting gene from a nuclear polyhedrosis virus encoding a polypeptide with Cys/His sequence motifs. *Journal of virology* **68**, 2521-2528 (1994).
- 233 Deshaies, R. J. & Joazeiro, C. A. RING domain E3 ubiquitin ligases. *Annual review of biochemistry* **78**, 399-434, doi:10.1146/annurev.biochem.78.101807.093809 (2009).
- 234 Hinds, M. G., Norton, R. S., Vaux, D. L. & Day, C. L. Solution structure of a baculoviral inhibitor of apoptosis (IAP) repeat. *Nature structural biology* **6**, 648-651, doi:10.1038/10701 (1999).
- 235 Blankenship, J. W. *et al.* Ubiquitin binding modulates IAP antagonist-stimulated proteasomal degradation of c-IAP1 and c-IAP2(1). *The Biochemical journal* **417**, 149-160, doi:10.1042/BJ20081885 (2009).
- 236 Vaux, D. L. & Silke, J. IAPs, RINGs and ubiquitylation. *Nature reviews. Molecular cell biology* **6**, 287-297, doi:10.1038/nrm1621 (2005).
- 237 Gyrd-Hansen, M. *et al.* IAPs contain an evolutionarily conserved ubiquitin-binding domain that regulates NF-kappaB as well as cell survival and oncogenesis. *Nat Cell Biol* **10**, 1309-1317, doi:10.1038/ncb1789 (2008).
- 238 Husnjak, K. & Dikic, I. Ubiquitin-binding proteins: decoders of ubiquitin-mediated cellular functions. *Annual review of biochemistry* **81**, 291-322, doi:10.1146/annurev-biochem-051810-094654 (2012).
- 239 Silke, J. *et al.* Determination of cell survival by RING-mediated regulation of inhibitor of apoptosis (IAP) protein abundance. *Proc Natl Acad Sci U S A* **102**, 16182-16187, doi:10.1073/pnas.0502828102 (2005).
- 240 Suzuki, Y., Nakabayashi, Y. & Takahashi, R. Ubiquitin-protein ligase activity of X-linked inhibitor of apoptosis protein promotes proteasomal degradation of caspase-3 and enhances its anti-apoptotic effect in Fas-induced cell death. *Proc Natl Acad Sci U S A* **98**, 8662-8667, doi:10.1073/pnas.161506698 (2001).
- 241 Morizane, Y., Honda, R., Fukami, K. & Yasuda, H. X-linked inhibitor of apoptosis functions as ubiquitin ligase toward mature caspase-9 and cytosolic Smac/DIABLO. *Journal of biochemistry* **137**, 125-132, doi:10.1093/jb/mvi029 (2005).
- 242 Hershko, A. & Ciechanover, A. The ubiquitin system. *Annual review of biochemistry* **67**, 425-479, doi:10.1146/annurev.biochem.67.1.425 (1998).
- 243 Hochstrasser, M. Ubiquitin-dependent protein degradation. *Annual review of genetics* **30**, 405-439, doi:10.1146/annurev.genet.30.1.405 (1996).
- 244 Hershko, A., Heller, H., Elias, S. & Ciechanover, A. Components of ubiquitin-protein ligase system. Resolution, affinity purification, and role in protein breakdown. *J Biol Chem* **258**, 8206-8214 (1983).

- 245 Pickart, C. M. Mechanisms underlying ubiquitination. *Annual review of biochemistry* **70**, 503-533, doi:10.1146/annurev.biochem.70.1.503 (2001).
- 246 Chau, V. *et al.* A multiubiquitin chain is confined to specific lysine in a targeted short-lived protein. *Science* **243**, 1576-1583 (1989).
- 247 Spence, J. *et al.* Cell cycle-regulated modification of the ribosome by a variant multiubiquitin chain. *Cell* **102**, 67-76 (2000).
- 248 Spence, J., Sadis, S., Haas, A. L. & Finley, D. A ubiquitin mutant with specific defects in DNA repair and multiubiquitination. *Molecular and cellular biology* **15**, 1265-1273 (1995).
- 249 Hofmann, R. M. & Pickart, C. M. Noncanonical MMS2-encoded ubiquitin-conjugating enzyme functions in assembly of novel polyubiquitin chains for DNA repair. *Cell* **96**, 645-653 (1999).
- 250 Koepp, D. M., Harper, J. W. & Elledge, S. J. How the cyclin became a cyclin: regulated proteolysis in the cell cycle. *Cell* **97**, 431-434 (1999).
- 251 Ghosh, S., May, M. J. & Kopp, E. B. NF-kappa B and Rel proteins: evolutionarily conserved mediators of immune responses. *Annual review of immunology* **16**, 225-260, doi:10.1146/annurev.immunol.16.1.225 (1998).
- 252 Rock, K. L. & Goldberg, A. L. Degradation of cell proteins and the generation of MHC class I-presented peptides. *Annual review of immunology* **17**, 739-779, doi:10.1146/annurev.immunol.17.1.739 (1999).
- 253 Deng, L. *et al.* Activation of the IkkappaB kinase complex by TRAF6 requires a dimeric ubiquitin-conjugating enzyme complex and a unique polyubiquitin chain. *Cell* **103**, 351-361 (2000).
- 254 Salvesen, G. S. & Duckett, C. S. IAP proteins: blocking the road to death's door. *Nature reviews. Molecular cell biology* **3**, 401-410, doi:10.1038/nrm830 (2002).
- 255 Tenev, T., Zachariou, A., Wilson, R., Ditzel, M. & Meier, P. IAPs are functionally non-equivalent and regulate effector caspases through distinct mechanisms. *Nat Cell Biol* **7**, 70-77, doi:10.1038/ncb1204 (2005).
- 256 Wei, Y., Fan, T. & Yu, M. Inhibitor of apoptosis proteins and apoptosis. *Acta biochimica et biophysica Sinica* **40**, 278-288 (2008).
- 257 Meier, P., Silke, J., Leever, S. J. & Evan, G. I. The Drosophila caspase DRONC is regulated by DIAP1. *EMBO J* **19**, 598-611, doi:10.1093/emboj/19.4.598 (2000).
- 258 Riedl, S. J. & Shi, Y. Molecular mechanisms of caspase regulation during apoptosis. *Nature reviews. Molecular cell biology* **5**, 897-907, doi:10.1038/nrm1496 (2004).
- 259 Xu, D. *et al.* Genetic control of programmed cell death (apoptosis) in Drosophila. *Fly* **3**, 78-90 (2009).
- 260 Deveraux, Q. L., Takahashi, R., Salvesen, G. S. & Reed, J. C. X-linked IAP is a direct inhibitor of cell-death proteases. *Nature* **388**, 300-304, doi:10.1038/40901 (1997).
- 261 Deveraux, Q. L. *et al.* IAPs block apoptotic events induced by caspase-8 and cytochrome c by direct inhibition of distinct caspases. *EMBO J* **17**, 2215-2223, doi:10.1093/emboj/17.8.2215 (1998).
- 262 Chai, J. *et al.* Structural basis of caspase-7 inhibition by XIAP. *Cell* **104**, 769-780 (2001).

- 263 Wilson, R. *et al.* The DIAP1 RING finger mediates ubiquitination of Dronc and is indispensable for regulating apoptosis. *Nat Cell Biol* **4**, 445-450, doi:10.1038/ncb799 (2002).
- 264 Hawkins, C. J. *et al.* The Drosophila caspase DRONC cleaves following glutamate or aspartate and is regulated by DIAP1, HID, and GRIM. *J Biol Chem* **275**, 27084-27093, doi:10.1074/jbc.M000869200 (2000).
- 265 Hawkins, C. J., Wang, S. L. & Hay, B. A. A cloning method to identify caspases and their regulators in yeast: identification of Drosophila IAP1 as an inhibitor of the Drosophila caspase DCP-1. *Proc Natl Acad Sci U S A* **96**, 2885-2890 (1999).
- 266 Gyrd-Hansen, M. & Meier, P. IAPs: from caspase inhibitors to modulators of NF-kappaB, inflammation and cancer. *Nature reviews. Cancer* **10**, 561-574, doi:10.1038/nrc2889 (2010).
- 267 Ribeiro, P. S. *et al.* DIAP2 functions as a mechanism-based regulator of drICE that contributes to the caspase activity threshold in living cells. *The Journal of cell biology* **179**, 1467-1480, doi:10.1083/jcb.200706027 (2007).
- 268 Leulier, F. *et al.* Systematic in vivo RNAi analysis of putative components of the Drosophila cell death machinery. *Cell death and differentiation* **13**, 1663-1674, doi:10.1038/sj.cdd.4401868 (2006).
- 269 Wang, S. L., Hawkins, C. J., Yoo, S. J., Muller, H. A. & Hay, B. A. The Drosophila caspase inhibitor DIAP1 is essential for cell survival and is negatively regulated by HID. *Cell* **98**, 453-463 (1999).
- 270 Lisi, S., Mazzon, I. & White, K. Diverse domains of THREAD/DIAP1 are required to inhibit apoptosis induced by REAPER and HID in Drosophila. *Genetics* **154**, 669-678 (2000).
- 271 Goyal, L., McCall, K., Agapite, J., Hartwig, E. & Steller, H. Induction of apoptosis by Drosophila reaper, hid and grim through inhibition of IAP function. *EMBO J* **19**, 589-597, doi:10.1093/emboj/19.4.589 (2000).
- 272 Valanne, S., Kleino, A., Myllymaki, H., Vuoristo, J. & Ramet, M. *lap2* is required for a sustained response in the Drosophila Imd pathway. *Developmental and comparative immunology* **31**, 991-1001, doi:10.1016/j.dci.2007.01.004 (2007).
- 273 Meinander, A. *et al.* Ubiquitylation of the initiator caspase DREDD is required for innate immune signalling. *EMBO J* **31**, 2770-2783, doi:10.1038/emboj.2012.121 (2012).
- 274 Grutter, M. G. Caspases: key players in programmed cell death. *Current opinion in structural biology* **10**, 649-655 (2000).
- 275 Chowdhury, I., Tharakan, B. & Bhat, G. K. Current concepts in apoptosis: the physiological suicide program revisited. *Cellular & molecular biology letters* **11**, 506-525, doi:10.2478/s11658-006-0041-3 (2006).
- 276 Varfolomeev, E. E. *et al.* Targeted disruption of the mouse Caspase 8 gene ablates cell death induction by the TNF receptors, Fas/Apo1, and DR3 and is lethal prenatally. *Immunity* **9**, 267-276 (1998).
- 277 Kroemer, G., Galluzzi, L. & Brenner, C. Mitochondrial membrane permeabilization in cell death. *Physiological reviews* **87**, 99-163, doi:10.1152/physrev.00013.2006 (2007).

- 278 Tait, S. W. & Green, D. R. Mitochondria and cell death: outer membrane permeabilization and beyond. *Nature reviews. Molecular cell biology* **11**, 621-632, doi:10.1038/nrm2952 (2010).
- 279 Riedl, S. J. & Salvesen, G. S. The apoptosome: signalling platform of cell death. *Nature reviews. Molecular cell biology* **8**, 405-413, doi:10.1038/nrm2153 (2007).
- 280 Li, P. *et al.* Cytochrome c and dATP-dependent formation of Apaf-1/caspase-9 complex initiates an apoptotic protease cascade. *Cell* **91**, 479-489 (1997).
- 281 Hill, M. M., Adrain, C. & Martin, S. J. Portrait of a killer: the mitochondrial apoptosome emerges from the shadows. *Molecular interventions* **3**, 19-26, doi:10.1124/mi.3.1.19 (2003).
- 282 Cullen, S. P. & Martin, S. J. Caspase activation pathways: some recent progress. *Cell death and differentiation* **16**, 935-938, doi:10.1038/cdd.2009.59 (2009).
- 283 White, K., Tahaoglu, E. & Steller, H. Cell killing by the Drosophila gene reaper. *Science* **271**, 805-807 (1996).
- 284 Chen, P., Lee, P., Otto, L. & Abrams, J. Apoptotic activity of REAPER is distinct from signaling by the tumor necrosis factor receptor 1 death domain. *J Biol Chem* **271**, 25735-25737 (1996).
- 285 Abbott, M. K. & Lengyel, J. A. Embryonic head involution and rotation of male terminalia require the Drosophila locus head involution defective. *Genetics* **129**, 783-789 (1991).
- 286 Grether, M. E., Abrams, J. M., Agapite, J., White, K. & Steller, H. The head involution defective gene of Drosophila melanogaster functions in programmed cell death. *Genes Dev* **9**, 1694-1708 (1995).
- 287 White, K. *et al.* Genetic control of programmed cell death in Drosophila. *Science* **264**, 677-683 (1994).
- 288 Nordstrom, W., Chen, P., Steller, H. & Abrams, J. M. Activation of the reaper gene during ectopic cell killing in Drosophila. *Developmental biology* **180**, 213-226, doi:10.1006/dbio.1996.0296 (1996).
- 289 Lohmann, I., McGinnis, N., Bodmer, M. & McGinnis, W. The Drosophila Hox gene deformed sculpts head morphology via direct regulation of the apoptosis activator reaper. *Cell* **110**, 457-466 (2002).
- 290 Jiang, C., Lamblin, A. F., Steller, H. & Thummel, C. S. A steroid-triggered transcriptional hierarchy controls salivary gland cell death during Drosophila metamorphosis. *Mol Cell* **5**, 445-455 (2000).
- 291 Ryoo, H. D., Bergmann, A., Gonen, H., Ciechanover, A. & Steller, H. Regulation of Drosophila IAP1 degradation and apoptosis by reaper and ubcD1. *Nat Cell Biol* **4**, 432-438, doi:10.1038/ncb795 (2002).
- 292 Yoo, S. J. Grim stimulates Diap1 poly-ubiquitination by binding to UbcD1. *Molecules and cells* **20**, 446-451 (2005).
- 293 Yoo, S. J. *et al.* Hid, Rpr and Grim negatively regulate DIAP1 levels through distinct mechanisms. *Nat Cell Biol* **4**, 416-424, doi:10.1038/ncb793 (2002).
- 294 Olson, M. R. *et al.* Reaper is regulated by IAP-mediated ubiquitination. *J Biol Chem* **278**, 4028-4034, doi:10.1074/jbc.M209734200 (2003).

- 295 Eckhart, L. *et al.* Terminal differentiation of human keratinocytes and stratum corneum formation is associated with caspase-14 activation. *The Journal of investigative dermatology* **115**, 1148-1151, doi:10.1046/j.1523-1747.2000.00205.x (2000).
- 296 Saleh, M. *et al.* Enhanced bacterial clearance and sepsis resistance in caspase-12-deficient mice. *Nature* **440**, 1064-1068, doi:10.1038/nature04656 (2006).
- 297 Saleh, M. *et al.* Differential modulation of endotoxin responsiveness by human caspase-12 polymorphisms. *Nature* **429**, 75-79, doi:10.1038/nature02451 (2004).
- 298 Wang, S. *et al.* Murine caspase-11, an ICE-interacting protease, is essential for the activation of ICE. *Cell* **92**, 501-509 (1998).
- 299 Santambrogio, L. *et al.* Involvement of caspase-cleaved and intact adaptor protein 1 complex in endosomal remodeling in maturing dendritic cells. *Nature immunology* **6**, 1020-1028, doi:10.1038/ni1250 (2005).
- 300 Kang, T. B. *et al.* Caspase-8 serves both apoptotic and nonapoptotic roles. *Journal of immunology* **173**, 2976-2984 (2004).
- 301 Sordet, O. *et al.* Specific involvement of caspases in the differentiation of monocytes into macrophages. *Blood* **100**, 4446-4453, doi:10.1182/blood-2002-06-1778 (2002).
- 302 Chaudhary, P. M. *et al.* Activation of the NF-kappaB pathway by caspase 8 and its homologs. *Oncogene* **19**, 4451-4460, doi:10.1038/sj.onc.1203812 (2000).
- 303 Jun, J. I. *et al.* Role of FLASH in caspase-8-mediated activation of NF-kappaB: dominant-negative function of FLASH mutant in NF-kappaB signaling pathway. *Oncogene* **24**, 688-696, doi:10.1038/sj.onc.1208186 (2005).
- 304 Su, H. *et al.* Requirement for caspase-8 in NF-kappaB activation by antigen receptor. *Science* **307**, 1465-1468, doi:10.1126/science.1104765 (2005).
- 305 Beisner, D. R., Ch'en, I. L., Kolla, R. V., Hoffmann, A. & Hedrick, S. M. Cutting edge: innate immunity conferred by B cells is regulated by caspase-8. *Journal of immunology* **175**, 3469-3473 (2005).
- 306 Chun, H. J. *et al.* Pleiotropic defects in lymphocyte activation caused by caspase-8 mutations lead to human immunodeficiency. *Nature* **419**, 395-399, doi:10.1038/nature01063 (2002).
- 307 Salmena, L. *et al.* Essential role for caspase 8 in T-cell homeostasis and T-cell-mediated immunity. *Genes Dev* **17**, 883-895, doi:10.1101/gad.1063703 (2003).
- 308 Martinon, F., Burns, K. & Tschopp, J. The inflammasome: a molecular platform triggering activation of inflammatory caspases and processing of proIL-beta. *Mol Cell* **10**, 417-426 (2002).
- 309 Zandy, A. J., Lakhani, S., Zheng, T., Flavell, R. A. & Bassnett, S. Role of the executioner caspases during lens development. *J Biol Chem* **280**, 30263-30272, doi:10.1074/jbc.M504007200 (2005).
- 310 Ghayur, T. *et al.* Caspase-1 processes IFN-gamma-inducing factor and regulates LPS-induced IFN-gamma production. *Nature* **386**, 619-623, doi:10.1038/386619a0 (1997).

- 311 Lamkanfi, M., Kalai, M., Saelens, X., Declercq, W. & Vandenabeele, P. Caspase-1 activates nuclear factor of the kappa-enhancer in B cells independently of its enzymatic activity. *J Biol Chem* **279**, 24785-24793, doi:10.1074/jbc.M400985200 (2004).
- 312 Lamkanfi, M. *et al.* A novel caspase-2 complex containing TRAF2 and RIP1. *J Biol Chem* **280**, 6923-6932, doi:10.1074/jbc.M411180200 (2005).
- 313 Zhivotovsky, B. & Orrenius, S. Caspase-2 function in response to DNA damage. *Biochemical and biophysical research communications* **331**, 859-867, doi:10.1016/j.bbrc.2005.03.191 (2005).
- 314 Yan, X. X. *et al.* Expression of active caspase-3 in mitotic and postmitotic cells of the rat forebrain. *The Journal of comparative neurology* **433**, 4-22 (2001).
- 315 Okuyama, R. *et al.* High commitment of embryonic keratinocytes to terminal differentiation through a Notch1-caspase 3 regulatory mechanism. *Dev Cell* **6**, 551-562 (2004).
- 316 Miura, M. *et al.* A crucial role of caspase-3 in osteogenic differentiation of bone marrow stromal stem cells. *The Journal of clinical investigation* **114**, 1704-1713, doi:10.1172/JCI20427 (2004).
- 317 Lippens, S. *et al.* Epidermal differentiation does not involve the pro-apoptotic executioner caspases, but is associated with caspase-14 induction and processing. *Cell death and differentiation* **7**, 1218-1224, doi:10.1038/sj.cdd.4400785 (2000).
- 318 Kondo, S., Senoo-Matsuda, N., Hiromi, Y. & Miura, M. DRONC coordinates cell death and compensatory proliferation. *Molecular and cellular biology* **26**, 7258-7268, doi:10.1128/MCB.00183-06 (2006).
- 319 Huh, J. R., Guo, M. & Hay, B. A. Compensatory proliferation induced by cell death in the Drosophila wing disc requires activity of the apical cell death caspase Dronc in a nonapoptotic role. *Curr Biol* **14**, 1262-1266, doi:10.1016/j.cub.2004.06.015 (2004).
- 320 Wells, B. S., Yoshida, E. & Johnston, L. A. Compensatory proliferation in Drosophila imaginal discs requires Dronc-dependent p53 activity. *Curr Biol* **16**, 1606-1615, doi:10.1016/j.cub.2006.07.046 (2006).
- 321 Muro, I. *et al.* The Drosophila caspase Ice is important for many apoptotic cell deaths and for spermatid individualization, a nonapoptotic process. *Development* **133**, 3305-3315, doi:10.1242/dev.02495 (2006).
- 322 Geisbrecht, E. R. & Montell, D. J. A role for Drosophila IAP1-mediated caspase inhibition in Rac-dependent cell migration. *Cell* **118**, 111-125, doi:10.1016/j.cell.2004.06.020 (2004).
- 323 Fan, Y. & Bergmann, A. Distinct mechanisms of apoptosis-induced compensatory proliferation in proliferating and differentiating tissues in the Drosophila eye. *Dev Cell* **14**, 399-410, doi:10.1016/j.devcel.2008.01.003 (2008).
- 324 Arama, E., Agapite, J. & Steller, H. Caspase activity and a specific cytochrome C are required for sperm differentiation in Drosophila. *Dev Cell* **4**, 687-697 (2003).
- 325 Kanuka, H. *et al.* Drosophila caspase transduces Shaggy/GSK-3beta kinase activity in neural precursor development. *EMBO J* **24**, 3793-3806, doi:10.1038/sj.emboj.7600822 (2005).

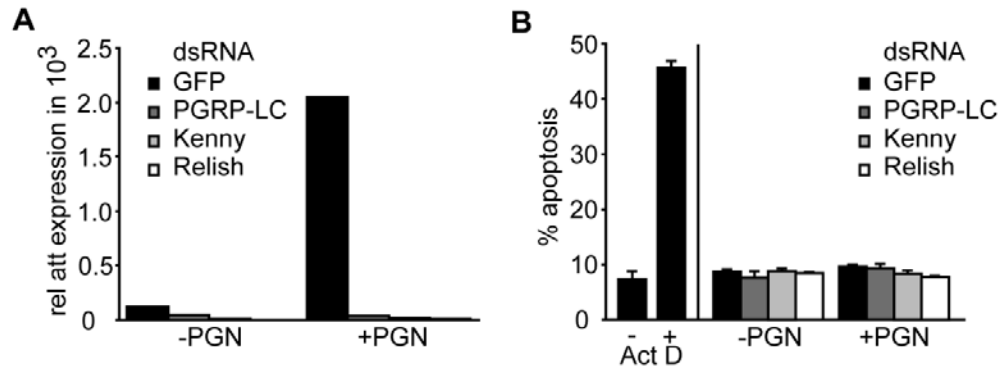
- 326 Foley, E. & O'Farrell, P. H. Functional dissection of an innate immune response by a genome-wide RNAi screen. *PLoS biology* **2**, E203, doi:10.1371/journal.pbio.0020203 (2004).
- 327 Maelfait, J. & Beyaert, R. Non-apoptotic functions of caspase-8. *Biochem Pharmacol* **76**, 1365-1373, doi:10.1016/j.bcp.2008.07.034 (2008).
- 328 Muzio, M. *et al.* FLICE, a novel FADD-homologous ICE/CED-3-like protease, is recruited to the CD95 (Fas/APO-1) death--inducing signaling complex. *Cell* **85**, 817-827 (1996).
- 329 Boldin, M. P., Goncharov, T. M., Goltsev, Y. V. & Wallach, D. Involvement of MACH, a novel MORT1/FADD-interacting protease, in Fas/APO-1- and TNF receptor-induced cell death. *Cell* **85**, 803-815 (1996).
- 330 Juo, P., Kuo, C. J., Yuan, J. & Blenis, J. Essential requirement for caspase-8/FLICE in the initiation of the Fas-induced apoptotic cascade. *Curr Biol* **8**, 1001-1008 (1998).
- 331 Los, M., Wesselborg, S. & Schulze-Osthoff, K. The role of caspases in development, immunity, and apoptotic signal transduction: lessons from knockout mice. *Immunity* **10**, 629-639 (1999).
- 332 Boatright, K. M. & Salvesen, G. S. Mechanisms of caspase activation. *Current opinion in cell biology* **15**, 725-731 (2003).
- 333 Li, H., Zhu, H., Xu, C. J. & Yuan, J. Cleavage of BID by caspase 8 mediates the mitochondrial damage in the Fas pathway of apoptosis. *Cell* **94**, 491-501 (1998).
- 334 Luo, X., Budihardjo, I., Zou, H., Slaughter, C. & Wang, X. Bid, a Bcl2 interacting protein, mediates cytochrome c release from mitochondria in response to activation of cell surface death receptors. *Cell* **94**, 481-490 (1998).
- 335 Chou, J. J., Li, H., Salvesen, G. S., Yuan, J. & Wagner, G. Solution structure of BID, an intracellular amplifier of apoptotic signaling. *Cell* **96**, 615-624 (1999).
- 336 Yin, X. M. *et al.* Bid-deficient mice are resistant to Fas-induced hepatocellular apoptosis. *Nature* **400**, 886-891, doi:10.1038/23730 (1999).
- 337 Brenner, C. & Grimm, S. The permeability transition pore complex in cancer cell death. *Oncogene* **25**, 4744-4756, doi:10.1038/sj.onc.1209609 (2006).
- 338 Inoue, S., Browne, G., Melino, G. & Cohen, G. M. Ordering of caspases in cells undergoing apoptosis by the intrinsic pathway. *Cell death and differentiation* **16**, 1053-1061, doi:10.1038/cdd.2009.29 (2009).
- 339 Slee, E. A. *et al.* Ordering the cytochrome c-initiated caspase cascade: hierarchical activation of caspases-2, -3, -6, -7, -8, and -10 in a caspase-9-dependent manner. *The Journal of cell biology* **144**, 281-292 (1999).
- 340 Sakamaki, K. *et al.* Ex vivo whole-embryo culture of caspase-8-deficient embryos normalize their aberrant phenotypes in the developing neural tube and heart. *Cell death and differentiation* **9**, 1196-1206, doi:10.1038/sj.cdd.4401090 (2002).
- 341 Lemmers, B. *et al.* Essential role for caspase-8 in Toll-like receptors and NFkappaB signaling. *J Biol Chem* **282**, 7416-7423, doi:10.1074/jbc.M606721200 (2007).

- 342 Ben Moshe, T. *et al.* Role of caspase-8 in hepatocyte response to infection and injury in mice. *Hepatology* **45**, 1014-1024, doi:10.1002/hep.21495 (2007).
- 343 Mielgo, A. *et al.* The death effector domains of caspase-8 induce terminal differentiation. *PLoS One* **4**, e7879, doi:10.1371/journal.pone.0007879 (2009).
- 344 Kreuz, S. *et al.* NFkappaB activation by Fas is mediated through FADD, caspase-8, and RIP and is inhibited by FLIP. *The Journal of cell biology* **166**, 369-380, doi:10.1083/jcb.200401036 (2004).
- 345 Shikama, Y., Yamada, M. & Miyashita, T. Caspase-8 and caspase-10 activate NF-kappaB through RIP, NIK and IKKalpha kinases. *European journal of immunology* **33**, 1998-2006, doi:10.1002/eji.200324013 (2003).
- 346 Cooper, D. M., Pio, F., Thi, E. P., Theilmann, D. & Lowenberger, C. Characterization of Aedes Dredd: a novel initiator caspase from the yellow fever mosquito, *Aedes aegypti*. *Insect biochemistry and molecular biology* **37**, 559-569, doi:10.1016/j.ibmb.2007.03.005 (2007).
- 347 Di Fruscio, M. *et al.* Kep1 interacts genetically with dredd/caspase-8, and kep1 mutants alter the balance of dredd isoforms. *Proc Natl Acad Sci U S A* **100**, 1814-1819, doi:10.1073/pnas.0236048100 (2003).
- 348 Rodriguez, A. *et al.* Dark is a Drosophila homologue of Apaf-1/CED-4 and functions in an evolutionarily conserved death pathway. *Nat Cell Biol* **1**, 272-279, doi:10.1038/12984 (1999).
- 349 Daish, T. J., Mills, K. & Kumar, S. Drosophila caspase DRONC is required for specific developmental cell death pathways and stress-induced apoptosis. *Dev Cell* **7**, 909-915, doi:10.1016/j.devcel.2004.09.018 (2004).
- 350 Guntermann, S. & Foley, E. The protein Dredd is an essential component of the c-Jun N-terminal kinase pathway in the Drosophila immune response. *J Biol Chem* **286**, 30284-30294, doi:10.1074/jbc.M111.220285 (2011).
- 351 Ditzel, M. *et al.* Degradation of DIAP1 by the N-end rule pathway is essential for regulating apoptosis. *Nat Cell Biol* **5**, 467-473 (2003).
- 352 Guntermann, S., Primrose, D. A. & Foley, E. Dnr1-dependent regulation of the Drosophila immune deficiency signaling pathway. *Developmental and comparative immunology* **33**, 127-134, doi:10.1016/j.dci.2008.07.021 (2009).
- 353 Bond, D., Primrose, D. A. & Foley, E. Quantitative evaluation of signaling events in Drosophila S2 cells. *Biological procedures online* **10**, 20-28, doi:10.1251/bpo139 (2008).
- 354 Bond, D. & Foley, E. Autocrine platelet-derived growth factor-vascular endothelial growth factor receptor-related (Pvr) pathway activity controls intestinal stem cell proliferation in the adult Drosophila midgut. *J Biol Chem* **287**, 27359-27370, doi:10.1074/jbc.M112.378018 (2012).
- 355 Harikrishnan, A., Ando, I. & Dearolf, C. R. in *Program and Abstracts. 41st Annual Drosophila Research Conference, Pittsburgh, 2000.* 625C.
- 356 Hazelrigg, T., Levis, R. & Rubin, G. M. Transformation of white locus DNA in drosophila: dosage compensation, zeste interaction, and position effects. *Cell* **36**, 469-481 (1984).

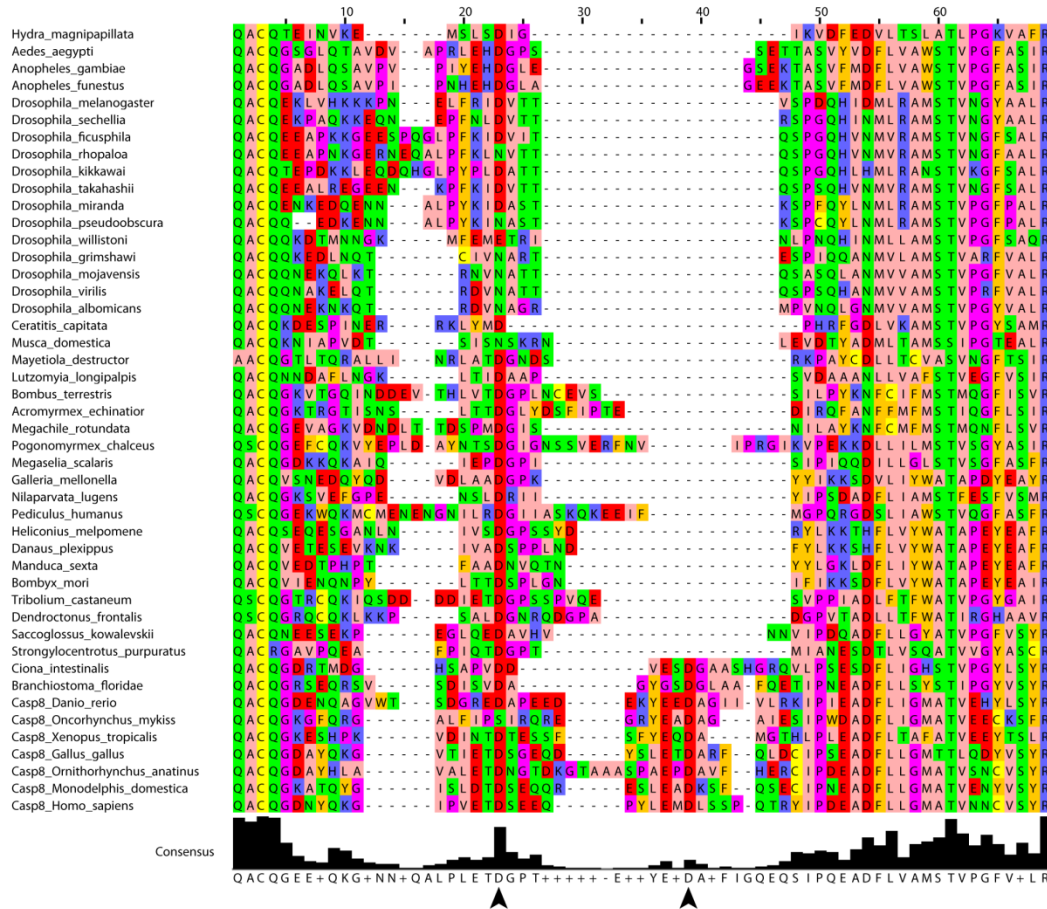
- 357 Saleh, M. C. *et al.* The endocytic pathway mediates cell entry of dsRNA to induce RNAi silencing. *Nat Cell Biol* **8**, 793-802, doi:10.1038/ncb1439 (2006).
- 358 Hay, B. A. & Guo, M. Caspase-dependent cell death in *Drosophila*. *Annual review of cell and developmental biology* **22**, 623-650, doi:10.1146/annurev.cellbio.21.012804.093845 (2006).
- 359 Brand, A. H. & Perrimon, N. Targeted gene expression as a means of altering cell fates and generating dominant phenotypes. *Development* **118**, 401-415 (1993).
- 360 Silke, J. & Meier, P. Inhibitor of apoptosis (IAP) proteins-modulators of cell death and inflammation. *Cold Spring Harbor perspectives in biology* **5**, doi:10.1101/cshperspect.a008730 (2013).
- 361 Muro, I., Hay, B. A. & Clem, R. J. The *Drosophila* DIAP1 protein is required to prevent accumulation of a continuously generated, processed form of the apical caspase DRONC. *J Biol Chem* **277**, 49644-49650, doi:10.1074/jbc.M203464200 (2002).
- 362 Chinnaiyan, A. M., O'Rourke, K., Tewari, M. & Dixit, V. M. FADD, a novel death domain-containing protein, interacts with the death domain of Fas and initiates apoptosis. *Cell* **81**, 505-512 (1995).
- 363 Kersse, K., Verspurten, J., Vanden Berghe, T. & Vandenabeele, P. The death-fold superfamily of homotypic interaction motifs. *Trends in biochemical sciences* **36**, 541-552, doi:10.1016/j.tibs.2011.06.006 (2011).
- 364 Boyer, L. *et al.* Pathogen-derived effectors trigger protective immunity via activation of the Rac2 enzyme and the IMD or Rip kinase signaling pathway. *Immunity* **35**, 536-549, doi:10.1016/j.immuni.2011.08.015 (2011).
- 365 Botas, J. *Drosophila* researchers focus on human disease. *Nature genetics* **39**, 589-591, doi:10.1038/ng0507-589 (2007).
- 366 Adams, M. D. *et al.* The genome sequence of *Drosophila melanogaster*. *Science* **287**, 2185-2195 (2000).
- 367 Oberst, A. & Green, D. R. It cuts both ways: reconciling the dual roles of caspase 8 in cell death and survival. *Nature reviews. Molecular cell biology* **12**, 757-763, doi:10.1038/nrm3214 (2011).
- 368 Lamkanfi, M., Festjens, N., Declercq, W., Vanden Berghe, T. & Vandenabeele, P. Caspases in cell survival, proliferation and differentiation. *Cell death and differentiation* **14**, 44-55, doi:10.1038/sj.cdd.4402047 (2007).
- 369 Cao, Y., Chtarbanova, S., Petersen, A. J. & Ganetzky, B. Dnr1 mutations cause neurodegeneration in *Drosophila* by activating the innate immune response in the brain. *Proc Natl Acad Sci U S A* **110**, E1752-1760, doi:10.1073/pnas.1306220110 (2013).
- 370 Yu, J. W., Jeffrey, P. D. & Shi, Y. Mechanism of procaspase-8 activation by c-FLIPL. *Proc Natl Acad Sci U S A* **106**, 8169-8174, doi:10.1073/pnas.0812453106 (2009).
- 371 Kataoka, T. & Tschopp, J. N-terminal fragment of c-FLIP(L) processed by caspase 8 specifically interacts with TRAF2 and induces activation of the NF-kappaB signaling pathway. *Molecular and cellular biology* **24**, 2627-2636 (2004).

- 372 Primrose, D. A. *et al.* Interactions of DNR1 with the apoptotic machinery of *Drosophila melanogaster*. *Journal of cell science* **120**, 1189-1199, doi:10.1242/jcs.03417 (2007).
- 373 Florentin, A. & Arama, E. Caspase levels and execution efficiencies determine the apoptotic potential of the cell. *The Journal of cell biology* **196**, 513-527, doi:10.1083/jcb.201107133 (2012).
- 374 Koto, A., Kuranaga, E. & Miura, M. Temporal regulation of *Drosophila* IAP1 determines caspase functions in sensory organ development. *The Journal of cell biology* **187**, 219-231, doi:10.1083/jcb.200905110 (2009).
- 375 Kaplan, Y., Gibbs-Bar, L., Kalifa, Y., Feinstein-Rotkopf, Y. & Arama, E. Gradients of a ubiquitin E3 ligase inhibitor and a caspase inhibitor determine differentiation or death in spermatids. *Dev Cell* **19**, 160-173, doi:10.1016/j.devcel.2010.06.009 (2010).

## **Appendix - Supplementary data**



**Supplementary Figure 1: by Edan Foley. The IMD signaling pathway does not induce apoptosis: A.** Quantitative real time PCR analysis of cells treated with the indicated dsRNAs and stimulated with PGN for 0 or 6 h. The relative expression levels for *attacin*, are standardized to *actin* levels. **B.** Quantification of apoptosis. As a control for the detection of apoptosis cells were treated with toxic doses of Actinomycin D (column 2). In the following columns, cells were treated with the indicated dsRNA and treated with PGN where shown. The extent of apoptosis was determined 8 hours after treatment. In each case, inactivation of the IKK-Rel axis blocks AMP expression, but did not results in apoptosis. This contrasts with mammalian systems where TNF induces death in cells that lack an IKK-NF- $\kappa$ B arm and suggest that the IMD pathway lacks an apoptotic component.



**Supplementary Figure 2:.** by Bart Hazes. **Caspase sequence alignment:** Sequence alignment of the linker motif between the large and small catalytic subunits of Caspase-8 orthologs. An arrowhead indicates auto-proteolytic cleavage sites in human Caspase-8, the consensus sequence is indicated below.